MODELING, SIMULATION AND STABILIZATION OF A DOUBLE QUAD INVERTED PENDULUM SYSTEM (DQIP) USING A LINEAR QUADRATIC REGULATOR (LQR) CONTROLLER

BY

MOHAMMAD ABDULLAHI

MSC/ENG/5992/2009-2010

(masani@abu.edu.ng)

SUPERVISORY TEAM:

Dr. M. B. Mu'azu (Major)

Prof. B. G. Bajoga (Minor)

A Thesis Submitted to the Department of Electrical and Computer Engineering, Ahmadu Bello University, Zaria, in Partial Fulfillment of the Requirements for the Award of Master of Science (M.Sc) Degree in Electrical Engineering.

August, 2014

DECLARATION

I Mohammad Abdullahi, hereby declare that this Thesis titled "Modeling, Simulation and Stabilization of a Double Quad Inverted Pendulum System (DQIP) using Linear Quadratic Regulator (LQR) Controller" was carried out by me under the supervision of Dr. M. B. Mu;azu and Prof. B. G. Bajoga as part of the Requirements for the Award of Degree of Master of Science in Electrical Engineering. This work to the best of my knowledge has never been submitted anywhere for the award of degree. All literatures used and cited are dully acknowledged in the reference pages.

Abdullahi MOHAMMAD	__________________	__________________
	(Signature)	**Date**

CERTIFICATION

This Thesis "Modeling, Simulation and Stabilization of a Double Quad Inverted Pendulum System (DQIP) using Linear Quadratic Regulator (LQR) Controller" meets the Requirements for the Award of Degree of Master of Science (MSc) in Electrical Engineering by Ahmadu Bello University, Zaria and it is approved for its contribution to knowledge and literature.

Dr. M. B. Mu;azu ______________________ ______________________
(Major Supervisor) **(Signature)** **Date**

Prof. B. G. Bajoga ______________________ ______________________
(Minor Supervisor) **(Signature)** **Date**

Dr. M. B. Mu;azu ______________________ ______________________
(Head of Department) **(Signature)** **Date**

Prof. A. A. Joshu ______________________ ______________________
(Dean Postgraduate School) **(Signature)** **Date**

DEDICATION

I dedicate this work to my late father and grant parents; Malam Muhammad Sani Umar, Alhaji Umar Abdullahi Tailor and Hajiya Fatima Abdullahi. May Allah forgive them and grant them Aljannatul Firdaus, Amin.

AKNOWLEDGEMENT

In the name of Allah, the beneficent and the most merciful, I begin by saying all praises are due to Allah, the Lord of universe. Peace and blessings be upon Prophet Muhammad (S.A.W), members of His households, His most guided companions and all those who follow their guidance till the end of time.

It is indeed a long journey having come all this way. I thank Allah (S.W.A) for seeing me through these hurdles. It was with His grace that this piece of work becomes reality.

My immeasurable thanks go to my able scholar, supervisor and a mentor Dr. M. B. Mu'azu for his time, patience and immense contributions towards making this work eccentrically special in terms of content richness. My appreciation goes to my grandfather and emeritus Professor, Prof. B. G. Bajoga for his constructive criticisms and valuable contributions. To my mentor, roll model and a father, Dr. S. M. Sani, I say thank you for having time to go through the manuscript. Your contributions are quite enormous and have indeed added material value to this Thesis, thus making it unique in terms content.

I am highly indebted to my late grandparents; Alhaji Umar Tailor and Hajiya Fatima Abdullahi; and my late father, Malam Muhammad Sani for their prayers and moral support. I cannot repay the favours you gave me during your life times. I pray may Allah forgive all your sins and make Aljannatul Firdaus your final abode. To my dear Mummy,Malama Sa'adatu Abdullahi, no amount of words can be used to express how grateful I am towards your kindness. I am what I am now because of you Mummy. May Allah reward you abundantly, Amin.

To my dear better half, Maryam Abdullahi and sweet daughter Sumayya Abdullahi, I thank both of you for your patience and prayers throughout the period of this Thesis compilation. Ummu-Sumayya, I honestly owe you so much. Allah Ya barmu tare, Amin.

I owe so much to my siblings and the entire members of my family for their prayers and moral support.

I am grateful to all my lecturers and colleagues; Dr. S. Garba, Engr Alhaji Malam Y. Jibril, Dr. Jimoh, Dr. D.D.Dajab, Dr. E. O. Akinsanmi, Dr. J.Y.Oricha, Engr. Kabir Ahmad Abu-Bilal, Engr. Mu'azu, Mal. M. D. Almustapha, Engr. Bashir S. Halliru and all those whose names cannot be captured.

I am also grateful to Engr. Y. A. Shaaban, a colleague, brother and a friend for his invaluable contributions. Without his contributions, this work would have been stranded.

My immense gratitude goes to my uncle and in-law, Alhaji Abdullahi M. Barau and his brother Alhaji Abubakar Lawal for their prayers and moral support. To my uncles; Alhaji Shuaibu Umar Abdullahi, Abubakar Umar and Husaini Umar, I say thank you for being there always for me. I cannot end this without mentioning a true friend Shehu Dikko and my aunty Ramatu Dikko for their constant prayers and moral support and all those who contributed to the success of this work in one way or the other

Abdullahi MOHAMMAD Abu Sumayyah (Minister)

Zaria

August, 2014.

TABLE OF CONTENTS

LIST OF FIGURES

LIST OF TABLES

LIST OF ABBREVIATIONS

Acronym	**Definition**
AKF	Adaptive Kalman Filter
ANN	Artificial Neural Networks
BIBO	Bounded Input Bounded Output
DQIP	Double Quad Inverted Pendulum
FLC	Fuzzy Logic Controller
GA	Genetic Algorithm
LQR	Linear Quadratic Regulator
LQG	Linear Quadratic Quasian
LQT	Linear Quadratic Tracking
LTI	Linear Time Invariant System
MIMO	Multiple Input Multiple Output
QIP	Quad Inverted Pendulum
SIMO	Single Input Multiple Output
SISO	Single Input Single Output
QEQC	Quadrature Encoder Quantization Compensator

ABSTRACT

Inverted Pendulum phenomenon has been critical in the modeling and stabilization of space-ships, rockets, humanoid robots, etc and also in understanding classical control systems. This research is aimed at extending the modeling and complexity of the inverted pendulum from single-link or double-link to a multilink type, with particular emphasis on the double-quad inverted pendulum (DQIP) i.e. 8-link system. The nonlinear model of the DQIP was obtained using Eular-Lagrange formulation. To ease the analysis and control of the DQIP, the model was linearized using the Jacobi Matrix based on the Taylor's series expansion approach. In order to validate the linear model, a comprehensive Simulink model of the DQIP was developed from which the Quad Inverted Pendulum (QIP) model was extracted. The response of the extracted QIP model was then compared with the responses reported in literatures for other QIP models and was found to outperform them. LQR was introduced after it was confirmed that the system was controllable and observable but not stable. This validated the DQIP model developed. The performance of the DQIP was then tested against the performance specifications of ≤ 2% maximum overshoot, ≤ 20 seconds settling time and zero steady-state error. With the following values of weighting matrices, which were used to penalize the states (Q) and input (R) respectively: *Q=dig[500, 5000, 5000, 5000, 5000, 5000, 5000, 5000, 5000] and R=[0.8]*, maximum overshoots of 2.05%, 1.7%, 1.575%, 1.52%, 1.45%, 1.26%, 1.21% and 0.106% for the first, second, third, fourth, fifth, sixth, seventh and eighth pendulum were obtained with settling time of 17.5 seconds and zero steady-state error. The LQR designed has therefore demonstrated its ability to stabilize all the pendulum links about a vertical position.

CHAPTER ONE

INTRODUCTION

1.1 Background

The compelling circumstances during a rocket vertical take-off brought about the early studies of inverted pendulum system (Mathew et al., 2013). At the point of take-off, the rocket is highly unstable (Chye and Sang, 1999). Inverted Pendulum, like the rocket at a point of launch, requires a series of continuous correction mechanisms to maintain a vertical position, since the system is unstable in an open loop configuration (Chye and Sang, 1999 and Li et al., 2004). The first Inverted Pendulum System was developed in the 1950's by the control experts group at MIT, USA (Li et al., 2004).

An Inverted Pendulum is a type of pendulum in which the mass of the pendulum is above the fulcrum (pivot point), while a conventional pendulum is normally stable when hanging downwards (Shen et al., 2004). An inverted pendulum is highly unstable in that it may trip over in any direction unless a suitable control force is applied (Astrom and Furuta, 1996). It is usually implemented with a rod hinged on a movable cart, which can move horizontally along X-axis as shown in Figure 1.1.

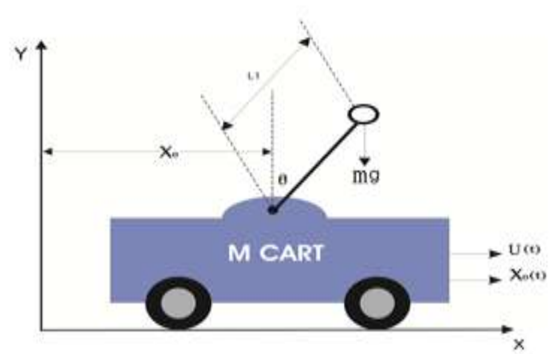

Figure 1.1. Single Inverted Pendulum on a Cart (Source: Prasad et al, 2011).

Sometimes it is referred to as a “cart and pole” (Fantoni and Lozano, 2003). The inverted pendulum on a cart remains one of the classical problems in dynamics and control theory that is widely used as a basis for testing and verifying control algorithms such as: Linear Quadratic Regulator (LQR), Proportional Integral Derivative (PID) controller, Artificial Intelligence - based controllers (Fuzzy controller, Genetic Algorithms, Neural Networks), etc (Khan et al., 2009 and Boubaker, 2012).

The peculiar features of an inverted pendulum have, over the time, attracted the interests of scholars and researchers such that it is used as one of the benchmarks for classical control theory demonstration especially with respect to stability studies and dynamics of non-linear systems (Yi and Yubazaki, 2000 and Geun and Suel., 2008).). The complexity of the physical modeling of the systems increases when multiple link systems are considered (Lam and Davison, 2006). Generally, an inverted pendulum is inherently an unstable system and it is made stable when firmly and actively balanced in a vertical position (Lam and Davison, 2005). This is achieved by either applying a torque at the pivot point or a horizontal force which forms part of a feedback mechanism. Control engineers have recently gone beyond stabilization of single inverted pendulum to double, triple and quadruple inverted pendulum systems (Li et al., 2002). The first successful control implementation of triple inverted pendulum was achieved in October 2001 (Li et al 2004) in the Department of Applied Mathematics , Beijing Normal University, Beijing, China. A year later, the same group of control experts implemented and stabilized the quadruple inverted pendulum using Variable Universe Adaptive Fuzzy Control method (VUAFC) (Li et al., 2002).

Inverted pendulum system is an important class of an under actuated mechanical system essentially used in teaching classical control systems with the following applications (Graf and Röfer, 2012; Slavka and Anna, 2010):

i. missile guidance
ii. modeling of a postural standing of human or humanoid robot
iii. self transport machine
iv. modeling and simulation of the unstable system of a human or robotic upper limb
v. modeling and stabilization of space-ships and rockets

What is evident in literature, to the best of my knowledge, is that the highest number of links reported in literature is the quadruple inverted pendulum and that the LQR Controller is a viable tool for the control and stabilization of the inverted pendulum. However, several attempts have been made over the last five years to develop the general procedure and solution to the inverted pendulum system of an arbitrary number of links by developing a block library lilted "Inverted Pendulum Modeling and Control (IPMaC)" (Slavka and Anna, 2009, 2010; Slavka and Sarnovsky, 2011; Jadlovska and Sarnovky, 2012; 2013). The block library was integrated into the MATLAB/Simulink Library browser. The validity of the developed block library was only tested on single and double inverted pendulum systems (Slavka and Anna, 2010). Further tests could have been carried out in order to justify the universality; validity and correctness of the developed library for systems with more number of links say three or four. This is because there are at the moment, evidences of experimental results on the stabilization of triple and quad inverted pendulum systems (Li et al., 2002; Giraldo, 2008; Yundong and Yanbin, 2008; Zhang et al., 2012).

1.2 Aim and Objectives

Until now, there has not been a unique control solution dedicated explicitly to the control of a double-quad inverted pendulum (DQIP). This research focused on modeling, simulation and stabilization of a double quad inverted pendulum (DQIP); a highly unstable and nonlinear system.

The research objectives therefore are:

1. Development of the linearized model of the double-quad inverted pendulum using Jacobian matrix based on Taylor's series expansion upon controllability.
2. Development of comprehensive simulation model of the double quad inverted pendulum using the MATLAB/Simulink control tool box.
3. Design of the LQR controller for the double quadruple inverted pendulum (DQIP).

1.3 Statement of the Problem

There have been several attempts to extend the study of a single inverted pendulum to multi-links inverted pendulum systems (Lam and Davison, 2005, 2006, Li et al, 2002; Zhang et al., 2012; Jadlovska and Sarnovky, 2012, 2013). The experimental stabilization of double, triple and quad inverted pendulums has been reported in number of literatures (Bogdanov, 2004; Li et al., 2002, 2004 and Zhang et al., 2012). The modeling and control stabilization of a multi-link inverted pendulum is an important concept used in describing the control and stability mechanism of a humanoid robot (Xiong et al., 2010). The complexity of the modeling increases as the number of links increases (Lam and Davison, 2005, 2006). In this thesis, possibility of extending the mathematical modeling to eight links (double quad) would be presented. LQR controller will be designed to investigate its viability in stabilizing such a complex system.

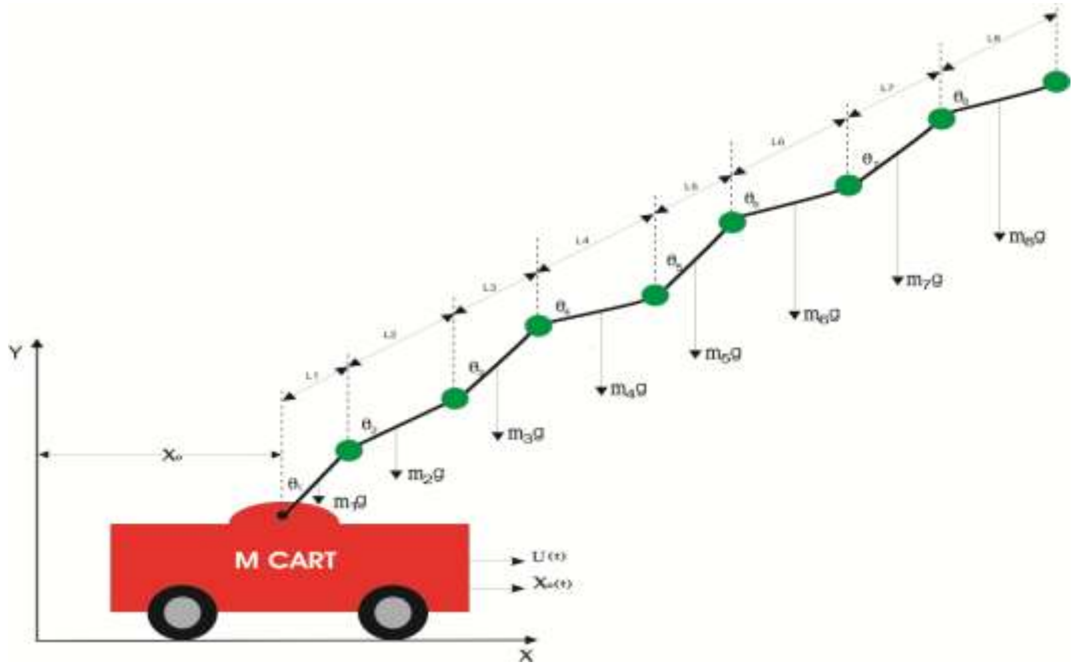

Figure 1.2. Double-Quad Inverted Pendulum

1.4 Methodology

Different control algorithms are used to implement control mechanisms of unstable systems. A multi-link inverted pendulum is sensitive to: joint friction, torque disturbance and noise (Lam and Davison, 2005 and 2006). In this research, an LQR controller being the simplest controller for optimal control regulator solution is proposed.

The methodology adopted is as follows:

1. Development of mathematical model based on Euler-Lagrange Equation.
2. Linearization of the model using Jacobian matrix based on Taylor's series expansion.

3. Control solution analysis
4. Extraction of the QIP model from the DQIP model.
5. Development of a simulink model of the QIP for comparison of responses and behaviour with other similar models developed.
6. Development of a comprehensive simulation model for the DQIP
7. Design of the LQR controller for the DQIP
8. Comparison of behaviour of the DQIP with and without the LQR controller.

1.5 Thesis Organization

The general introduction has been presented in Chapter One. The remaining chapters are structured as follows:

The detailed review of the relevant literatures and pertinent fundamental concepts is carried out in Chapter Two.

An in-depth approach to mathematical modeling of the DQIP and the development of its simulation model from which the QIP model is extracted for analysis is presented in Chapter Three. The details of the derivations are presented in the appendix A1 and A2. A logical approach to LQR controller design and implementation is also presented in this Chapter.

The analysis and discussions of the results are presented in Chapter Four.

The results obtained are analyzed and discussed in Chapter Five. Quoted references and appendices are also provided at the end of the thesis.

CHAPTER TWO

LITERATURE REVIEW AND THEORITHICAL BACKGROUND

2.1 Introduction

This chapter is divided into two parts. The first part discusses the fundamental concepts relevant to the study and control analysis of the inverted pendulum system. While, the second part provides details of some literature reviews relevant to the inverted pendulum system.

2.2 Review of Fundamental Concepts

This section presents the review of theoretical background and fundamental concepts pertinent to the control of an inverted pendulum system.

2.2.1 Linear and Nonlinear Control Systems

A linear control system is the control system in which the input/output relationship is generally represented by linear differential equations (Mohandas, 2006). The most fundamental property of a linear system is the validity of the principles of superposition and homogeneity (Kailath, 1980). It is on the basis of these properties that a linear system is designed to guarantee satisfactory performance when excited by a standard test signal (step, ramp, impulse, exponential, etc) (Dorf and Bishop, 2011). In this way the system may exhibit satisfactory behaviour under any circumstances.

On the other hand, a control system in which nonlinearity plays an important role, either in the controlled process (plant or system) or in the controller itself is known as nonlinear control system (Sastry, 2004; Binder et al., 2009). Nonlinear systems occur naturally in many engineering and natural systems, such as electrical, mechanical, aeronautics, automotive control, industrial control processes, biological systems and many others.

Nonlinear control systems do not obey the principles of superposition and homogeneity (Najmeijer, 2006). These systems are represented mathematically by set of nonlinear differential equations (Sastry, 2004). Many real-world processes and systems are nonlinear in their baheviour and therefore they require nonlinear control (Binder et al., 2009). The nonlinear systems are also difficult to handle and control (Binder et al., 2009). However, the control of nonlinear systems is simplified if they are controlled linearly based on the concept of piecewise approximation of nonlinear equations (Najmeijer, 2006). This therefore means that the nonlinear systems will be linearized and controlled about a specified operating point. The following are the general properties of linear and nonlinear systems (Najmeijer, 2006):

1. Linear systems obey the principles of superposition and homogeneity while nonlinear systems do not.
2. Linear systems have one equilibrium point at the origin. Nonlinear systems may have many equilibrium points.
3. Stability needs to be precisely defined for nonlinear systems. Stability for linear systems is uniquely determined by the location of poles or eigenvalues.
4. The principle of superposition does not necessarily hold for forced response for nonlinear systems.

The most typical nonlinear systems that are used in teaching classical control system and testing control algorithms are: inverted pendulum, magnetic suspension system, ball and beam and pitch control (Boubaker, 2013). Based on this, inverted pendulum is considered among as one of the fundamental benchmarks for teaching linear feedback control theory because of its wide applications (Kailath, 1980 and Boubaker, 2013).

2.2.2 Theory of Inverted Pendulum

For over four decades, the inverted pendulum especially the cart type has been used as a standard tool for teaching linear feedback control theory to demonstrate how open-loop unstable systems can be stabilized (Kailath, 1980). The first classical approach to solving inverted pendulum problem based on root locus analysis was done by Roberge (Roberge, 1960) and then later by Cannon (Cannon, 1966). It was later used in solving linear optimal control problems and complex nonlinear control problems for unstable systems (Kwakernaak, 1972; Khalil, 2002). Despite the fact that inverted pendulum has a simple structure, it is however a typical nonlinear dynamic system with two equilibrium positions; a stable equilibrium position when the pendulum is hanging downward and an unstable equilibrium position when the pendulum is in an inverted vertical position with its mass above the pivot point. The system becomes highly nonlinear if it is in an inverted position (Boubaker, 2013). Here, the inverted pendulum control is achieved when the pendulum swings from the stable equilibrium position and then later balances in an upright position by moving the cart to and forth to a specified position.

Based on the principle of inverted pendulum stabilization, many new concepts in robotics have evolved with quite new control applications (Boubaker, 2013). The recent major achievements of control and stabilization of inverted pendulum model are:

1. Control of under-actuated robotic systems (Liu et al., 2008; Boubaker, 2013): Under-actuated robotic systems are systems with fewer independent control inputs

(actuators) than degrees of freedom to be controlled (output states). Inverted pendulum on a cart is a typical system of under-actuated mechanical system with number of outputs to be controlled greater than the number of controlled inputs.

2. Design of mobile inverted pendulums (self transport machine): The design and implementation of mobile wheeled inverted pendulum systems have recently attracted a lot of attention (Younis and Abdelati, 2009). Plate 2.1 shows a pictorial view of mobile inverted pendulum.

Plate 2.1. Mobile wheeled inverted pendulum (Younis and Abdelati, 2009)

3. Gait pattern generation for humanoid robots: The control and stabilization of humanoid robots is one of the exigent tasks in the field of control and robotics engineering (Aloulou and Boubaker, 2010). The main issue in control and stabilization of humanoid robot is gait pattern generation (Arous and Boubaker, 2012). Inverted pendulum motion has been extensively used to bipedal gait in order to simplify the trajectory generation (Kiemel S., 2012). Linear Inverted Pendulum Model (LIPM) is a current research topic in this context; and it is generally

combined with Zero Moment Point concept to ensure gait stability (Kajita et al. 2010). The pictorial representation of a humanoid robot is shown in Plate 2.2.

Plate 2.2. Walking Humanoid Robot under Linear Inverted Pendulum Model (Kiemel S., 2012)

2.2.3 Modeling Techniques

The dynamics of mechanical systems are derived from either Mathieu equation, Newtonian formulation or Eular-Lagrange equation (Lasenby et al., 1993). Mathieu and Newton's equations are best suited if the dynamic transformations involved are for simple dynamical systems which yields set of single order ordinary differential equations (Lasenby et al., 1993). However, for complex dynamic systems, these formulations may not produce accurate dynamic equations and therefore, Eular-Lagrange equation is used (Doran and Lasenby, 2003). This is because Eular-Lagrange equation gives a set of higher order ordinary differential equations with the following advantages (Lasenby et al., 1993):

1. It takes into account the dynamics and control energy requirements (derivation is based on energy calculations of the physical system). In real experimental implementation, energy calculation is of great importance for the purpose of power consumption by the system and proper design of suitable actuators that could derive the system (Doran and Lasenby, 2003).
2. The use of generalized coordinates to describe the system degrees of freedom simplifies and illustrates more naturally the problem using much more simple coordinates (it is simpler) (Ni, 2011; Mladenov, 2011).
3. It can be used when the nature of some control force during constrained motion is not known (it is viable) (Lasenby et al., 1993).

Therefore, based on the above stated advantages, Euler-Lagrange equation of motion is used to derive the nonlinear dynamic equations of motion of the double quad inverted pendulum (DQIP). The Lagrangian function is given by (Doran and Lasenby, 2003):

$$L = K.E - P.E \tag{2.1}$$

Where L is the Lagrangian function, $K.E$ and $P.E$ are the kinetic and potential energies respectively.

The general Euler-Lagrange equation of motion that describes the dynamics of any mechanical system is given by (Lasenby et al., 1993):

$$\frac{d}{dt}\left(\frac{\partial L}{\partial \dot{\phi}}\right) - \frac{\partial L}{\partial \phi} + \frac{\partial F}{\partial \dot{\phi}} = \psi \tag{2.2}$$

Where ψ is a vector of the generalized co-ordinates (forces or moments) acting on the direction of the generalized coordinates $(\dot{\phi}, \phi)$ and F the fricative (dissipative) energy. Applying (2.2) on the double quad inverted pendulum system, the following equations are obtained:

Non-linear equation for pendulum angle;

$$\frac{d}{dt}\left(\frac{\partial L}{\partial \dot{\theta}}\right) - \frac{\partial L}{\partial \theta} + \frac{\partial F}{\partial \dot{\theta}} = \psi_1 \tag{2.3}$$

Non-linear equation for cart position;

$$\frac{d}{dt}\left(\frac{\partial L}{\partial \dot{x}}\right) - \frac{\partial L}{\partial x} + \frac{\partial F}{\partial \dot{x}} = \psi_2 \tag{2.4}$$

Where: ψ_1 and ψ_2 are vectors of total forces or moments acting in the direction of all the components of θ and x (pendulums' angles and cart position).

2.2.4 Control Analysis Techniques

Control theory has emerged over the last ten decades (Fernandez-Cara and Zuazua, 2003). The theory has over the time undergone series of changes in the way and manner by which control laws and solutions are formulated. There are basically two major distinctions in control theory: classical and modern control approaches (Andrei, 2006). These techniques have direct repercussions on control system design and its applications.

2.2.4.1 Classical Control Theory

Classical control methods typically are concerned with system response shaping using frequency domain techniques (e.g. Bode, Root-locus and Nyquist plots) (Kim and Faruqi

2010). These analyses are based on the transfer functions and thus its limitations are tied down to the limitations of transfer. The extent of classical control theory is simply restricted to single-input and single-output (SISO) system design in time domain (Kim and Faruqi, 2010 and Stang, 2005). However, for Multiple-Input Multiple-Output (MIMO) systems the application of classical control technique requires that each input and output be separated. This means that the whole system is treated as a group of SISO systems with each having a controller designed specifically for it (Kim and Faruqi 2010). The following are the drawbacks of classical control approach based on transfer function:

i. It is generally defined under zero initial conditions
ii. It is applicable to only LTI systems
iii. It is limited to only SISO systems
iv. It cannot provide information about the system internal state
v. It involves trial and error procedures

The implications of these drawbacks led to the following:

i. Difficulty when handling MIMO systems
ii. Optimal control system with respect to performance may not be guaranteed.
iii. Instability may result as a result of lack of information about internal state.

In order to address these shortcomings, particularly when dealing with Time-Varying Systems (TVS), modern control system was born (Dorf and Bishop, 2011).

2.2.4.2 Modern Control

The shift from classical control approach to modern control approach is as a result of the growth in system complexity, sophistication and the need for high accuracy (Dorf and Bishop, 2011). The pressing demand on the performance of control systems has largely increased the accessibility of large scale computers. Modern control therefore has been developed around 1960s to serve as a new approach to analysis and design of complex control systems (Ogata, 2007). Modern control theory is built upon the concept of state space approach (Ogata, 2007).

Modern control theory is extended to time-varying multi-input and multi-output (MIMO) systems in time domain (Wright, 2004). In this way, more sophisticated problems, aircraft fighter control, space ships, missiles control, robots, etc involving multi-variables can be addressed. This indeed overcomes the limitations of classical control theory in analyzing such systems. Instead of representing the system in terms of output/input description (transfer function), modern control design approach represents the system as a set of first order differential equations described using state variables. Modern control system requires sometimes that controllers are designed not only to efficiently control the behaviour of the system but also to extremize certain specifications (e.g. energy, settling time, overshoot, rise time or some physical constraints enforced on the environment) defined by the controller designer.

The following are the advantages of using state space representation as compared to classical approach (Dorf and Bishop, 2011):

1. It provides a time domain solution.
2. It has the ability to handle MIMO, SIMO or MISO systems.

3. It provides information about both the internal and output state of the system.
4. The effect of initial conditions can be integrated easily in the solution.
5. The use of vector/matrix modeling provides efficiency from the point of view for computer implementation.

Based on the foregoing and the fact that DQIP is a typical SIMO system, modern control approach is chosen as the control technique for modeling the linear dynamic model of the DQIP in state space.

2.2.4.2.1 Classes of Modern Control System

The need for better and fast system response stability necessitated the development of more robust controllers (Stang, 2005). This is important because of the growth in complexity and sophistication of systems, which has led to the extension of modern control theory to other control theories: Optimal, Adaptive and Robust Theories (Stang, 2005, Kim and Faruqi, 2010).

2.2.4.2.2 Classification of Controllers

Controllers may be classified as classical, modern or intelligent (Mladenov et al., 2006).

a. **Classical Controller:** PID Controllers are the most common and popular classical controllers used in industrial control systems (Araki, 2002). The general applicability of the controllers is attributed to their operational and functional simplicity. PID controller as shown in Figure 2.1 is characterized by three parameters: proportional gain, integral gain and derivative gain. In a heuristic sense, these parameters are defined in terms of time. ‘P’ is dependent on the present error, ‘I’ on the accumulation of past errors, and ‘D’ on the prediction of future errors (Araki, 2002).

In many control processes, PID controllers have been proved useful in providing satisfactory control. In many situations, however, they may not yield optimal control performance.

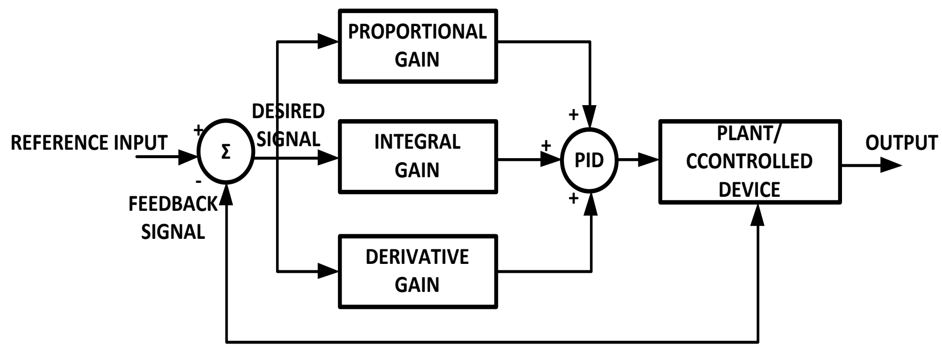

Figure 2.1. Block Diagram of PID Controller (Source: Norma, 2011).

b. **Intelligent Controllers:** These are controllers that employ artificial neural networks (ANN), genetic algorithms (GA) or neuro-fuzzy logic (NFL) as control algorithms (Samad, 2009). They are generally popular in the control of nonlinear systems because of their universal function approximation abilities (Bogdanov, 2004 and Samad, 2009). A typical example of this controller is fuzzy logic controller and is shown in Figure 2.2. These controllers can work very well even on linear systems and on system whose mathematical model is difficult to obtain (Cibilić et al, 2010).

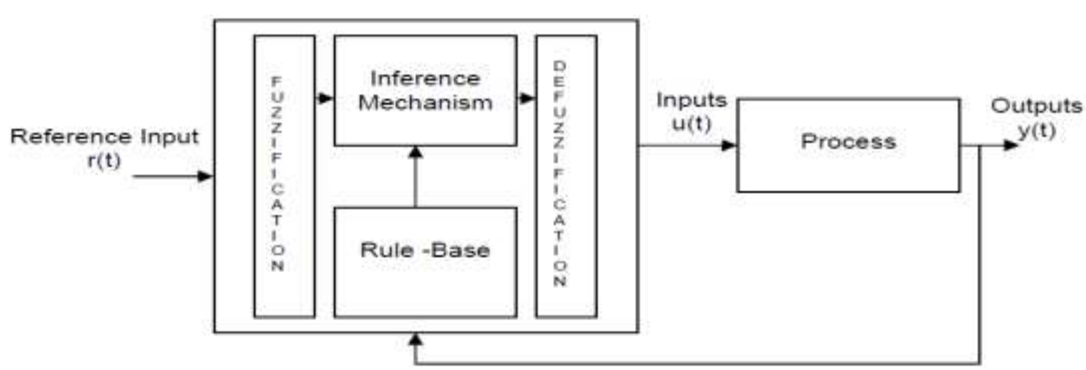

Figure 2.2. Block diagram of Fuzzy Controller (Cibilić et al., 2010)

c. **Modern Controllers:** These are controllers that are designed based on the modern control system approach. These controllers may be further categorized as optimal, adaptive and robust controllers (Wright, 2004). Controllers that are designed to work properly in the presence of uncertainties are called robust controllers (Damen and Weiland, 2002). Similarly, a controller that is designed with an ability to modify or change its behaviour in order to accommodate the changes in the dynamic characteristics of the plant or circumstances is called an adaptive controller (Kanellakopoulos et al., 1991). Optimal controller on the other hand is the one that seeks to optimize a certain system performance index with minimum input control energy (Oral et al., 2010). A typical block diagram of an optimal controller (LQR) is shown in Figure 2.3.

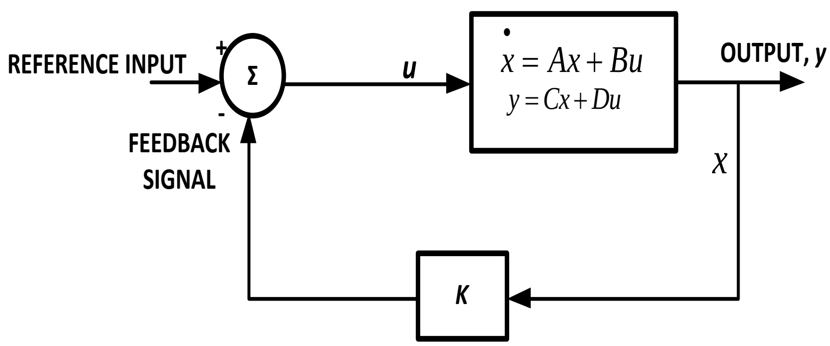

Figure 2.3. A typical Block Diagram of Optimal Controller (LQR) (source: Ogata, 2007).

It is also important to note that modern control theory approach is mainly based on the concept of state space (Dorf and Bishop, 2011). Therefore, it is important at this point to define the state and the state space model.

The mathematical modeling of a physical system is derived from the system of differential equations known as state space (Ogata, 2007). State is therefore, as defined as the "set of small elements $(x_{1,} x_2,..., x_n)$ called state variables such that the knowledge of these variables at some initial condition *(t = t₀)*, together with the knowledge of input function $(u_{1,} u_2,..., u_n)$ for $t \geq t_0$, completely determines the output $(y_{1,} y_2,..., y_n)$ of the system for any time $t \geq t$" (Dorf and Bishop, 2011). This definition is pictorially depicted in Figure 2.4.

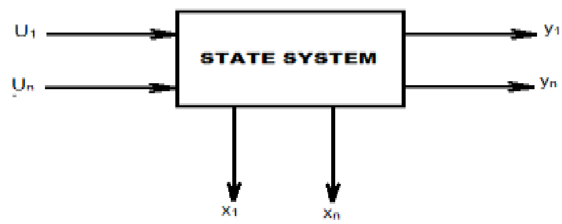

Figure 2.4. General Block Diagram of System Model Dynamics (Dorf and Bishop, 2011)

The representation of nth order dynamic system as a first order differential equation in an n-vector in terms is called state space model and is given by (Dorf and Bishop, 2011):

$$\dot{x} = Ax + Bu \tag{2.5}$$

$$y = Cx + Du \tag{2.6}$$

Where:

$\dot{x}$ is the derivative of the vector, x is the state vector, A the state variable matrix, B the input matrix, u the control or input vector, y the output vector, C the output state matrix and D the transition or disturbance matrix.

2.2.5 State Space Model Scaling

The implementation of linear control laws on Linear Time Invariant system (LTI) is simplified when the system is presented in a state space model form (Braslavasky, nd). For higher order systems however, representing the systems in state space models may not guarantee accuracy due to internal computational error ("finite word length arithmetic") by the computer as a result of round-off error. Moreover, an ill-conditioned state model may also sometimes be as a result of mismatch in the unit of two or more of the state variables in the system dynamics (Braslavasky, nd). This difference in units of the state variables may result in the presence of small and large entries (elements) in the state matrix *A*. The mix up in these small and large entries could alter some essential properties of the state model and could eventually lead to wrong results (Braslavasky, nd and Mathwork MATLAB® 12). Dealing with an ill-conditioned model yields inaccurate and inconsistent results. Therefore, a good state space model is essential to obtaining precise results. Provided that the model of a system is correct, its numerical state can be improved by scaling or normalizing the system matrices *(A, B, C, and D).*

Scaling provides reasonable deduction to be drawn about the extent of controllability and observability of different inputs and outputs (Braslavasky nd; Pulgar et al, 2011). Scaling can be performed manually, automatically or auto-manually.

2.2.5.1 Manual Scaling

The theory behind model scaling involves the use of diagonal scaling matrices S_x, S_u and S_y to normalize u, x and y (Braslavasky, nd; Zhang, 2002).

$$u = S_u u_s \, , x = S_S x \, , y = S_y y_s \tag{2.7}$$

The scaled system is as follows:

$$\dot{x}_s = A_s x_s + B_s u \, , \tag{2.8}$$

$$y_s = C_s x_s + D_s u_s \tag{2.9}$$

Where:

$$A_s = S_x^{-1} A S_x \tag{2.10}$$

$$B_s = S_x^{-1} B S_u \tag{2.11}$$

$$C_s = S_y^{-1} C S_x \tag{2.12}$$

$$D_s = S_y^{-1} D S_u \tag{2.13}$$

Analytical method of finding the scaled system matrices of equations (2.10) and (2.11) could be so stressful and involves serious iterative process especially for complex system like double quad inverted pendulum.

2.2.5.2 Automatic Scaling

Automatic scaling is possible by using a command line "*ssbal(sys*)" in MATLAB. Typing this command line provides means of generating state scaled model without the loss of accuracy by automatic selection of frequency range in order to achieve accuracy based on system dynamics (Mathwork MATLAB® 12a; Braslavasky, nd).

2.2.5.3 Auto- manual Scaling

For most complex models, that are physically realizable and having dynamics over a wide frequency range, automatic scaling may not give accurate model (Braslavasky, nd). Double quad inverted pendulum is one of those systems because of the order and complexity of its modeling. For such systems, there is always a tradeoff of accuracy at different frequency intervals (Mathwork MATLAB® 12a). Consequently, the system model may not be accurate. If the model is verified to be in order, proper scaled model can be obtained for high accuracy by manually adjusting the frequency interval (Mathwork MATLAB® 12a). The band within which the model is accurate is referred to as “scaling factor” (Mathwork MATLAB® 12a, Braslavasky nd). This factor is used to obtain the normalized state matrix and system input vector.

This method combines some properties of both manual and automatic scaling methods. Unlike manual scaling, this method uses a more robust way of finding scaling factor. It involves the use of MATLAB command *“prescale(sys)”*. This command has in it a graphical user interface (GUI) scaling tool that pops up on typing the syntax on a MATLAB command window as shown in Figure 2.5 (Mathwork MATLAB R2012a). The *prescale(sys)* GUI tool allows the visualization of the accuracy tradeoffs so that frequency bands can be adjusted for maximum accuracy.

When scaling a model using scaling tool GUI, the following steps are followed:

i. Lunching the scaling tool GUI
ii. Defining the frequency axis limits
iii. Defining the frequency band for maximum accuracy
iv. Saving the scaled model

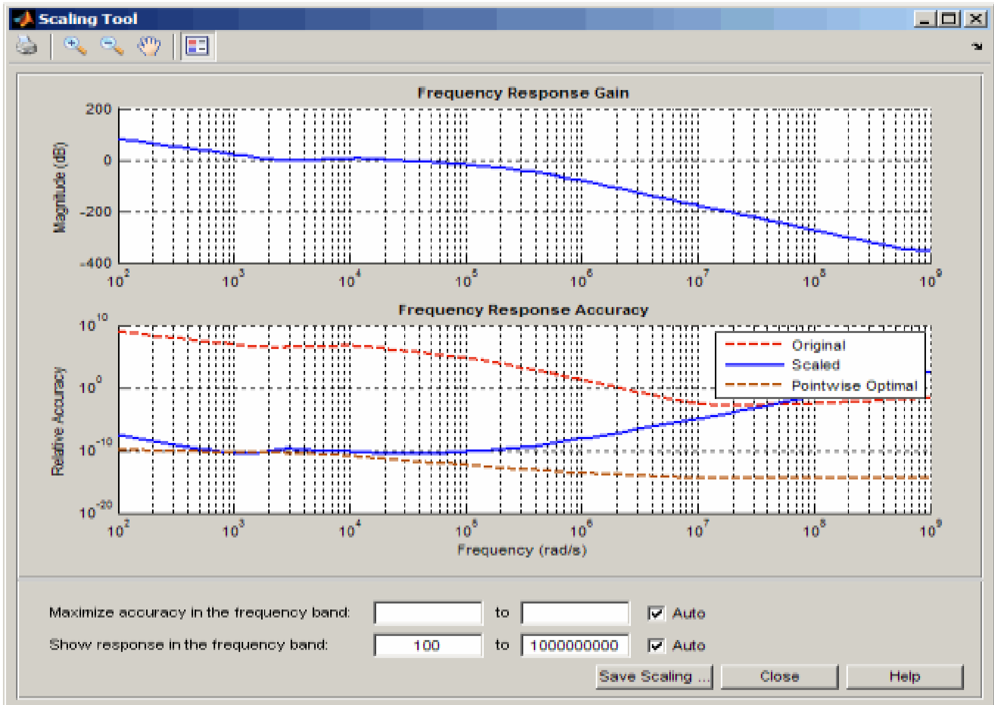

Figure 2.5. Graphical User Interface (GUI) Scaling Tool (Mathwork MATLAB® 12a)

2.2.5.3.1 Components of Scaling Tool GUI

The following are the constituents of Scaling Tool GUI (Figure 2.5):

1. Frequency Response Gain: this helps in determining the frequency band over which the scaling is maximized
2. Frequency Response Accuracy: this curve allows the visualization of accuracy tradeoffs of the model at certain frequency band when maximizing accuracy.

From the frequency response accuracy, the following could be observed:

Red line: this curve shows the relative accuracy response of the original un-scaled model

Blue line: this curve indicates the relative accuracy response of the scaled model

Brown line: this curve presents the best accuracy that can be achieved using different scaling at some frequencies.

The relative accuracy in this context refers to the measure of the worst scenario of the relative difference between the original model frequency and the perturbed model (scaled model). Accurate model is obtained when the blue curve is closer to or almost in phase with Brown Pont-wise optimal curve" at a certain frequency band (Mathwork MATLAB® 12a). Frequency bands are specified in two fields as shown in the scaling tool GUI are:

i. Frequency band field: this shows the frequency response plots within a specific frequency range.

ii. The second is the frequency field: this shows how a maximize accuracy in the frequency band can be achieved. As stated earlier, the accuracy is maximized by adjusting the frequency in the field provided.

Frequency response plots are always updated producing new scaling any time a new frequency band is specified. To obtain the approximate and most accurate scaling factor, comparison is made between the scaled model curve (blue line) and a point wise optimal curve (brown line) (Mathwork MATLAB® 12a). This is done in order to find where the new scaling is close to optimal.

After finding a good scaling, the model is saved in a dialog box called "save to work space". This dialog box contains two small sub dialog boxes. One of these boxes is used to save the scaled model while the other contains the information about the scaling factor, the frequencies used to test the accuracy and relative frequency at each test frequency.

2.2.6 Principle of Optimality

The term "Optimal Control" is used to describe the best way of controlling a system by means of extremizing (minimizing or maximizing) system functional performance (Oral et al., 2010). Over the last four decades, Optimal Control theory has been the area of research and interest by control engineers (Elggerd, 1966; Naslin, 1968; Bryson and Ho, 1975; Anderson and More, 1989; Oral et al., 2010). Many analytical approaches to implementing control strategies in accordance with the given design specification/s have been proposed by the evolution of modern optimal control theory (Anderson and Moore, 1989; Gupta et al., 2007). Not only that, the theory has also provided the best possible way to achieving the required system performance (Gupta et al., 2007). Optimal control design, therefore, requires the knowledge of the plant (system) in order to make the system to behave in a desired way (Anderson and Moore, 1989 and Oral et al., 2010). On this background, principle of optimality may be defined as the control policy that tries to maximize the performance of a system with a minimum cost (Oral et al., 2010). This is done by first defining the system performance index known as cost function and it is given (Gupta et al., 2007):

$$\boldsymbol{J_t} = \sum_{\boldsymbol{t}=0}^{\boldsymbol{t_\infty}} \boldsymbol{L_t}\left(\boldsymbol{x_{t,}}\boldsymbol{u_t}\right) \tag{2.14}$$

Where; t_∞ = *final time*, J_t is the total cost sequence of the state of the system and controls ($x_{t,}$ u_t).

Equation (2.1) can be written in integral notation:

$$\boldsymbol{J} = \int_0^\infty \left(\boldsymbol{x^T Q x} + \boldsymbol{u^T R u}\right) \boldsymbol{dt} \tag{2.15}$$

Where; Q and R are positive-definite Hermitian or real matrices (weighting matrices) used to determine the relative importance of the state variables and expenditure of energy. x^T *and* u^T are the transpose matrices of x and u (state variables and input function).

2.2.6.1 Types of Optimal Control Problems:

1. Terminal Control Problem: a problem that is used to bring the system as close as possible to a given terminal state within a given period of time, e.g. aircraft landing system (Remsing, 2006).

2. Minimum-Time Control Problem: this problem involves reaching the terminal state in the shortest possible time, e.g. a car driver that keeps his foot flat on the accelerator for the entire duration of his journey and applies the brakes as hard as possible at his final destination. It is also known as the 'Bang-Bang control problem (Remsing, 2006).

3. Minimum Energy Control Problem: this is used when a system is transferred from an initial state with minimum expenditure of control energy, e.g. in satellite control (Agrachev et al., 2004; Remsing, 2006).

4. Regulator Control Problem: this is used to return the system that was initially displaced from equilibrium state to the equilibrium state in order to minimize a given performance index. Inverted pendulum falls under the category of this problem. There other classical control problems such as magnetic suspension, ball and beam, etc. that may be categorized as regulator control problems (Agrachev et al., 2004; Claudiu and Remsing, 2006). Hence, the inverted pendulum problem is a classical optimisation problem that requires an optimal control strategy.

5. Tracking Control Problem: this is used to cause the state of a system to track as close as possible some desired state time history in such a manner as to minimize a given performance index (Agrachev et al., 2004; Claudiu and Remsing, 2006).

2.2.6.1.1 Formulation of Optimal Control Problem

The formulation of optimal control problem requires the following:

1. Mathematical description (or model) of the system (process) to be controlled (generally in state space variable form)
2. Specification of the performance index.
3. Stating the boundary conditions and the physical constraints on the states and/or controls.

Optimal control theory therefore provides an analytical and computational technique to solving problems involving MIMO, SIMO or MISO systems. The solution to such problems is obtained either analytically or by recapitulation process using computer. This is done by expressing the user defined criteria into some function known as "cost function" (Ni, 2011; Prasad et al 2012). In line with the above, the control solution of the DQIP problem is formulated using linear method based on optimal control theory. This is because DQIP just like normal single inverted pendulum may be classified as a regulator control problem that can be solved using optimal control technique.

2.2.6.2 Linear Quadratic Regulator (LQR)

Linear Quadratic Regulator (LQR) is a class of linear control design methodology in which cost function (quadratic performance indices) relating the control signal and the state variables are minimized in an optimal way (Oral et al, 2010; Ozana et al., 2012). LQR is one of the simplest optimal control methods implemented on the linear model so that appropriate feedback gains (*K* matrix) are obtained (Morari and Furrer, 2010; Abdullah et al, 2011). The objective of this technique is to ensure stability with a minimum control input (Morari and Furrer, 2010; Rashid and Sidek, 2012). The advantage of this method is that the closed loop gain values required to stabilize the system with a minimum amount of energy can be determined (Rashid and Sidek, 2012). The system performance measure is given by some cost function and is defined in equation (2.15). The optimal control problem is to find a control vector *u* which causes the system (Burns, 2001; Dorf and Bishop, 2011);

$$\dot{x} = g\left(x(t), u(t)\right) \tag{2.16}$$

to follow an optimal trajectory that minimizes the cost function. For LTI systems, equation (2.16) becomes:

$$\dot{x} = Ax + Bu \tag{2.17}$$

A Hamilton-Jacobi equation can be expressed as (Burns, 2001; Dorf and Bishop, 2011):

$$\frac{\partial f}{\partial t} = -\min_{u}\left[h(x,u) + \left(\frac{\partial f}{\partial x}\right)^{T} g(x,u)\right] \tag{2.18}$$

Substituting equations (2.17) and (2.15) into equation (2.18);

$$\frac{\partial f}{\partial t} = -\min_{u}\left[x^{T}Qx + u^{T}Ru + \left(\frac{\partial f}{\partial x}\right)^{T}(Ax + Bu)\right] \tag{2.19}$$

Equation (2.19) is solved if a square matrix P is introduced such that (Burns, 2001; Dorf and Bishop, 2011);

$$f(x,t) = x^{T}Px \tag{2.20}$$

From equation (2.20);

$$\frac{\partial f}{\partial t} = x^T \frac{\partial}{\partial t} Px \tag{2.21}$$

And $$\frac{\partial f}{\partial x} = 2Px \tag{2.22}$$

$$\left[\frac{\partial f}{\partial x}\right] = 2x^T P \tag{2.23}$$

Substituting equations (2.21) and (2.23) into equation (2.19) gives;

$$x^T \frac{\partial}{\partial t} Px = -\min_{u}\left[x^T Qx + u^T Ru + 2x^T P(Ax + Bu)\right] \tag{2.24}$$

The control vector u is minimized from equation (2.24) as follows;

$$\frac{\partial\left(\partial f / \partial t\right)}{\partial u} = 2u^T R + 2x^T PB = 0 \tag{2.25}$$

Substituting equation (2.25) back into equation (2.23) yields;

$$x^T Px = -x^T\left(Q + 2PA - PBR^{-1}B^T P\right)x \tag{2.26}$$

And finally, equation (2.26) becomes;

$$A^T P + PA - PBR^{-1}B^T P + Q = 0 \tag{2.27}$$

Equation (2.27) is called the Algebraic Riccati equation (ARE) and it is used to find the optimal closed-loop control law given by (Carlsson and ÖRBÄCK, 2009; Rashid and Sidek, 2012; Das et al., 2013):

$$u = -Kx \tag{2.28}$$

Where: $$K = R^{-1}B^T P \tag{2.29}$$

K is the optimal feedback gain matrix, and it is used to determine the proper location of the closed loop poles so that the performance index *J* is minimized. Therefore the feedback gain matrix K depends on the matrices A, B, Q, and R. P is a positive definite symmetric matrix and it is found by solving equation (2.27).

2.2.6.2.1 Determination of LQR Weighting Matrices (Q and R)

The design of LQR controller is based on the choice of weighting factors or elements known as weighting matrices (Q and R) (Quanser Manual, 2004, Logan, 2006; Hashim and Ahmed, 2012). These parameters determine largely the relative importance of the individual state variables and input control signal (Rashid and Sidek, 2012). Therefore, weighting matrices Q and R are essential parts of the optimization process using an LQR method as they have a significant effect on the performance of the system (Das et al, 2013). Selection of weighting matrices is absolutely at the discretion of the designer based on the knowledge of the system, the problem involved and the specifications defined (Anderson and Moroe, 1989; Oral et al, 2010).

Since Q matrix defines the relative importance of the state variables and R matrix is used to impose some constraints on the input control signal; then the dimensions of Q and R are given by the sizes of state matrix A and the input control vector u respectively. If there is n number of state variables, then A is a square matrix of dimension nxn and this results in a diagonal matrix Q of equal dimension as A. Similarly, input vector of dimension say mxm results in a diagonal matrix R of equal dimension as u.

$$Q = \begin{pmatrix} Q_{11} & 0 & 0 & 0 & \cdots & 0 \\ 0 & Q_{22} & 0 & 0 & \cdots & 0 \\ 0 & 0 & Q_{33} & 0 & \cdots & 0 \\ 0 & 0 & 0 & Q_{44} & \cdots & 0 \\ \vdots & \vdots & \vdots & \vdots & \ddots & 0 \\ 0 & 0 & 0 & 0 & 0 & Q_{nn} \end{pmatrix} \tag{2.30}$$

$$R = \begin{pmatrix} R_{11} & 0 & 0 & 0 & \cdots & 0 \\ 0 & R_{22} & 0 & 0 & \ldots & 0 \\ 0 & 0 & R_{33} & 0 & \cdots & 0 \\ 0 & 0 & 0 & R_{44} & \cdots & 0 \\ \vdots & \vdots & \vdots & \vdots & \ddots & 0 \\ 0 & 0 & 0 & 0 & 0 & R_{mm} \end{pmatrix} \tag{2.31}$$

If the diagonal elements of the weighting matrices are chosen, the measure of performance (quadratic performance index) is just simply the integral of the weighted square error of the states variable and the control input (Hashim and Ahmed, 2012). It is also important to note that the performance index is always scalar, irrespective of the dimensions of the *Q* and *R* matrices (Hashim and Ahmed, 2012).

There has not been up till now, a universal way of finding the values of the weighting matrices (Oral et al, 2010 and Das et al, 2013). The most common method of finding these weighting elements is the one proposed by Bryson and Ho in 1975 (Oral et al., 2010 and Rashid and Sidek, 2012). The weighting matrices can be written as (Oral et al., 2010 and Rashid and Sidek, 2012):

$$Q_{ii} = \left[x_{i(\max)}{}^{2} \right]^{-1} \tag{2.32}$$

Where i = 1, 2, 3,…n

$$R_{jj} = \left[u_{j(\max)}{}^{2} \right]^{-1} \tag{2.33}$$

Where j = 1, 2, 3,…m

The following are the issues to consider when selecting *Q* and *R* (Prasad et al, 2012).

a. Larger values of Q_{ii} will cause the control signal to reduce values of the state x_i relative to other state and vice-versa

b. If R is large in relation to $\left[{x_{i(\max)}}^2 \right]$, the control will be affluent and hence results in gradual (slow) response.

c. If R is small in relation to $\left[{x_{i(\max)}}^2 \right]$, the control will be easy with a fast response.

However, a typical way of selecting a weighting matrix is to choose Q as the identity matrix:

$$Q = \begin{pmatrix} 1 & 0 & 0 & 0 & \cdots & 0 \\ 0 & 1 & 0 & 0 & \cdots & 0 \\ 0 & 0 & 1 & 0 & \cdots & 0 \\ 0 & 0 & 0 & 1 & \cdots & 0 \\ \vdots & \vdots & \vdots & \vdots & \ddots & 0 \\ 0 & 0 & 0 & 0 & 0 & 1 \end{pmatrix} \tag{2.34}$$

The relative easiness of LQR implementation on multivariable systems (MIMO, SIMO and MISO) and its ability to provide asymptotically stable closed loop response explains its choice in this thesis. And its objective is to ensure that the system outputs (pendulum angles) are regulated to zero (brought to the inverted position) while maintaining closed loop stability. To achieve this, different values of Q are used and system time responses based on these values are analyzed. The set of values of Q that gives the system the best response based on the design specifications (optimal performance) is selected to compute the controller gain matrix (K) and closed loop poles (eigenvalues). Solving the Algebraic Riccati Equation (ARE) analytically for complex system is very tedious, because of the complexity of the matrix computations involved. However, MATLAB provides a simple command *'lqr'* that can perform these computations.

2.2.6.2.2 Linear Controller Design for Inverted Pendulum Systems

Controllers are devices, or software programs that are used to compensate the feedback error for the purpose of achieving the desired system response (Ogata, 2007). The controller's input is the error between the desired and measured system outputs (Kim and Faruqi 2010). A compensated signal based on the error is the controller's output. Generally, the design of the controller involves selecting poles, zeros, and gains (Kim and Faruqi, 2010).

On this note, the implementation of control algorithm for control stabilization of inverted pendulum system is in two folds (Stimac, 1999):

1) **Vertical Position Routine:** In this position, the pendulums are initially at their resting positions hanging downward (natural stable equilibrium). The continuous back and forth movement of the cart along the horizontal track elevates the pendulums to their inverted positions, so that a linear controller can be used to stabilize them. The basic concept here is that the cart is moves in back and forth fashion so that energy is added gradually to the pendulums. In this way, the pendulums will be brought to an inverted position. This therefore means the cart will be subjected to a position control, which then requires a repetitive process to drive the cart to a desired position.

2) **Vertical Stabilization:** Vertical stabilization may be achieved by the use of a linear control algorism based on state feedback control law by solving the algebraic riccati equation (ARE). In this position, the pendulums are made to remain in an upright position without falling over.

2.2.7 Control Solution and Stability

In this section, the concept of control test solution and stability are presented. A detailed but conscience approach to the fundamental theories behind the subject of control and stability with relevant formulations are also given.

2.2.7.1 Controllability and Observability

Before any controller is designed for any system, it is necessary to check and find out if the system has a control solution (Furrer and Gohl 2010; Jarczyk et al 2011). This is done by finding the system controllability and observabilty matrices.

Controllability: A given system is said to be completely state controllable if by means of some control action it can be shifted from any initial state $x(t_0)$ at t_0 to any other final state within a finite time interval (Ogata 2007). This is achieved by finding a controllability matrix given by (Jarczyk et al 2011; Bawek 2012):

$$MC_r = \left[B \vdots AB \vdots \cdots \vdots A^{n-1}B \right] \tag{2.35}$$

such that MC_r is a nonsingular matrix with n linearly independent column vectors.

Where: A is represents the state variable matrix, B the state input matrix and n defines the dimension of the state matrix A. The state controllable if the controllability matrix (MC_r) is of full rank. This means that is its rank equals the dimension of A (i.e. MC_r is nonsingular).

Observability: A system is said to be completely state observable at a time t_0 if it is possible to find its state from the observation of its output within a given finite time interval (Ogata, 2007). The observability is found if the obsevability matrix given by (Ogata 2007; Jansson and Klempic, 2012):

$$MC_o = \left[C^T \vdots A^T C^T \vdots \cdots \vdots A^{T(n-1)} C^T \right] \quad (2.36)$$

is nonsingular with n linearly independent column vectors.

Where: *A* is the state input matrix, *C* is the output state matrix and *n* is the dimension of the state matrix. For a system to be completely state observable, the observability matrix (MC_o) must be of full rank (i.e. its rank must be equal the dimension of *A*) (Ogata, 2007).

2.2.7.2 Concept of Stability

The ultimate goal of any control system design is stability (Dorf and Bishop, 2011). An unstable system has no practical implication from the control point of view. Most dynamic systems are described by their input/output relationships based on transfer function or matrix (Dorf and Bishop, 2011). Such systems are stable if all bounded inputs they generate bounded outputs. This is known as “bounded-input bounded-output (BIBO) stability” (Gu et al., 2013). BIBO stability may be explained in terms of location of poles (roots of the characteristics equation) for a linear time-invariant system that has been modeled by a transfer function matrix (Gu et al., 2013). BIBO stability is determined by the presence all the poles of the transfer function in the open-left-half complex plane (i.e. with negative real part). For a system described in state space, the concept of asymptotic stability is assumed. For a linear time-invariant system described in state space, it is asymptotically stable if and only if all the eigenvalues of the state matrix *A* are in the open-left-half complex plane (i.e. with negative real part) (Gu et al., 2013). Generally, a system that is asymptotically stable is also BIBO stable, but not vice versa (Gu et al., 2013).

2.2.8 MATLAB and Simulink

MATLAB stands for MATrix LABoratory. It was initially developed to simplify matrix computations using matrix software developed by the LINPACK (linear system package) and EISPACK (Eigen system package) projects (Mathwork MATLAB® 12). MATLAB is a high level language for scientific and technical computations (Mathwork MATLAB® 12). It incorporates computation, visualization, and programming environment. In addition, MATLAB is a modern programming language environment with advanced data structures that contains in-built tools for editing and debugging program syntax; and also supports object-oriented programming (Mathwork MATLAB® 12). These features make MATLAB a very good tool for teaching and research.

Simulation of Dynamic Systems has been over the years proven to be immensely useful when it comes to control design, saving time and money that would otherwise be spent in prototyping a physical system. Simulink is software that is integrated into the MATLAB (Mathwork MATLAB® 12). Simulink is a tool used to program a dynamic system (systems described by Differential equations) pictorially (Mathwork MATLAB® 12). It has a library that contains standard building blocks used for building logic circuits or a control system. Furthermore, various toolboxes are also available for different applications, such as Neural Networks, Fuzzy Logic, DSP, Statistics etc. (Mathwork MATLAB® 12).

2.3 Review of Similar Works

This section will deal with the review of some literatures on works carried out the in area of modeling, control and stabilization of the inverted pendulum system.

Quintero (2001) discussed the strategies involved in swinging up and balancing of an inverted pendulum. The modeled equation was derived from the pendulum energy. The stabilization was achieved by:

i. Two controllers that used digital linear quadratic regulator (LQR) based on the linearized model of the system about upright position.
ii. Use of relays with hysteresis to establish smooth transition between the two controllers.

The central idea of the paper was to investigate the nonlinear dynamics of an inverted pendulum. The main drawback was the difficulty in consolidating the two controllers. However, the use of LQR controller yielded satisfactory performance in terms of quadratic cost function reduction.

Bogdanov (2004) carried out an investigative study of the performance of different number of control algorithms for a double inverted pendulum. In the report, optimal control problem in minimizing a quadratic cost function was considered. Combinations of Linear Quadratic Regulator (LQR) and State Dependent Riccati Equation (SDRE) or Artificial Neural Network controllers were simulated. The results of the simulation showed that:

i. SDRE had a potential advantage over LQR design, but with higher recovery region (maximum pendulum deflection from which the control forces the pendulum to equilibrium position).
ii. Better performance when optimization was done directly using NN, but with the same recovery region as LQR.

iii. The combined NN with LQR or with SDRE gave both large recovery region and better performance.

In control theory however, all control designs are better enhanced for optimal performance when limited number of control authority is considered. Although the paper showed that optimal performance could be improved when different controllers were combined, no limits were imposed on the magnitude of the control force in all simulations.

Lam and Davison (2006) studied the stabilizablity robustness properties of a multilink inverted pendulum system, by arbitrarily decreasing the real stabilizablity radius of the system. It was established that a linearized n-link system was both controllable and observable but with no practical controller because of the small stabilizability radius. However, when an n-torque was applied at various n-links, the stabilization difficulty was alleviated. Even though, the paper proved the possibility of stabilizing an n-link inverted pendulum system, the position of a cart was not taken into consideration (the cart was assumed fixed); and this may affect the overall stability of the system.

Giraldo (2008) designed an LQR controller using MAPLE for the stabilization of triple and quadruple inverted pendulum systems with a view to demonstrating in simple and precise manner, the solutions to some abstract ideas associated with control in system dynamics. But the work, however, limited the complexity and mathematical modeling to four links systems only.

Lee and Perkins (2008) investigated and compared the control performances of LQR and Q-learning algorithms in the stabilization of a triple inverted pendulum. The LQR controller was found to be more accurate in terms of cost function minimization, and was able to balance the system given certain constraints, while Q-learning was not successful as a result of system constraints. Although, the LQR controller successfully stabilized the system but it was limited to four degrees of freedom and small angle approximation.

Kwon and Hodgins (2010) presented an approach to constructing a control system for human running using inverted pendulum. The performance of the system was looked into and the performance index was minimized for the adjustment of set of parameters in order to make the motion much more natural and robust. The paper is centered around analysis of a reference motion data sequence for information extraction on human running mechanism using an LQR controller for an inverted pendulum. The placement of the foot was used by the control system for balance recovery. Arms motions or upper-body motions are used by humans to help recover balance. The approach in question lacked robustness; because the control mechanism is based on a single inverted pendulum. However, the use of a more complex model (multilink inverted pendulum) in the design of the controller may yield better performance and improve robustness thereby allowing motion to be integrated into the upper body.

Application of mobile inverted pendulum to Boxingbots for a Boxing Game was presented by **G. Lee et al (2009).** The Boxingbot was implemented and controlled by two different controllers: Two PID controllers were used as primary controllers; one for the pendulum angle and other for the cart position. The other controller was an intelligent controller (Neural Network controller based on reference compensation technique (RCT) implemented on a DSP chip) and was used as a secondary controller to compensate for the degradation of the Boxingbot performance under uncertainty conditions (i.e. robustness against external disturbance such as bits from opponent Boxingbot or friction). Looking closely at the problem at hand from the optimal control point of view, PID controller could not yield optimal solution to the problem since it is not an optimal controller. However, replacing the PID controller with more robust optimal controllers like LQR, LQT or LQG will yield better performance. In this way, the optimal controller (primary controller) together with the secondary controller (RCT) embedded on the DSP chip board can work quite well in providing past learning algorithm to improve both balancing of the pendulum and tracking of the Boxingbot.

Marholt and Gazdoš (2010) modeled, identified and simulated an inverted pendulum PS600. The modeled equation was implemented into MATLAB/Simulink environment and its properties were compared with the real system. The control was implemented using a proportional derivative (PID) controller; and yielded conformity between the mathematical model and the real system. However, the performance indices of the control variables were not taken into consideration when a conventional PID controller was used.

Kowalczy et al, (2012) developed a model dynamics of human balancing mechanism using a switched system based on feedback control. The human postural balancing in an upright position was successfully modeled using a single-link inverted pendulum. The balance was achieved by altering the time delay in muscle activation and neural transmission using proportional derivative (PD) algorithm. However, two issues were not adequately addressed:

1. Optimal performance: - limiting the control strategy to PD controller will not provide optimal solution to the control problem in question (balancing mechanism).
2. The model did not fully represent the human postural mechanism since it was based on a single-link inverted pendulum.

If the model could be based on a multilink-inverted pendulum, the dynamics of postural balancing would have been more realistic.

Prasad et al (2012) carried out a comparative analysis of PID and LQR control algorithms on a single inverted pendulum. The two controllers were developed based on the linear state space model of the equivalent nonlinear dynamics of the system. Simulation was performed with measurable system variable parameters in a MATLAB/Simulink control tool box. The results of simulation showed that both the controllers based on the two approaches stabilized the pendulum around the vicinity of an upright position. The results also showed a comparative advantage of LQR over PID because of its optimal performance. The analysis presented in the paper is however limited to a single inverted pendulum which could not be extended to precisely model the dynamics of a system having more than two degrees of freedom (such as a humanoid robot; Colin and Thomas (2010).

Singh and Yadav (2012) developed a model for an optimal control of a double inverted pendulum using an LQR controller. The control mechanism for the system was successfully achieved. The nonlinear equations representing the double inverted pendulum were linearized using small angle approximation. The implication of such approach however, is that the conformity between the nonlinear and linear model is not always guaranteed; and that the model was limited to only two-links system.

Jadlovska and Sarnovky (2013) presented a general approach to solving classical and rotary inverted pendulum systems by building a customized block library within the MATALB/Simulink library. The developed library was used to solve an arbitrary n-link inverted pendulum system and validated with the single and double inverted pendulum models reported in literature. However, there have been evidences of the experimental stabilization of the triple and quad inverted pendulum systems reported in literature (Li et al., 2002, Li et al., 2004 and Zhang et al., 2012). The vailidity of the model could have been further extended to these pendulum systems in order to justfy the efficacy of the control library developed.

Most of the existing works on inverted pendulum reviewed in this work are limited to maximum five degrees of freedom (quadruple inverted pendulum including cart position). However, the possibility of extending the study to a multi-link inverted pendulum system has been proposed by Lam and Davison (2006). In order to explore the possibility of developing a linear model of a muli-link inverted pendulum system, this work tries to model a double-quad inverted pendulum system. A linear control algorithm (LQR) will be used to implement control stabilization of the system about an upright position.

CHAPTER THREE

DESIGN METHODOLOGY

3.1 Introduction

In this chapter, procedures leading to the development of the mathematical model of DQIP and LQR controller designed as outlined in the methodology are presented. The mathematical model is derived from the first principle based on Lagrangian formulation. The model is be validated by extracting the model of the QIP and the resulting extracted model is compared with similar models reported in literatures.

3.2 Mathematical Modeling of the Nonlinear DQIP System

The development of the mathematical model of DQIP requires that the physical parameters making the system are defined. These parameters are described in Table 3.1.

Table 3.1 Description of the DQIP Parameters

Parameter	**Description**	**Unit**
m_0	Mass of the Cart	kg
m_n	Mass of the n-th pendulum link (n = 1, 2, 3, …, 8)	kg
l_n	Length of the n-th pendulum link from the pivot point to its center of mass	m
L_n	Length of the n-th pendulum link	m
θ_n	Angular displacement of the n-th pendulum link with respect to the vertical axis	rad
I_n	Moment of inertia of the n-th pendulum link with respect to its center of mass	kgm^2
X	Position of the cart along the horizontal track	m
U	Applied horizontal control force	N
$K.E$	Kinetic energy	J
$P.E$	Potential energy	J
L	Lagarangian function	J
μ_0	Frictional Coefficient between the Cart and the Horizontal Track	kgm^2
μ_n	Frictional Coefficient between of the various nth pivot pendulum joints (n = 1, 2, 3,…,8)	Nsm^{-1}
g	gravitational constant	$kgms^{-2}$

In order to reduce the complexity of the mathematical modeling, the effect of the surrounding wind is neglected (Li et al, 2002; Bogdanov, 2004).

The dynamic equations of the system can be derived by vector resolution of the vector components of velocity and displacement as shown in the free body diagram of the system Figure 3.1 (see Appendix A1 for the details of the derivation).

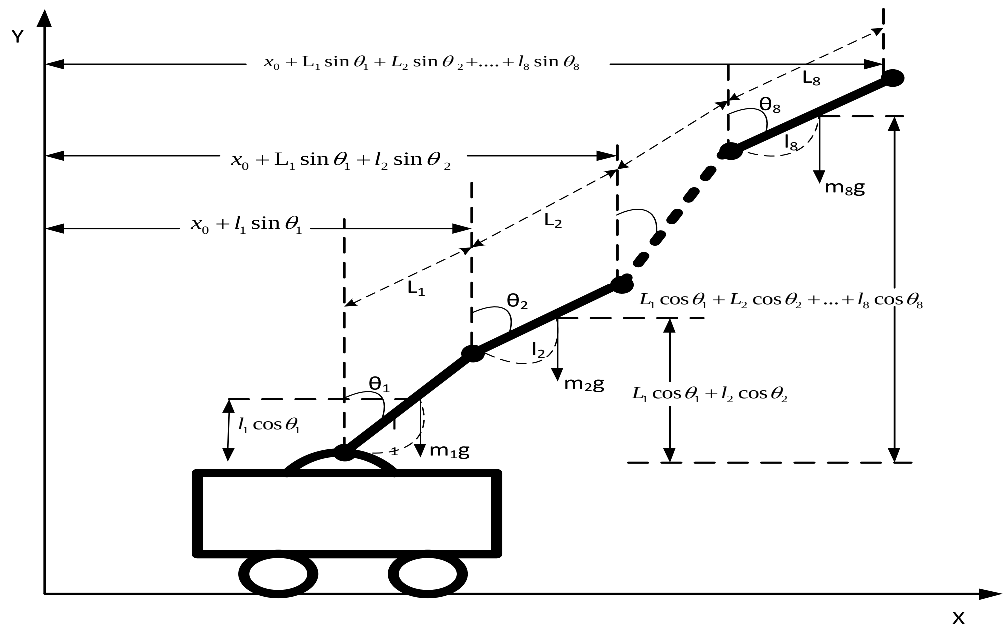

Figure 3.1 Free body Diagram of the Double Quad Inverted Pendulum System.

The kinetic and potential energies of the system (DQIP) are given by the sum of energies of its individual components (wheeled cart and eight pendulum links) (Bogdanov, 2004).

$$K.E_T = \sum_{n=0}^{8} K.E_n \tag{3.1}$$

$$P.E_T = \sum_{n=0}^{8} P.E_n \tag{3.2}$$

Where $K.E_T$ is the total kinetic energy and $P.E_T$ is the total potential energy of the system including the wheeled cart and the pendulums.

Using equations (3.1) and (3.2), the total kinetic energy of the DQIP is given by:

$$
\begin{aligned}
&\sum_{n=1}^{8} K.E_n = \frac{1}{2}a_0\,\dot{x} + \frac{1}{2}a_1\,\dot{\theta}_1^2 + \frac{1}{2}a_2\,\dot{\theta}_2^2 + \frac{1}{2}a_3\,\dot{\theta}_3^2 + \frac{1}{2}a_4\,\dot{\theta}_4^2 + \frac{1}{2}a_5\,\dot{\theta}_5^2 + \frac{1}{2}a_6\,\dot{\theta}_6^2 + \frac{1}{2}a_7\,\dot{\theta}_7^2 + \frac{1}{2}a_8\,\dot{\theta}_8^2 + \\
&b_0\,\dot{x}\,\dot{\theta}_1\cos\theta_1 + b_1\,\dot{x}\,\dot{\theta}_2\cos\theta_2 + b_2\,\dot{x}\,\dot{\theta}_3\cos\theta_3 + b_3\,\dot{x}\,\dot{\theta}_4\cos\theta_4 + b_4\,\dot{x}\,\dot{\theta}_5\cos\theta_5 + b_5\,\dot{x}\,\dot{\theta}_6\cos\theta_6 + b_6\,\dot{x}\,\dot{\theta}_7\cos\theta_7 + \\
&b_7\,\dot{x}\,\dot{\theta}_8\cos\theta_8 + b_1L_1\,\dot{\theta}_1\,\dot{\theta}_2\cos(\theta_1-\theta_2) + L_1b_2\,\dot{\theta}_1\,\dot{\theta}_3\cos(\theta_1-\theta_3) + L_1b_3\,\dot{\theta}_1\,\dot{\theta}_4\cos(\theta_1-\theta_4) + \\
&L_1b_4\,\dot{\theta}_1\,\dot{\theta}_5\cos(\theta_1-\theta_5) + L_1b_5\,\dot{\theta}_1\,\dot{\theta}_6\cos(\theta_1-\theta_6) + L_1b_6\,\dot{\theta}_1\,\dot{\theta}_7\cos(\theta_1-\theta_7) + L_1b_7\,\dot{\theta}_1\,\dot{\theta}_8\cos(\theta_1-\theta_8) + \\
&L_2b_2\,\dot{\theta}_2\,\dot{\theta}_3\cos(\theta_2-\theta_3) + L_2b_3\,\dot{\theta}_2\,\dot{\theta}_4\cos(\theta_2-\theta_4) + L_2b_4\,\dot{\theta}_2\,\dot{\theta}_5\cos(\theta_2-\theta_5) + L_2b_5\,\dot{\theta}_2\,\dot{\theta}_6\cos(\theta_2-\theta_6) + \\
&L_2b_6\,\dot{\theta}_2\,\dot{\theta}_7\cos(\theta_2-\theta_7) + L_2b_7\,\dot{\theta}_2\,\dot{\theta}_8\cos(\theta_2-\theta_8) + L_3b_3\,\dot{\theta}_3\,\dot{\theta}_4\cos(\theta_3-\theta_4) + L_3b_4\,\dot{\theta}_3\,\dot{\theta}_5\cos(\theta_3-\theta_5) + \\
&L_3b_5\,\dot{\theta}_3\,\dot{\theta}_6\cos(\theta_3-\theta_6) + L_3b_6\,\dot{\theta}_3\,\dot{\theta}_7\cos(\theta_3-\theta_7) + L_3b_7\,\dot{\theta}_3\,\dot{\theta}_7\cos(\theta_3-\theta_8) + L_4b_4\,\dot{\theta}_4\,\dot{\theta}_5\cos(\theta_4-\theta_5) + \\
&L_4b_5\,\dot{\theta}_4\,\dot{\theta}_6\cos(\theta_4-\theta_6) + L_4b_6\,\dot{\theta}_4\,\dot{\theta}_7\cos(\theta_4-\theta_7) + L_4b_7\,\dot{\theta}_4\,\dot{\theta}_8\cos(\theta_4-\theta_8) + L_5b_5\,\dot{\theta}_5\,\dot{\theta}_6\cos(\theta_5-\theta_6) + \\
&L_5b_6\,\dot{\theta}_5\,\dot{\theta}_7\cos(\theta_5-\theta_7) + L_5b_7\,\dot{\theta}_5\,\dot{\theta}_8\cos(\theta_5-\theta_8) + L_6b_6\,\dot{\theta}_6\,\dot{\theta}_7\cos(\theta_6-\theta_7) + L_6b_7\,\dot{\theta}_6\,\dot{\theta}_8\cos(\theta_6-\theta_8) + \\
&L_7b_7\,\dot{\theta}_7\,\dot{\theta}_8\cos(\theta_7-\theta_8)
\end{aligned}
\tag{3.3}
$$

The potential energy of the system is completely determined by the angular displacement of the pendulum, since the wheeled cart only move in the horizontal direction. Thus the potential energy of the cart is zero.

$$
\begin{aligned}
&\sum_{n=1}^{8} P.E_n = b_0g\cos\theta_1 + b_1g\cos\theta_2 + b_2g\cos\theta_3 + b_3g\cos\theta_4 + b_4g\cos\theta_5 + b_5g\cos\theta_6 + b_6g\cos\theta_7 \\
&+b_7g\cos\theta_8
\end{aligned}
\tag{3.4}
$$

Equations (3.3) and (3.4) are the total kinetic and potential energies of the DQIP system respectively (see appendix A for the details of the derivation).

Where a_i (i = 0, 1, 2,… 8) and b_j (j = 0, 1, 2, …, 7) are used to replace the coefficients of the variables $(x, \theta_n \; and \; \dot{x}, \dot{\theta}_n)$. (Details of Derivation is given in Appendix A1).

The Lagrangian function, L that describes the dynamics of the DQIP as indicated by equation (2.3) is obtained by the difference between equations (3.3) and (3.4);

$$
\begin{aligned}
L &= \frac{1}{2}a_0\dot{x} + \frac{1}{2}a_1\dot{\theta}_1^2 + \frac{1}{2}a_2\dot{\theta}_2^2 + \frac{1}{2}a_3\dot{\theta}_3^2 + \frac{1}{2}a_4\dot{\theta}_4^2 + \frac{1}{2}a_5\dot{\theta}_5^2 + \frac{1}{2}a_6\dot{\theta}_6^2 + \frac{1}{2}a_7\dot{\theta}_7^2 + \frac{1}{2}a_8\dot{\theta}_8^2 + \\
& b_0\dot{x}\dot{\theta}_1\cos\theta_1 + b_1\dot{x}\dot{\theta}_2\cos\theta_2 + b_2\dot{x}\dot{\theta}_3\cos\theta_3 + b_3\dot{x}\dot{\theta}_4\cos\theta_4 + b_4\dot{x}\dot{\theta}_5\cos\theta_5 + b_5\dot{x}\dot{\theta}_6\cos\theta_6 + b_6\dot{x}\dot{\theta}_7\cos\theta_7 + \\
& b_7\dot{x}\dot{\theta}_8\cos\theta_8 + b_1L_1\dot{\theta}_1\dot{\theta}_2\cos(\theta_1-\theta_2) + L_1b_2\dot{\theta}_1\dot{\theta}_3\cos(\theta_1-\theta_3) + L_1b_3\dot{\theta}_1\dot{\theta}_4\cos(\theta_1-\theta_4) + \\
& L_1b_4\dot{\theta}_1\dot{\theta}_5\cos(\theta_1-\theta_5) + L_1b_5\dot{\theta}_1\dot{\theta}_6\cos(\theta_1-\theta_6) + L_1b_6\dot{\theta}_1\dot{\theta}_7\cos(\theta_1-\theta_7) + L_1b_7\dot{\theta}_1\dot{\theta}_8\cos(\theta_1-\theta_8) + \\
& L_2b_2\dot{\theta}_2\dot{\theta}_3\cos(\theta_2-\theta_3) + L_2b_3\dot{\theta}_2\dot{\theta}_4\cos(\theta_2-\theta_4) + L_2b_4\dot{\theta}_2\dot{\theta}_5\cos(\theta_2-\theta_5) + L_2b_5\dot{\theta}_2\dot{\theta}_6\cos(\theta_2-\theta_6) + \\
& L_2b_6\dot{\theta}_2\dot{\theta}_7\cos(\theta_2-\theta_7) + L_2b_7\dot{\theta}_2\dot{\theta}_8\cos(\theta_2-\theta_8) + L_3b_3\dot{\theta}_3\dot{\theta}_4\cos(\theta_3-\theta_4) + L_3b_4\dot{\theta}_3\dot{\theta}_5\cos(\theta_3-\theta_5) + \\
& L_3b_5\dot{\theta}_3\dot{\theta}_6\cos(\theta_3-\theta_6) + L_3b_6\dot{\theta}_3\dot{\theta}_7\cos(\theta_3-\theta_7) + L_3b_7\dot{\theta}_3\dot{\theta}_7\cos(\theta_3-\theta_8) + L_4b_4\dot{\theta}_4\dot{\theta}_5\cos(\theta_4-\theta_5) + \\
& L_4b_5\dot{\theta}_4\dot{\theta}_6\cos(\theta_4-\theta_6) + L_4b_6\dot{\theta}_4\dot{\theta}_7\cos(\theta_4-\theta_7) + L_4b_7\dot{\theta}_4\dot{\theta}_8\cos(\theta_4-\theta_8) + L_5b_5\dot{\theta}_5\dot{\theta}_6\cos(\theta_5-\theta_6) + \\
& L_5b_6\dot{\theta}_5\dot{\theta}_7\cos(\theta_5-\theta_7) + L_5b_7\dot{\theta}_5\dot{\theta}_8\cos(\theta_5-\theta_8) + L_6b_6\dot{\theta}_6\dot{\theta}_7\cos(\theta_6-\theta_7) + L_6b_7\dot{\theta}_6\dot{\theta}_8\cos(\theta_6-\theta_8) + \\
& L_7b_7\dot{\theta}_7\dot{\theta}_8\cos(\theta_7-\theta_8) - b_0g\cos\theta_1 + b_1g\cos\theta_2 + b_2g\cos\theta_3 + b_3g\cos\theta_4 + b_4g\cos\theta_5 + b_5g\cos\theta_6 + b_6g\cos\theta_7 \\
& + b_7g\cos\theta_8
\end{aligned}
\tag{3.5}
$$

The energy of the DQIP system (both cart and pendulum links) due to friction is given by Raleigh function and this describes the frictional (viscous) force within the system (Li et al, 2002; Jadlovska and Sarnovsky, 2011).

$$F_0 = \frac{1}{2}\mu_0\dot{x}^2 \tag{3.6}$$

$$F_n = \frac{1}{2}\mu_n\left(\dot{\theta}_n - \dot{\theta}_{n-1}\right)^2 \tag{3.7}$$

F_0 is the energy due to friction between the cart and the surface track. F_n is the energy due to friction at the various nth pivot pendulum joints. μ_0 and μ_n are the coefficient of friction of the cart and the pendulums respectively.

Applying the Euler-Lagrange equation of motion to the cart position and the pendulum angles, the Lagrangian function, L described by equation (3.5) gives the resultant nonlinear dynamic equations that represent the double-quad inverted pendulum (DQIP) are as follows:

Non-linear dynamic equation of motion for the cart position is given by;

$$\frac{d}{dt}\left(\frac{\partial L}{\partial \dot{x}}\right) - \frac{\partial L}{\partial x} + \frac{\partial F}{\partial \dot{x}} = \psi \text{ , } (\psi = u) \tag{3.8}$$

Non-linear dynamic equation of motions for the pendulum angles is given by;

$$\frac{d}{dt}\left(\frac{\partial L}{\partial \dot{\theta}_n}\right) - \frac{\partial L}{\partial \theta_n} + \frac{\partial F_n}{\partial \dot{\theta}_n} = \psi \tag{3.9}$$

(θ_n = 1, 2, 3, .., 8. $\psi = 0$, since the control force u was only applied to the cart)

Based on equations (3.8) and (3.9), the nonlinear equations that describe the dynamics of the double quad inverted pendulum (DQIP) are as follows:

$$\begin{aligned} & a_0\ddot{x} + b_0 \cos\theta_1\ddot{\theta}_1 + b_1 \cos\theta_2\ddot{\theta}_2 + b_2 \cos\theta_3\ddot{\theta}_3 + b_2 \cos\theta_3\ddot{\theta}_3 + b_3 \cos\theta_4\ddot{\theta}_4 + b_4 \cos\theta_5\ddot{\theta}_5 + b_5 \cos\theta_6\ddot{\theta}_6 + \\ & b_6 \cos\theta_7\ddot{\theta}_7 + b_7 \cos\theta_8\ddot{\theta}_8 + \mu_0\dot{x} - b_0\dot{\theta}_1 \sin\theta_1(\dot{\theta}_1) - b_1\dot{\theta}_2 \sin\theta_2(\dot{\theta}_2) - b_2\dot{\theta}_3 \sin\theta_3(\dot{\theta}_3) - b_3\dot{\theta}_4 \sin\theta_4(\dot{\theta}_4) - \\ & b_4\dot{\theta}_5 \sin\theta_5(\dot{\theta}_5) - b_5\dot{\theta}_6 \sin\theta_6(\dot{\theta}_6) - b_6\dot{\theta}_7 \sin\theta_7(\dot{\theta}_7) - b_7\dot{\theta}_8 \sin\theta_8(\dot{\theta}_8) = u \end{aligned} \tag{3.10}$$

$$\begin{aligned} & b_0\cos\theta_1\ddot{x} + a_1\ddot{\theta}_1 + L_1b_1\cos(\theta_1-\theta_2)\ddot{\theta}_2 + L_1b_2\cos(\theta_1-\theta_3)\ddot{\theta}_3 + L_1b_3\cos(\theta_1-\theta_4)\ddot{\theta}_4 + L_1b_4\cos(\theta_1-\theta_5)\ddot{\theta}_5 + \\ & L_1b_5\cos(\theta_1-\theta_6)\ddot{\theta}_6 + L_1b_6\cos(\theta_1-\theta_7)\ddot{\theta}_7 + L_1b_7\cos(\theta_1-\theta_8)\ddot{\theta}_8 + (\mu_1+\mu_2)\dot{\theta}_1 + (L_1b_1\dot{\theta}_2\sin(\theta_1-\theta_2) - \mu_2)\dot{\theta}_2 + \\ & L_1b_2\dot{\theta}_3\sin(\theta_1-\theta_3)\dot{\theta}_3 + L_1b_3\dot{\theta}_4\sin(\theta_1-\theta_4)\dot{\theta}_4 + L_1b_4\dot{\theta}_5\sin(\theta_1-\theta_5)\dot{\theta}_5 + L_1b_5\dot{\theta}_6\sin(\theta_1-\theta_6)\dot{\theta}_6 + L_1b_6\dot{\theta}_7\sin(\theta_1-\theta_7)\dot{\theta}_7 + \\ & L_1b_7\dot{\theta}_8\sin(\theta_1-\theta_8)\dot{\theta}_8 - b_0 g\sin\theta_1 = 0 \end{aligned} \tag{3.11}$$

$$\begin{aligned} & b_1\cos\theta_2\ddot{x} + L_1b_1\cos(\theta_1-\theta_2)\ddot{\theta}_1 + a_2\ddot{\theta}_2 + L_2b_2\cos(\theta_2-\theta_3)\ddot{\theta}_3 + L_2b_3\cos(\theta_2-\theta_4)\ddot{\theta}_4 + L_2b_4\cos(\theta_2-\theta_5)\ddot{\theta}_5 + \\ & L_2b_5\cos(\theta_2-\theta_6)\ddot{\theta}_6 + L_2b_6\cos(\theta_2-\theta_7)\ddot{\theta}_7 + L_2b_7\cos(\theta_2-\theta_8)\ddot{\theta}_8 - (L_1b_1\dot{\theta}_1\sin(\theta_1-\theta_2) + \mu_2)\dot{\theta}_1 + (\mu_2+\mu_3)\dot{\theta}_2 + \\ & (L_2b_2\dot{\theta}_3\sin(\theta_2-\theta_3) - \mu_3)\dot{\theta}_3 + L_2b_3\dot{\theta}_4\sin(\theta_2-\theta_4)\dot{\theta}_4 + L_2b_4\dot{\theta}_5\sin(\theta_2-\theta_5)\dot{\theta}_5 + L_2b_5\dot{\theta}_6\sin(\theta_2-\theta_6)\dot{\theta}_6 + \\ & L_2b_6\dot{\theta}_7\sin(\theta_2-\theta_7)\dot{\theta}_7 + L_2b_7\dot{\theta}_8\sin(\theta_2-\theta_8)\dot{\theta}_8 - b_1 g\sin\theta_2 = 0 \end{aligned} \tag{3.12}$$

$$\begin{aligned}
&b_2 \cos\theta_3 \ddot{x} + L_1 b_2 \cos(\theta_1-\theta_3)\ddot{\theta}_1 + L_2 b_2 \cos(\theta_2-\theta_3)\ddot{\theta}_2 + a_3\ddot{\theta}_3 + L_3 b_3 \cos(\theta_3-\theta_4)\ddot{\theta}_4 + L_3 b_4 \cos(\theta_3-\theta_5)\ddot{\theta}_5 + \\
&L_3 b_5 \cos(\theta_3-\theta_6)\ddot{\theta}_6 + L_3 b_6 \cos(\theta_3-\theta_7)\ddot{\theta}_7 + L_3 b_7 \cos(\theta_3-\theta_8)\ddot{\theta}_8 - L_1 b_2\dot{\theta}_1 \sin(\theta_1-\theta_3)\dot{\theta}_1 - (L_2 b_2 \dot{\theta}_2 \sin(\theta_2-\theta_3)+\mu_3)\dot{\theta}_2 + \\
&(\mu_3+\mu_4)\dot{\theta}_3 + (L_3 b_3\dot{\theta}_4 \sin(\theta_3-\theta_4)-\mu_4)\dot{\theta}_4 + L_3 b_4\dot{\theta}_5 \sin(\theta_3-\theta_5)\dot{\theta}_5 + L_3 b_5\dot{\theta}_6 \sin(\theta_3-\theta_6)\dot{\theta}_6 + L_3 b_6\dot{\theta}_7 \sin(\theta_3-\theta_7)\dot{\theta}_7 + \\
&L_3 b_7\dot{\theta}_8 \sin(\theta_3-\theta_8)\dot{\theta}_8 - b_2 g \sin\theta_3 = 0
\end{aligned} \tag{3.13}$$

$$\begin{aligned}
&b_3 \cos\theta_4 \ddot{x} + L_1 b_3 \cos(\theta_1-\theta_4)\ddot{\theta}_1 + L_2 b_3 \cos(\theta_2-\theta_4)\ddot{\theta}_2 + L_3 b_3 \cos(\theta_3-\theta_4)\ddot{\theta}_3 + a_4\ddot{\theta}_4 + L_4 b_4 \cos(\theta_4-\theta_5)\ddot{\theta}_5 + \\
&L_4 b_5 \cos(\theta_4-\theta_6)\ddot{\theta}_6 + L_4 b_6 \cos(\theta_4-\theta_7)\ddot{\theta}_7 + L_4 b_7 \cos(\theta_4-\theta_8)\ddot{\theta}_8 - L_1 b_3\dot{\theta}_1 \sin(\theta_1-\theta_4)\dot{\theta}_1 - L_2 b_3\dot{\theta}_2 \sin(\theta_2-\theta_4)\dot{\theta}_2 - \\
&(L_3 b_3\dot{\theta}_3 \sin(\theta_3-\theta_4)+\mu_4)\dot{\theta}_3 + (\mu_4+\mu_5)\dot{\theta}_4 + (L_4 b_4\dot{\theta}_5 \sin(\theta_4-\theta_5)-\mu_5)\dot{\theta}_5 + L_4 b_5\dot{\theta}_6 \sin(\theta_4-\theta_6)\dot{\theta}_6 + \\
&L_4 b_6\dot{\theta}_7 \sin(\theta_4-\theta_7)\dot{\theta}_7 + L_4 b_7\dot{\theta}_8 \sin(\theta_4-\theta_8)\dot{\theta}_8 - b_3 g \sin\theta_4 = 0
\end{aligned} \tag{3.14}$$

$$\begin{aligned}
&b_4 \cos\theta_5 \ddot{x} + L_1 b_4 \cos(\theta_1-\theta_5)\ddot{\theta}_1 + L_2 b_4 \cos(\theta_2-\theta_5)\ddot{\theta}_2 + L_3 b_4 \cos(\theta_3-\theta_5)\ddot{\theta}_3 + L_4 b_4 \cos(\theta_4-\theta_5)\ddot{\theta}_4 + a_5\ddot{\theta}_5 + \\
&L_5 b_5 \cos(\theta_5-\theta_6)\ddot{\theta}_6 + L_5 b_6 \cos(\theta_5-\theta_7)\ddot{\theta}_7 + L_5 b_7 \cos(\theta_5-\theta_8)\ddot{\theta}_8 - L_1 b_4\dot{\theta}_1 \sin(\theta_1-\theta_5)\dot{\theta}_1 - L_2 b_4\dot{\theta}_2 \sin(\theta_2-\theta_5)\dot{\theta}_2 - \\
&L_3 b_4\dot{\theta}_3 \sin(\theta_3-\theta_5)\dot{\theta}_3 - (L_4 b_4\dot{\theta}_4 \sin(\theta_4-\theta_5)+\mu_5)\dot{\theta}_4 + (\mu_5+\mu_6)\dot{\theta}_5 + (L_5 b_5\dot{\theta}_6 \sin(\theta_5-\theta_6)-\mu_6)\dot{\theta}_6 + \\
&L_5 b_6\dot{\theta}_7 \sin(\theta_5-\theta_7)\dot{\theta}_7 + L_5 b_7\dot{\theta}_8 \sin(\theta_5-\theta_8)\dot{\theta}_8 - b_4 g \sin\theta_5 = 0
\end{aligned} \tag{3.15}$$

$$\begin{aligned}
&b_5 \cos\theta_6 \ddot{x} + L_1 b_5 \cos(\theta_1-\theta_6)\ddot{\theta}_1 + L_2 b_5 \cos(\theta_2-\theta_6)\ddot{\theta}_2 + L_3 b_5 \cos(\theta_3-\theta_6)\ddot{\theta}_3 + L_4 b_5 \cos(\theta_4-\theta_6)\ddot{\theta}_4 + \\
&L_5 b_5 \cos(\theta_5-\theta_6)\ddot{\theta}_5 + a_6\ddot{\theta}_6 + L_6 b_6 \cos(\theta_6-\theta_7)\ddot{\theta}_7 + L_6 b_7 \cos(\theta_6-\theta_8)\ddot{\theta}_8 - L_1 b_5\dot{\theta}_1 \sin(\theta_1-\theta_6)\dot{\theta}_1 - \\
&L_2 b_5\dot{\theta}_2 \sin(\theta_2-\theta_6)\dot{\theta}_2 - L_3 b_5\dot{\theta}_3 \sin(\theta_3-\theta_6)\dot{\theta}_3 - L_4 b_5\dot{\theta}_4 \sin(\theta_4-\theta_6)\dot{\theta}_4 - (L_5 b_5\dot{\theta}_5 \sin(\theta_5-\theta_6)+\mu_6)\dot{\theta}_5 + \\
&(\mu_6+\mu_7)\dot{\theta}_6 + (L_6 b_6\dot{\theta}_7 \sin(\theta_6-\theta_7)-\mu_7)\dot{\theta}_7 + L_6 b_7\dot{\theta}_8 \sin(\theta_6-\theta_8)\dot{\theta}_8 - b_5 g \sin\theta_6 = 0
\end{aligned} \tag{3.16}$$

$$\begin{aligned}
&b_6 \cos\theta_7 \ddot{x} + L_1 b_6 \cos(\theta_1-\theta_7)\ddot{\theta}_1 + L_2 b_6 \cos(\theta_2-\theta_7)\ddot{\theta}_2 + L_3 b_6 \cos(\theta_3-\theta_7)\ddot{\theta}_3 + L_4 b_6 \cos(\theta_4-\theta_7)\ddot{\theta}_4 + \\
&L_5 b_6 \cos(\theta_5-\theta_7)\ddot{\theta}_5 + L_6 b_6 \cos(\theta_6-\theta_7)\ddot{\theta}_6 + a_7\ddot{\theta}_7 + L_7 b_7 \cos(\theta_7-\theta_8)\ddot{\theta}_8 - L_1 b_6\dot{\theta}_1 \sin(\theta_1-\theta_7)\dot{\theta}_1 - \\
&L_2 b_6\dot{\theta}_2 \sin(\theta_2-\theta_7)\dot{\theta}_2 - L_3 b_6\dot{\theta}_3 \sin(\theta_3-\theta_7)\dot{\theta}_3 - L_4 b_6\dot{\theta}_4 \sin(\theta_4-\theta_7)\dot{\theta}_4 - L_5 b_6\dot{\theta}_5 \sin(\theta_5-\theta_7)\dot{\theta}_5 - \\
&(L_6 b_6\dot{\theta}_6 \sin(\theta_6-\theta_7)+\mu_7)\dot{\theta}_6 + (\mu_7+\mu_8)\dot{\theta}_7 + (L_7 b_7\dot{\theta}_8 \sin(\theta_7-\theta_8)-\mu_8)\dot{\theta}_8 - b_6 g \sin\theta_7 = 0
\end{aligned} \tag{3.17}$$

$$\begin{aligned}
&b_7 \cos\theta_8 \ddot{x} + L_1 b_7 \cos(\theta_1-\theta_8)\ddot{\theta}_1 + L_2 b_7 \cos(\theta_2-\theta_8)\ddot{\theta}_2 + L_3 b_7 \cos(\theta_3-\theta_8)\ddot{\theta}_3 + L_4 b_7 \cos(\theta_4-\theta_8)\ddot{\theta}_4 + \\
&L_5 b_7 \cos(\theta_5-\theta_8)\ddot{\theta}_5 + L_6 b_7 \cos(\theta_6-\theta_8)\ddot{\theta}_6 + L_7 b_7 \cos(\theta_7-\theta_8)\ddot{\theta}_7 + a_8\ddot{\theta}_8 - L_1 b_7\dot{\theta}_1 \sin(\theta_1-\theta_8)\dot{\theta}_1 - \\
&L_2 b_7\dot{\theta}_2 \sin(\theta_2-\theta_8)\dot{\theta}_2 - L_3 b_7\dot{\theta}_3 \sin(\theta_3-\theta_8)\dot{\theta}_3 - L_4 b_7\dot{\theta}_4 \sin(\theta_4-\theta_8)\dot{\theta}_4 - L_5 b_7\dot{\theta}_5 \sin(\theta_5-\theta_8)\dot{\theta}_5 - \\
&L_6 b_7\dot{\theta}_6 \sin(\theta_6-\theta_8)\dot{\theta}_6 - (L_7 b_7\dot{\theta}_7 \sin(\theta_7+\theta_8)+\mu_8)\dot{\theta}_7 + \mu_8\dot{\theta}_8 - b_7 g \sin\theta_8 = 0
\end{aligned} \tag{3.18}$$

Equations (3.10) to (3.18) can be written in a single line equation in matrix form given by equation (3.19)

$$M(x,\theta)\left(\ddot{x}\ddot{\theta}\right) + N((x,\theta),(\dot{x},\dot{\theta}))\left(\dot{x}\dot{\theta}\right) + D(x,\theta) + Gu \tag{3.19}$$

(See Appendix A1 for details of derivation).

Where:

$$M(x,\theta)=\begin{pmatrix}
a_0 & b_0\cos\theta_1 & b_1\cos\theta_2 & b_2\cos\theta_3 & b_3\cos\theta_4 & b_4\cos\theta_5 & b_5\cos\theta_6 & b_6\cos\theta_7 & b_7\cos\theta_8 \\
b_0\cos\theta_1 & a_1 & L_1b_1\cos(\theta_1-\theta_2) & L_1b_2\cos(\theta_1-\theta_3) & L_1b_3\cos(\theta_1-\theta_4) & L_1b_4\cos(\theta_1-\theta_5) & L_1b_5\cos(\theta_1-\theta_6) & L_1b_6\cos(\theta_1-\theta_7) & L_1b_7\cos(\theta_1-\theta_8) \\
b_1\cos\theta_2 & L_1b_1\cos(\theta_1-\theta_2) & a_2 & L_2b_2\cos(\theta_2-\theta_3) & L_2b_3\cos(\theta_2-\theta_4) & L_2b_4\cos(\theta_2-\theta_5) & L_2b_5\cos(\theta_2-\theta_6) & L_2b_6\cos(\theta_2-\theta_7) & L_2b_7\cos(\theta_2-\theta_8) \\
b_2\cos\theta_3 & L_1b_2\cos(\theta_1-\theta_3) & L_2b_2\cos(\theta_2-\theta_3) & a_3 & L_3b_3\cos(\theta_3-\theta_4) & L_3b_4\cos(\theta_3-\theta_5) & L_3b_5\cos(\theta_3-\theta_6) & L_3b_6\cos(\theta_3-\theta_7) & L_3b_7\cos(\theta_3-\theta_8) \\
b_3\cos\theta_4 & L_1b_3\cos(\theta_1-\theta_4) & L_2b_3\cos(\theta_2-\theta_4) & L_3b_3\cos(\theta_3-\theta_4) & a_4 & L_4b_4\cos(\theta_4-\theta_5) & L_4b_5\cos(\theta_4-\theta_6) & L_4b_6\cos(\theta_4-\theta_7) & L_4b_7\cos(\theta_4-\theta_8) \\
b_4\cos\theta_5 & L_1b_4\cos(\theta_1-\theta_5) & L_2b_4\cos(\theta_2-\theta_5) & L_3b_4\cos(\theta_3-\theta_5) & L_4b_4\cos(\theta_4-\theta_5) & a_5 & L_5b_5\cos(\theta_5-\theta_6) & L_5b_6\cos(\theta_5-\theta_7) & L_5b_7\cos(\theta_5-\theta_8) \\
b_5\cos\theta_6 & L_1b_5\cos(\theta_1-\theta_6) & L_2b_5\cos(\theta_2-\theta_6) & L_3b_5\cos(\theta_3-\theta_6) & L_4b_5\cos(\theta_4-\theta_6) & L_5b_5\cos(\theta_5-\theta_6) & a_6 & L_6b_6\cos(\theta_6-\theta_7) & L_6b_7\cos(\theta_6-\theta_8) \\
b_6\cos\theta_7 & L_1b_6\cos(\theta_1-\theta_7) & L_2b_6\cos(\theta_2-\theta_7) & L_3b_6\cos(\theta_3-\theta_7) & L_4b_6\cos(\theta_4-\theta_7) & L_5b_6\cos(\theta_5-\theta_7) & L_6b_6\cos(\theta_6-\theta_7) & a_7 & L_7b_7\cos(\theta_7-\theta_8) \\
b_7\cos\theta_8 & L_1b_7\cos(\theta_1-\theta_8) & L_2b_7\cos(\theta_2-\theta_8) & L_3b_7\cos(\theta_3-\theta_8) & L_4b_7\cos(\theta_4-\theta_8) & L_5b_7\cos(\theta_5-\theta_8) & L_6b_7\cos(\theta_6-\theta_8) & L_7b_7\cos(\theta_7-\theta_8) & a_8
\end{pmatrix} \tag{3.20}$$

$$N((x,\theta),(\dot{x},\dot{\theta}))=\begin{pmatrix}
\mu_0 & -b_0\dot{\theta}_1\sin\theta_1 & -b_1\dot{\theta}_2\sin\theta_2 & -b_2\dot{\theta}_3\sin\theta_3 & -b_3\dot{\theta}_4\sin\theta_4 & -b_4\dot{\theta}_5\sin\theta_5 & -b_5\dot{\theta}_6\sin\theta_6 & -b_6\dot{\theta}_7\sin\theta_7 & -b_7\dot{\theta}_8\sin\theta_8 \\
0 & \mu_1+\mu_2 & L_1b_1\dot{\theta}_2\sin(\theta_1-\theta_2)-\mu_2 & L_1b_2\dot{\theta}_3\sin(\theta_1-\theta_3) & L_1b_3\dot{\theta}_4\sin(\theta_1-\theta_4) & L_1b_4\dot{\theta}_5\sin(\theta_1-\theta_5) & L_1b_5\dot{\theta}_6\sin(\theta_1-\theta_6) & L_1b_6\dot{\theta}_7\sin(\theta_1-\theta_7) & L_1b_7\dot{\theta}_8\sin(\theta_1-\theta_8) \\
0 & -L_1b_1\dot{\theta}_1\sin(\theta_1-\theta_2)-\mu_2 & \mu_2+\mu_3 & L_2b_2\dot{\theta}_3\sin(\theta_2-\theta_3)-\mu_3 & L_2b_3\dot{\theta}_4\sin(\theta_2-\theta_4) & L_2b_4\dot{\theta}_5\sin(\theta_2-\theta_5) & L_2b_5\dot{\theta}_6\sin(\theta_2-\theta_6) & L_2b_6\dot{\theta}_7\sin(\theta_2-\theta_7) & L_2b_7\dot{\theta}_8\sin(\theta_2-\theta_8) \\
0 & -L_1b_2\dot{\theta}_1\sin(\theta_1-\theta_3) & -L_2b_2\dot{\theta}_2\sin(\theta_2-\theta_3)-\mu_3 & \mu_3+\mu_4 & L_3b_3\dot{\theta}_4\sin(\theta_3-\theta_4)-\mu_4 & L_3b_4\dot{\theta}_5\sin(\theta_3-\theta_5) & L_3b_5\dot{\theta}_6\sin(\theta_3-\theta_6) & L_3b_6\dot{\theta}_7\sin(\theta_3-\theta_7) & L_3b_7\dot{\theta}_8\sin(\theta_3-\theta_8) \\
0 & -L_1b_3\dot{\theta}_1\sin(\theta_1-\theta_4) & -L_2b_3\dot{\theta}_2\sin(\theta_2-\theta_4) & -L_3b_3\dot{\theta}_3\sin(\theta_3-\theta_4)-\mu_4 & \mu_4+\mu_5 & L_4b_4\dot{\theta}_5\sin(\theta_4-\theta_5)-\mu_5 & L_4b_5\dot{\theta}_6\sin(\theta_4-\theta_6) & L_4b_6\dot{\theta}_7\sin(\theta_4-\theta_7) & L_4b_7\dot{\theta}_8\sin(\theta_4-\theta_8) \\
0 & -L_1b_4\dot{\theta}_1\sin(\theta_1-\theta_5) & -L_2b_4\dot{\theta}_2\sin(\theta_2-\theta_5) & -L_3b_4\dot{\theta}_3\sin(\theta_3-\theta_5) & -L_4b_4\dot{\theta}_4\sin(\theta_4-\theta_5)-\mu_5 & \mu_5+\mu_6 & L_5b_5\dot{\theta}_6\sin(\theta_5-\theta_6)-\mu_6 & L_5b_6\dot{\theta}_7\sin(\theta_5-\theta_7) & L_5b_7\dot{\theta}_8\sin(\theta_5-\theta_8) \\
0 & -L_1b_5\dot{\theta}_1\sin(\theta_1-\theta_6) & -L_2b_5\dot{\theta}_2\sin(\theta_2-\theta_6) & -L_3b_5\dot{\theta}_3\sin(\theta_3-\theta_6) & -L_4b_5\dot{\theta}_4\sin(\theta_4-\theta_6) & -L_5b_5\dot{\theta}_5\sin(\theta_5-\theta_6)-\mu_6 & \mu_6+\mu_7 & L_6b_6\dot{\theta}_7\sin(\theta_6-\theta_7)-\mu_7 & L_6b_7\dot{\theta}_8\sin(\theta_6-\theta_8) \\
0 & -L_1b_6\dot{\theta}_1\sin(\theta_1-\theta_7) & -L_2b_6\dot{\theta}_2\sin(\theta_2-\theta_7) & -L_3b_6\dot{\theta}_3\sin(\theta_3-\theta_7) & -L_4b_6\dot{\theta}_4\sin(\theta_4-\theta_7) & -L_5b_6\dot{\theta}_5\sin(\theta_5-\theta_7) & -L_6b_6\dot{\theta}_6\sin(\theta_6-\theta_7)-\mu_7 & \mu_7+\mu_8 & L_7b_7\dot{\theta}_8\sin(\theta_7-\theta_8)-\mu_8 \\
0 & -L_1b_7\dot{\theta}_1\sin(\theta_1-\theta_8) & -L_2b_7\dot{\theta}_2\sin(\theta_2-\theta_8) & -L_3b_7\dot{\theta}_3\sin(\theta_3-\theta_8) & -L_4b_7\dot{\theta}_4\sin(\theta_4-\theta_8) & -L_5b_7\dot{\theta}_5\sin(\theta_5-\theta_8) & -L_6b_7\dot{\theta}_6\sin(\theta_6-\theta_8) & -L_7b_7\dot{\theta}_7\sin(\theta_7-\theta_8)-\mu_7 & \mu_8
\end{pmatrix} \tag{3.21}$$

$$D(x,\theta) = \begin{pmatrix} 0 \\ -b_0 g\sin\theta_1 \\ -b_1 g\sin\theta_2 \\ -b_2 g\sin\theta_3 \\ -b_3 g\sin\theta_4 \\ -b_4 g\sin\theta_5 \\ -b_5 g\sin\theta_6 \\ -b_6 g\sin\theta_7 \\ -b_7 g\sin\theta_8 \end{pmatrix} = \begin{pmatrix} 0 & 0 & 0 & 0 & 0 & 0 & 0 & 0 & 0 \\ 0 & -b_0 & 0 & 0 & 0 & 0 & 0 & 0 & 0 \\ 0 & 0 & -b_1 & 0 & 0 & 0 & 0 & 0 & 0 \\ 0 & 0 & 0 & -b_2 & 0 & 0 & 0 & 0 & 0 \\ 0 & 0 & 0 & 0 & b_3 & 0 & 0 & 0 & 0 \\ 0 & 0 & 0 & 0 & 0 & b_4 & 0 & 0 & 0 \\ 0 & 0 & 0 & 0 & 0 & 0 & b_5 & 0 & 0 \\ 0 & 0 & 0 & 0 & 0 & 0 & 0 & -b_6 & 0 \\ 0 & 0 & 0 & 0 & 0 & 0 & 0 & 0 & -b_7 \end{pmatrix} \times \begin{pmatrix} x \\ \sin\theta_1 \\ \sin\theta_2 \\ \sin\theta_3 \\ \sin\theta_4 \\ \sin\theta_5 \\ \sin\theta_6 \\ \sin\theta_7 \\ \sin\theta_8 \end{pmatrix} g \tag{3.22}$$

And
$$G = \begin{pmatrix} 1 \\ 0 \\ 0 \\ 0 \\ 0 \\ 0 \\ 0 \\ 0 \\ 0 \end{pmatrix} \tag{3.23}$$

Replacing the generalized co-ordinates of equation (3.19) with a single parameter β, the equation is further simplified as;

$$M(\beta)\left(\ddot{\beta}\right) + N(\beta,\dot{\beta})\left(\dot{\beta}\right) + D(\beta) = Gu \tag{3.24}$$

Where $\beta = (x, \theta)$

To make the control implementation easier, the system dynamic equations represented in a compact form by equation (3.24) is reformulated into 18th *(9x9)* order system of ordinary differential equation (Christoper et al., 2012; Jadlosvka and Sarnovsky, 2012; Jadlovska and Sarnovsk, 2013).

In order to achieve this, a state vector Z ϵ R^{18} such that $Z = (\beta, \dot{\beta})^T$ is used. Dropping the dependencies and their derivatives of the generalized co-ordinates $(\beta, \dot{\beta})$ in the system matrix, the dynamic equation (3.24) is written as;

$$M\ddot{\beta} + N\dot{\beta} + D\beta = Gu \tag{3.25}$$

$$\dot{Z} = \begin{pmatrix} 0_{9x9} & I_{9x9} \\ 0_{9x9} & -M^{-1}N \end{pmatrix} Z + \begin{pmatrix} 0_{9x1} \\ -M^{-1}D \end{pmatrix} + \begin{pmatrix} 0_{9x1} \\ M^{-1}G \end{pmatrix} u \tag{3.26}$$

Equation (3.26) represents a compact nonlinear state space dynamics of the DQIP.

3.2.1 Linear Equivalent Model of the DQIP

The central idea of this thesis is to design a linear controller (LQR) that can stabilize the DQIP around an upright unstable equilibrium position. The control policy is achieved when the nonlinear equation that describes the dynamics of the DQIP represented by equation (3.26) is linearized about an upright position ($\theta = 0$). Before proceeding with further analysis that could lead to the design and implementation of LQR controller, equation (3.26) must be linearized about an operating point. Two equilibrium points are identified:

1. $\theta_n = 0$ (unstable position when the pendulum is pointing vertically upward)
2. $\theta_n = \pi$ (stable position when the pendulum is pointing vertically downward)

There would have been no need of trying to implement control techniques if the pendulums were in their inherent stable equilibrium position ($\theta_n = \pi$). Therefore, the problem at hand is to balance the pendula system in an upright unstable equilibrium position ($\theta_n = 0$).

By means of Taylor's Series expansion and Jacobian Matrix transformation with small angle approximation, equation (3.26) is linearized about:

$$Z = 0\left((\beta, \dot{\beta})^T = (x, \theta)^T = (0,0)^T\right) \tag{3.27}$$

That is θ is very small and approaching zero. This yields an equivalent linear equation of the form:

$$\dot{Z} = \begin{pmatrix} 0_{9x9} & I_{9x9} \\ -M^{-1}(0)\dfrac{\partial D(0)}{\partial \theta} & -M^{-1}(0)N(0) \end{pmatrix} Z + \begin{pmatrix} 0_{9x1} \\ M^{-1}(0)G \end{pmatrix} u \tag{3.28}$$

(Details of linearization are provided in Appendix A1)

Equation (3.30) is the approximate linear equation of the nonlinear dynamics of the double quad inverted pendulum in an open-loop configuration (without the controller) represented in a State Space form. Recall that the state space equations of any linear time-invariant system are given by (Dorf, 2011):

$$\dot{x} = Ax + Bu \tag{3.29}$$

$$y = Cx + Du \tag{3.30}$$

Equations (3.29) and (3.30) represent input and output state equations respectively. Comparing equation (3.28) with equation (3.29), equation (3.29) becomes;

$$\dot{Z} = AZ + Bu \tag{3.31}$$

Since the external disturbance is assumed negligible, then the state space output equation will be;

$$y = CZ\,,\ (D = 0) \tag{3.32}$$

Where A represents the state transition matrix, B is the input matrix, C is the output matrix, D is the direct transition matrix known as a disturbance matrix and Z is the variable state vector. u and y are the input and output vectors respectively.

Where $$A = \begin{pmatrix} 0_{9x9} & I_{9x9} \\ -M^{-1}(0)\dfrac{\partial D(0)}{\partial \theta} & -M^{-1}(0)N(0) \end{pmatrix} \tag{3.33}$$

And $$B = \begin{pmatrix} 0_{9x1} \\ M^{-1}(0)G \end{pmatrix} \tag{3.34}$$

$$M(0) = \begin{pmatrix} a_0 & b_0 & b_1 & b_2 & b_3 & b_4 & b_5 & b_6 & b_7 \\ b_0 & a_1 & L_1b_1 & L_1b_2 & L_1b_3 & L_1b_4 & L_1b_5 & L_1b_6 & L_1b_7 \\ b_1 & L_1b_1 & a_2 & L_2b_2 & L_2b_3 & L_2b_4 & L_2b_5 & L_2b_6 & L_2b_7 \\ b_2 & L_1b_2 & L_2b_2 & a_3 & L_3b_3 & L_3b_4 & L_3b_5 & L_3b_6 & L_3b_7 \\ b_3 & L_1b_3 & L_2b_3 & L_3b_3 & a_4 & L_4b_4 & L_4b_5 & L_4b_6 & L_4b_7 \\ b_4 & L_1b_4 & L_2b_4 & L_3b_4 & L_4b_4 & a_5 & L_5b_5 & L_5b_6 & L_5b_7 \\ b_5 & L_1b_5 & L_2b_5 & L_3b_5 & L_4b_5 & L_5b_5 & a_6 & L_6b_6 & L_6b_7 \\ b_6 & L_1b_6 & L_2b_6 & L_3b_6 & L_4b_6 & L_5b_6 & L_6b_6 & a_7 & L_7b_7 \\ b_7 & L_1b_7 & L_2b_7 & L_3b_7 & L_4b_7 & L_5b_7 & L_6b_7 & L_7b_7 & a_8 \end{pmatrix} \tag{3.35}$$

$$\frac{\partial D(0)}{\partial \theta} = \begin{pmatrix} 0 & 0 & 0 & 0 & 0 & 0 & 0 & 0 & 0 \\ 0 & -b_0 & 0 & 0 & 0 & 0 & 0 & 0 & 0 \\ 0 & 0 & -b_1 & 0 & 0 & 0 & 0 & 0 & 0 \\ 0 & 0 & 0 & -b_2 & 0 & 0 & 0 & 0 & 0 \\ 0 & 0 & 0 & 0 & b_3 & 0 & 0 & 0 & 0 \\ 0 & 0 & 0 & 0 & 0 & b_4 & 0 & 0 & 0 \\ 0 & 0 & 0 & 0 & 0 & 0 & b_5 & 0 & 0 \\ 0 & 0 & 0 & 0 & 0 & 0 & 0 & -b_6 & 0 \\ 0 & 0 & 0 & 0 & 0 & 0 & 0 & 0 & -b_7 \end{pmatrix} \times g \tag{3.36}$$

$$
N(0) = \begin{pmatrix}
\mu_0 & 0 & 0 & 0 & 0 & 0 & 0 & 0 & 0 \\
0 & \mu_1 + \mu_2 & -\mu_2 & 0 & 0 & 0 & 0 & 0 & 0 \\
0 & -\mu_2 & \mu_2 + \mu_3 & -\mu_3 & 0 & 0 & 0 & 0 & 0 \\
0 & 0 & -\mu_3 & \mu_3 + \mu_4 & -\mu_4 & 0 & 0 & 0 & 0 \\
0 & 0 & 0 & -\mu_4 & \mu_4 + \mu_5 & -\mu_5 & 0 & 0 & 0 \\
0 & 0 & 0 & 0 & -\mu_5 & \mu_5 + \mu_6 & -\mu_6 & 0 & 0 \\
0 & 0 & 0 & 0 & 0 & -\mu_6 & \mu_6 + \mu_7 & -\mu_7 & 0 \\
0 & 0 & 0 & 0 & 0 & 0 & -\mu_7 & \mu_7 + \mu_8 & -\mu_8 \\
0 & 0 & 0 & 0 & 0 & 0 & 0 & -\mu_7 & \mu_8
\end{pmatrix} \tag{3.37}
$$

The DQIP system is an under actuated mechanical system, because a single control signal is used to control nine degrees of freedom (the position of the cart and the eight pendulum angles). Therefore, to balance the system (DQIP) in an upright position, nine output state variables are considered (position of the cart and the eight pendulum angles). The output state space equation is, therefore given by:

$$
y = \begin{pmatrix}
1 & 0 & 0 & 0 & 0 & 0 & 0 & 0 & 0 & 0 & 0 & 0 & 0 & 0 & 0 & 0 & 0 & 0 \\
0 & 1 & 0 & 0 & 0 & 0 & 0 & 0 & 0 & 0 & 0 & 0 & 0 & 0 & 0 & 0 & 0 & 0 \\
0 & 0 & 1 & 0 & 0 & 0 & 0 & 0 & 0 & 0 & 0 & 0 & 0 & 0 & 0 & 0 & 0 & 0 \\
0 & 0 & 0 & 1 & 0 & 0 & 0 & 0 & 0 & 0 & 0 & 0 & 0 & 0 & 0 & 0 & 0 & 0 \\
0 & 0 & 0 & 0 & 1 & 0 & 0 & 0 & 0 & 0 & 0 & 0 & 0 & 0 & 0 & 0 & 0 & 0 \\
0 & 0 & 0 & 0 & 0 & 1 & 0 & 0 & 0 & 0 & 0 & 0 & 0 & 0 & 0 & 0 & 0 & 0 \\
0 & 0 & 0 & 0 & 0 & 0 & 1 & 0 & 0 & 0 & 0 & 0 & 0 & 0 & 0 & 0 & 0 & 0 \\
0 & 0 & 0 & 0 & 0 & 0 & 0 & 1 & 0 & 0 & 0 & 0 & 0 & 0 & 0 & 0 & 0 & 0 \\
0 & 0 & 0 & 0 & 0 & 0 & 0 & 0 & 1 & 0 & 0 & 0 & 0 & 0 & 0 & 0 & 0 & 0
\end{pmatrix} \times \begin{pmatrix}
x \\ \theta_1 \\ \theta_2 \\ \theta_3 \\ \theta_4 \\ \theta_5 \\ \theta_6 \\ \theta_7 \\ \theta_8 \\ \dot{x} \\ \dot{\theta}_1 \\ \dot{\theta}_2 \\ \dot{\theta}_3 \\ \dot{\theta}_4 \\ \dot{\theta}_5 \\ \dot{\theta}_6 \\ \dot{\theta}_7 \\ \dot{\theta}_8
\end{pmatrix} Z \tag{3.38}
$$

3.3 Tests for Control Solution on DQIP

In order to verify the viability of the developed linear model of the DQIP, numerical values of the state variables and state input matrices (*A* and *B*) must be found. The linear model can better be represented if these values are found by physical measurement on simple DQIP prototype or physical experimentation or using verified or verifiable data. Simulation approach based on the data Table 3.2 is adopted here. Table 3.2 is a replication of the experimental data used by Li et al., 2002; Zhang et al., 2012 for QIP system.

Table 3.2 Simulation Parameters for the DQIP

Parameter	Cart	First Pendulum	Second Pendulum	Third Pendulum	Fourth Pendulum	Fifth Pendulum	Sixth Pendulum	Seventh Pendulum	Eighth Pendulum
Mass (kg)	1.3282	0.2200	0.2200	0.2200	0.2200	0.2200	0.2200	0.2200	0.1870
Frictional Coefficient (kgm^2/Nsm^{-1})	22.914	0.0049	0.0049	0.0049	0.0049	0.0049	0.0049	0.0049	0.004824
Length (m)	0.5	0.5	0.5	0.5	0.5	0.5	0.5	0.5	0.7
$g = 9.81ms^{-2}$									

Based on equations (3.33), (3.34), (3.35), (3.36), (3.37) and (3.38) and the data in Table 3.2, the state model matrices of the DQIP *A*, *B*, *C* and *D* are determined as follows (see Appendix B2 for details of numerical computations):

$$A=\begin{bmatrix}
0 & 0 & 0 & 0 & 0 & 0 & 0 & 0 & 0 & 1 & 0 & 0 & 0 & 0 & 0 & 0 & 0 & 0 \\
0 & 0 & 0 & 0 & 0 & 0 & 0 & 0 & 0 & 0 & 1 & 0 & 0 & 0 & 0 & 0 & 0 & 0 \\
0 & 0 & 0 & 0 & 0 & 0 & 0 & 0 & 0 & 0 & 0 & 1 & 0 & 0 & 0 & 0 & 0 & 0 \\
0 & 0 & 0 & 0 & 0 & 0 & 0 & 0 & 0 & 0 & 0 & 0 & 1 & 0 & 0 & 0 & 0 & 0 \\
0 & 0 & 0 & 0 & 0 & 0 & 0 & 0 & 0 & 0 & 0 & 0 & 0 & 1 & 0 & 0 & 0 & 0 \\
0 & 0 & 0 & 0 & 0 & 0 & 0 & 0 & 0 & 0 & 0 & 0 & 0 & 0 & 1 & 0 & 0 & 0 \\
0 & 0 & 0 & 0 & 0 & 0 & 0 & 0 & 0 & 0 & 0 & 0 & 0 & 0 & 0 & 1 & 0 & 0 \\
0 & 0 & 0 & 0 & 0 & 0 & 0 & 0 & 0 & 0 & 0 & 0 & 0 & 0 & 0 & 0 & 1 & 0 \\
0 & 0 & 0 & 0 & 0 & 0 & 0 & 0 & 0 & 0 & 0 & 0 & 0 & 0 & 0 & 0 & 0 & 1 \\
0 & -14.4522 & 3.3456 & -0.7553 & 0.1646 & -0.0340 & 0.0064 & -0.0010 & 0.0001 & -16.4652 & 0.0175 & -0.0059 & 0.0016 & -0.0004 & 0.0001 & -0.0000 & 0.0000 & -0.0000 \\
0 & 268.4901 & -262.4517 & 59.2492 & -12.9085 & 2.6642 & -0.5021 & 0.0802 & -0.0089 & 41.7540 & -0.3832 & 0.2414 & -0.1232 & 0.0330 & -0.0088 & 0.0024 & -0.0006 & 0.0001 \\
0 & -303.7826 & 524.5893 & -287.1826 & 62.5680 & -12.9135 & 2.4339 & -0.3888 & 0.0429 & -11.1879 & 0.5000 & -0.4823 & 0.3787 & -0.1599 & 0.0429 & -0.0115 & 0.0031 & -0.0007 \\
0 & 81.3984 & -340.8615 & 459.6791 & -237.3634 & 48.9899 & -9.2333 & 1.4748 & -0.1629 & 2.9978 & -0.1924 & 0.3787 & -0.5191 & 0.3886 & -0.1626 & 0.0437 & -0.0118 & 0.0025 \\
0 & -21.8109 & 91.3349 & -291.9297 & 374.8035 & -183.0460 & 34.4995 & -5.5106 & 0.6087 & -0.8033 & 0.0516 & -0.1599 & 0.3886 & -0.5218 & 0.3894 & -0.1633 & 0.0442 & -0.0095 \\
0 & 5.8454 & -24.4779 & 78.2376 & -237.6866 & 288.8320 & -128.7646 & 20.5676 & -2.2719 & 0.2153 & -0.0138 & 0.0429 & -0.1626 & 0.3894 & -0.5224 & 0.3911 & -0.1651 & 0.0353 \\
0 & -1.5705 & 6.5766 & -21.0206 & 63.8607 & -183.5580 & 203.9168 & -76.7597 & 8.4790 & -0.0578 & 0.0037 & -0.0115 & 0.0437 & -0.1633 & 0.3911 & -0.5286 & 0.3980 & -0.1318 \\
0 & 0.4367 & -1.8286 & 5.8447 & -17.7564 & 51.0381 & -133.6188 & 127.5494 & -31.6440 & 0.0161 & -0.0010 & 0.0032 & -0.0121 & 0.0454 & -0.1694 & 0.4141 & -0.5542 & 0.2737 \\
0 & -0.1094 & 0.4583 & -1.4648 & 4.4502 & -12.7915 & 33.4884 & -71.7973 & 47.7609 & -0.0040 & 0.0003 & -0.0008 & 0.0030 & -0.0114 & 0.0425 & -0.1585 & 0.3723 & -0.2473
\end{bmatrix} \tag{3.39}$$

$$\boldsymbol{B}=\begin{bmatrix} 0 \\ 0 \\ 0 \\ 0 \\ 0 \\ 0 \\ 0 \\ 0 \\ 0 \\ 0.7185 \\ -1.8221 \\ 0.4882 \\ -0.1308 \\ 0.0351 \\ -0.0094 \\ 0.0025 \\ -0.0007 \\ 0.0002 \end{bmatrix} \tag{3.40}$$

$$C = \begin{pmatrix} 1 & 0 & 0 & 0 & 0 & 0 & 0 & 0 & 0 & 0 & 0 & 0 & 0 & 0 & 0 & 0 & 0 & 0 \\ 0 & 1 & 0 & 0 & 0 & 0 & 0 & 0 & 0 & 0 & 0 & 0 & 0 & 0 & 0 & 0 & 0 & 0 \\ 0 & 0 & 1 & 0 & 0 & 0 & 0 & 0 & 0 & 0 & 0 & 0 & 0 & 0 & 0 & 0 & 0 & 0 \\ 0 & 0 & 0 & 1 & 0 & 0 & 0 & 0 & 0 & 0 & 0 & 0 & 0 & 0 & 0 & 0 & 0 & 0 \\ 0 & 0 & 0 & 0 & 1 & 0 & 0 & 0 & 0 & 0 & 0 & 0 & 0 & 0 & 0 & 0 & 0 & 0 \\ 0 & 0 & 0 & 0 & 0 & 1 & 0 & 0 & 0 & 0 & 0 & 0 & 0 & 0 & 0 & 0 & 0 & 0 \\ 0 & 0 & 0 & 0 & 0 & 0 & 1 & 0 & 0 & 0 & 0 & 0 & 0 & 0 & 0 & 0 & 0 & 0 \\ 0 & 0 & 0 & 0 & 0 & 0 & 0 & 1 & 0 & 0 & 0 & 0 & 0 & 0 & 0 & 0 & 0 & 0 \\ 0 & 0 & 0 & 0 & 0 & 0 & 0 & 0 & 1 & 0 & 0 & 0 & 0 & 0 & 0 & 0 & 0 & 0 \end{pmatrix} \tag{3.41}$$

$$D = 0 \tag{3.42}$$

Control test solution was carried out to determine the controllability and observability status of the DQIP before LQR controller was designed for it. The MATLAB codes used for these tests are:

```
MCr = ctrb(A, B);
MCo = obsv(A, C);
CONTR = rank(MCr)
OBSVB = rank(MCo)
if rank(MCr)==size(A)
    'THE SYSTEM IS CONTROLLABLE'
else 'THE SYSTEM IS NOT CONTROLLABLE'
end
    if rank(MCo)==size(A)
        'THE SYSTEM IS OBSERVABLE'
    else 'THE SYSTEM IS NOT OBSERVABLE'
    end
>> CONTR = 13

ans =

THE SYSTEM IS NOT CONTROLLABLE

>> OBSVB = 17

ans =

THE SYSTEM IS NOT OBSERVABLE
```

It can be concluded from these tests that the controllability and observabilty matrices are not of full ranks and hence the system is not controllable and obervable.

3.4 DQIP Model Verification

Before the controller was designed and implemented on the linear model of the DQIP, the validity of the model was first verified. Therefore, a basis must be established in order to justify the correctness of the model developed. Careful study of the various inverted pendulum models reveals the presence of some repetitive terms and replications in the models parameters. A single inverted pendulum model can be extracted from the model of the double inverted. Similarly the model of the double inverted pendulum can be extracted from the model of the quad inverted pendulum (Bogdanov, 2004; Giraldo, 2008). By implication, this means the QIP model could be extracted from the model of the DQIP. A typical QIP is as shown in Figure 3.2.

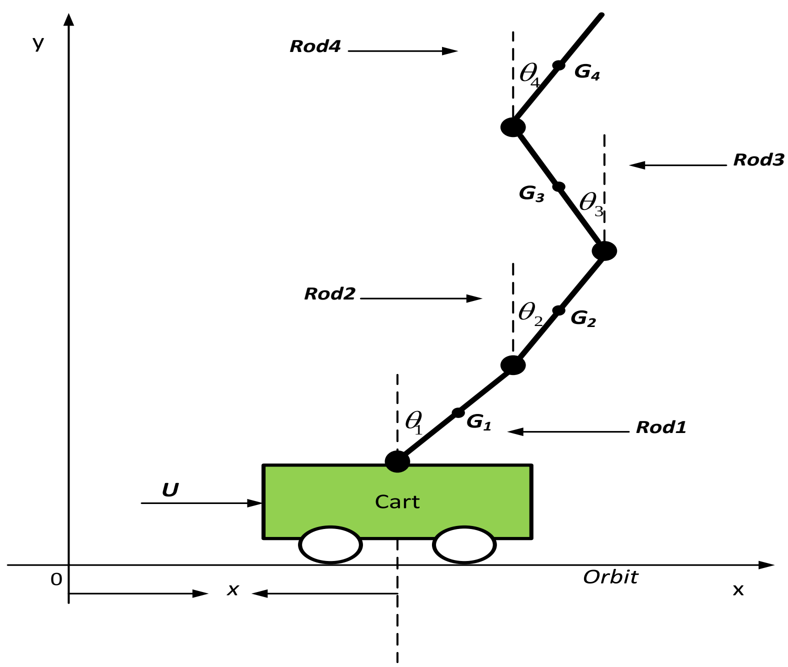

Figure 3.2 Structure of the QIP (Zhang et al, 2012)

The model of the QIP is obtained from the DQIP model by truncating the mathematical modeling at the fourth link (refer to Appendix A2 for the details). The truncated non-linear model equations of the QIP are given by equations (3.43) to (3.47).

$$a_0\ddot{x}+b_0\cos\theta_1\ddot{\theta}_1+b_1\cos\theta_2\ddot{\theta}_2+b_2\cos\theta_3\ddot{\theta}_3+b_2\cos\theta_3\ddot{\theta}_3+b_3\cos\theta_4\ddot{\theta}_4+\mu_0\dot{x}-b_0\dot{\theta}_1\sin\theta_1(\dot{\theta}_1)-b_1\dot{\theta}_2\sin\theta_2(\dot{\theta}_2)$$
$$-b_2\dot{\theta}_3\sin\theta_3(\dot{\theta}_3)-b_3\dot{\theta}_4\sin\theta_4(\dot{\theta}_4)=u \tag{3.43}$$

$$b_0\cos\theta_1\ddot{x}+a_1\ddot{\theta}_1+L_1b_1\cos(\theta_1-\theta_2)\ddot{\theta}_2+L_1b_2\cos(\theta_1-\theta_3)\ddot{\theta}_3+L_1b_3\cos(\theta_1-\theta_4)\ddot{\theta}_4+(\mu_1+\mu_2)\dot{\theta}_1+$$
$$(L_1b_1\dot{\theta}_2\sin(\theta_1-\theta_2)-\mu_2)\dot{\theta}_2+L_1b_2\dot{\theta}_3\sin(\theta_1-\theta_3)\dot{\theta}_3+L_1b_3\dot{\theta}_4\sin(\theta_1-\theta_4)\dot{\theta}_4-b_0g\sin\theta_1=0 \tag{3.44}$$

$$b_1\cos\theta_2\ddot{x}+L_1b_1\cos(\theta_1-\theta_2)\ddot{\theta}_1+a_2\ddot{\theta}_2+L_2b_2\cos(\theta_2-\theta_3)\ddot{\theta}_3+L_2b_3\cos(\theta_2-\theta_4)\ddot{\theta}_4-(L_1b_1\dot{\theta}_1\sin(\theta_1-\theta_2)+\mu_2)\dot{\theta}_1+$$
$$(\mu_2+\mu_3)\dot{\theta}_2+(L_2b_2\dot{\theta}_3\sin(\theta_2-\theta_3)-\mu_3)\dot{\theta}_3+L_2b_3\dot{\theta}_4\sin(\theta_2-\theta_4)\dot{\theta}_4-b_1g\sin\theta_2=0 \tag{3.45}$$

$$b_2\cos\theta_3\ddot{x}+L_1b_2\cos(\theta_1-\theta_3)\ddot{\theta}_1+L_2b_2\cos(\theta_2-\theta_3)\ddot{\theta}_2+a_3\ddot{\theta}_3+L_3b_3\cos(\theta_3-\theta_4)\ddot{\theta}_4-L_1b_2\dot{\theta}_1\sin(\theta_1-\theta_3)\dot{\theta}_1-$$
$$(L_2b_2\dot{\theta}_2\sin(\theta_2-\theta_3)+\mu_3)\dot{\theta}_2+(\mu_3+\mu_4)\dot{\theta}_3+(L_3b_3\dot{\theta}_4\sin(\theta_3-\theta_4)-\mu_4)\dot{\theta}_4-b_2g\sin\theta_3=0 \tag{3.46}$$

$$b_3\cos\theta_4\ddot{x}+L_1b_3\cos(\theta_1-\theta_4)\ddot{\theta}_1+L_2b_3\cos(\theta_2-\theta_4)\ddot{\theta}_2+L_3b_3\cos(\theta_3-\theta_4)\ddot{\theta}_3+a_4\ddot{\theta}_4-L_1b_3\dot{\theta}_1\sin(\theta_1-\theta_4)\dot{\theta}_1-$$
$$L_2b_3\dot{\theta}_2\sin(\theta_2-\theta_4)\dot{\theta}_2-(L_3b_3\dot{\theta}_3\sin(\theta_3-\theta_4)+\mu_4)\dot{\theta}_3+(\mu_4+\mu_5)\dot{\theta}_4-b_3g\sin\theta_4=0 \tag{3.47}$$

Using equations (3.43) to (3.47), the resulting truncated linear state-space model equation of the QIP in compact form is determined to be;

$$\underline{\dot{x}}=\begin{pmatrix}0_{5x5} & I_{5x5}\\ -\underline{M}^{-1}(0)\dfrac{\partial\underline{D}(0)}{\partial\theta} & -\underline{M}^{-1}(0)\underline{N}(0)\end{pmatrix}\underline{x}+\begin{pmatrix}0_{5x1}\\ \underline{M}^{-1}(0)\underline{G}\end{pmatrix}\underline{u} \tag{3.48}$$

Equation (3.48) corresponds to the standard state-space equation given by (3.51).

$$\underline{\dot{x}}=\underline{A}\underline{x}+\underline{B}\underline{u} \tag{3.49}$$

$$\underline{y}=\underline{C}\underline{x}+\underline{D}\underline{u} \tag{3.50}$$

Where: $$\underline{A}=\begin{pmatrix}0_{5x5} & I_{5x5}\\ -\underline{M}^{-1}(0)\dfrac{\partial\underline{D}(0)}{\partial\theta} & -\underline{M}^{-1}(0)\underline{N}(0)\end{pmatrix} \tag{3.51}$$

$$\underline{B} = \begin{pmatrix} 0_{5x1} \\ \underline{M}^{-1}(0)\underline{G} \end{pmatrix} \tag{3.52}$$

The details of the derivation is provided in the Appendix A2

The data in Table 3.3 were the experimental parameters used by Zhang et al, (2012) for computing the state matrices of the QIP he had developed. The same data were also used for the computation of the state-space model matrices of the extracted QIP model.

Table 3.3 Parameters of the Quad inverted Pendulum (Zhang et al 2012)

Parameter	Cart	First Pendulum	Second Pendulum	Third Pendulum	Fourth Pendulum
Mass (kg)	1.3282	0.2200	0.2200	0.2200	0.1870
Frictional Coefficient (kgm^2/Nsm^{-1})	22.91470	0.00490	0.00490	0.00490	0.004824
Length (m)	0.5	0.5	0.5	0.5	0.7
$g = 9.81ms^{-2}$					

Using the data in Table 3.3 and equations (3.51) and (3.52), the state space model matrices of the quad inverted pendulum are determined as follows:

$$\underline{A} = \begin{pmatrix} 0 & 0 & 0 & 0 & 0 & 1 & 0 & 0 & 0 & 0 \\ 0 & 0 & 0 & 0 & 0 & 0 & 1 & 0 & 0 & 0 \\ 0 & 0 & 0 & 0 & 0 & 0 & 0 & 1 & 0 & 0 \\ 0 & 0 & 0 & 0 & 0 & 0 & 0 & 0 & 1 & 0 \\ 0 & 0 & 0 & 0 & 0 & 0 & 0 & 0 & 0 & 1 \\ 0 & -6.5881 & 1.2417 & -0.1983 & 0.0219 & -16.4652 & 0.0194 & -0.0079 & 0.0022 & -0.0005 \\ 0 & 124.9542 & -99.3947 & 15.8763 & -1.7537 & 42.6129 & -0.4480 & 0.3344 & -0.1759 & 0.0406 \\ 0 & -141.6903 & 199.4814 & -76.9531 & 8.5003 & -11.4491 & 0.6004 & -0.6732 & 0.5519 & -0.1969 \\ 0 & 39.3968 & -133.9553 & 129.7706 & -32.2476 & 3.1834 & -0.2505 & 0.5552 & -0.8295 & 0.4463 \\ 0 & -14.9856 & 50.9534 & -111.0453 & 73.9500 & -1.2109 & 0.0953 & -0.3255 & 0.9378 & -0.6778 \end{pmatrix} \tag{3.53}$$

$$\underline{B} = \begin{pmatrix} 0 \\ 0 \\ 0 \\ 0 \\ 0 \\ 0.7185 \\ -1.8596 \\ 0.4996 \\ -0.1389 \\ 0.0528 \end{pmatrix} \tag{3.54}$$

$$\underline{C} = \begin{pmatrix} 1 & 0 & 0 & 0 & 0 & 0 & 0 & 0 & 0 & 0 \\ 0 & 1 & 0 & 0 & 0 & 0 & 0 & 0 & 0 & 0 \\ 0 & 0 & 1 & 0 & 0 & 0 & 0 & 0 & 0 & 0 \\ 0 & 0 & 0 & 1 & 0 & 0 & 0 & 0 & 0 & 0 \\ 0 & 0 & 0 & 0 & 1 & 0 & 0 & 0 & 0 & 0 \end{pmatrix} \tag{3.55}$$

And

$$\underline{D} = 0 \tag{3.56}$$

3.4.1 Control Tests Solution on QIP

Before the controller was designed for QIP, control test was carried out to verify whether control solution exists. This is done by determining its controllability and observability status. Recall that a system is said to be controllable and observable if it is of full rank. The MATLAB scripts for the controllability and observability tests are as follows:

```
MCr = ctrb(A, B);
MCo = obsv(A, C);
CONTR = rank(MCr)
OBSVB = rank(MCo)
if rank(MCr)==size(A)
    'THE SYSTEM IS CONTROLLABLE'
else 'THE SYSTEM IS NOT CONTROLLABLE'
end
    if rank(MCo)==size(A)
        'THE SYSTEM IS OBSERVABLE'
    else 'THE SYSTEM IS NOT OBSERVABLE'
    end
```

```
>> CONTR = 10
ans =
THE SYSTEM IS CONTROLLABLE
>> OBSVB = 10
ans =
THE SYSTEM IS OBSERVABLE
```

The stability status of the system (QIP) was further checked by determining the location of eigenvalues in the complex s-plane. This is achieved using the *eig* and *ltview* MATLAB commads.

```
eig(A) = [0   17.5896   -20.3218   -16.3751   -11.2214   10.9160
-6.3685   6.4960   -2.6221   2.8135]
ltiview(sys_ss) %% this MATLAB command is used to plot the system
response in different configurations (step response, impulse, bode
plot, nyquist, pole-zero map, etc).
```

From the results of the control test, it can be seen that the QIP model is both controllable and observable. Similarly, the presence of positive eigenvalues is an indication of instability. The eigenvalues were plotted on the complex s-plane to determine their locations in the plane.

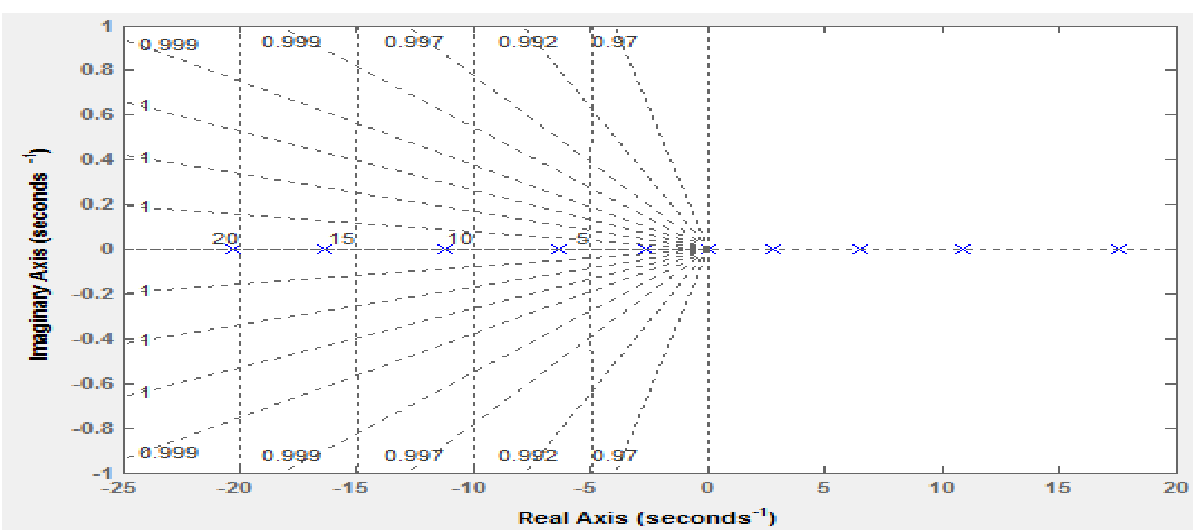

Figure 3.3 Pole-Zero Map of the QIP in an Open Loop Configuration.

The pole-zero map of the system in Figure 3.3 shows the location of the eigenvalues in the complex s-plane.

The eigenvalues are indicated by a mark‘x’. From this plot, total of 10 eigenvalues are observed. Five of these values are on the negative half of the s-plane, one at the origin and four on the on the positive half of the s-plane. This, from control perspective, confirms that the QIP is unstable in an open loop configuration (without the feedback controller).

Having established that QIP is both state controllable and observable and that it is unstable without the controller, then a controller could be designed to stabilize it.

3.4.2 Simulink Model Design of LQR Controller for QIP

The design of the LQR controller for QIP was based on the linear model presented in state space form. LQR controller was designed in MATLAB/Simulink block library. The Simulink model of the entire QIP with the controller is shown in Figure 3.4. In order to validate the model of the QIP extracted from the DQIP model, LQR controller was developed using equations (3.53), (3.54), (3.55) and (3.56) based on the data in Table 3.3. The results of using the LQR are the plots shown in Figures 3.5a to 3.9a.

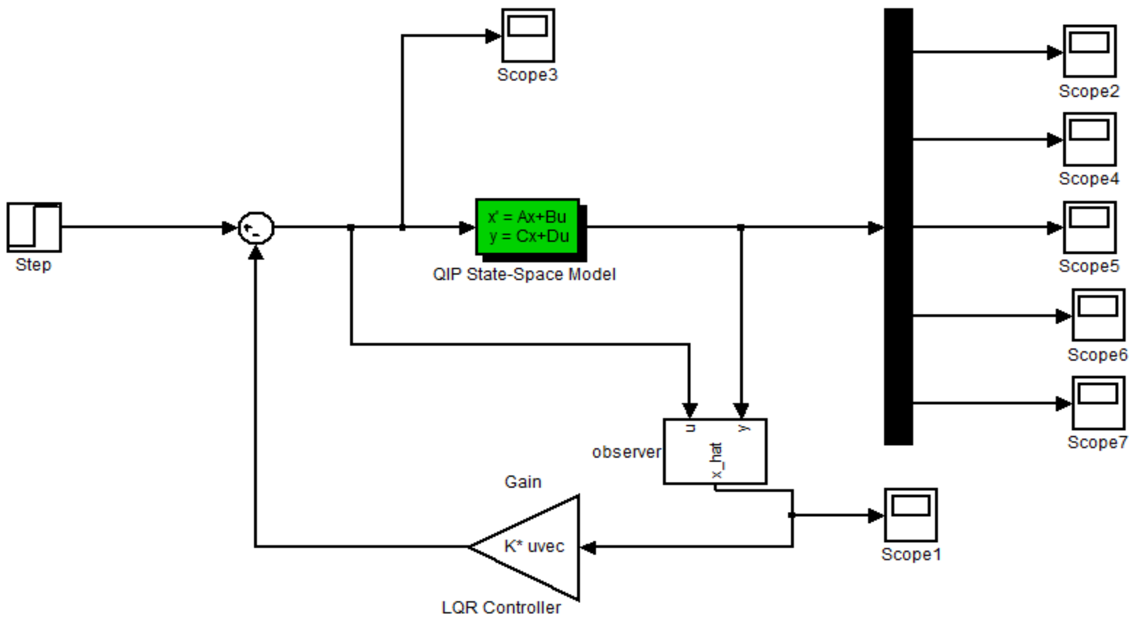

Figure 3.4. Linearized Simulink Model of the QIP with LQR Controller

3.4.2.1 Comparison of Responses using LQR and Fuzzy Logic Controllers on QIP

QIP model was developed by Li et al., (2002) and successfully stabilized using Variable Universe Adaptive Fuzzy Logic Controller. A similar model was also developed by Zhang et al., (2012). The control was implemented using Variable Universe Adaptive Fuzzy Logic Controller based on H-Infinity Variable Gain (H_∞) Regulator to stabilize the QIP about a vertical position based on the data in Table 3.3. The purpose of this was to improve on the work previously done by Li et al., (2002). The plots in Figures 3.5b to Figure 3.9b are the responses obtained by Zhang et al, 2012. From these plots, the solid blue lines show the responses obtained by Zhang et al., (2012) and the doted green lines are the responses obtained by Li et al., (2002). These plots are compared with the ones obtained from the extracted QIP model in Figures 3.5a to 3.9a. Table 3.4 summarizes the results obtained by Zhang et al., (2012).

Table 3.4 Summary of the Results obtained by Zhang et al., (2012)

Variable	Maximum Overshoot (%)	Settling Time (s)	Steady State Error (s)
Cart's Position	5.75	6.00	0.00
First Pendulum Angle	3.80	7.50	0.00
Second Pendulum Angle	2.10	7.50	0.00
Third Pendulum Angle	1.40	7.51	0.00
Fourth Pendulum Angle	0.90	7.51	0.00
Initial Conditions x_0 = [2 -0.04 0.02 -0.01 0.005 0 0 0 0 0]^T			

3.4.2.2 Time Responses of QIP using LQR and Fuzzy Logic Controllers

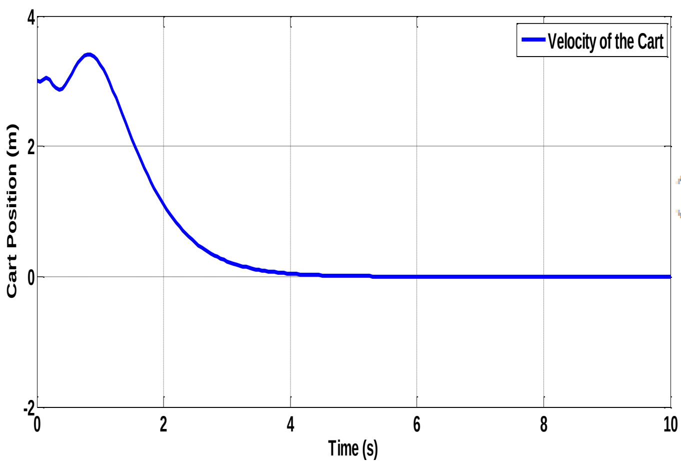

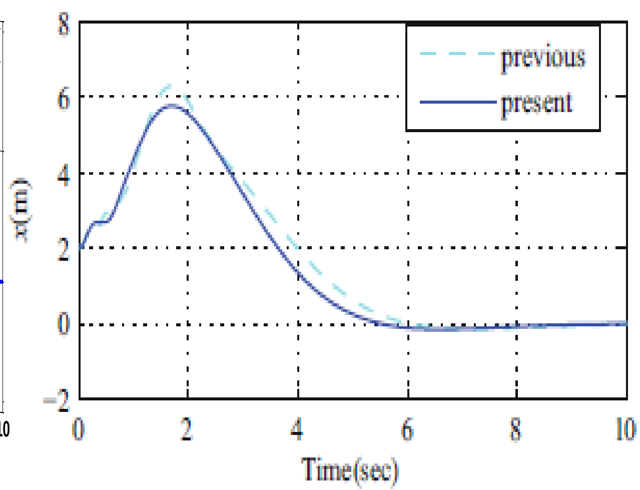

Figure 3.5a. Time Respose of the Cart with LQR the Cart controller

Figure 3.5b. Time Response of with Fuzzy Logic controller

From Figure 3.5a it can be seen that with LQR controller, the cart took about 5 seconds to reach a steady state with a maximum overshoot of 3.4%. The time response in Figure 3.5b showed that the cart moved back and forth and reached a maximum overshoot of about 5.75% and finally stablized in 6 seconds.

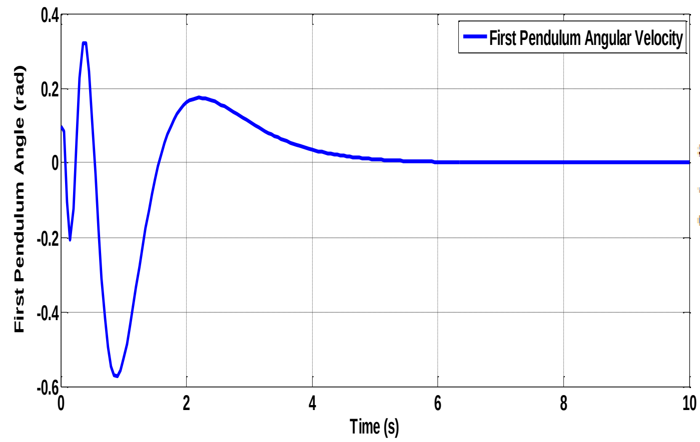

Figure.3.6a.Time Response of the First Pendulum the First angle Pendulum with LQR Controller

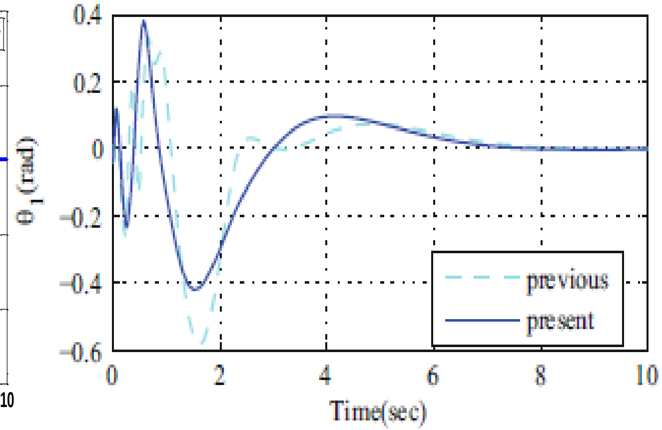

Figure.3.6b.Time response of Pendulum angle with Fuzzy Logic Controller

Figure 3.6a shows that the first pendulum has a maximum overshoot of about 3.21% and settles to a steady state in 5.8 seconds. From Figure 3.6b, the first pendulum has maximum overshoot of 3.8% and finally settles at about 7.5 seconds.

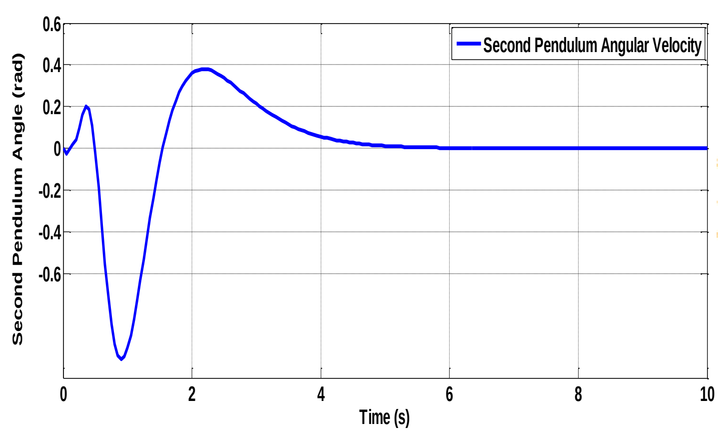

Figure.3.7a. Time Response of the Second Pendulum using LQR Controller

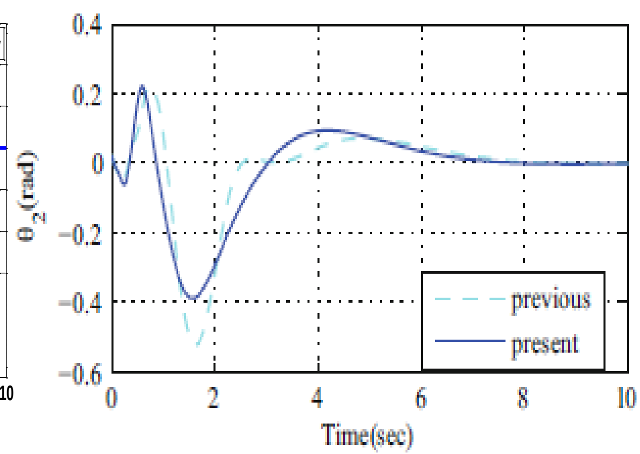

Figure.3.7b.Time Response of the Second Pendulum angle using Fuzzy Logic Controller

The settling time and maximum overshoot from Figure 3.7a are respectively 5.8 seconds and 3.79%. From Figure 3.7b, it can be seen that the second pendulum oscillates has a maximum overshoot of 2.1% and finally reaches steady state at 7.5 seconds.

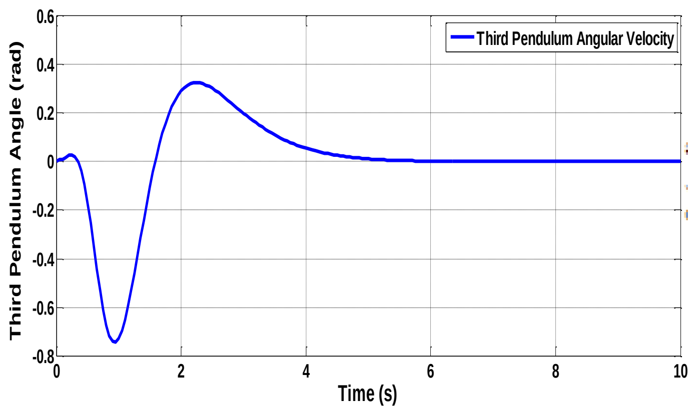

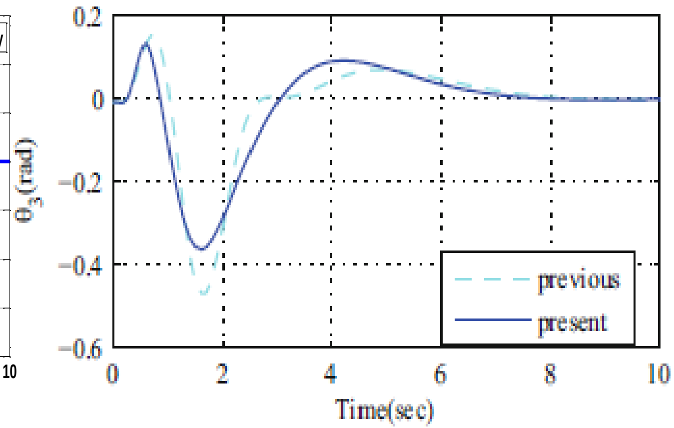

Figure 3.8a. Time Response of the Third angle with Pendulum LQR Controller

Figure 3.8b. Time Response of the Third Pendulum with Fuzzy Logic Controller

In Figure 3.8a, it can be seen that the third pendulum initially swings downwards but rises to reach a maximum over shoot 3.26% and finally settles to steady state in 5.8 seconds. The third pendulum as shown in Figure 3.8b swings up and down reaches and has maximum overshoot of 1.4% attaining steady-state in 7.51 seconds.

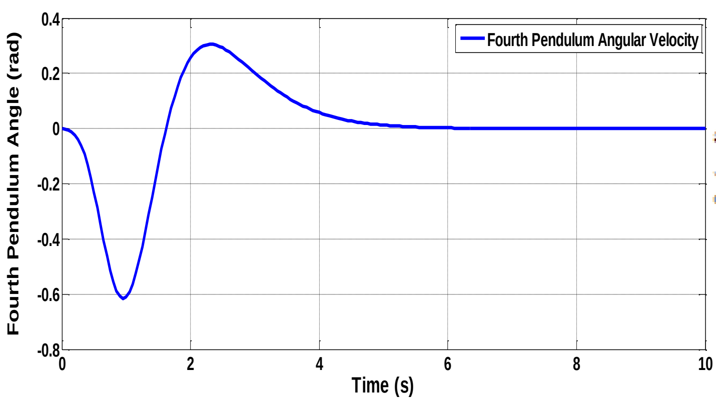

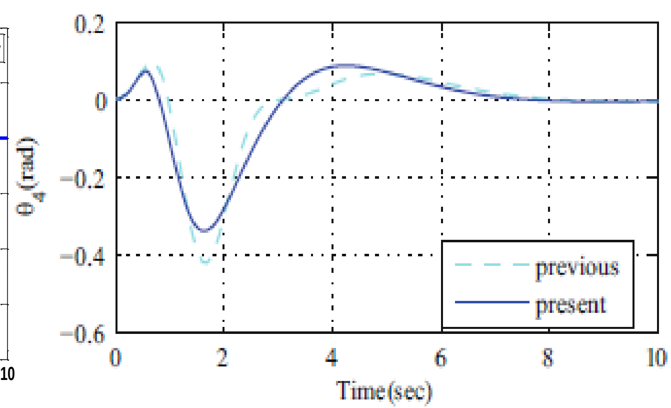

Figure 3.9a Time Response of the Fourth Pendulum angle using LQR Controller

Figure 3.9b.Time Response of the Fourth Pendulum using Fuzzy Logic Controller

The response of Figure 3.9a shows that the fourth pendulum swings downwards and starts as the cart moves back and forth attaining maximum over shoot of 3.16% and finally attaining steady-state in 5.8 seconds. For Figure 3.9b, the pendulum swings up and attains a maximum angular displacement of about 0.9% and finally brought to a steady state in 7.51 seconds.

Table 3.5 summarizes the performance of LQR on the extracted QIP model and the performance using Fuzzy Logic controller as reported by Zhang et al., (2012).

Table 3.5 Comparison of Fuzzy Logic and LQR Controllers on QIP

Variable	Maximum Overshoot (%)		Settling Time (s)		Steady State Error (s)	
	Fuzzy Logic	LQR Controller	Fuzzy Logic	LQR Controller	Fuzzy Logic	LQR Controller
Cart’s Position	5.75	3.40	6.00	6.10	0.00	0.00
First Pendulum Angle	3.80	3.21	7.50	5.80	0.00	0.00
Second Pendulum Angle	2.10	3.79	7.50	5.80	0.00	0.00
Third Pendulum Angle	1.40	3.26	7.51	5.80	0.00	0.00
Fourth Pendulum Angle	0.90	3.16	7.51	5.80	0.00	0.00
Initial Conditions $x_0 = [2\ \ -0.04\ \ 0.02\ \ -0.01\ \ 0.005\ \ 0\ \ 0\ \ 0\ \ 0\ \ 0]^T$						

The results in Table 3.5 show that the extracted model of QIP is correct and conforms to the ones reported in literature by Li et al, (2002) and Zhang et al, (2012). It can also be seen that LQR provided improved performances in terms of maximum overshoot, settling time and steady state error comparable to the ones obtained using Fuzzy Logic controller. Therefore, it can be concluded that the model of the DQIP developed is appropriate.

Before a linear controller was designed to stabilize the DQIP, controllability and observability tests were carried out. These are necessary in order to find out the possibility of extending a linear regulator control algorithm (LQR) to DQIP.

3.5 DQIP State Model Scaling

It can be recalled that the results of control test on DQIP model were inconsistence in terms of controllability and obsevability. Form the DQIP state matrix given by equation (3.41), presence of very small and large entries in the state matrix *A* is observed. This has led to a state matrix divergence which gives rise to an ill-conditioned state model. This, therefore, made it difficult to arrive at the best possible conclusions with respect to system stability. Provided that the model is correct, the presence of the small and large elements in the state matrix can be addressed by state model normalization or scaling using an appropriate scaling factor. This factor is used to multiply both the state and control input matrixes so that the uncontrolled parts of the state model represented by these small and large entries are converged for proper control implementation (Braslavasky nd). Auto-Manual scaling is therefore used to find the best possible scaling factor for the DQIP. This is because the auto-manual scaling is used for complex systems having dynamics over a wide range of frequencies (Braslavasky, nd). DQIP model was scaled using the following MATLAB commands:

sys_ss = ss(A, B, C, D);

prescale(sys_ss)

Where *A*, *B*, *C* and *D* are the state, input, output and disturbance (transition) matrices. These resulted in the frequency response accuracy and frequency response gain plots as shown in Figure 3.10.

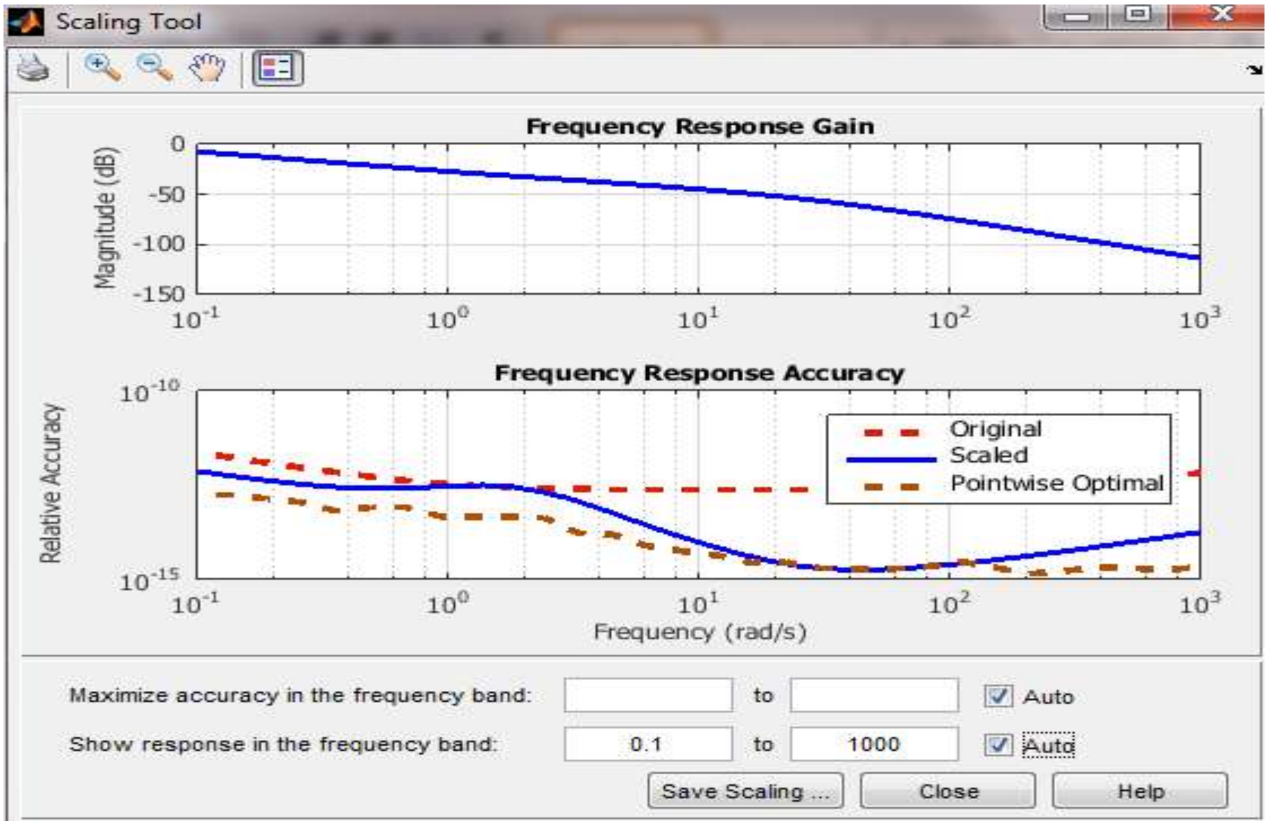

Figure 3.10. Frequency Response Accuracy and Frequency Response Gain of the DQIP (Before Scaling)

It can be seen from the Figure 3.10 that there is a significant difference between the Scaled model curve (blue curve) and the point-wise optimal model curve (brown curve). This is an indication of an ill-state model.

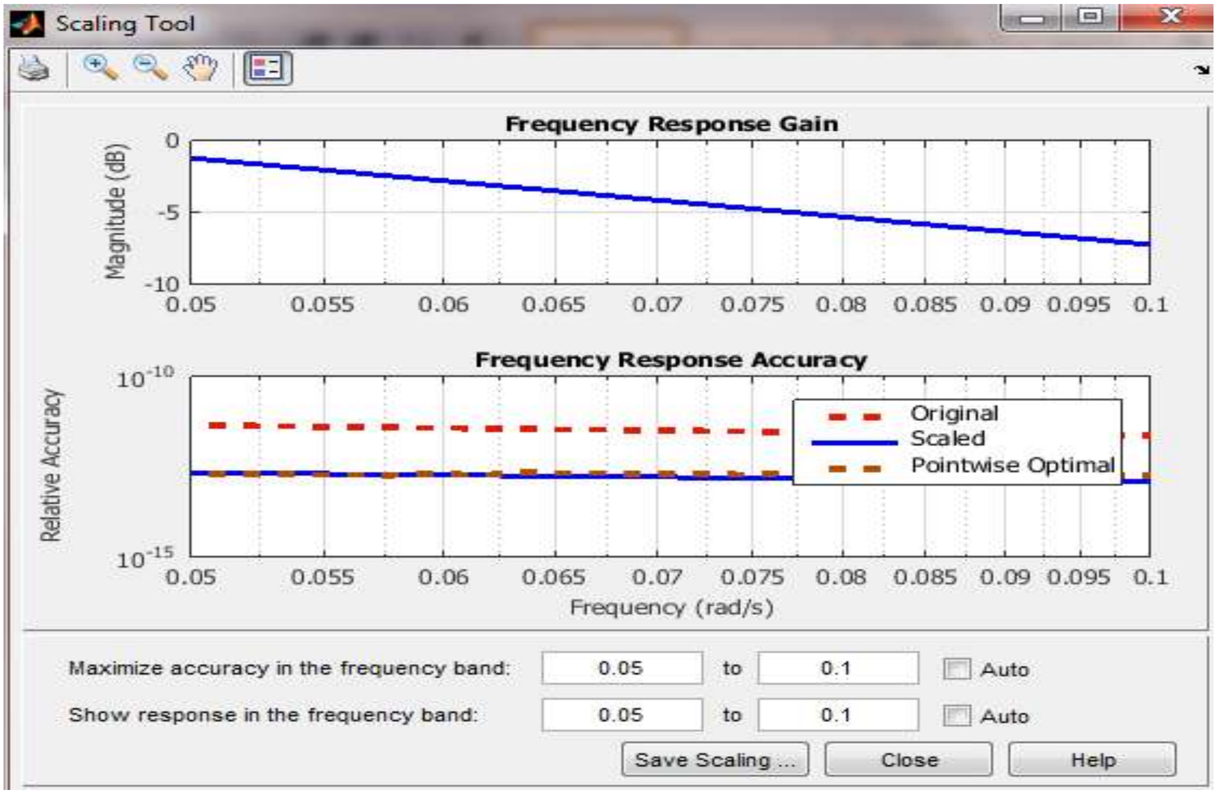

Figure 3.11. Frequency Response Accuracy and Frequency Response Gain of the DQIP (After Scaling)

By adjusting the frequency band, a scaled model is obtained within the range of 0.05 - 0.1. The scaled model (blue curve) has been found to be very close to a point-wise optimal model (brown curve). The choice of the scaling factor must be within some acceptable range and is relative to the accuracy of the model. For this model, 0.075 was selected as a scaling factor and was used to normalize the state matrix model because it is within specified frequency band (Figure 3.11). It gives the best relative close proximity between the scaled model and a point-wise optimal model. Therefore, the scaled state matrix model of the DQIP is given by:

$$A_S = 0.75e^{-1} * A \tag{3.57}$$

$$B_S = 0.75e^{-1} * B \tag{3.58}$$

Where A_s and B_s are the state variable and control input matrices of the scaled model.

With this scaled model, control tests were again performed and the system (DQIP) was found to be both completely state controllable and observable. The MATLAB codes used are:

```
MCr = ctrb(As, Bs);
MCo = obsv(As, Cs);
CONTR = rank(MCr)
OBSVB = rank(MCo)
if rank(MCr)==size(As)
    'THE SYSTEM IS CONTROLLABLE'
else 'THE SYSTEM IS NOT CONTROLLABLE'
end
    if rank(MCo)==size(As)
        'THE SYSTEM IS OBSERVABLE'
    else 'THE SYSTEM IS NOT OBSERVABLE'
    end
>> CONTR = 18

ans =

THE SYSTEM IS CONTROLLABLE

>> OBSVB = 18

ans =

THE SYSTEM IS OBSERVABLE
```

Since the control tests has been passed, a linear controller that could stabilize the DQIP is designed for DQIP

3.6 LQR Controller Design for DQIP

Before LQR controller was designed, Simulink model of the nonlinear system was developed (Figure 3.12). The nonlinear characteristics of the various system components (cart and the pendulums) were investigated.

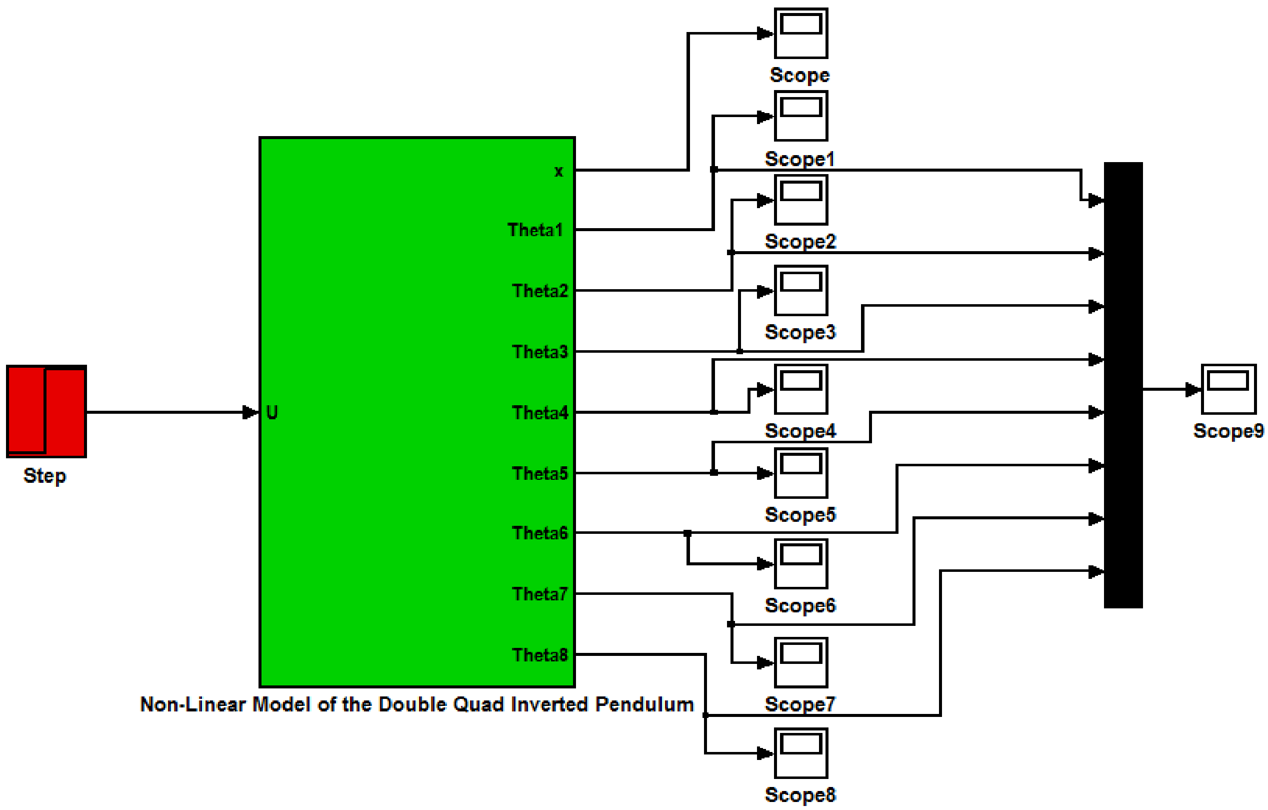

Figure 3.12. Subsystems Simulink Model of the Nonlinear DQIP with a Step Input without a Controller.

Within the subsystems model in Figure 3.12, nonlinear Simulink blocks were designed. All the nonlinear computations are performed within the subsystems block. The internal configuration of the nonlinear subsystems model where all the nonlinear algebraic computations are done is shown in Figure 3.13.

It is also important to investigate the time response of the DQIP linear model without the controller. This will provide the basis of designing the controller to stabilize it. The complete Simulink configuration of the DQIP linear model in open-loop configuration (without controller) is shown in Figure 3.14.

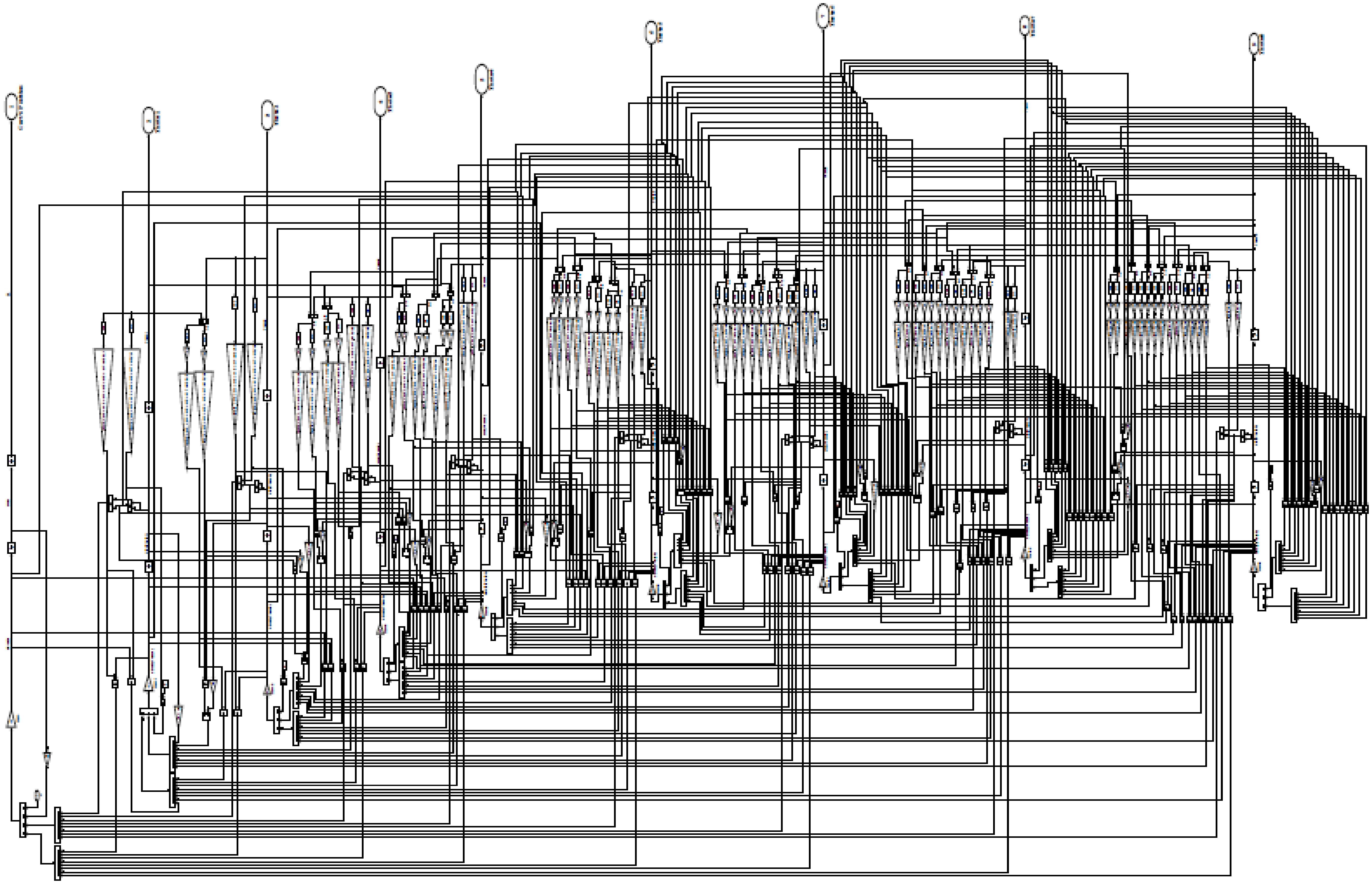

Figure.3.13. Internal Configuration Simulink Model of the Nonlinear DQIP

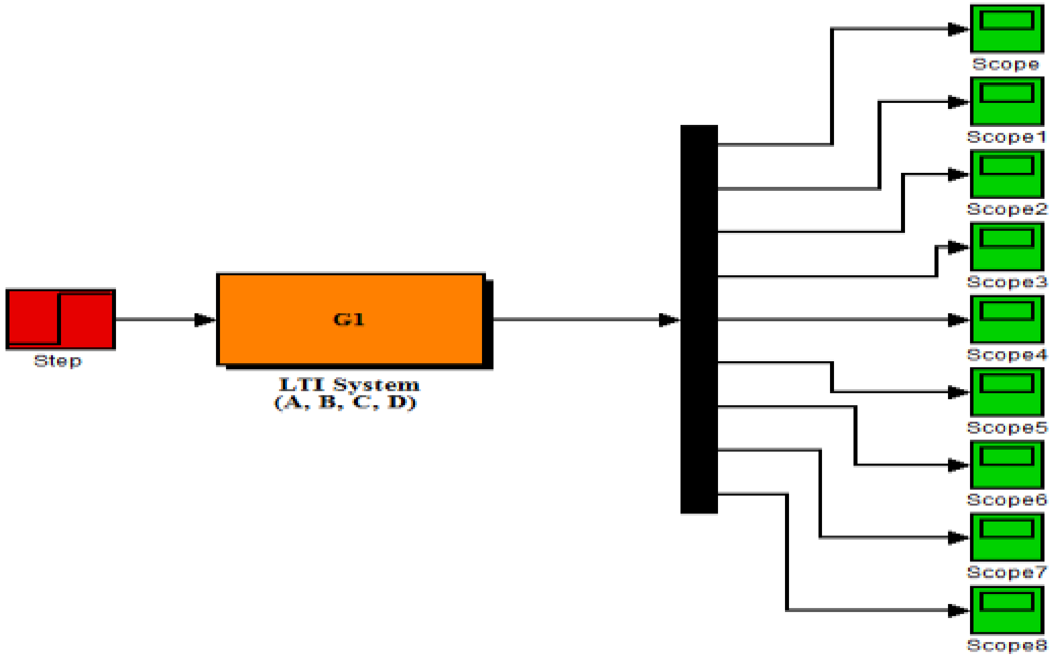

Figure 3.14. Simulink Model Configuration of the DQIP Linear Model without LQR Controller

3.6.1 Design Specifications

In this problem, the control action is performed so that the cart is moved to a position where all the pendulum links are in an upright un-equilibrium position. This means that the variables to be controlled are the cart's position and pendulum angles ($\boldsymbol{\theta}_1$, $\boldsymbol{\theta}_2$, $\boldsymbol{\theta}_3$, $\boldsymbol{\theta}_4$, $\boldsymbol{\theta}_5$, $\boldsymbol{\theta}_6$, $\boldsymbol{\theta}_7$ and $\boldsymbol{\theta}_8$) and these correspond to $Q_{11}, Q_{22}, Q_{33}, Q_{44}, Q_{55}, Q_{66}, Q_{77}, Q_{88} and Q_{99}$ (output states). Therefore, the output responses of the pendulum angles are improved by imposing penalty on these parameters. Therefore the emphasis will be on the output states not on the control input signal. To achieve an optimum time response, the relative weights imposed on the cart's position, first, second, third, fourth, fifth, sixth, seventh and eighth pendulums ($Q_{11}, Q_{22}, Q_{33}, Q_{44}, Q_{55}, Q_{66}, Q_{77}, Q_8$ and Q_9) were varied until desired system responses were obtained.

In designing a controller, some specifications must be defined. The optimal performance is achieved when these specifications are met. Given zero initial conditions, the controller was designed to ensure that the maximum overshoot for the entire pendulum angles was less than or equal to 2%, the settling time less than or equal to 20 seconds and the zero steady state error. The controller was tuned to different values of the weighting matrices until a set of values were obtained that gave the responses whose characteristics satisfy the design requirements. The 2% maximum overshoot is to ensure minimal angular fluctuations. The settling time is to ensure that the controller is relatively fast. Zero steady state is to make sure that all the pendulums are approximately balanced and stabilized in an upright position (zero degrees angular displacements).

The LQR was designed based on the scaled state space model matrices of equations (3.41), (3.42), (3.57) and (3.58). The complete Simulink configuration of the DQIP linear model with the LQR controller is shown in Figure 3.15.

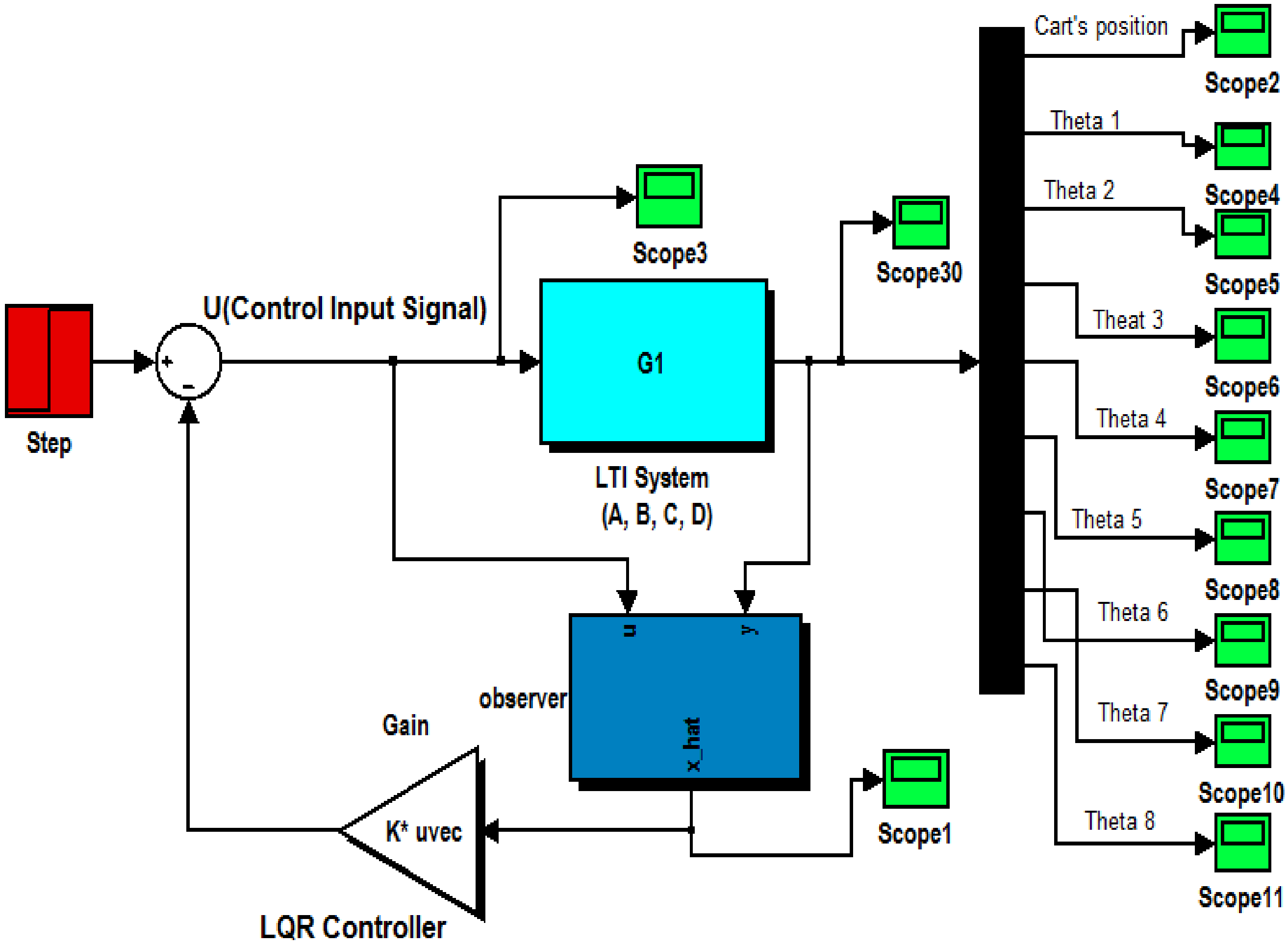

Figure 3.15 Simulink Model of the DQIP Linear Model with LQR Controller

Flowchart of the complete Control Algorithm

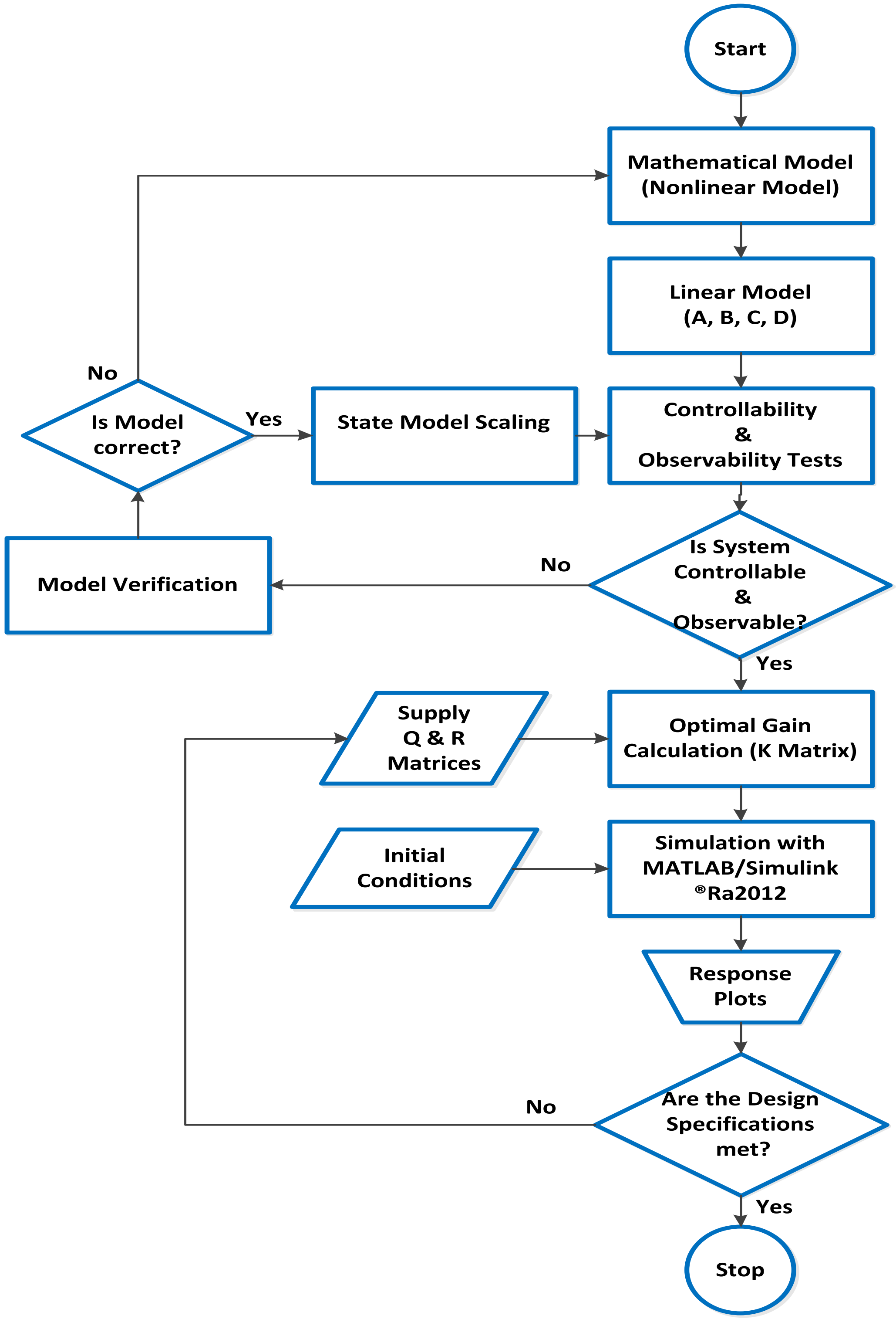

Figure 3.16. Flowchart of the LQR Controller Design approach for DQIP

3.7 Proposed Experimental Validation of the DQIP System

The proposed experimental layout for the practical implementation of the DQIP system is shown in Figure 3.17. The experimental equipment are manufactured by one of these popular companies: Googol Technology (HK) Limited or Quanser Limited. These companies are specialists in manufacturing experimental modules for Electronics, Telecommunications and Control Systems Engineering for both industrial and research purposes (Quanser User Manual, 2004 and Duan et al., 2005). They provide different experimental modules ranging from single to triple inverted pendulum both in linear and rotary forms (Googol Technology, 2004).

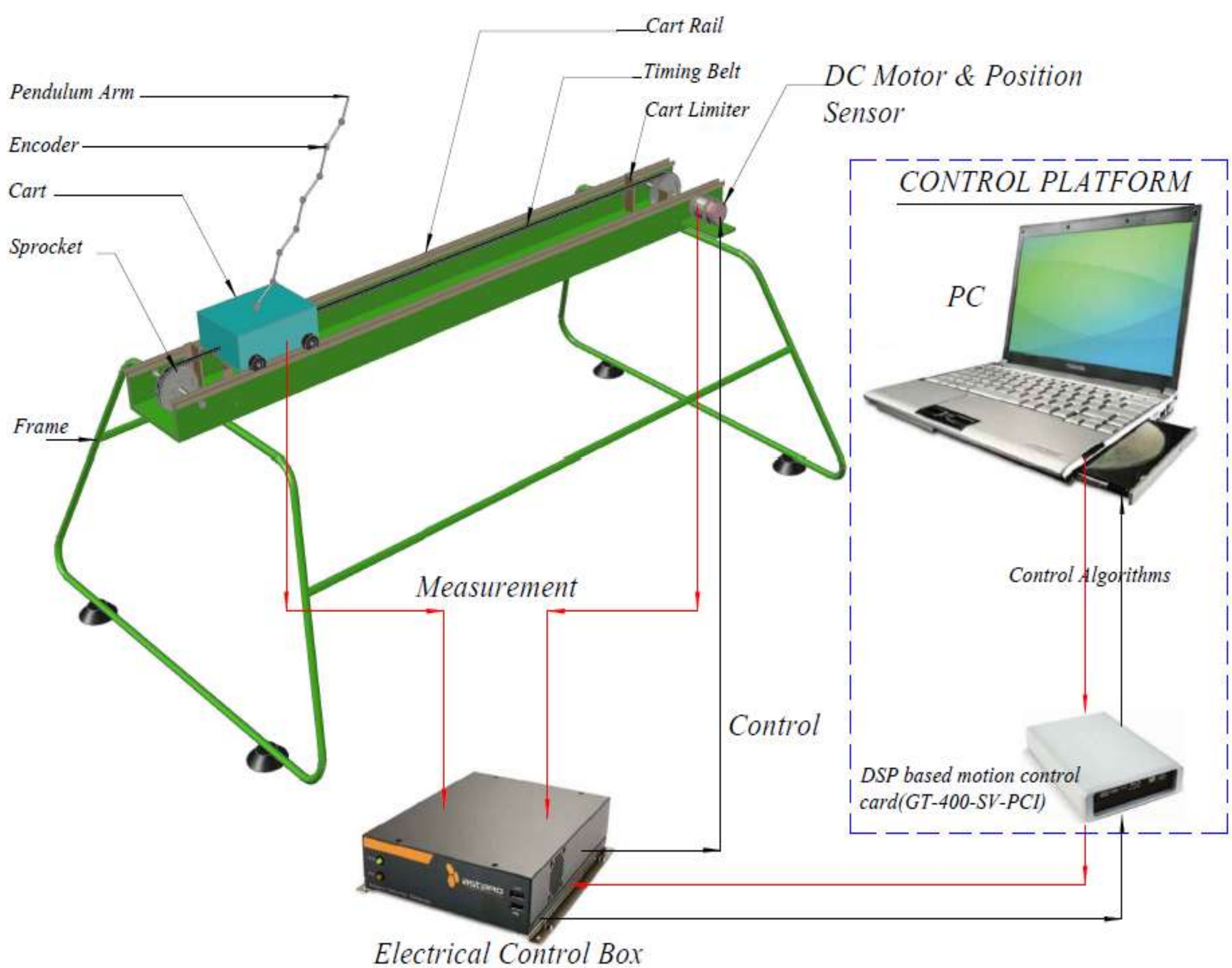

Figure.3.17. Complete real time experimental set up for the control and stabilization of DQIP

The experimental validation of the model of the model developed was not carried out as it was outside the scope of the research. Therefore, validation was only limited to software simulation in MATLAB/Simulink. However, layout of the experimental demonstration of the system has been proposed. The following equipment are required for the experimental demonstration of the DQIP stabilization:

1. Electric control Box: this contains the power supply, a servo amplifier, protection circuit and connecting terminals.
2. Data Acquisition Board: this together with the PC forms the complete control platform. It is a DSP-based motion control card (GT-400-SV-PC1) with advanced I/O with storage ability. It has several connection cables for connecting PC to the control box and the control box to the cart.
3. Real-Time Control Software (MATLAB/Simulink Ra2012): this is the software that is used to develop the control algorithm.
4. Encoders: These are used for measuring Angular displacements.

3.8 Conclusion

Mathematical modeling of a DQIP has been presented. The developed model has been verified and validated by extracting the model of the QIP and compared with those reported in literatures. Nonlinear and Linear Simulink models of the DQIP in open-loop configurations have been developed. LQR controller has been designed based on the linear model. It can therefore be concluded that it is possible to extend the modeling of an inverted pendulum system beyond four links and that LQR can be used to stabilize a multi-link inverted pendulum of nine degree of freedoms.

CHAPTER FOUR

RESULTS ANALYSIS AND DISCUSSIONS

4.1 Introduction

This chapter discusses the results obtained from the responses of the system before and after the application of an LQR controller. It also explains the various results obtained when LQR was applied with different values of weighting matrices. The stabilization of the DQIP in a closed-loop configuration has been proven by the location of system eigenvalues on the left hand side of the s-plane. The chapter discusses further how an optimal control stabilization of the DQIP is achieved; by designing an LQR controller with the best possible gain in accordance with the prescribed design specifications.

4.2 Open-loop Time Response of the DQIP (without a feedback controller)

The plots in Figures 4.1 to 4.9 are obtained from the linear model equations of the DQIP using linear Simulink model of Figure 3.14 based on the data in Table 3.2. All the MATLAB scripts used for plotting the open-loop time responses are given in the Appendix B2.

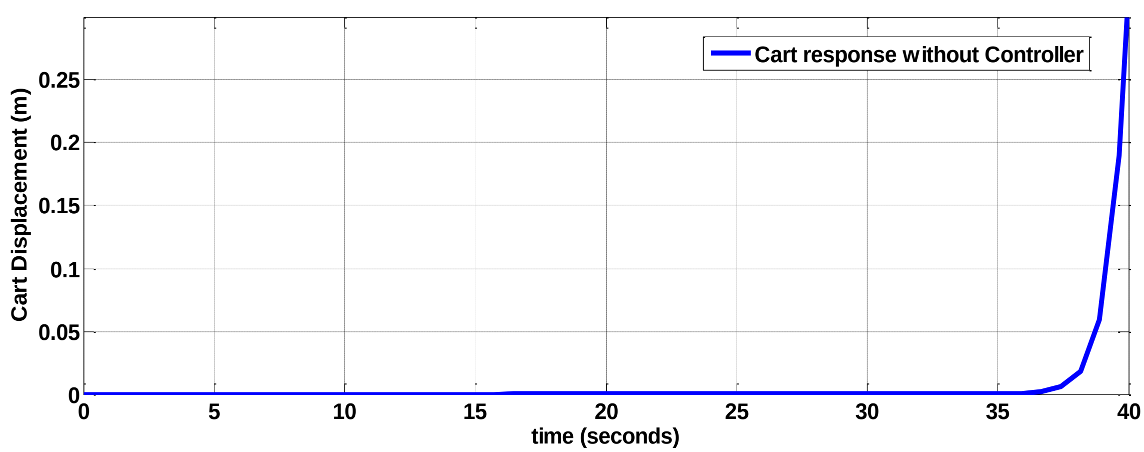

Figure 4.1. Linear Response of the Cart Without Controller

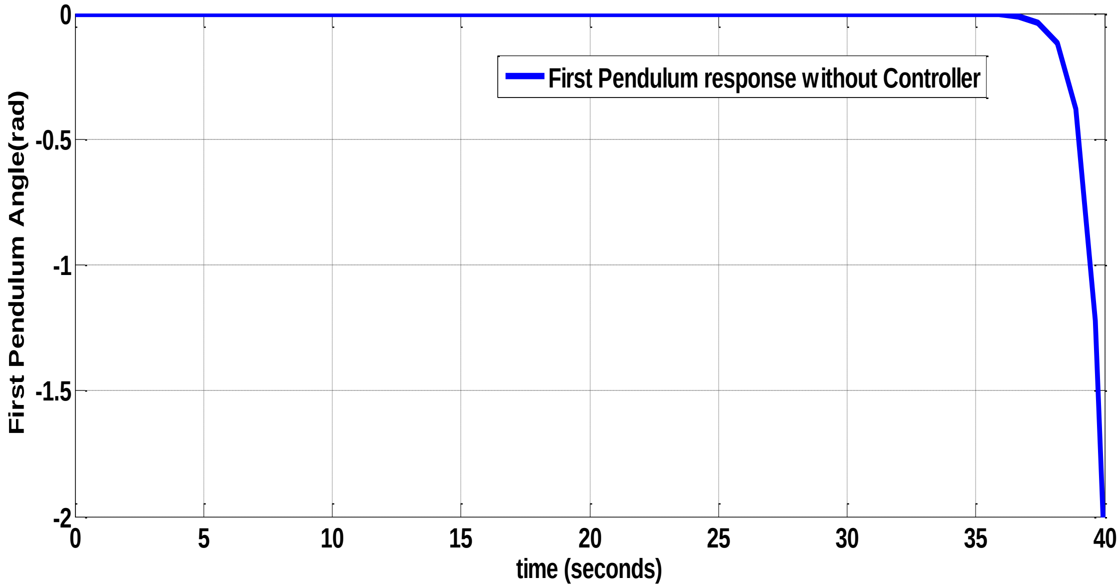

Figure 4.2. Linear Response of the First Pendulum Without Controller

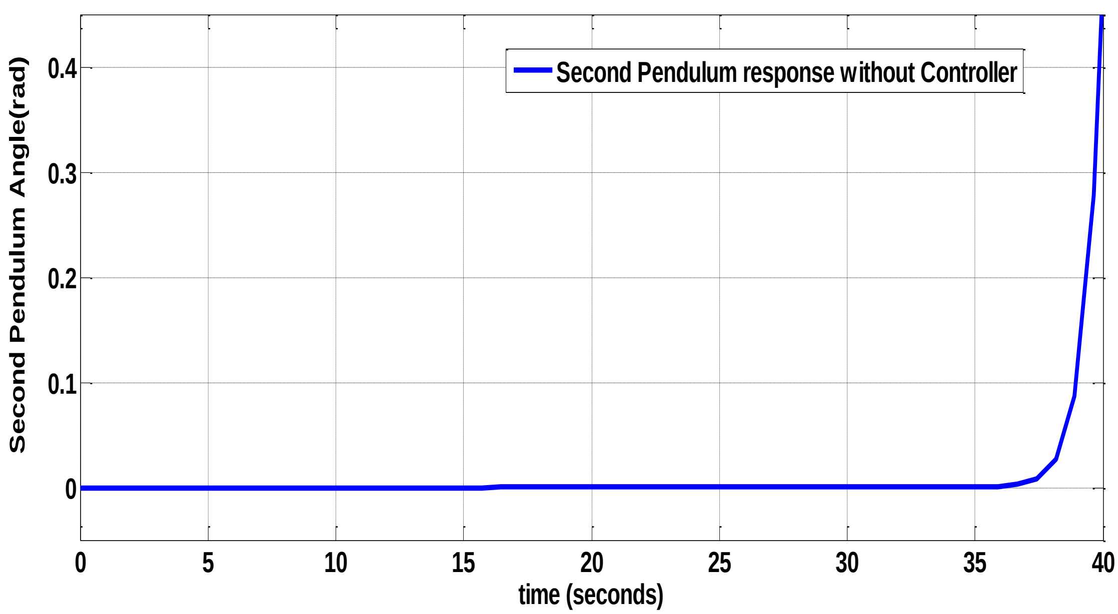

Figure 4.3. Linear Response of the Second Pendulum Without Controller

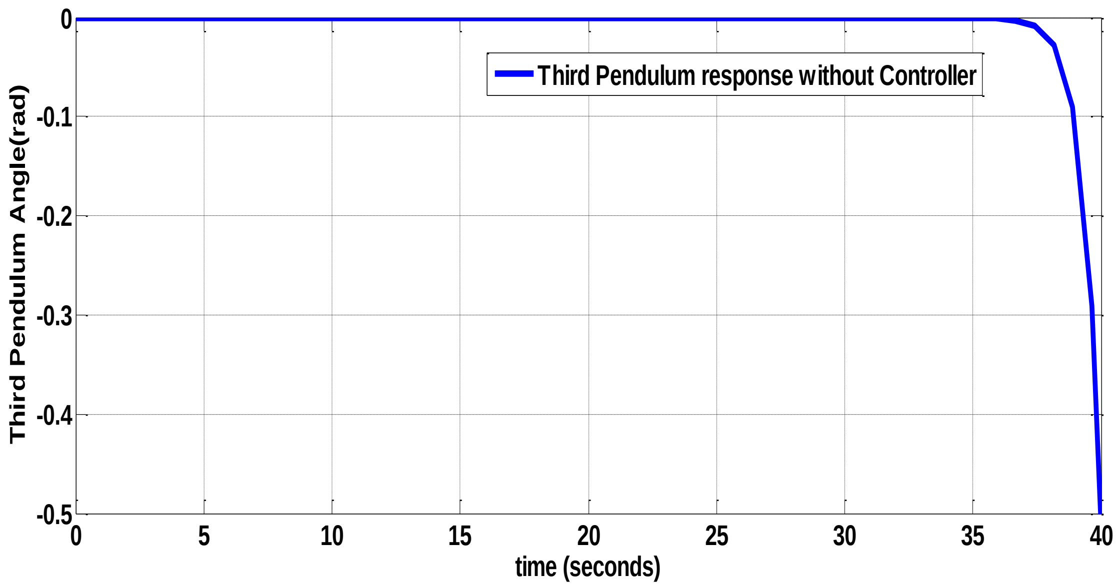

Figure 4.4. Linear Response of the Third Pendulum Without Controller

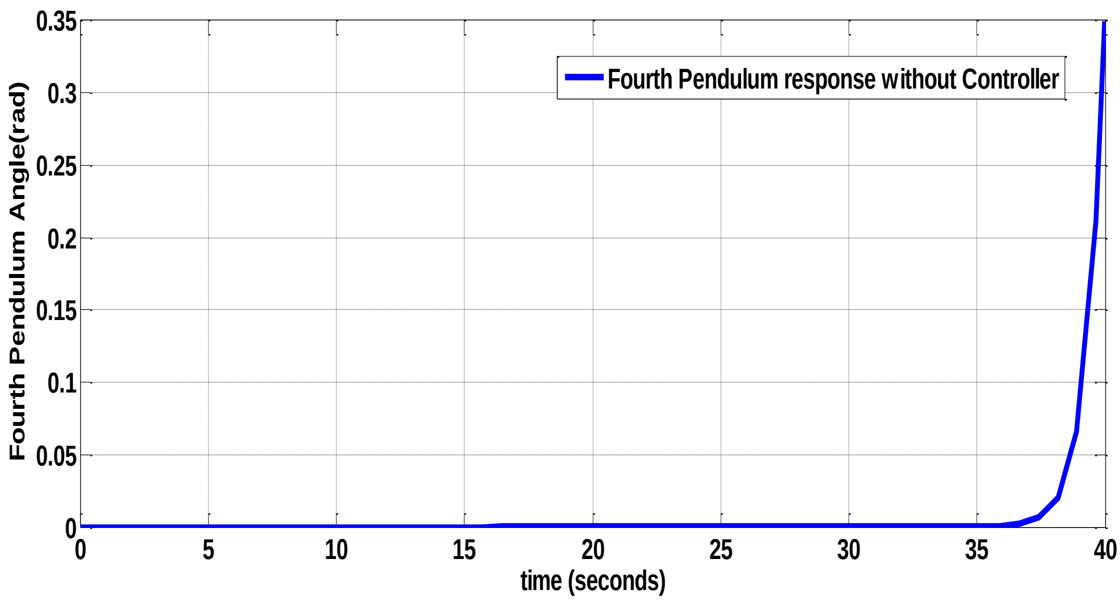

Figure 4.5. Linear Response of the Fourth Pendulum Without Controller

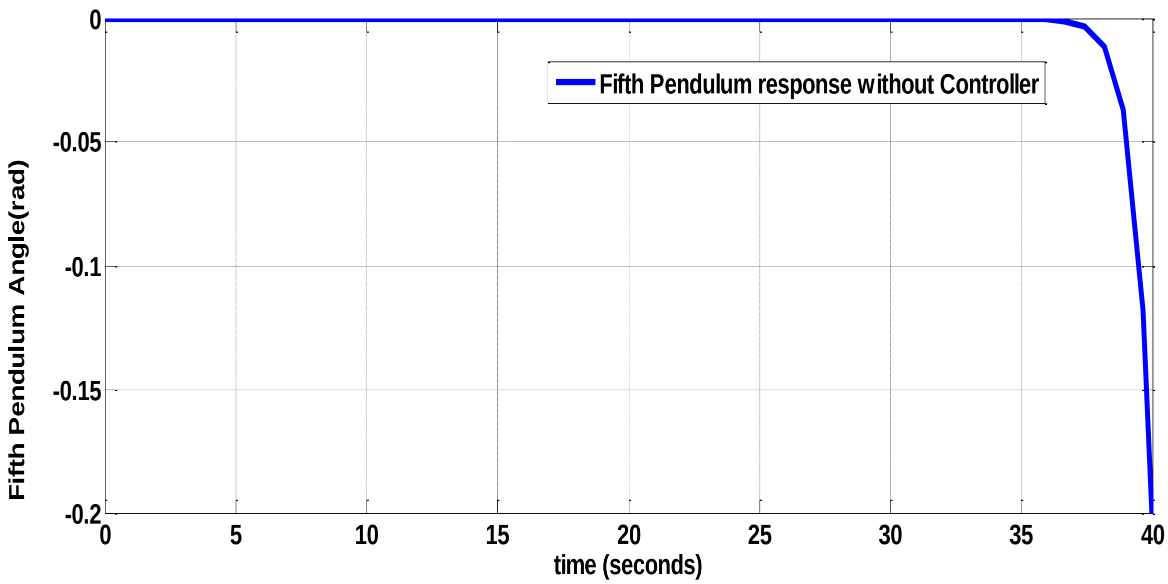

Figure 4.6. Linear Response of the Fifth Pendulum Without Controller

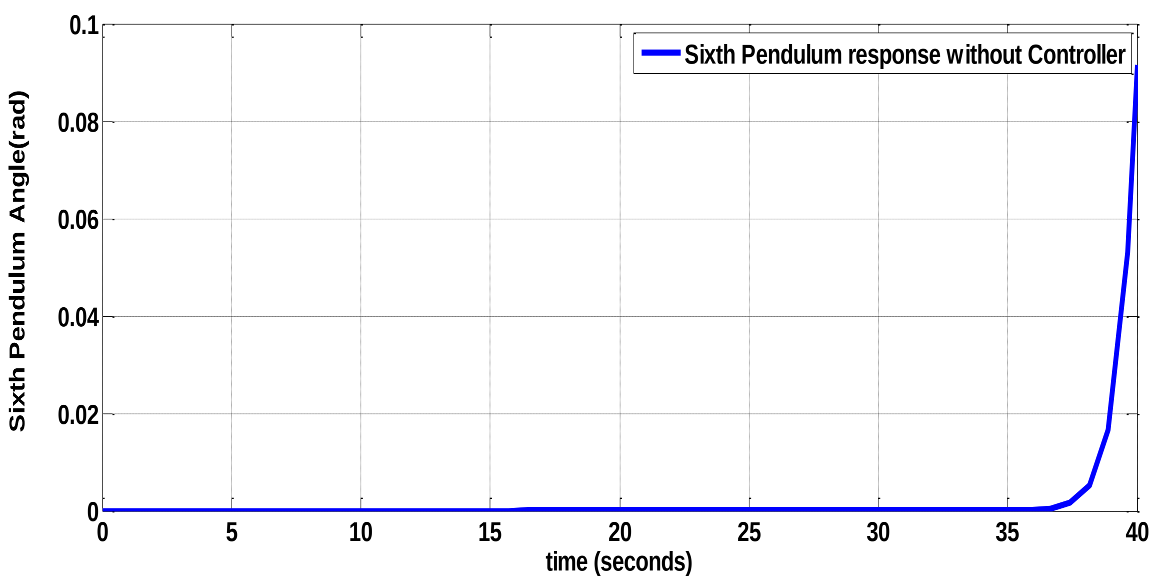

Figure 4.7. Linear Response of the Sixth Pendulum Without Controller

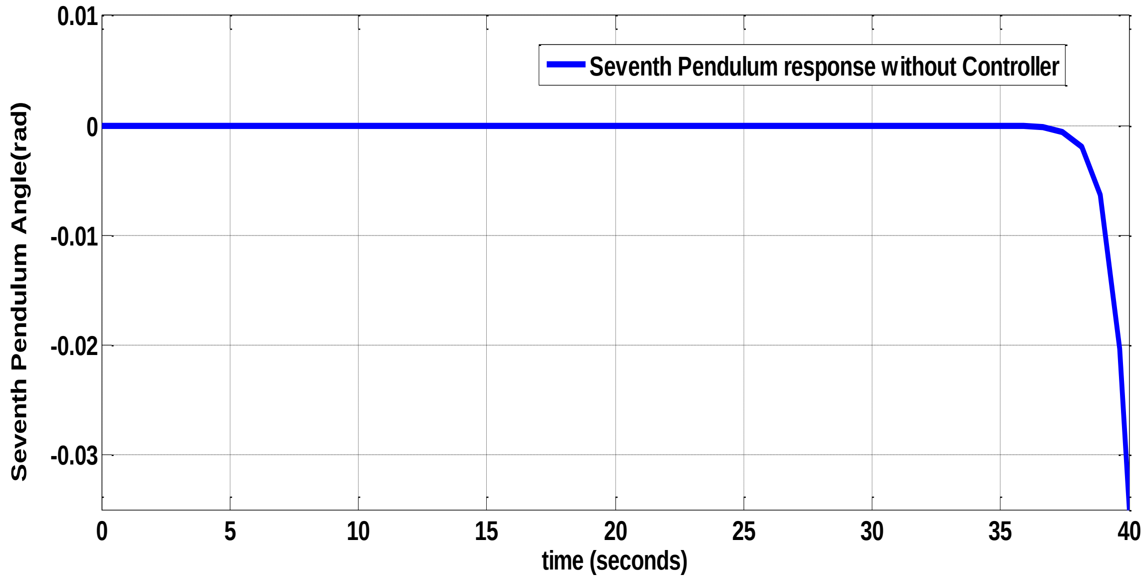

Figure 4.8. Linear Response of the Seventh Pendulum Without Controller

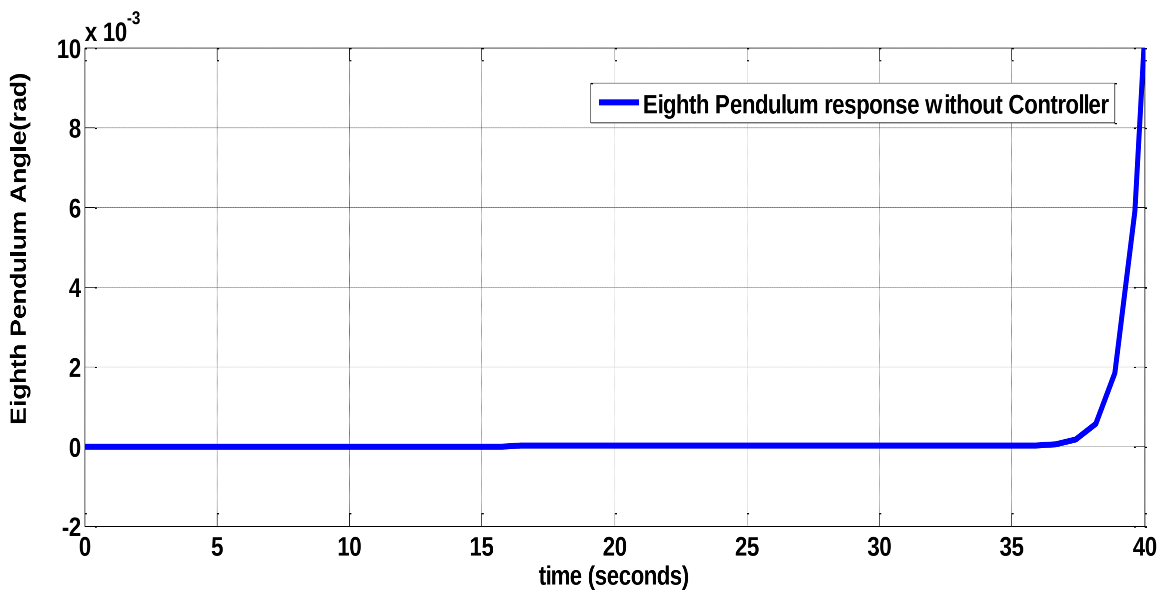

Figure 4.9. Linear Response of the Eighth Pendulum Without Controller

The plots in Figures 4.1, 4.3, 4.5, 4.7 and 4.9 show the open-loop time responses of the cart, second, fourth, sixth and eighth pendulums respectively. It can be seen from Figures 4.1, 4.3, 4.5, 4.7 and 4.9 that there is an exponential growth in the responses when a controller is not used. Figures 4.2, 4.4, 4.6 and 4.8 show the open-loop time responses of the first, third, fifth and seventh pendulums respectively. As depicted in this Figures 4.2, 4.4, 4.6 and 4.8, an exponential increase in the opposite sense is observed. This is as a result of the reactions against the impact from the cart, second, fourth and sixth pendulums. It can be concluded from these plots that DQIP is unstable without the controller as none of these responses from theses plots attains a steady state. Stability of DQIP is further investigated by the locations of the open-loop eigenvalues in the complex s-plane as shown in Figure 4.10.

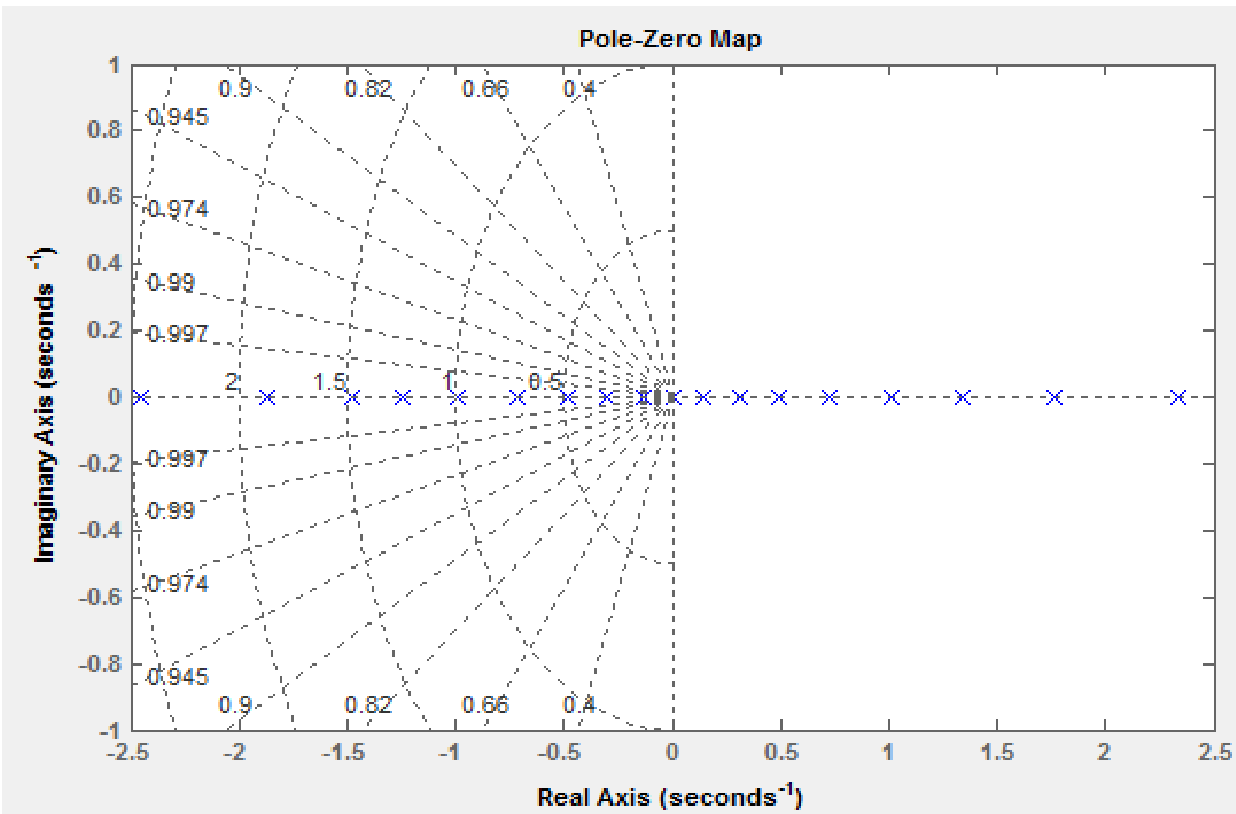

Figure 4.10 Pole-Zero map of the DQIP without a feedback controller.

Figure 4.10 shows that there is presence of some roots in the right half side of the s-plane. This indicates instability from control perspective (i.e. DQIP is not asymptotically stable without a feedback controller).

4.3 Closed-loop Time Response of the DQIP (with a feedback controller)

In designing an LQR controller, the optimal performance is largely dependent on how the controller is tuned. The tuning in this sense means careful selection of the values of *Q* and *R* until a best response is obtained based on the designer's specifications. The designer's specifications are relative terms and are sometimes based on the application in question. Table 4.1 gives the set of different values of the weighting matrices used.

Table 4.1 Weighting Matrices Values

First Case																		
Diag(Q)	1	1	1	1	1	1	1	1	1	1	1	1	1	1	1	1	1	1
R	1.0																	
Second Case																		
Diag(Q)	100	500	500	500	500	500	500	500	500	1	1	1	1	1	1	1	1	1
R	0.6																	
Third Case																		
Diag(Q)	500	5000	5000	5000	5000	5000	5000	5000	5000	1	1	1	1	1	1	1	1	1
R	0.8																	
Fourth Case																		
Diag(Q)	1000	10000	10000	10000	10000	10000	10000	10000	10000	1	1	1	1	1	1	1	1	1
R	0.4																	

The results of the system (DQIP) responses from the Simulink model of Figure 3.15 with different weighting matrices based on equations (3.43), (3.44), (3.59) and (3.60) and the data in Table 3.2 are shown in Figures 4.1 to 4.39; and they are given in the following cases.

4.3.1 First Case

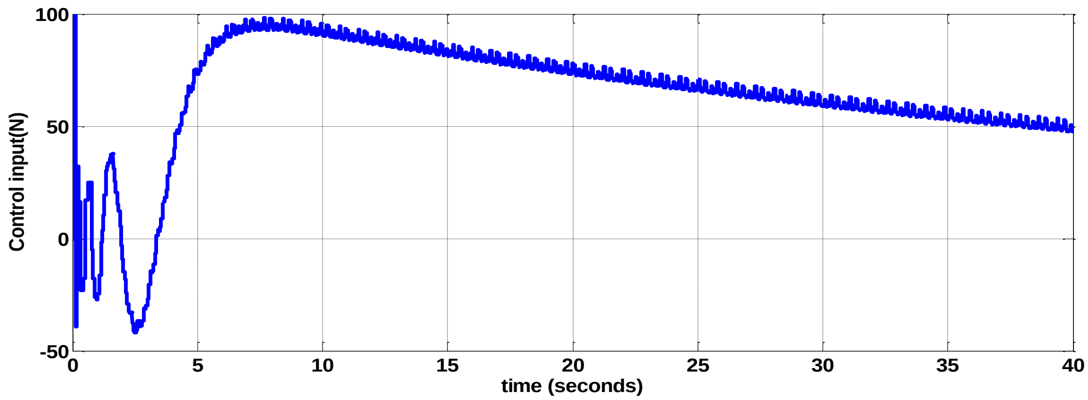

Figure 4.11 Control Input signal (First Case)

From Figure 4.11, it can be seen that the applied control input is significantly high. Smooth and fast are required with little control effort. The chatter in the response is as a result of noise in the input signal.

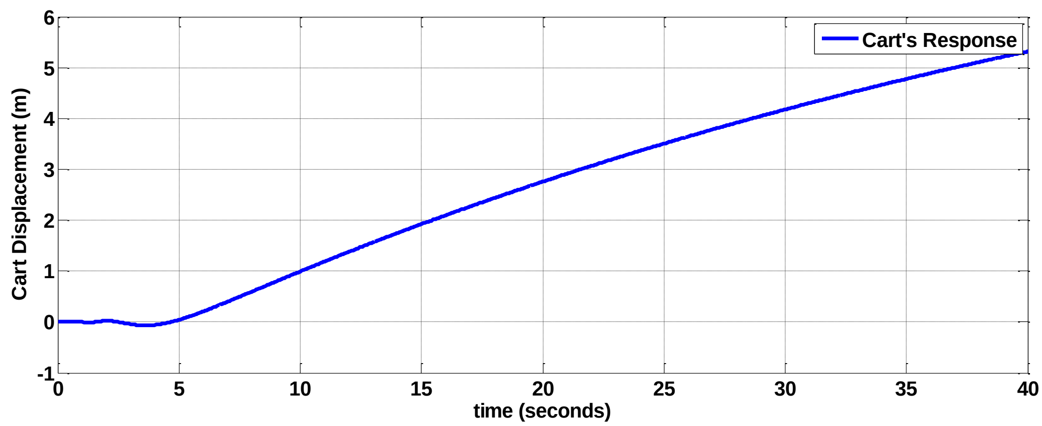

Figure 4.12 Cart's Response (First Case)

It can be seen from this plot that the cart moves from initial resting position and does not settle at any reference point. The implication of this is that a long track is needed for the cart to move to a stable position; and this may be practically impossible.

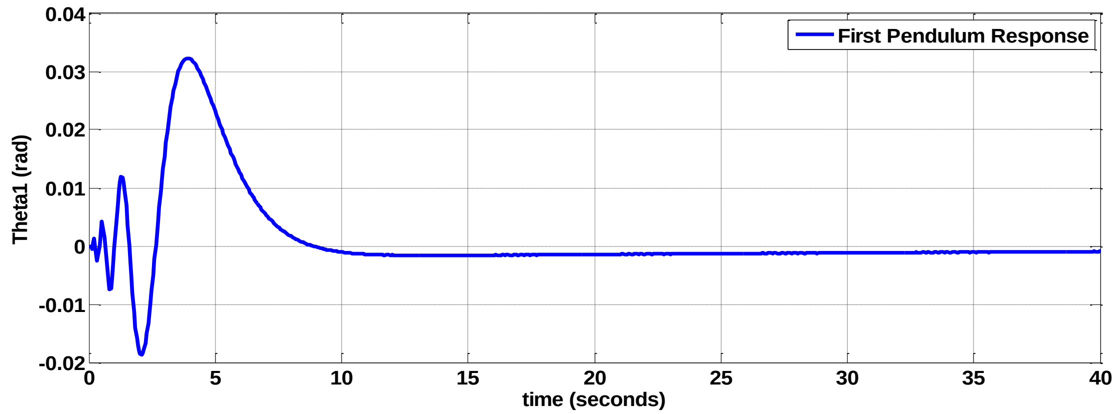

Figure 4.13 First Pendulum Response (First Case)

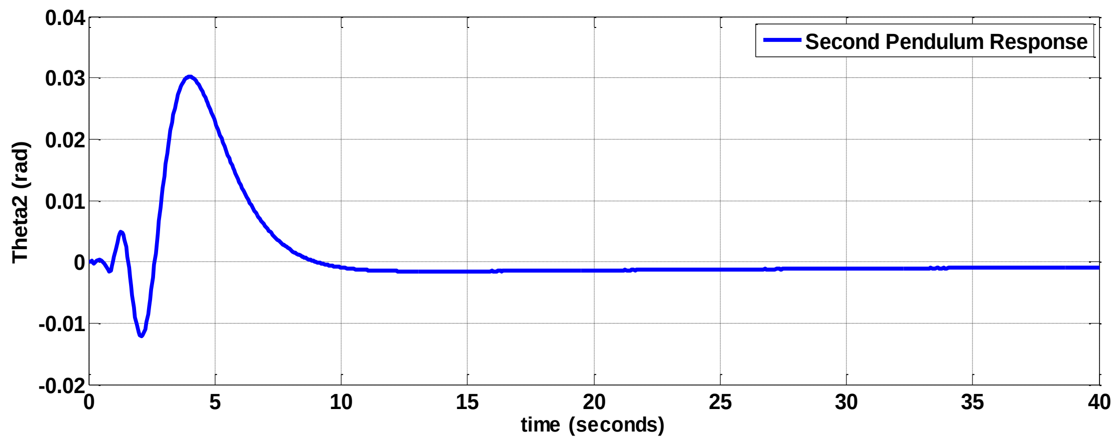

Figure 4.14 Second Pendulum Response (First Case)

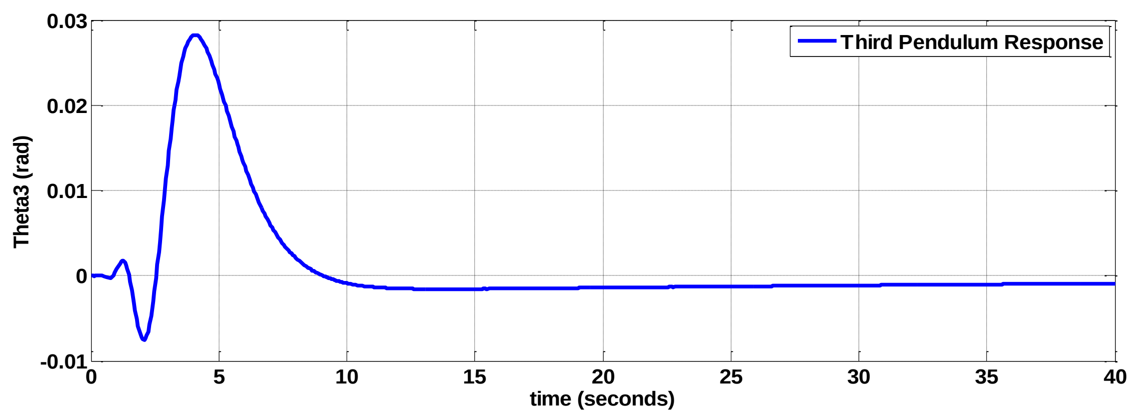

Figure 4.15 Third Pendulum Response (First Case)

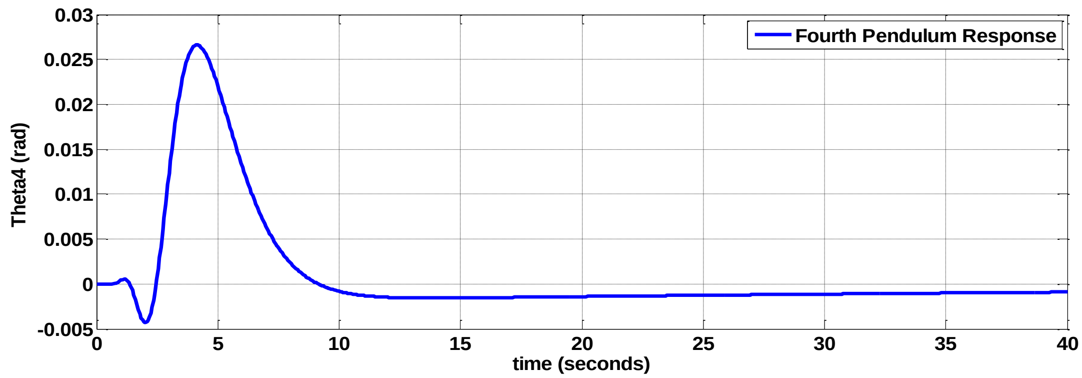

Figure 4.16 Fourth Pendulum Response (First Case)

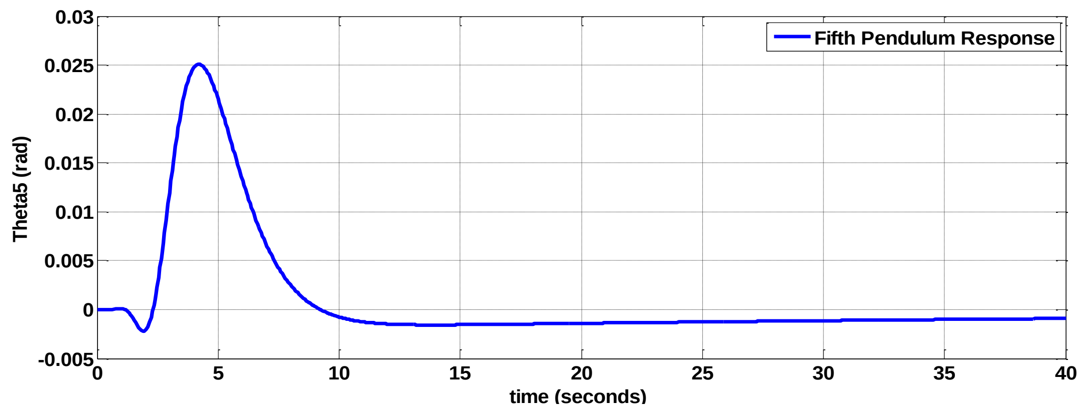

Figure 4.17 Fifth Pendulum Response (First Case)

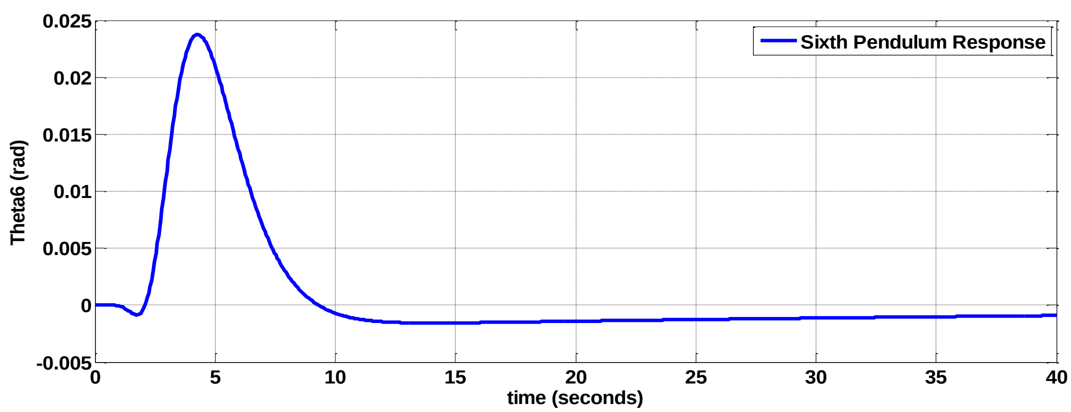

Figure 4.18 Sixth Pendulum Response (First Case)

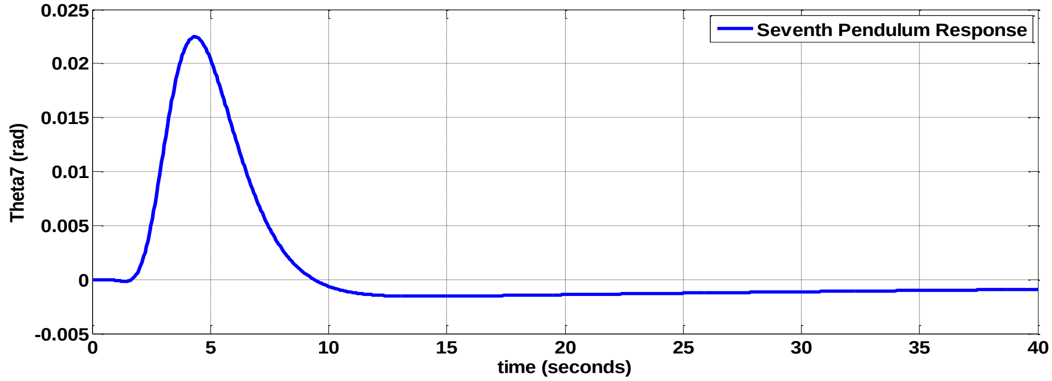

Figure 4.19 Seventh Pendulum Response (First Case)

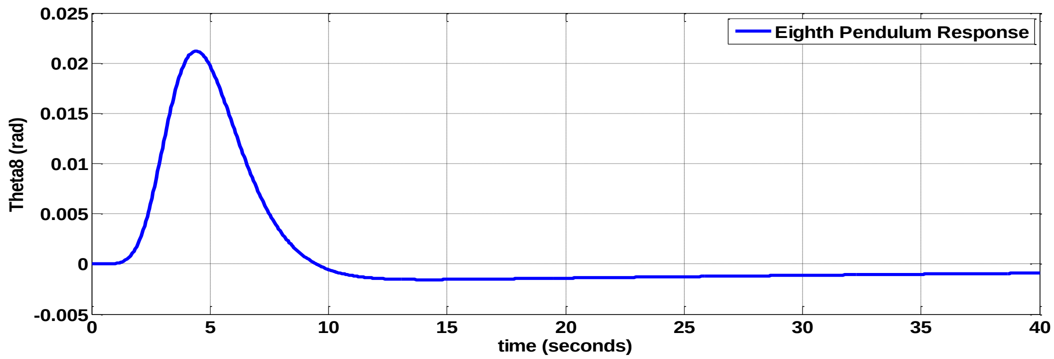

Figure 4.20 Eighth Pendulum Response (First Case)

Figures 4.13 to 4.20 show the responses of all the eight pendulums respectively. It can deduce from these plots that the pendulums finally attain a steady state over a period of about 13seconds but with a steady state error (an angular deflection of about 0.02rad (0.115^0) and maximum overshoot of about 2.21%.

4.3.2 Second Case

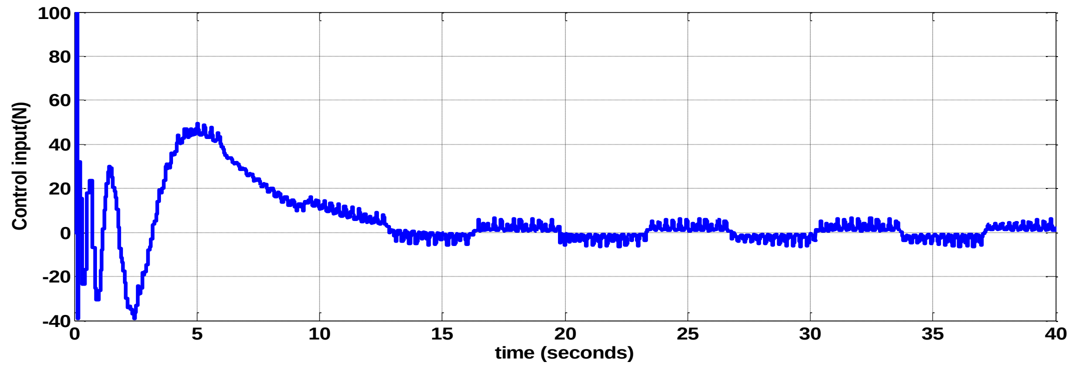

Figure 4.21 Control Signal (Second Case)

When R was reduced from 1 to 0.6 and the values of Q_{ii} are increased, a significant decrease in the control effort was observed as compared to the one in case one (see Figure 4.1.) but with some noise introduced. This is as a result of change of weighting factor corresponding to the control input (see Table 4.1).

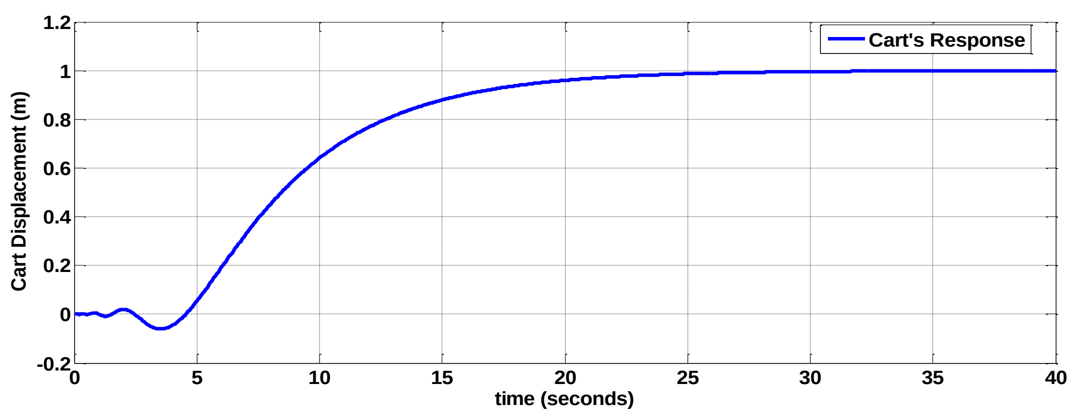

Figure 4.22 Cart's Response (Second Case)

This shows a better response as compared to the first case. This is as a result of change in the weighting matrix corresponding to the cart's position. It can be seen the cart initially oscillates, rises and finally reaches a steady state in 26seconds with zero overshoot.

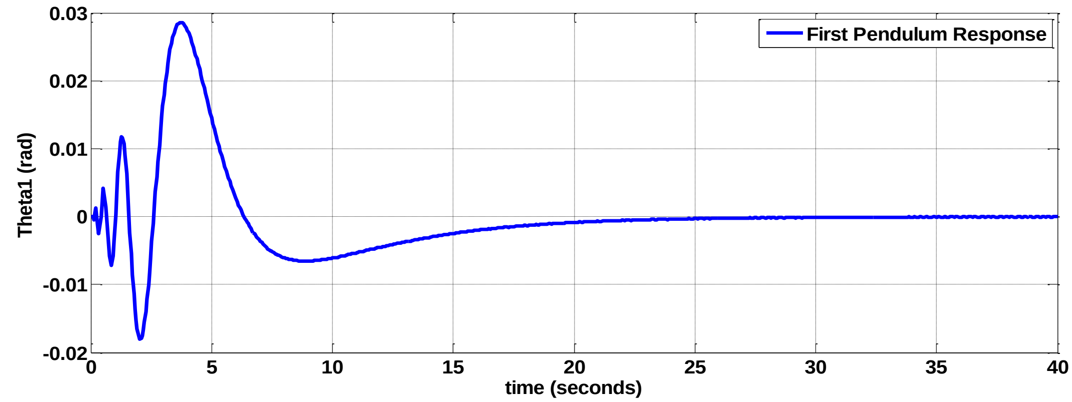

Figure 4.23 First Pendulum Response (Second Case)

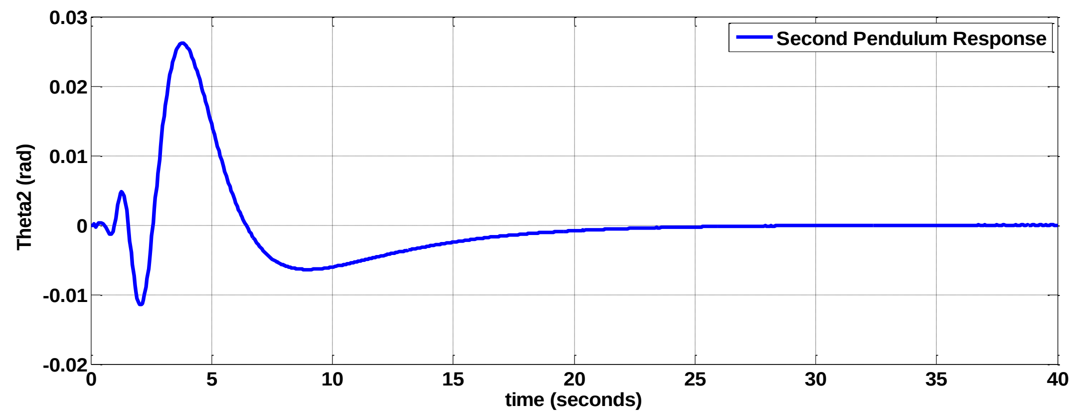

Figure 4.24 Second Pendulum Response (Second Case)

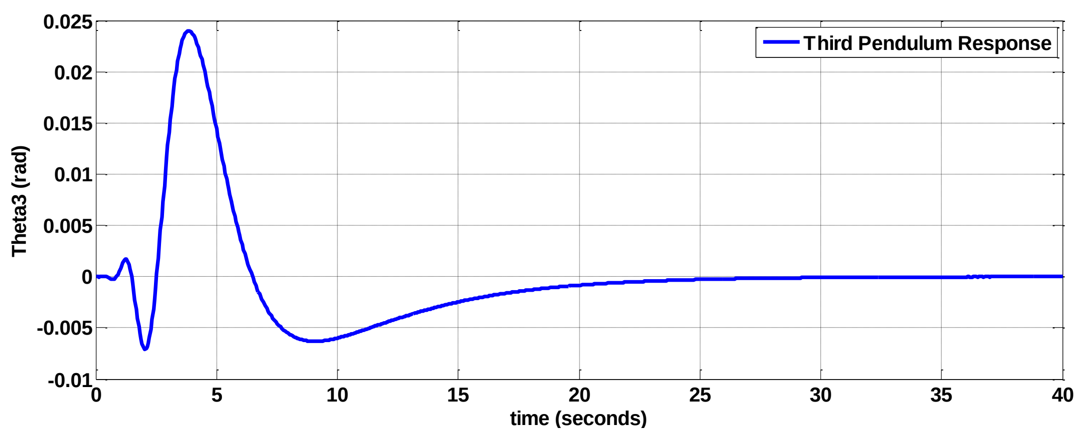

Figure 4.25 Third Pendulum Response (Second Case)

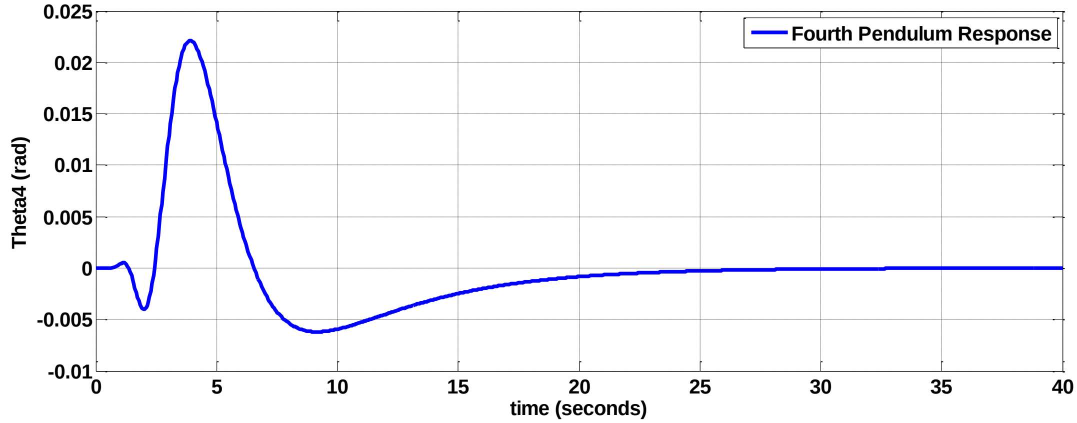

Figure 4.26 Fourth Pendulum Response (Second Case)

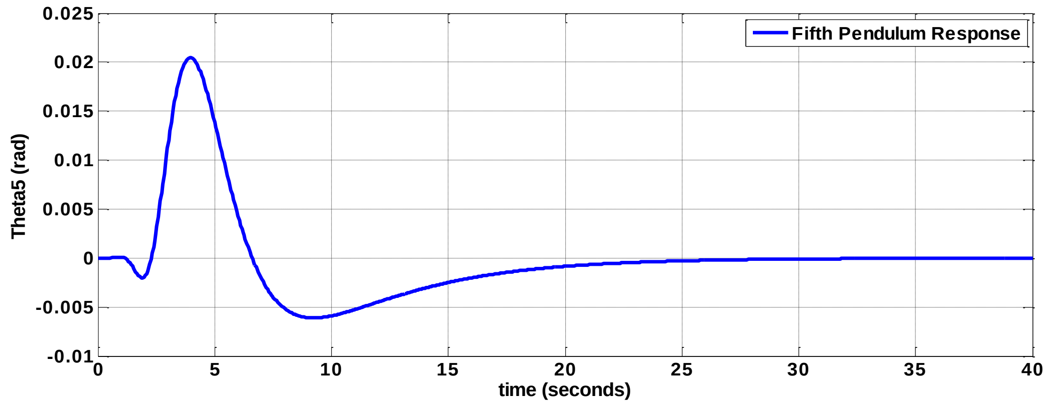

Figure 4.27 Fifth Pendulum Response (Second Case)

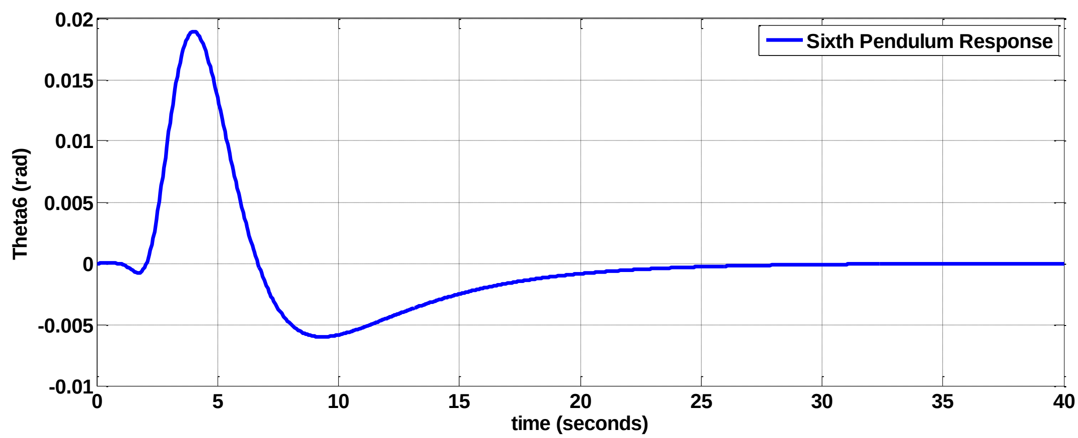

Figure 4.28 Sixth Pendulum Response (Second Case)

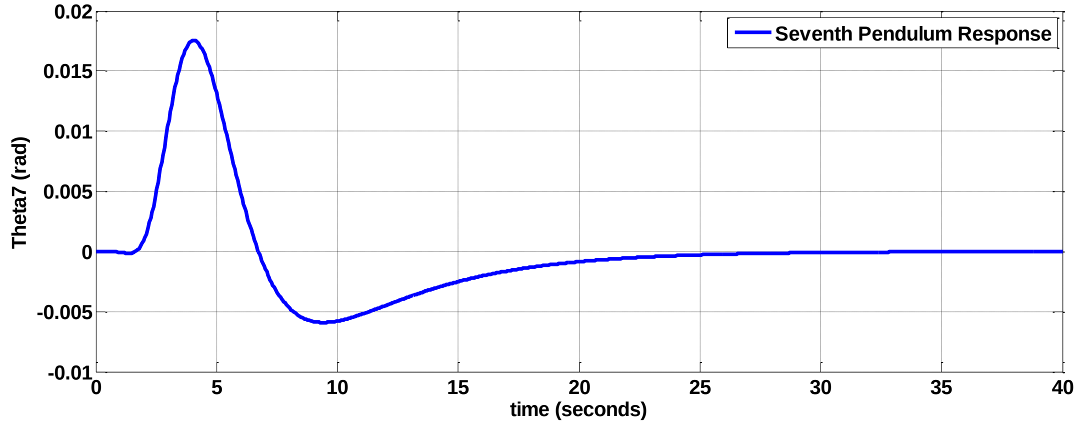

Figure 4.29 Seventh Pendulum Response (Second Case)

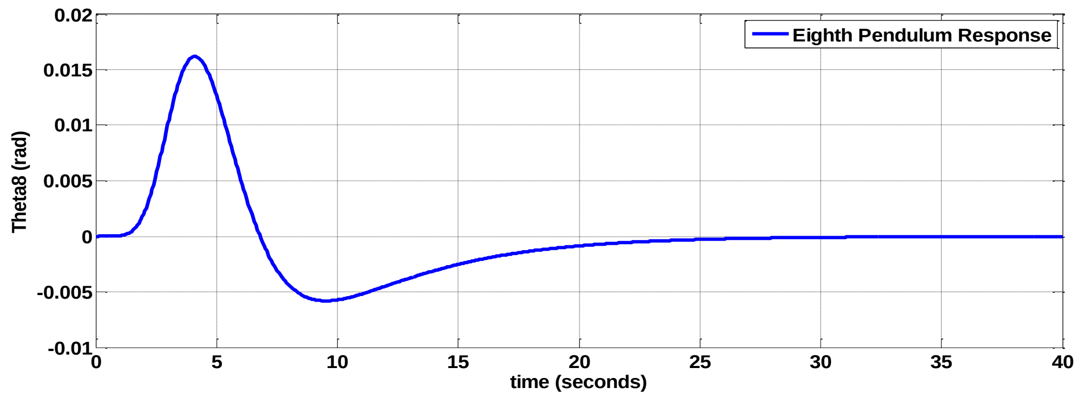

Figure 4.30 Eighth Pendulum Response (Second Case)

The pendulum plots in Figures 4.23 to 4.30 depict the responses of the pendulums. It can be seen from the plots that the maximum overshoots for all the pendulums are within the specified value (less than 2%) but the settling time for all the pendulums is 26seconds. This is more than the specified value of less than 20seconds.

4.3.3 Third Case

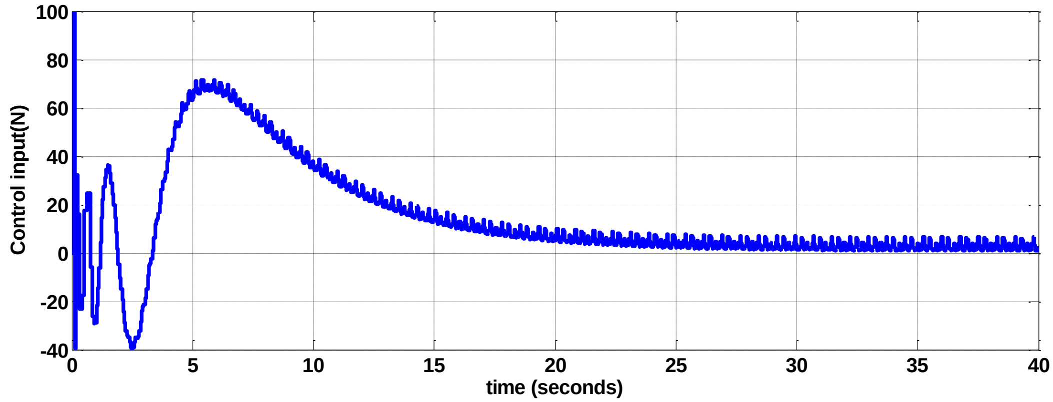

Figure 4.31 Control Signal (Third Case)

When R was increased from 0.6 to 0.8 and values of Q_{ii} were further increased, the control input signal and the noise are significantly reduced.

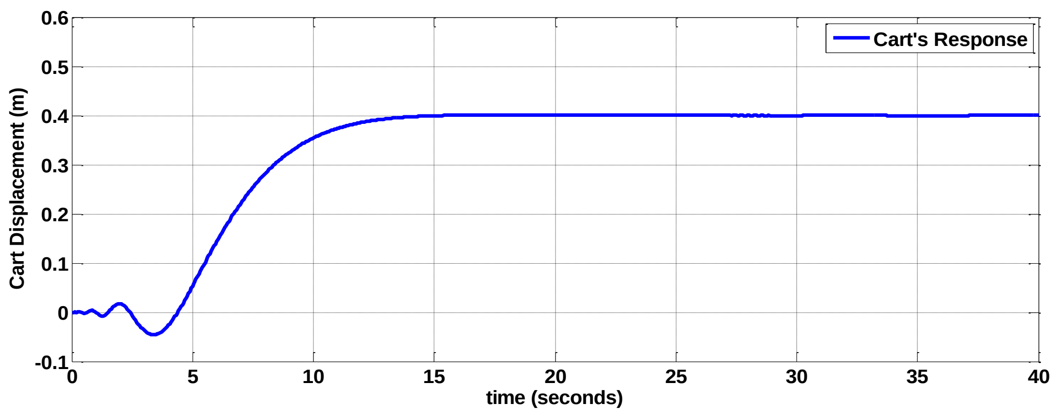

Figure 4.32 Cart’s Response (Third Case)

As the weighting value corresponding to the cart’s position is further increased, a better response is obtained. It can be seen from this plot that the steady state is attained at about 15 seconds with zero overshoot.

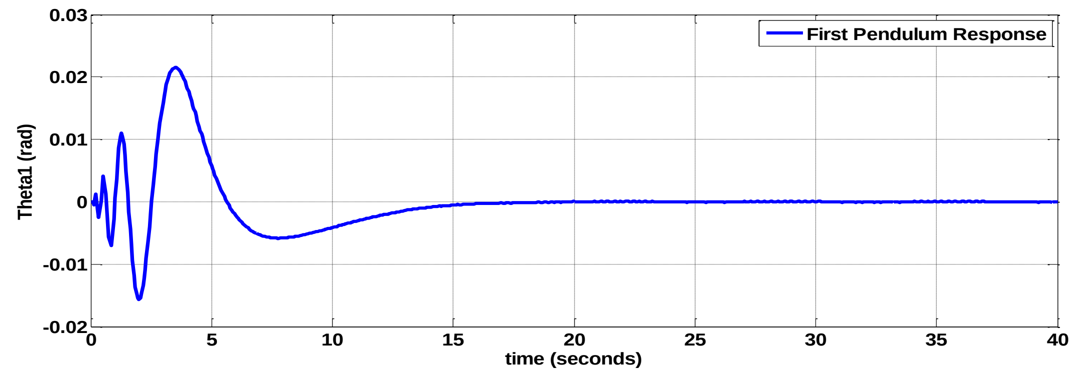

Figure 4.33 First Pendulum Response (Third Case)

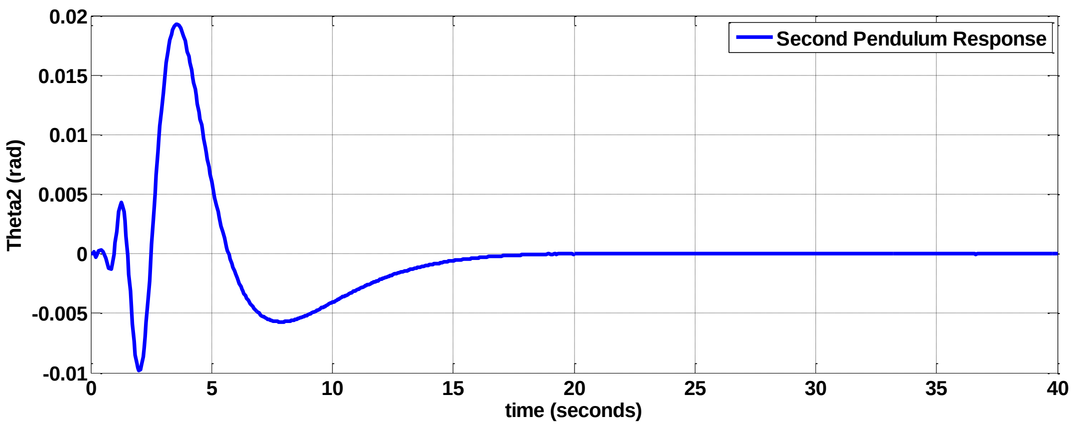

Figure 4.34 Second Pendulum Response (Third Case)

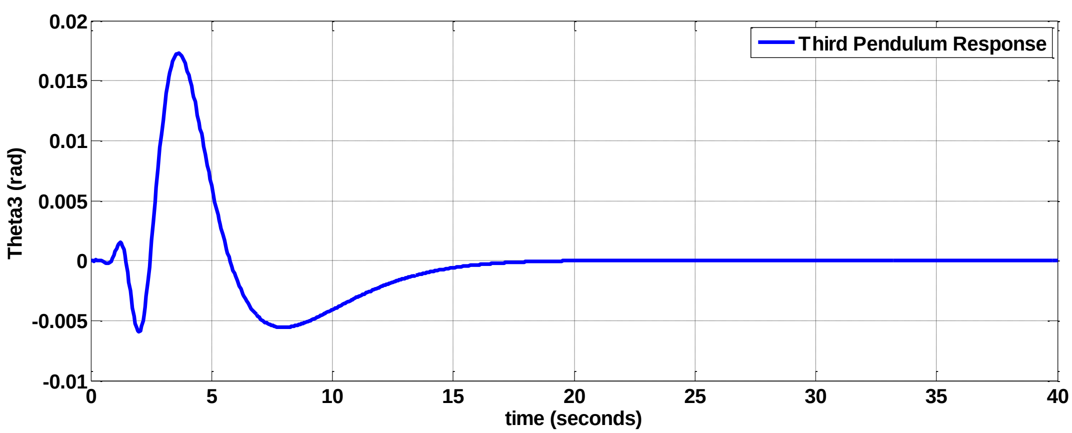

Figure 4.35 Third Pendulum Response (Third Case)

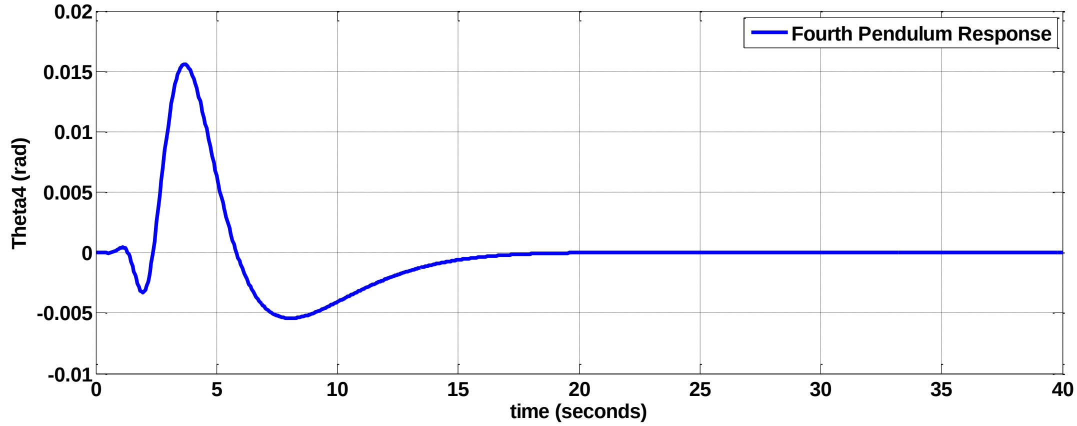

Figure 4.36 Fourth Pendulum Response (Third Case)

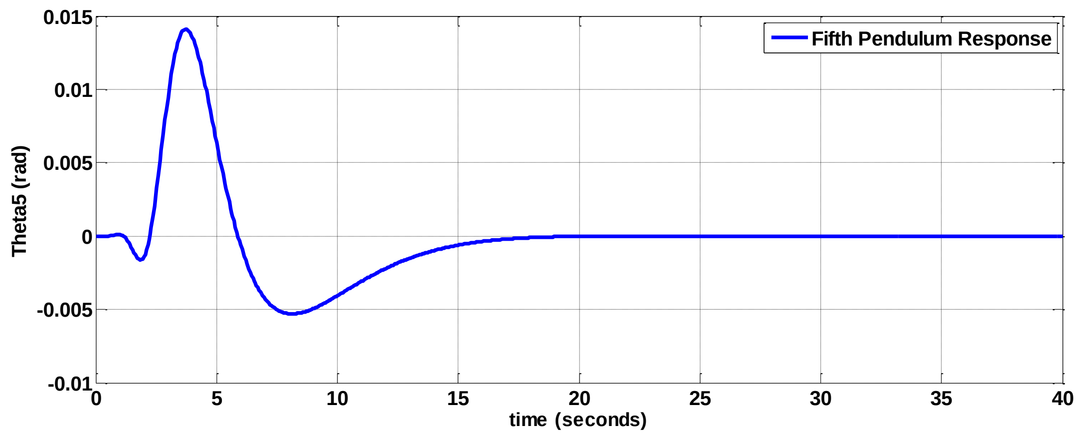

Figure 4.37 Fifth Pendulum Response (Third Case)

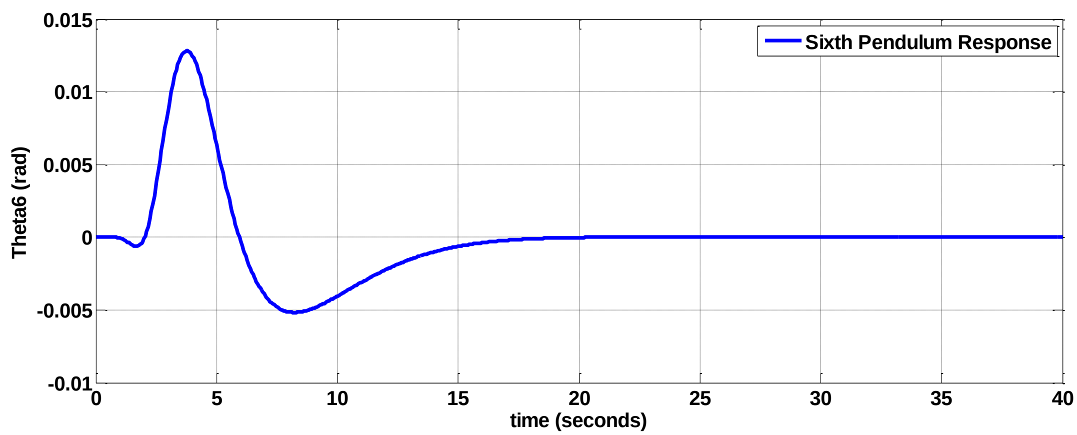

Figure 4.38 Sixth Pendulum Response (Third Case)

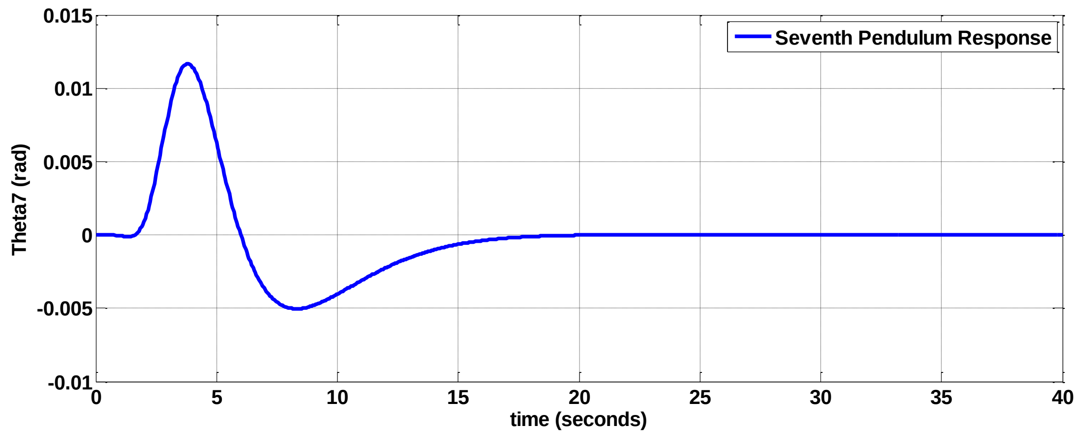

Figure 4.39 Seventh Pendulum Response (Third Case)

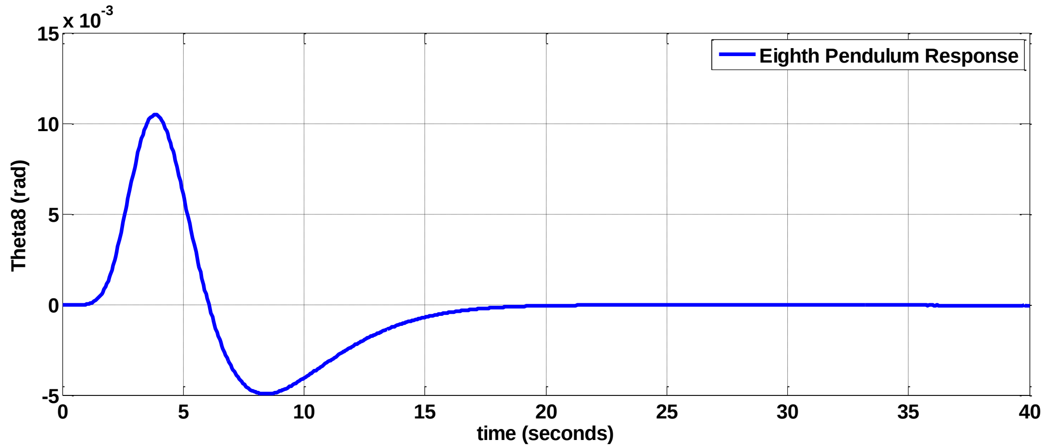

Figure 4.40 Eighth Pendulum Response (Third Case)

The results of responses in Figures 4.33 to 4.40 indicate that for the selected weighting matrices used all the controller design requirement have been satisfied (maximum overshoot less than 2% and settling time less than 20 seconds). However, the control effort is relatively expensive and needs to be further decrease. Although this may not constitute a problem once the specifications spelt are met, but further work may be required to see if the cost can be reduced.

4.3.4 Fourth Case

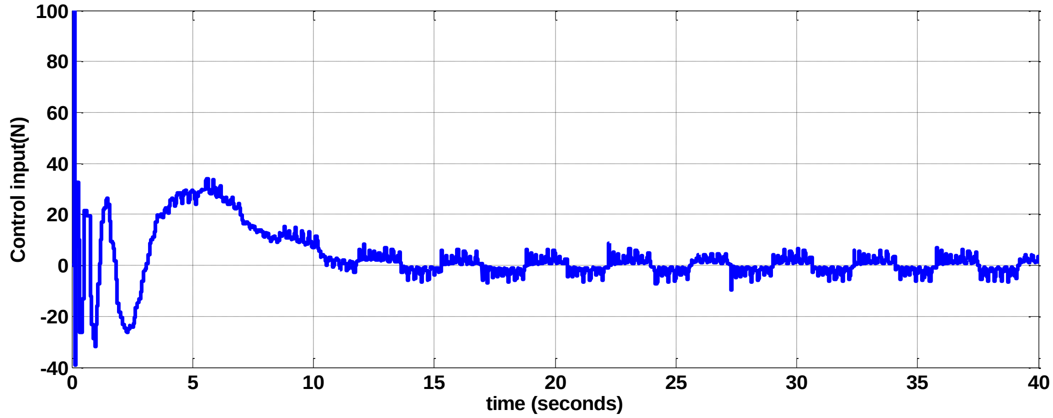

Figure 4.41 Control Signal (Fourth Case)

Further decrease in R and increase in Q_{ii} has resulted in a faster response but with more noise introduced.

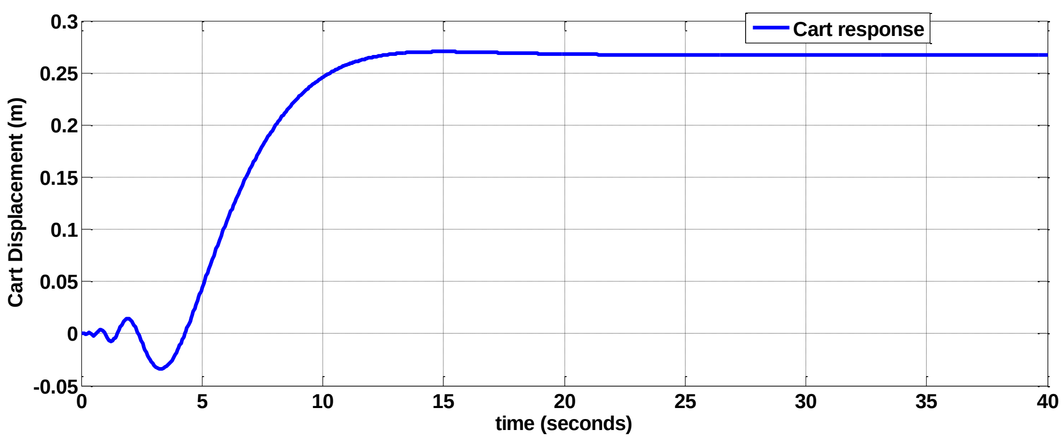

Figure 4.42 Cart's Response (Fourth Case)

Increase in the weighting value corresponding to the car's position gives a better response with respect displacement of the cart from its reference point to maximum distance it will cover before reaching a steady state. It can also be seen that no overshoot is observed.

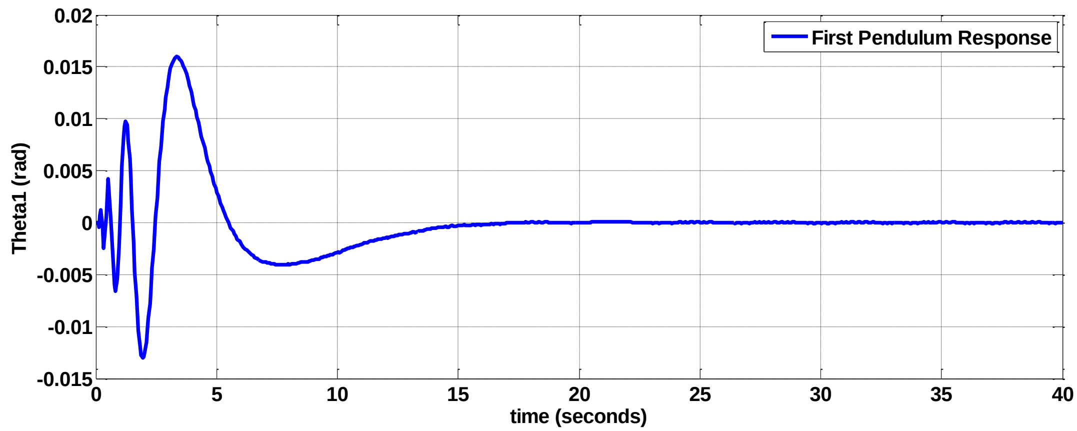

Figure 4.43 Fist Pendulum Response (Fourth Case)

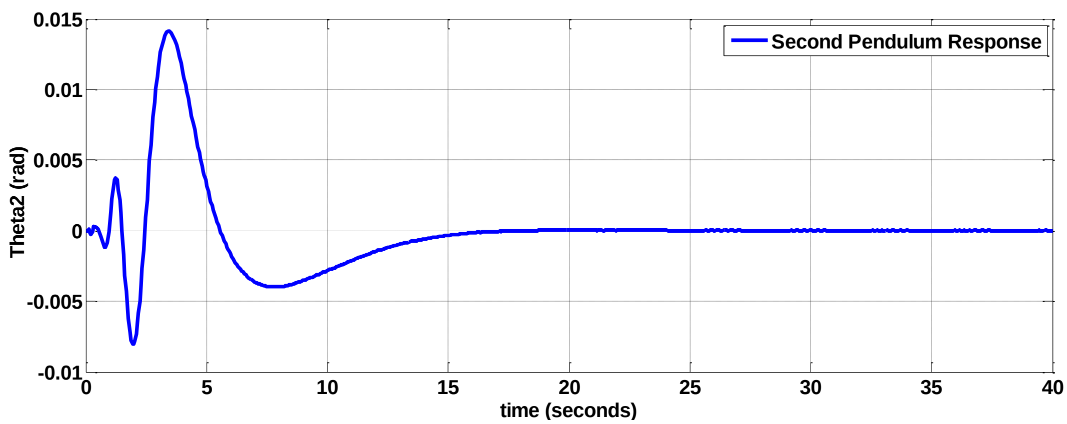

Figure 4.44 Second Pendulum Response (Fourth Case)

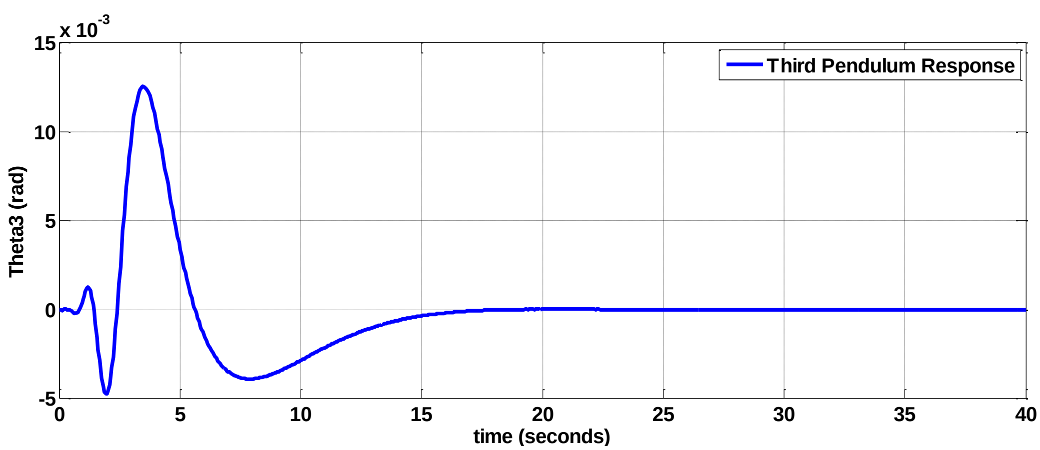

Figure 4.45 Third Pendulum Response (Fourth Case)

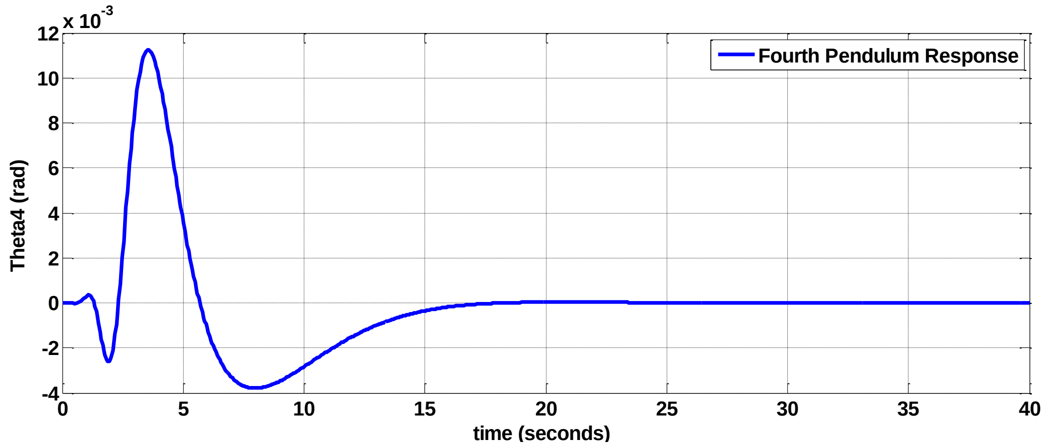

Figure 4.46 Fourth Pendulum Response (Fourth Case)

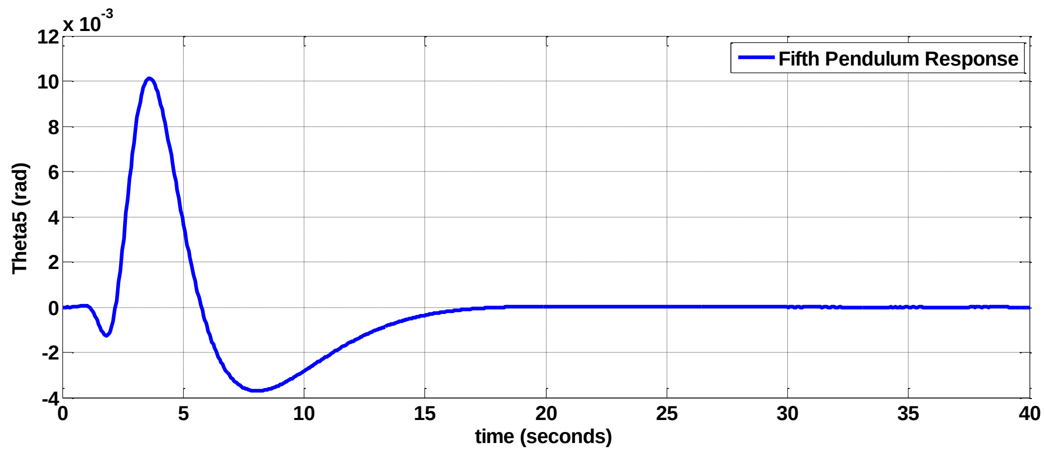

Figure 4.47 Fifth Pendulum Response (Fourth Case)

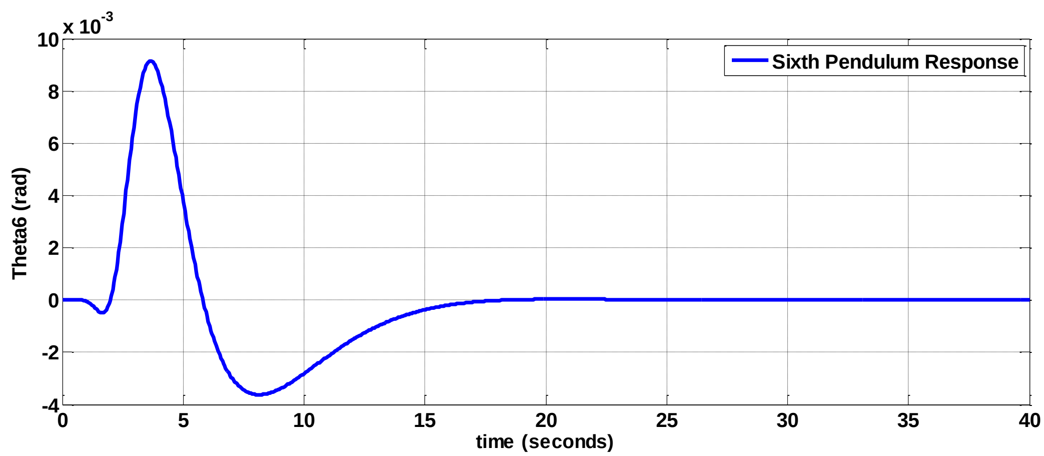

Figure 4.48 Sixth Pendulum Response (Fourth Case)

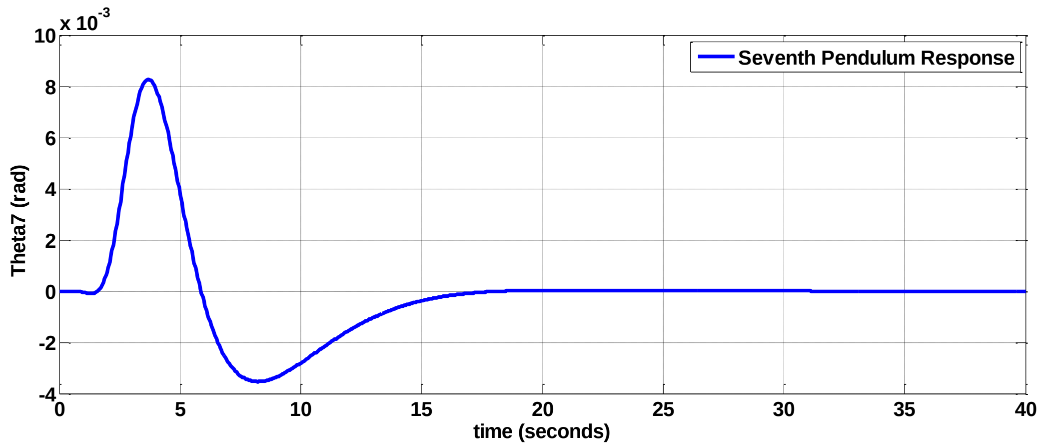

Figure 4.49 Seventh Pendulum Response (Fourth Case)

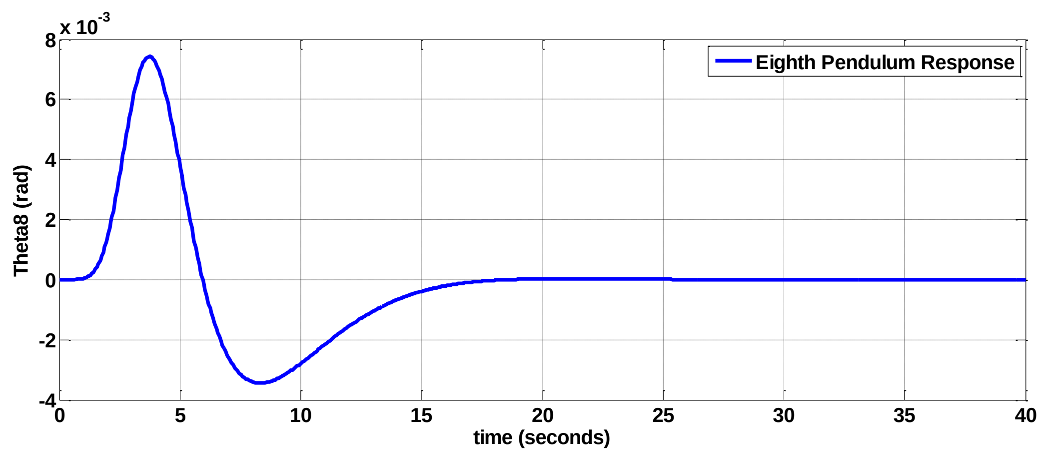

Figure 4.50 Eighth Pendulum Response (Fourth Case)

It can be deduced from Figures 4.43 to 4.50 that the pendulums responses with respect to the inverted position according to the design requirements (zero overshoot for the cart's response and less than 2% maximum over shoot, settling time less than or equal to 20 seconds and zero steady state error) have been achieved.

The stability of the pendulums with respect to the inverted position has already been achieved in all the four cases. It is important, however, to select the case that gives the best optimal response in terms of smoothness and conformity with the design specifications spelt out. On the basis of this, the third Case has been found to give the required optimal responses in accordance with the design specifications and smooth input control signal with minimal noise (see Figure 4.31). Therefore, a controller with gain matrix *K3* was chosen (Table 4.2).

Table 4.2 Controller Gain Values

Controller Gain for the First Case *(1.0e+06)	
K1	0.0000 0.0001 -0.0079 -0.0105 0.3848 -1.5283 2.5796 -2.0166 0.5994 0.0000 -0.0000 -0.0003 0.0030 -0.0016 -0.0409 0.1231 -0.1316 0.0490
Controller Gain for the Second Case *(1.0e+06)	
K2	0.0000 0.0001 -0.0081 -0.0091 0.3848 -1.5506 2.6429 -2.0838 0.6245 0.0000 0.0000 -0.0003 0.0031 -0.0018 -0.0410 0.1258 -0.1362 0.0514
Controller Gain for the Third Case *(1.0e+06)	
K3	0.0000 0.0001 -0.0086 -0.0045 0.3857 -1.6237 2.8422 -2.2885 0.6987 0.0001 0.0000 -0.0002 0.0032 -0.0026 -0.0416 0.1344 -0.1501 0.0584
Controller Gain for the Fourth Case *(1.0e+06)	
K4	0.0000 0.0001 -0.0093 0.0018 0.3873 -1.7263 3.1177 -2.6004 0.8116 0.0001 0.0001 -0.0002 0.0035 -0.0038 -0.0426 0.1475 -0.1712 0.0691

Table 4.3 Closed-Loop Eigen Values

	First Case	Second Case	Third Case	Fourth Case
Eigen-values (E)	-1.6465	-1.6420	-1.6022 + 0.0525i	-1.6078 + 0.1095i
	-1.5472	-1.5528	-1.6022 - 0.0525i	-1.6078 - 0.1095i
	-1.2636	-1.2509	-1.2253 + 0.0932i	-1.2290 + 0.1518i
	-1.1581	-1.1763	-1.2253 - 0.0932i	-1.2290 - 0.1518i
	-1.0066	-0.9719	-0.9616 + 0.1239i	-0.9660 + 0.1843i
	-0.8583 + 0.0329i	-0.9206	-0.9616 - 0.1239i	-0.9660 - 0.1843i
	-0.8583 - 0.0329i	-0.7995	-0.7597 + 0.1213i	-0.7748 + 0.1723i
	-0.6637 + 0.0316i	-0.7198	-0.7597 - 0.1213i	-0.7748 - 0.1723i
	-0.6637 - 0.0316i	-0.6128	-0.5705 + 0.0988i	-0.5866 + 0.1415i
	-0.4815 + 0.0207i	-0.5354	-0.5705 - 0.0988i	-0.5866 - 0.1415i
	-0.4815 - 0.0207i	-0.4243	-0.3984 + 0.0742i	-0.4155 + 0.1201i
	-0.3249 + 0.0131i	-0.3840	-0.3984 - 0.0742i	-0.4155 - 0.1201i
	-0.3249 - 0.0131i	-0.2641 + 0.0253i	-0.2695 + 0.0501i	-0.2738 + 0.1004i
	-0.2041 + 0.0066i	-0.2641 - 0.0253i	-0.2695 - 0.0501i	-0.2738 - 0.1004i
	-0.2041 - 0.0066i	-0.1455 + 0.0153i	-0.1613 + 0.0613i	-0.1557 + 0.0825i
	-0.0022	-0.1455 - 0.0153i	-0.1613 - 0.0613i	-0.1557 - 0.0825i
	-0.0976	-0.0220	-0.0425 + 0.0209i	-0.0377 + 0.0249i
	-0.0894	-0.0695	-0.0425 - 0.0209i	-0.0377 - 0.0249i

Table 4.3 shows the eigenvalues of the closed-loop system (DQIP) with feedback controller (LQR). It can be seen from Table 4.3 that all the eigenvalues are either negatives or complex pair. This means that all the roots of the characteristic equation are located in the negative half of the s-plane; and this, from control perspective is an indication of stability. The third case gave the best responses in accordance with the defined specifications. Therefore, the egienvalues of obtained in the third case were plotted in a complex s-plane Figure 4.51.

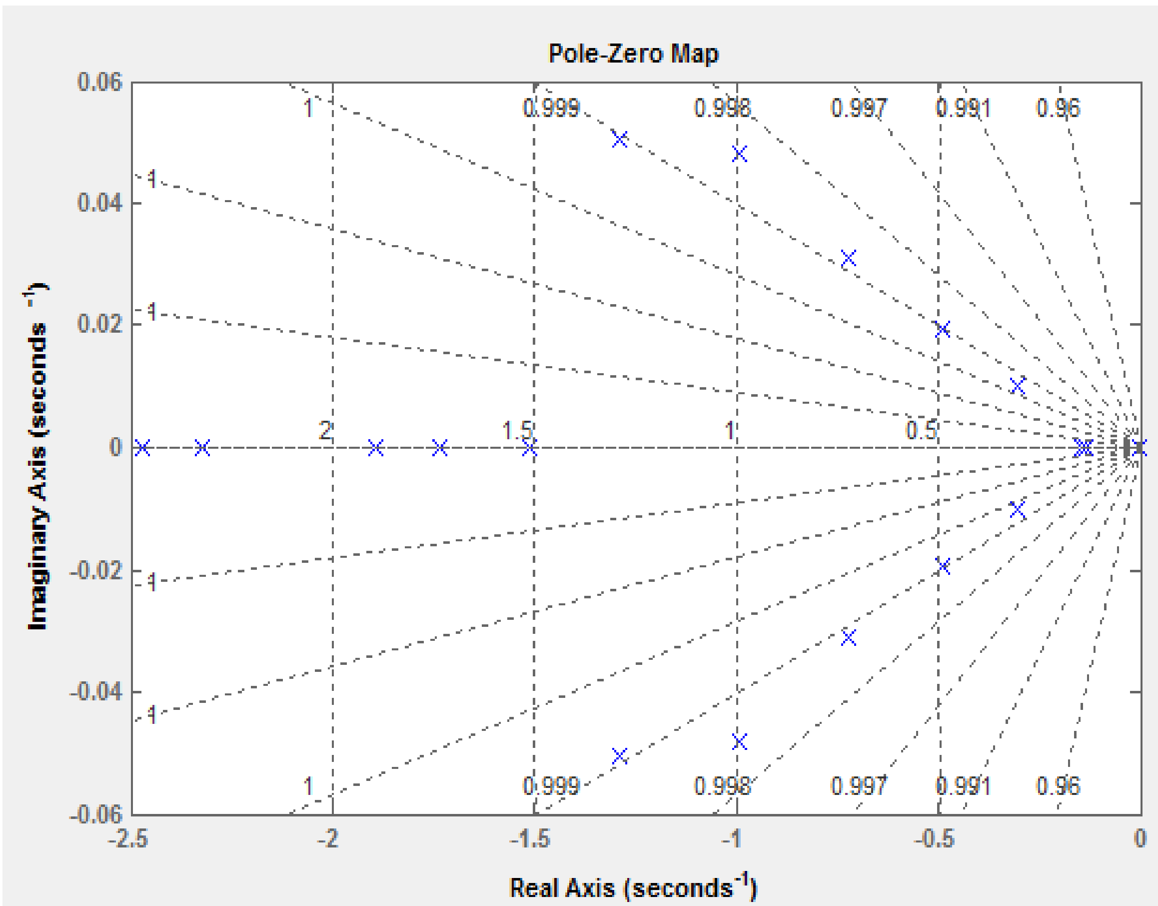

Figure 4.51 Pole-Zero Plot of the Eigenvalues of the DQIP System with the Controller**.**

It can be seen from Figure 4.51 that all the eigenvalues are located at the half left side of the s-plane. This confirms that DQIP is asymptotically stable with a feedback controller. And this also means that the controller was able to stabilize the DQIP. The details of how the pole-zero map was plotted is in the Appendix B2.

4.4 Conclusion

Stability analysis of the DQIP System with and without controller has been presented. The design and implementation of linear quadratic regulator controller (LQR) for DQIP have been accomplished. The open-loop responses show that DQIP is unstable without a feedback controller. The LQR controller was tuned to different weighting matrices. This gave rise to different time responses in accordance with the selected values of the weighting matrices. Optimal performance of the controller was analyzed in four different cases. Form theses cases, third case has been found to provide the controller with the best optimal performance in terms overshoot, settling time and steady state error as specified in design requirements. The results from the various plots and the egeinvalues have shown that both asymptotic and BIBO stabilities have been attained. This, therefore, means that the LQR controller has been able to stabilize the DQIP about an upright position.

CHAPTER FIVE

CONCLUSION AND RECOMMENDATIONS

5.1 Introduction

In this chapter the summary of the research contribution is presented. The summary of the entire thesis is captured in the conclusion. The work in this thesis has been limited to simulation in a virtual environment. However, areas for further works which include prototyping have been recommended. Finally, limitations encountered are also explicitly outlined.

5.2 Significant Contribution of the Research

So many works have been done in the area of control and stabilization of inverted pendulum. Most of the works in this area are limited to either single, double or triple inverted pendulum with very few works reported in literatures on quadruple inverted pendulum. The following are contributions this research:

i. From the study of inverted pendulum, a multi-link inverted pendulum system has been developed with particular emphasis on DQIP.

ii. Comprehensive Simulink model of the DQIP from which the QIP model was extracted has been presented.

iii. The stability issue latent within a multi-link inverted pendulum system has been investigated and addressed.

iv. The viability of LQR controller to stabilize a multi-link inverted pendulum has been achieved.

5.3 Limitations

1. The scope of this research is limited to simulation in a virtual environment using MATLAB/Simulink R2012a. Therefore, the model could be developed and implemented in real time to verify its validity.
2. Development of the comprehensive simulation models of the DQIP system.
3. Difficulty in getting the experimental values of the DQIP parameters.

5.4 Conclusion

Inverted Pendulum is a classical control problem that is widely used in teaching linear and nonlinear control systems. Different configurations of inverted pendulum system from linear to circular with one, two or three links have been reported with few literatures on inverted pendulum with four links. The applications of inverted pendulum system in robotics engineering, modeling of human postural standing missile guidance and space ships have also been widely reported. This thesis presents analytical approach to modeling of a multi-link inverted pendulum system with nine degree of freedoms. The nonlinear equations representing the dynamics of the DQIP were derived from the first Principle based on Eular-Lagrange equation. The equations were then compressed to a single linear equation to represent the nonlinear model of the DQIP. The resulting nonlinear model was than linearized using Jacobian matrix based on Taylor's series expansion. State space representation was used to present the linear model in state space form.

Linear and nonlinear Simulink models of the DQIP were developed based on the linear and nonlinear model equations using MATLAB/Simulink control tool box. QIP model was extracted from the DQIP. The extracted model was compared with similar models reported in literature to ascertain the validity of the developed DQIP model.

LQR controller was designed and implemented in MATLAB/Simulink to stabilize DQIP about an operating position (inverted position). A state observer model was in-cooperated along side with the LQR controller to measure those state that are not readily available for measurement. This inclusion does not seem to cause any deterioration of the controller performance.

Although the analysis in the thesis was limited to simulations in a virtual environment (MATLAB® 2012a), a real time experimental set up has been proposed. The results of the time responses of different pendulums and the movable cart have shown the viability of LQR algorithm in stabilizing a system of such order. The success of this research could serve as an avenue to modeling of complex under actuated dynamic systems of higher degree of freedoms. By simply adjusting the RQ/ ratio, desired fast response at a reasonably small control effort has been achieved.

5.5 Recommendations for Further Works.

The following are the recommendations for further work:

1. Experimental modeling of the DQIP: This will involve integrating the DC motor voltage-torque model equation and also attachment of the encoder to measure the angular displacement of the pendulums.

2. A hinge joint was used so that the pendulums movements were restricted to only two-dimensional plane. A three-dimensional plane could be used so that a more general dynamic behaviour could be developed.
3. The use of Adaptive Kalman Filter (AKF) and Quadrature Encoder Quantization Compensation (QEQC) could be investigated in order to minimize noise and modeling errors due to linearization of the model.
4. The use of symbolic modeling technique for the modeling of the DQIP could be investigated using such tools as MAPLE software, MATHEMATICA, etc.

REFERENCES

Abdullah J., Ruslee R., and Jalani J. (2011). Performance Comarison between LQR and FLC for Automatic 3 DOF Crane Systems. *International Journal of Control and Automation Volume 4.*

Agrachev A. A., Morse A. S., Sontag E. D., Sussmann H. J. and Utkin V. I., (2004). Nonlinear and Optimal Control Theory, *C.I.M.E., Cetraro, Italy*.

Ahmed A., Hashim O. (2012). Optimal Speed Control for Direct Current Motors using Linear Quadratic Regulator. *Journal of Science and Technology, Volume 13*.

Aloulou A. and Boubaker O., (2010). Control of a step walking combined to arms swinging for a three dimensional humanoid prototype. *Journal of Computer Science, Vol. 6, pp. 886-895.*

Araki, Mituhiko, (2002).PID control. Control systems, Robotics and Automation, volume 2.

Astrom, K.J. and Furuta, K. (1996). Swinging up a pendulum by energy control. *IFAC 13th World Congress, San Francisco.*

Anderson and J. B. Moore (1989). Optimal Control, A linear Quadratic Methods, *New Jersey, Prentice Hall.*

Andrei N. (2006). Modern Control Theory. Studies in Informatics and Control 15, 51, *Research Institute for Informatics, Center for Advanced Modeling and Optimization, Romania.*

Arous Y. and Boubaker O., (2012). Gait trajectory generation for a five link bipedal robot based on a reduced dynamical model. *In Proceedings of the 16th IEEE Mediterranean Electro-technical Conference, Yasmine Hammamet, pp. 993-996.*

Bawek D. (2012). Design and Implimentation of a Control System for a Quadrotor MAV. MSc *Thesis, University of Maryland.*

Bogdanov, A. (2004). Optimal control of a double inverted pendulum on a cart. *Oregon Health and Science University, Tech. Rep. CSE-04-006, OGI School of Science and Engineering, Beaverton, OR.*

Boubaker O. (2012). The Inverted Pendulum Benchmark in Nonlinear Control Theory: A Survey. *International Jounrnal of Advanced Robotic Systems, Volume 10.*

Boubaker O. (2013). The Inverted Pendulum Benchmark in Nonlinear Control Theory: A Survey. *International Jounrnal of Advanced Robotic Systems, Volume 10.*

Braslavsky J. H. (n, d). Control Systems Design. *(Lecture note)*, University of Newcastle.

Bryson A. E. Jr. and Yu-Chi H. (1975). Applied Optimal Control. *USA Hemisphere Publishing Corporation.*

Cannon R. H and Schaefer J. F., (1966). On the control of unstable mechanical systems. *In Proceedings of the third Automatic and Remote Control, London, vol. 3, pp. 12-24, 1966.*

Carlsson B. and ÖRBÄCK P. (2009). Mobile Inverted Pendulm-Control of an unstable process using open source real-time operating system. *MSc Thesis, Department of Signals and Systems, Division of Automatic Control, Chalmers University of Technology, Gothenburg, Sweden. Report No. EX055/2009.*

Cibilić A. Antonić R. and Golub, I., (2010). Application of fuzzy logic in control system using simulator Gunt RT124. *Conference Proceedings of the 14th International Research/Expert, Mediterranean Cruise.*

Chye T. K and Sang, T. C, (1999). Rotary Inverted Pendulum. B.Eng Project, *School of Electrical and Electronic Engineering, Nanyang Technological University, Chaina.*
Claudiu C. Remsing, (2006). Optimal Control.

Damen A. and Weiland S., (2002). Robust control. Measurement and Control Group Department of Electrical Engineering, Eindhoven University of Technology.

Das S., Pan I., Halder K., Das S. and Gupta A. (2013). Optimum Weight Selection based on LQR formulation for the Design of Fractional Order PIλDμ Controllers to Handle a Class of Fractional Order Systems. *In Computer Communication and Informatics (ICCCI), 2013 International Conference on (IEEE), pp. 1-6.*

Dorf R. C. and Bishop R. H. (2011). Modern Control Systems *(Twelfth ed.), pp. 189-228.*

Doran C. and Lasenby A.N., (2003). Geometric algebra for physicists. *Cambridge University Press New York.*

Driver J. and Thorpe D. (2004). Design , Build and Control of Single/Double Rotational Inverted Pendulum. *MSc Thesis University of Adelaide, School of Mechanical Engineering , Australia.*

Duan B, Ling Keck-voon, Mir H., Hosseini M. and Gay, R.K.L., (2005). An online laboratory Framework for Control Engineering Courses. *International Journal of Engineering Education, Volume 21, No. 6, ISBN 0949-149X, Tempus Publications Dublin INST Technology, Bolton ST, Dublin, Ireland.*

Elgerd O. I. (1966). Control Systems Theory. *Tokyo McGraw-Hill.*

Fantoni I., and Lozano R. (2003). Global Stabilization of the Cart-Pendulum System using Saturation Functions. *Proceedings of the 42nd IEEE Conference on Decision.*

Fernandez-Cara E. and Zuazua E. (2003). Control Theory: History, Mathematical Achievement and Perspectives. *Notes, Universidad de Sevilla and Universidad Autonoma Madrid, Spain.*

Geun H. L. and Suel J. (2008). Control of Inverted Pendulum System Using a Neuro-Fuzzy Controller for Intelligent Control Education. *IEEE International Conference on Mechatronics and Automation, pp. 965-969.*

Giraldo L. (2008). LQR for A Multi-Inverted Pendulum using Maple. *In CSC, pp. 242-245.*

Graf C. and R¨ofer T. (2012) A closed-loop 3D-LIPM gait for the RoboCup Standard Platform League humanoid. *In Proceedings of the Fifth Workshop on Humanoid Soccer Robots.*

Gu, Da-Wei, Petkov P.H, Konatantinov M.M., (2013). Robust control design with MATLAB® (2nd ed.). Springer, *Advaced Textbooks in Control and Signal Processing, Volume 1, ISBN-10: 1852339837.*

Gupta V., Hassibi B., and Murray R. M. (2007). Optimal LQG Control across packets-dropping links. *Systems and Conrol Letters Volume 56, pp. 439-449.*

Jadlovska, S, and Jadlovska A. (2009). A Simulink library for inverted pendula modeling and simulation. *In 17th Annual Conference Proceedings of the International Scientific Conference-Technical Computing Prague.*

Jadlovská S. and Jadlovská A., (2010). Inverted Pendula Simulation and Modeling–a Generalized Approach. *Proceedings of the 9th International Scientific–Technical Conference on Process Control, University of Pardubice, Czech Republic, ISBN 978-80-7399-951-3.*

Jadlovska S. and Sarnovsky, J. (2011). An extended Simulink library for modeling and control of inverted pendula systems. *In Proceeding of the International Conference in Technical Computing Prague.*

Jadlovska S. and Sarnovky J. (2012). Classical double Inverted Pendulum Systems A complex overview of a system in Applied Machine Intelligence and Informatics (SAMI). *IEEE 10th International Symposium on (IEEE), ISBN 978-1-4577-0196-2, pp 103-108.*

Jadlovska S. and Sarnovky J. (2013). Modeling of Classical and Rotary Inverted Pendulum Systems A Generalized Approach. *Journal of Electrical Engineering Volume 64, pp12-19, ISSN 1335-3632*.

Jansson A. and Klempic A. (2012). One Axel Light Weight Truck Dynamical Modeling and Implementation of a one Axel Vehicle. *MSc Thesis, Chalmers University of Technology, Gothenburg, Sweden. Report No. EX022/2012.*

Jarczyk J. C., Svaricek F. and Alt B. (2011). Strong Structural Contollability of Linear Systems revisited. In ECE, pp. 1213-1218.

Jiri M. and Frantisek G. (2010). Modeling, Identification and Simulation of the Inverted Pendulum PS600. *Department of Process Control, Faculty of Applied Informatics, Tomas Bata University in Zlin, Zlin Czech Republic, pp. 14-17.*

Junqi, G.W.C.W.L.U.O. (2007). Model building, simulation and real-time control of an inverted pendulum. *Journal of Shenzhen Institute of Information Technology Volume 2, 018.*

Kajita S., Morisawa M., Miura K., Nakaoka S., K., Harada and Kaneko K., (2010).Biped walking stabilization based on linear inverted pendulum tracking. *In Proceedings of the IEEE/RSJ 2010 International Conference on Intelligent Robots and Systems, Taipei, pp. 4489-449.*

Kailath T., (1980). Linear Systems. *Englewood Cliffs, Prentice-Hall.*

Kanellakopoulos I., Kokotovic P.V and Morse A.S., (1991).Systematic design of adaptive controllers for feedback linearizable systems. *Automatic Control, IEEE Transactions, V 36, No. 11, pp. 1241-1253.*

Khan J., Munawar K., Azeem R.A., and Salman M. (2009). Inverted pendulum with moving reference for benchmarking control systems performance. *In American Control Conference, pp. 3764-3768.*

Kiemel S., (2012). Balance maintenance of a humanoid robot using the hip-ankle strategy. *Master of Science Thesis, Department of Bio-Mechanical Design, Faculty of Mechanical, Maritime and Materials Engineering, Delft University of Technology.*

Kim J. and Faruqi F. (2010). A Design of Optimal Flight Controller for Genetic Linearized Missile Model in Hypersonic Regime. *Weapons Systems Division Defence Science and Technology Organisation, Edinburgh South Australia 5111 Australia.*

Kowalczyk P., Glendinning, P., Brown, M., Medrano-Cerda G., Dallali, H. and Shapiro J., (2012). Modelling human balance using switched systems with linear feedback control. *Journal of the Royal Society Interface, Volume 9 No. 67, pp. 234-245.*

Kwakernaak H. and Sivan R., (1972). Linear Optimal Control Systems, Wiley, New York.
Khalil H. K., (2002). Nonlinear Systems. *New Jersey, Prentice Hall, 2002.*

Kwon T. and Hodgins, J., (2010). Control systems for human running using an inverted pendulum model and a reference motion capture sequence. *Proceedings of the 2010 ACM SIGGRAPH/Eurographics Symposium on Computer Animation, Eurographics Association, pp. 129-138.*

Lam S., and Davison E.J. (2005). Real Stabiliy and Stabilizability Radii of the Multi-Link Inverted Pendulum. (Citeseer).

Lam S. and Davison E. J. (2006). The real stabilizability radius of the multi-link inverted pendulum. *In American Control Conference, 2006 (IEEE), p. 6.*

Lasenby A., Doran C. and Gull S., (1993). A Multivector Derivative Approach to Lagrangian field theory. *Foundations of Physics, Volume: 23(10), pp. 1295–1327.*

Lee G. H., Lee H. J, Choi H. J., Jeon H. J and Jung. S., (2009). Application of mobile inverted pendulum systems to Boxingbots for a boxing game. *Proceedings of the International Conference on Advanced Intelligent Mechatronics, IEEE/ASME, pp. 963-968.*

Lee E. and Perkins J. (2008). Comparison of Techniques for Stabilization of a Triple Inverted Pendulum.

Li, H., Zhihong M. and Jiayin W. (2002). Variable Universe Adapitive Fuzzy Control on the Quadruple Inverted Pendulum. *Science in China Series E: Technological Science Volume 45, No.2, pp.213-224.*

Li H., Wang J., Gu Y., and Feng Y., (2004). Hardware Implementation of the Quadruple Inverted Pendulum with Single Motor. *A project supported by the National Natural Science Foundation of China (Grant No. 60174013), pp. 1-4.*

Liu Y., Yu H., Wane S. and Yang T., (2008). On tracking control of a pendulum driven cart-pole underactuated system. *International Journal of Modelling, Identification and Control, vol. 4, pp. 357-372.*

Marcel L. and Giraldo C. (2008)**.** LQR Control for a Multi-Inverted Pendulum using MAPLE. Logic and Computation Group. EAFIT University, Medellin, Colombia.

Marholt, Jiří and Gazdoš, František, (2010). Modelling, identification and simulation of the inverted pendulum PS600. *Acta Montanistica Slovaca, Volume 15, No. 1, pp.14-18.*

Mathew N. J., Rao K. K. and Sivakumaran N. (2013). Swing Up and Stabilization Control of a Rotary Inverted Pendulum. *Preprints of the 10th IFAC International Symposium on Dynamics and Control of Process Systems, International Federation of Automatic Control, Mumbai, India, pp. 654-659.*

Mladenov V., Tsenov G., Ekonomou L., Harkiolakis N. and Karampelas P., (2006). Neural Network Control of an Inverted Pendulum on a Cart. *Proceedings of the 9th WSEAS International Conference on Robotics, Control and Manufacturing Technology, ISSN: 1790-5117, pp. 112-120.*

Morari M., and Furrer F. (2010). Control of an Autonomous Sailing Catamaran on the Concept of Hydrofoils.

Naslin P. (1968). Essentials of Optimal Control. London Iliffe Books Ltd.

Ogata K. (2007). Modern Control Engineering (4th ed.). Prentice –Hall of India Private Ltd.

Ni J. (2011). Control of the Spatial Double Inverted Pendulum. *MSc Thesis, McGill University Montreal, Canada.*

Oral O., Cetin L. and Uyar E. (2010). A Novel Method on Selection of Q and R Matrices in the Theory of Optimal Control. *International Journal of Systems Control. Volume 1, pp.84-92.*

Ozana S., Pies M., Slanina Z., and Hajovsky R. (2012). Design and Implementation of LQR Controller for Inverted Pendulum by use of REX Control System. *In control, Automation and Systems (ICCAS), 12th International Conference on (IEEE), pp. 356-359.*

Prasad L.B., Tyagi B., and Gupta H.O. (2011). Optimal control of nonlinear inverted pendulum dynamical system with disturbance input using PID controller & LQR. *In Control System, Computing and Engineering (ICCSCE), 2011 IEEE International Conference on (IEEE), pp. 540-545.*

Prasad L.B., Tyagi B. and Gupta H.O. (2012) Modelling and Simulation for Optimal Control of Nonlinear Inverted Pendulum Dynamical System Using PID Controller and LQR. *In Modelling Symposium (AMS), Sixth Asia (IEEE), pp. 138-143.*

Pulgar S., Silva E. and Salgado M. (2011). Optimal State-Feedback Design for MIMO Syatems subject to Multiple SNR Constraints. In Proceedings of the 18th IFAC World Congress, p. 14.

Quanser User Manual, (2004). L.M.S. Plants: IP01 and IP02. Single Inverted Pendulum.

Quintero, Steven A. P, (2001). Controlling the Inverted Pendulum. *Department of Electrical and Computer Engineering, University of California, Santa Barbara, pp. 1-5.*

Rashid Ab. and Sidek (2012). Controller Design Of Unicycle Mobile Robot. *IIUM Engineering Journal, Volume 13, No.2, pp.176-197.*

Roberge J. K., (1960). The Mechanical Seal. *Bachelor's thesis, Massachusetts Institute of Technology, USA.*

Samad T., (2009). Intelligent Control: *An Overview of Techniques. Wiley-IEEE Press, ISSN 0470545488.*

Singh N., and Yadav S. K. (2012). Comparison of LQR and PD controller for stabilizing Double Inverted Pendulum System. *International Journal of Engineering Volume 1, pp. 69-74.*

Shen J., Sanyal, A. K., and Chaturved, N. A. (2004). Dynamics and Control of ED Pendulum, *43rd IEEE Conference on Decision and Control, Bahamas.*

Stang J. (2005). The inverted Pendulum. *M.Eng Thesis (Cornell University).*

Stimac, A.K. (1999). Standup and stabilization of the inverted pendulum. *(Massachusetts Institute of Technology).*

Wright A. D. (2004). Modern Control Design for flexible Wind Turbines *(National Renewable Energy Laboratory).*

Xionga R., Suna Y. Chua, J., Zhoub C., (2010). An Inverted Pendulum Model Based Humanoid Gait Generation Using Convex Optimization. *Journal of Information and Computational Science, Volume 7: 12, pp. 2529-2538.*

MATHEWORKS Simulink Block Library. Retrieved from http://www.mathworks.com/ (June, 2013).

Yi J. and Yubanzaki N. (2000). Stabilization Fuzzy Control of Inverted Pendulum Systems. *Artificial Intelligence in Engineering. Ukyo, Kyoto 616-8303, Japan, pp. 153-155.*

Younis W. and Abdelati M., (2009). Design and implementation of an experimental segway model. *AIP Conference Proceedings, vol. 1107, pp. 350-354.*

Yundong, L.H.W.J.G. and Yanbin F. (2008). Hardware Implementation of the Quadruple Inverted Pendulum with Single Motor.

Zhang Q. (2002). Adaptive Observer for Multiple-Input-Multiple-Output (MIMO) Linear Time-Varying Systems. *Automatic Control, IEEE Transactions Volume 47, pp. 525-529.*

Zhang, Y., Wang, J., and Li, H. (2012). Stabilization of the quadruple inverted pendulum by variable universe adaptive fuzzy controller based on variable gain Hα regulator. *Journal of Systems Science and Complexity Volume 25, pp.856-872.*

APPENDIX A1
MATHEMATICAL DERIVATION OF THE DYNAMIC EQUATIONS OF THE DOUBLE QUAD INVERTED PPENDULUM SYSTEM

The Double-quad inverted pendulum has nine degrees of freedom and can thus be represented using nine generalized co-ordinates. These generalized co-ordinates are the horizontal displacement of the wheeled cart, *x* and the rotational displacement of the pendulum links, θ_n (n = 1, 2, 3, …, 8).

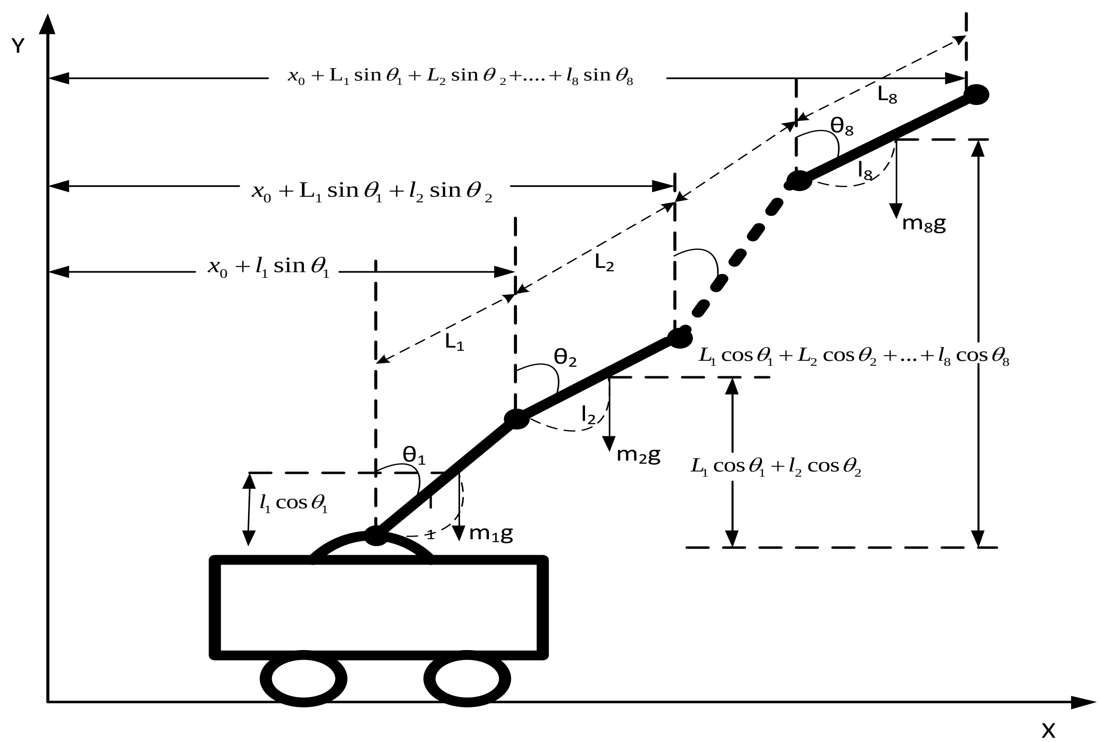

Figure A.1. Free body Diagram of the Double Quad Inverted Pendulum System.

Components of displacement with respect to the pendulum links center of gravities as in Figure A.1 are as follows:

$$S_x = x + l \sin\theta \qquad \text{A1.1}$$

$$S_y = l \cos\theta \qquad \text{A1.2}$$

If V_x and V_y are the components of velocity along horizontal and vertical axes, then;

$$V_x = \frac{dS_x}{dt} = \dot{x} + l\dot{\theta}\cos\theta \quad \text{A1.3}$$

$$V_y = \frac{dS_y}{dt} = -l\dot{\theta}\sin\theta \quad \text{A1.4}$$

Squaring equation (A1.1) and (A1.2) and add the results, gives the resultant velocity, given by;

$$V_R{}^2 = (\dot{x} + l\cos\theta)^2 + (-l\, sin\theta)^2 \quad \text{A1.5}$$

Where V_R is the resultant velocity given by;

$$V_R{}^2 = V_x{}^2 + V_y{}^2 \quad \text{A1.6}$$

The kinetic energy of a moving rod is given by; (Doran and Lasenby, 2003)

$$K\ 1/2\, m.E = V_R{}^2 + 1/2\ I\omega^2 \quad \text{A1.7}$$

$$K.E = 1/2\, mV_R{}^2 + 1/2\ I\dot{\theta}^2 \quad \text{A1.8}$$

(Where V_R is the linear velocity, m is the mass, I is the moment of inertia and ω is the angular velocity and is given by; $\omega = \frac{d\theta}{dt} = \dot{\theta}$).

Kinetic energy of the cart is given by;

$$K.E_0 = {}^1\!/_2\, m_c\dot{x}^2 \quad \text{A1.9}$$

Using equations (A1.6) and (A1.8), the kinetic energies of the various pendulum links can be written as:

For the first pendulum link, its kinetic energy based on equation (A1.8) is;

$$K.E_1 = 1/2\ m_1\left[\left(\dot{x} + l_1\dot{\theta}_1\cos\theta_1\right)^2 + \left(l_1\dot{\theta}_1\sin\theta_1\right)^2\right] + 1/2\ I_1\dot{\theta}_1{}^2 \quad \text{A1.10}$$

For the second pendulum link;

$$K.E_2 = 1/2\, m_2 \Big[\big(\dot{x} + L_1\dot{\theta}_1 \cos\theta_1 + l_2\dot{\theta}_2 \cos\theta_2\big)^2 + \big(L_1\dot{\theta}_1 \sin\theta_1 + l_2\dot{\theta}_2 \sin\theta_2)^2 + 1/2\, I_2{\dot{\theta}_2}^2\Big] \qquad \text{A1.11}$$

For the third pendulum;

$$K.E_3 = 1/2\, m_3 \Big[\big(\dot{x} + L_1\dot{\theta}_1 \cos\theta_1 + L_2\dot{\theta}_2 \cos\theta_2 + l_3\dot{\theta}_3 \cos\theta_3\big)^2 + \big(L_1\dot{\theta}_1 \sin\theta_1 + L_2\dot{\theta}_2 \sin\theta_2 + l_3\dot{\theta}_3 \sin\theta_3)^2 + 1/2\, I_3{\dot{\theta}_3}^2\Big] \qquad \text{A1.12}$$

For the fourth pendulum;

$$K.E_4 = 1/2\, m_4 \Big[\big(\dot{x} + L_1\dot{\theta}_1 \cos\theta_1 + L_2\dot{\theta}_2 \cos\theta_2 + L_3\dot{\theta}_3 \cos\theta_3 + l_4\dot{\theta}_4 \cos\theta_4\big)^2 + \big(L_1\dot{\theta}_1 \sin\theta_1 + L_2\dot{\theta}_2 \sin\theta_2 + L_3\dot{\theta}_3 \sin\theta_3 + l_4\dot{\theta}_4 \sin\theta_4\big)^2 + 1/2\, I_4{\dot{\theta}_4}^2\Big] \qquad \text{A1.13}$$

For the fifth pendulum;

$$K.E_5 = 1/2\, m_5 \Big[\big(\dot{x} + L_1\dot{\theta}_1 \cos\theta_1 + L_2\dot{\theta}_2 \cos\theta_2 + L_3\dot{\theta}_3 \cos\theta_3 + L_4\dot{\theta}_4 \cos\theta_4 + l_5\dot{\theta}_5 \cos\theta_5)^2 + \big(L_1\dot{\theta}_1 \sin\theta_1 + L_2\dot{\theta}_2 \sin\theta_2 + L_3\dot{\theta}_3 \sin\theta_3 + L_4\dot{\theta}_4 \sin\theta_4 + l_5\dot{\theta}_5 \sin\theta_5\big)^2 + 1/2\, I_5{\dot{\theta}_5}^2\Big] \qquad \text{A1.14}$$

For the sixth pendulum;

$$K.E_6 = 1/2\, m_5 \Big[\big(\dot{x} + L_1\dot{\theta}_1 \cos\theta_1 + L_2\dot{\theta}_2 \cos\theta_2 + L_3\dot{\theta}_3 \cos\theta_3 + L_4\dot{\theta}_4 \cos\theta_4 + L_5\dot{\theta}_5 \cos\theta_5 + l_6\dot{\theta}_6 \cos\theta_6)^2 + \big(L_1\dot{\theta}_1 \sin\theta_1 + L_2\dot{\theta}_2 \sin\theta_2 + L_3\dot{\theta}_3 \sin\theta_3 + L_4\dot{\theta}_4 \sin\theta_4 + L_5\dot{\theta}_5 \sin\theta_5 + l_6\dot{\theta}_6 \sin\theta_6\,)^2 + 1/2\, I_6{\dot{\theta}_6}^2\Big] \qquad \text{A1.15}$$

For the seventh pendulum;

$$K.E_7 = 1/2\, m_7 \Big[\big(\dot{x} + L_1\dot{\theta}_1 \cos\theta_1 + L_2\dot{\theta}_2 \cos\theta_2 + L_3\dot{\theta}_3 \cos\theta_3 + L_4\dot{\theta}_4 \cos\theta_4 + L_5\dot{\theta}_5 \cos\theta_5 + L\dot{\theta}_6 \cos\theta_6 + l_7\dot{\theta}_7 \cos\theta_7\big)^2 + \big(L_1\dot{\theta}_1 \sin\theta_1 + L_2\dot{\theta}_2 \sin\theta_2 + L_3\dot{\theta}_3 \sin\theta_3 + L_4\dot{\theta}_4 \sin\theta_4 + L_5\dot{\theta}_5 \sin\theta_5 + L_6\dot{\theta}_6 \sin\theta_6 + l_7\dot{\theta}_7 \sin\theta_7\big)^2 + 1/2\, I_7{\dot{\theta}_7}^{2}\Big] \qquad \text{A1.1}$$

For the eighth pendulum;

$$K.E_8 = 1/2\, m_7 \Big[\big(\dot{x} + L_1\dot{\theta}_1 \cos\theta_1 + L_2\dot{\theta}_2 \cos\theta_2 + L_3\dot{\theta}_3 \cos\theta_3 + L_4\dot{\theta}_4 \cos\theta_4 + L_5\dot{\theta}_5 \cos\theta_5 + L\dot{\theta}_6 \cos\theta_6 + L_7\dot{\theta}_7 \cos\theta_7 + l_8\dot{\theta}_8 \cos\theta_8\big)^2 + \big(L_1\dot{\theta}_1 \sin\theta_1 + L_2\dot{\theta}_2 \sin\theta_2 + L_3\dot{\theta}_3 \sin\theta_3 + L_4\dot{\theta}_4 \sin\theta_4 + L_5\dot{\theta}_5 \sin\theta_5 + L_6\dot{\theta}_6 \sin\theta_6 + L_7\dot{\theta}_7 \sin\theta_7 + l_8\dot{\theta}_8 \sin\theta_8\big)^2 + 1/2\, I_8{\dot{\theta}_8}^{2}\Big] \qquad \text{A1.17}$$

Expanding from equation (A.10)-(A1.17), the following equations are obtained;

$$K.E_1 = \tfrac{1}{2} m_1\dot{x}^2 + \tfrac{1}{2}\left(m_1 l^2 + I_1\right)\dot{\theta}_1^{\,2} + m_1\dot{x} l_1\dot{\theta}_1 \cos\theta_1 \qquad \text{A1.18}$$

$$K.E_2 = 1/2\, m_2 \dot{x}^2 + 1/2\, m_2 L_1^2 \dot{\theta}_1^2 + 1/2\,(m_2 l^2{}_2 + I_2)\dot{\theta}^2{}_2 + m_2 \dot{x} L_1 \dot{\theta}_1 \cos\theta_1 + m_2 \dot{x} l_2 \dot{\theta}_2 \cos\theta_2 + m_2 L_1 l_2 \dot{\theta}_1 \dot{\theta}_2 \cos(\theta_1 - \theta_2) \qquad \text{A1.19}$$

$$K.E_3 = 1/2\, m_3 \dot{x}^2 + 1/2\, m_3 L_1^2 \dot{\theta}_1^2 + 1/2\, m_3 L_2^2 \dot{\theta}_2^2 + 1/2\,(m_3 l^2{}_3 + I_3)\dot{\theta}^2{}_3 + m_3 \dot{x} L_1 \dot{\theta}_1 \cos\theta_1 + m_3 \dot{x} L_2 \dot{\theta}_2 \cos\theta_2 + m_3 \dot{x} l_3 \dot{\theta}_3 \cos\theta_3 + m_3 L_1 L_2 \dot{\theta}_1 \dot{\theta}_2 \cos(\theta_1 - \theta_2) + m_3 L_1 l_3 \dot{\theta}_1 \dot{\theta}_3 \cos(\theta_1 - \theta_3) + m_3 L_2 l_3 \dot{\theta}_2 \dot{\theta}_3 \cos(\theta_2 - \theta_3) \qquad \text{A1.20}$$

$$K.E_4 = 1/2\, m_4 \dot{x}^2 + 1/2\, m_4 L_1^2 \dot{\theta}_1^2 + 1/2\, m_4 L_2^2 \dot{\theta}_2^2 + 1/2\, m_4 L_3^2 \dot{\theta}_3^2 + 1/2\,(m_4 l^2{}_4 + I_4)\dot{\theta}_4^2 + m_4 \dot{x} L_1 \dot{\theta}_1 \cos\theta_1 + m_4 \dot{x} L_2 \dot{\theta}_2 \cos\theta_2 + m_4 \dot{x} L_3 \dot{\theta}_3 \cos\theta_3 + m_4 \dot{x} l_4 \dot{\theta}_4 \cos\theta_4 + m_4 L_1 L_2 \dot{\theta}_1 \dot{\theta}_2 \cos(\theta_1 - \theta_2) + m_4 L_1 L_3 \dot{\theta}_1 \dot{\theta}_3 \cos(\theta_1 - \theta_3) + m_4 L_1 l_4 \dot{\theta}_1 \dot{\theta}_4 \cos(\theta_1 - \theta_4) + m_4 L_2 L_3 \dot{\theta}_2 \dot{\theta}_3 \cos(\theta_2 - \theta_3) + m_4 L_2 l_4 \dot{\theta}_2 \dot{\theta}_4 \cos(\theta_2 - \theta_4) + m_4 L_3 l_4 \dot{\theta}_3 \dot{\theta}_4 \cos(\theta_3 - \theta_4) \qquad \text{A1.21}$$

$$
\begin{aligned}
&K.E_5 = 1/2\, m_5\, \dot{x}^2 + 1/2\, m_5 L_1^{\,2}\, \dot{\theta}_1^{\,2} + 1/2\, m_5 L_2^{\,2}\, \dot{\theta}_2^{\,2} + 1/2\, m_5 L_3^{\,2}\, \dot{\theta}_3^{\,2} + 1/2\, m_5 L_4^{\,2}\, \dot{\theta}_4^{\,2} + 1/2\,(m_5 l^2{}_5 + I_5)\, \dot{\theta}^2{}_5 \\
&+m_5\, \dot{x}\, L_1\, \dot{\theta}_1 \cos\theta_1 + m_5\, \dot{x}\, L_2\, \dot{\theta}_2 \cos\theta_2 + m_5\, \dot{x}\, L_3\, \dot{\theta}_3 \cos\theta_3 + m_5\, \dot{x}\, L_4\, \dot{\theta}_4 \cos\theta_4 + m_5\, \dot{x}\, l_5\, \dot{\theta}_5 \cos\theta_5 + \\
&+m_5 L_1 L_2\, \dot{\theta}_1 \dot{\theta}_2 \cos(\theta_1 - \theta_2) + m_5 L_1 L_3\, \dot{\theta}_1 \dot{\theta}_3 \cos(\theta_1 - \theta_3) + m_5 L_1 L_4\, \dot{\theta}_1 \dot{\theta}_4 \cos(\theta_1 - \theta_4) + m_6 L_1 l_5\, \dot{\theta}_1 \dot{\theta}_5 \cos(\theta_1 - \theta_5) + \\
&m_5 L_2 L_3\, \dot{\theta}_2 \dot{\theta}_3 \cos(\theta_2 - \theta_3) + m_5 L_2 L_4\, \dot{\theta}_2 \dot{\theta}_4 \cos(\theta_2 - \theta_4) + m_5 L_2 l_5\, \dot{\theta}_2 \dot{\theta}_5 \cos(\theta_2 - \theta_5) + m_5 L_3 L_4\, \dot{\theta}_3 \dot{\theta}_4 \cos(\theta_3 - \theta_4) + \\
&m_5 L_3 l_5\, \dot{\theta}_3 \dot{\theta}_5 \cos(\theta_3 - \theta_5) + m_5 L_4 l_5\, \dot{\theta}_4 \dot{\theta}_5 \cos(\theta_4 - \theta_5)
\end{aligned}
\tag{A1.22}
$$

$$
\begin{aligned}
&K.E_6 = 1/2\, m_6\, \dot{x}^2 + 1/2\, m_6 L_1^{\,2}\, \dot{\theta}_1^{\,2} + 1/2\, m_6 L_2^{\,2}\, \dot{\theta}_2^{\,2} + 1/2\, m_6 L_3^{\,2}\, \dot{\theta}_3^{\,2} + 1/2\, m_6 L_4^{\,2}\, \dot{\theta}_4^{\,2} + 1/2\, m_6 L_5^{\,2}\, \dot{\theta}_5^{\,2} + 1/2\,(m_6 l^2{}_6 + I_6)\, \dot{\theta}^2{}_6 \\
&+m_6\, \dot{x}\, L_1\, \dot{\theta}_1 \cos\theta_1 + m_6\, \dot{x}\, L_2\, \dot{\theta}_2 \cos\theta_2 + m_6\, \dot{x}\, L_3\, \dot{\theta}_3 \cos\theta_3 + m_6\, \dot{x}\, L_4\, \dot{\theta}_4 \cos\theta_4 + m_6\, \dot{x}\, L_5\, \dot{\theta}_5 \cos\theta_5 + m_6\, \dot{x}\, l_6\, \dot{\theta}_6 \cos\theta_6 \\
&+m_6 L_1 L_2\, \dot{\theta}_1 \dot{\theta}_2 \cos(\theta_1 - \theta_2) + m_6 L_1 L_3\, \dot{\theta}_1 \dot{\theta}_3 \cos(\theta_1 - \theta_3) + m_6 L_1 L_4\, \dot{\theta}_1 \dot{\theta}_4 \cos(\theta_1 - \theta_4) + m_6 L_1 L_5\, \dot{\theta}_1 \dot{\theta}_5 \cos(\theta_1 - \theta_5) + \\
&m_6 L_1 l_6\, \dot{\theta}_1 \dot{\theta}_6 \cos(\theta_1 - \theta_6) + m_6 L_2 L_3\, \dot{\theta}_2 \dot{\theta}_3 \cos(\theta_2 - \theta_3) + m_6 L_2 L_4\, \dot{\theta}_2 \dot{\theta}_4 \cos(\theta_2 - \theta_4) + m_6 L_2 L_5\, \dot{\theta}_2 \dot{\theta}_5 \cos(\theta_2 - \theta_5) + \\
&m_6 L_2 l_6\, \dot{\theta}_2 \dot{\theta}_6 \cos(\theta_2 - \theta_6) + m_6 L_3 L_4\, \dot{\theta}_3 \dot{\theta}_4 \cos(\theta_3 - \theta_4) + m_6 L_3 L_5\, \dot{\theta}_3 \dot{\theta}_5 \cos(\theta_3 - \theta_5) + m_6 L_3 l_6\, \dot{\theta}_3 \dot{\theta}_6 \cos(\theta_3 - \theta_6) + \\
&m_6 L_4 L_5\, \dot{\theta}_4 \dot{\theta}_5 \cos(\theta_4 - \theta_5) + m_6 L_4 l_6\, \dot{\theta}_4 \dot{\theta}_6 \cos(\theta_4 - \theta_6) + m_6 L_5 l_6\, \dot{\theta}_5 \dot{\theta}_6 \cos(\theta_5 - \theta_6)
\end{aligned}
\tag{A1.23}
$$

$$
\begin{aligned}
&K.E_7 = 1/2\, m_7\, \dot{x}^2 + 1/2\, m_7 L_1^{\,2}\, \dot{\theta}_1^{\,2} + 1/2\, m_7 L_2^{\,2}\, \dot{\theta}_2^{\,2} + 1/2\, m_7 L_3^{\,2}\, \dot{\theta}_3^{\,2} + 1/2\, m_7 L_4^{\,2}\, \dot{\theta}_4^{\,2} + 1/2\, m_7 L_5^{\,2}\, \dot{\theta}_5^{\,2} + 1/2\, m_7 L_6^{\,2}\, \dot{\theta}_6^{\,2} + \\
&1/2\,(m_7 l^2{}_7 + I_7)\, \dot{\theta}^2{}_7 + m_7\, \dot{x}\, L_1\, \dot{\theta}_1 \cos\theta_1 + m_7\, \dot{x}\, L_2\, \dot{\theta}_2 \cos\theta_2 + m_7\, \dot{x}\, L_3\, \dot{\theta}_3 \cos\theta_3 + m_7\, \dot{x}\, L_4\, \dot{\theta}_4 \cos\theta_4 + m_7\, \dot{x}\, L_5\, \dot{\theta}_5 \cos\theta_5 \\
&+m_7\, \dot{x}\, L_6\, \dot{\theta}_6 \cos\theta_6 + m_7\, \dot{x}\, l_7\, \dot{\theta}_7 \cos\theta_7 + m_7 L_1 L_2\, \dot{\theta}_1 \dot{\theta}_2 \cos(\theta_1 - \theta_2) + m_7 L_1 L_3\, \dot{\theta}_1 \dot{\theta}_3 \cos(\theta_1 - \theta_3) + m_7 L_1 L_4\, \dot{\theta}_1 \dot{\theta}_4 \cos(\theta_1 - \theta_4) \\
&+m_7 L_1 L_5\, \dot{\theta}_1 \dot{\theta}_5 \cos(\theta_1 - \theta_5) + m_7 L_1 L_6\, \dot{\theta}_1 \dot{\theta}_6 \cos(\theta_1 - \theta_6) + m_7 L_1 l_7\, \dot{\theta}_1 \dot{\theta}_7 \cos(\theta_1 - \theta_7) + m_7 L_2 L_3\, \dot{\theta}_2 \dot{\theta}_3 \cos(\theta_2 - \theta_3) + \\
&m_7 L_2 L_4\, \dot{\theta}_2 \dot{\theta}_4 \cos(\theta_2 - \theta_4) + m_7 L_2 L_5\, \dot{\theta}_2 \dot{\theta}_5 \cos(\theta_2 - \theta_5) + m_7 L_2 L_6\, \dot{\theta}_2 \dot{\theta}_6 \cos(\theta_2 - \theta_6) + m_7 L_2 l_7\, \dot{\theta}_2 \dot{\theta}_7 \cos(\theta_2 - \theta_7) + \\
&m_7 L_3 L_4\, \dot{\theta}_3 \dot{\theta}_4 \cos(\theta_3 - \theta_4) + m_7 L_3 L_5\, \dot{\theta}_3 \dot{\theta}_5 \cos(\theta_3 - \theta_5) + m_7 L_3 L_6\, \dot{\theta}_3 \dot{\theta}_6 \cos(\theta_3 - \theta_6) + m_7 L_3 l_7\, \dot{\theta}_3 \dot{\theta}_7 \cos(\theta_3 - \theta_7) + \\
&m_7 L_4 L_5\, \dot{\theta}_4 \dot{\theta}_5 \cos(\theta_4 - \theta_5) + m_7 L_4 L_6\, \dot{\theta}_4 \dot{\theta}_6 \cos(\theta_4 - \theta_6) + m_7 L_4 l_7\, \dot{\theta}_4 \dot{\theta}_7 \cos(\theta_4 - \theta_7) + m_7 L_5 L_6\, \dot{\theta}_5 \dot{\theta}_6 \cos(\theta_5 - \theta_6) + \\
&m_7 L_5 l_7\, \dot{\theta}_5 \dot{\theta}_7 \cos(\theta_5 - \theta_7) + m_7 L_6 l_7\, \dot{\theta}_6 \dot{\theta}_7 \cos(\theta_6 - \theta_7)
\end{aligned}
\tag{A1.24}
$$

$$
\begin{aligned}
K.E_8 &= 1/2\, m_8 \dot{x}^2 + 1/2\, m_8 L_1^2 \dot{\theta}_1^2 + 1/2\, m_8 L_2^2 \dot{\theta}_2^2 + 1/2\, m_8 L_3^2 \dot{\theta}_3^2 + 1/2\, m_8 L_4^2 \dot{\theta}_4^2 + 1/2\, m_8 L_5^2 \dot{\theta}_5^2 + 1/2\, m_8 L_6^2 \dot{\theta}_6^2 + \\
&1/2\, m_8 L_7^2 \dot{\theta}_7^2 + 1/2\,(m_8 l^2_8 + I_8)\dot{\theta}^2_8 + m_8 \dot{x} L_1 \dot{\theta}_1 \cos\theta_1 + m_8 \dot{x} L_2 \dot{\theta}_2 \cos\theta_2 + m_8 \dot{x} L_3 \dot{\theta}_3 \cos\theta_3 + m_8 \dot{x} L_4 \dot{\theta}_4 \cos\theta_4 + \\
&m_8 \dot{x} L_5 \dot{\theta}_5 \cos\theta_5 + m_8 \dot{x} L_6 \dot{\theta}_6 \cos\theta_6 + m_8 \dot{x} L_7 \dot{\theta}_7 \cos\theta_7 + m_8 \dot{x} l_8 \dot{\theta}_8 \cos\theta_8 + m_8 L_1 L_2 \dot{\theta}_1 \dot{\theta}_2 \cos(\theta_1 - \theta_2) + \\
&m_8 L_1 L_3 \dot{\theta}_1 \dot{\theta}_3 \cos(\theta_1 - \theta_3) + m_8 L_1 L_4 \dot{\theta}_1 \dot{\theta}_4 \cos(\theta_1 - \theta_4) + m_8 L_1 L_5 \dot{\theta}_1 \dot{\theta}_5 \cos(\theta_1 - \theta_5) + m_8 L_1 L_6 \dot{\theta}_1 \dot{\theta}_6 \cos(\theta_1 - \theta_6) + \\
&m_8 L_1 L_7 \dot{\theta}_1 \dot{\theta}_7 \cos(\theta_1 - \theta_7) + m_8 L_1 l_8 \dot{\theta}_1 \dot{\theta}_8 \cos(\theta_1 - \theta_8) + m_8 L_2 L_3 \dot{\theta}_2 \dot{\theta}_3 \cos(\theta_2 - \theta_3) + m_8 L_2 L_4 \dot{\theta}_2 \dot{\theta}_4 \cos(\theta_2 - \theta_4) + \\
&m_8 L_2 L_5 \dot{\theta}_2 \dot{\theta}_5 \cos(\theta_2 - \theta_5) + m_8 L_2 L_6 \dot{\theta}_2 \dot{\theta}_6 \cos(\theta_2 - \theta_6) + m_8 L_2 L_7 \dot{\theta}_2 \dot{\theta}_7 \cos(\theta_2 - \theta_7) + m_8 L_1 l_8 \dot{\theta}_2 \dot{\theta}_8 \cos(\theta_2 - \theta_8) + \\
&m_8 L_3 L_4 \dot{\theta}_3 \dot{\theta}_4 \cos(\theta_3 - \theta_4) + m_8 L_3 L_5 \dot{\theta}_3 \dot{\theta}_5 \cos(\theta_3 - \theta_5) + m_8 L_3 L_6 \dot{\theta}_3 \dot{\theta}_6 \cos(\theta_3 - \theta_6) + m_8 L_3 L_7 \dot{\theta}_3 \dot{\theta}_7 \cos(\theta_3 - \theta_7) + \\
&m_8 L_3 l_8 \dot{\theta}_3 \dot{\theta}_8 \cos(\theta_3 - \theta_8) + m_8 L_4 L_5 \dot{\theta}_4 \dot{\theta}_5 \cos(\theta_4 - \theta_5) + m_8 L_4 L_6 \dot{\theta}_4 \dot{\theta}_6 \cos(\theta_4 - \theta_6) + m_8 L_4 L_7 \dot{\theta}_4 \dot{\theta}_7 \cos(\theta_4 - \theta_7) + \\
&m_8 L_4 l_8 \dot{\theta}_4 \dot{\theta}_8 \cos(\theta_4 - \theta_8) + m_8 L_5 L_6 \dot{\theta}_5 \dot{\theta}_6 \cos(\theta_5 - \theta_6) + m_8 L_5 L_7 \dot{\theta}_5 \dot{\theta}_7 \cos(\theta_5 - \theta_7) + m_8 L_5 l_8 \dot{\theta}_5 \dot{\theta}_8 \cos(\theta_5 - \theta_8) + \\
&m_8 L_6 L_7 \dot{\theta}_6 \dot{\theta}_7 \cos(\theta_6 - \theta_7) + m_8 L_6 l_8 \dot{\theta}_6 \dot{\theta}_8 \cos(\theta_6 - \theta_8) + m_8 L_7 l_8 \dot{\theta}_7 \dot{\theta}_8 \cos(\theta_7 - \theta_8)
\end{aligned}
\qquad \text{A1.25}
$$

To reduce the complexity of the modeling, it is assumed that the centers of the pendulums are situated at the geometric centers of the links, then;

$$l_n = \frac{L_n}{2}, \ (n = 1, 2, 3, 8) \qquad \text{A1.26}$$

The moment of inertia about the center of rod of mass M and length L is given by:

$$I = \frac{ML}{12} \quad \text{(Bogdanov, 2004).} \qquad \text{A1.27}$$

Therefore, for n number of pendulum links, the moment of inertia for n-number of links will be:

$$I_n = \frac{m_n L_n^2}{12}, \ (n = 1, 2, 3, 8) \qquad \text{A1.28}$$

The potential energy of the system is completely determined by the angular displacement of the pendulum, since the wheeled cart only moves in the horizontal direction. Thus the potential energy of the cart is zero;

$$P.E_0 = 0 \qquad \text{A1.29}$$

$$P.E_1 = m_1 g l_1 \cos\theta_1 \qquad \text{A1.30}$$

$$P.E_2 = m_2 g(L_1 \cos\theta_1 + l_2 \cos\theta_2) \qquad \text{A1.31}$$

$$P.E_3 = m_3 g(L_1 \cos\theta_1 + L_2 \cos\theta_2 + l_3 \cos\theta_3) \qquad \text{A1.32}$$

$$P.E_4 = m_4 g(L_1 \cos\theta_1 + L_2 \cos\theta_2 + L_3 \cos\theta_3 + l_4 \cos\theta_4) \qquad \text{A1.33}$$

$$P.E_5 = m_5 g(L_1 \cos\theta_1 + L_2 \cos\theta_2 + L_3 \cos\theta_3 + L_4 \cos\theta_4 + l_5 \cos\theta_5) \qquad \text{A1.34}$$

$$P.E_6 = m_6 g(L_1 \cos\theta_1 + L_2 \cos\theta_2 + L_3 \cos\theta_3 + L_4 \cos\theta_4 + L_5 \cos\theta_5 + l_6 \cos\theta_6) \qquad \text{A1.35}$$

$$P.E_7 = m_7 g(L_1 \cos\theta_1 + L_2 \cos\theta_2 + L_3 \cos\theta_3 + L_4 \cos\theta_4 + L_5 \cos\theta_5 + L_6 \cos\theta_6 + l_7 \cos\theta_7) \qquad \text{A1.36}$$

$$P.E_8 = m_8 g(L_1 \cos\theta_1 + L_2 \cos\theta_2 + L_3 \cos\theta_3 + L_4 \cos\theta_4 + L_5 \cos\theta_5 + L_6 \cos\theta_6 + L_7 \cos\theta_7 + l_8 \cos\theta_8) \qquad \text{A1.37}$$

Let: $a_0 = \left[m_0 + m_1 + m_2 + m_3 + m_4 + m_5 + m_6 + m_7 + m_8 \right]$ A1.38

$$a_1 = \left[(m_1 l_1^2 + I_1) + m_2 L_1^2 + m_3 L_1^2 + m_4 L_1^2 + m_5 L_1^2 + m_6 L_1^2 + m_7 L_1^2 + m_8 L_1^2 \right] \qquad \text{A1.39}$$

$$a_1 = \left[\frac{m_1}{3} + m_2 + m_3 + m_4 + m_5 + m_6 + m_7 + m_8 \right] L_1^2 \qquad \text{A1.40}$$

$$a_2 = \left[\frac{m_2}{3} + m_3 + m_4 + m_5 + m_6 + m_7 + m_8 \right] L_2^2 \qquad \text{A1.41}$$

$$a_3 = \left[\frac{m_3}{3} + m_4 + m_5 + m_6 + m_7 + m_8 \right] L_3^2 \qquad \text{A1.42}$$

$$a_4 = \left[\frac{m_4}{3} + m_5 + m_6 + m_7 + m_8 \right] L_4^2 \qquad \text{A1.43}$$

$$a_5 = \left[\frac{m_5}{3} + m_6 + m_7 + m_8 \right] L_5^2 \qquad \text{A1.44}$$

$$a_6 = \left[\frac{m_6}{3} + m_7 + m_8 \right] L_6^2 \qquad \text{A1.45}$$

$$a_7 = \left[\frac{m_7}{3} + m_8 \right] L_7^2 \qquad \text{A1.46}$$

$$a_8 = \left[\frac{m_8}{3}\right] L^2{}_8 \qquad \text{A1.47}$$

$$b_0 = \left[m_1 l_1 + m_2 L_1 + m_3 L_1 + m_4 L_1 + m_5 L_1 + m_6 L_1 + m_7 L_1 + m_8 L_1\right] \qquad \text{A1.48}$$

$$b_0 = \left[\frac{m_1}{2} + m_2 + m_3 + m_4 + m_5 + m_6 + m_7 + m_8\right] L_1 \qquad \text{A1.49}$$

$$b_1 = \left[\frac{m_2}{2} + m_3 + m_4 + m_5 + m_6 + m_7 + m_8\right] L_2 \qquad \text{A1.50}$$

$$b_2 = \left[\frac{m_3}{2} + m_4 + m_5 + m_6 + m_7 + m_8\right] L_3 \qquad \text{A1.51}$$

$$b_3 = \left[\frac{m_4}{2} + m_5 + m_6 + m_7 + m_8\right] L_4 \qquad \text{A1.52}$$

$$b_4 = \left[\frac{m_5}{2} + m_6 + m_7 + m_8\right] L_5 \qquad \text{A1.53}$$

$$b_5 = \left[\frac{m_6}{2} + m_7 + m_8\right] L_6 \qquad \text{A1.54}$$

$$b_6 = \left[\frac{m_7}{2} + m_8\right] L_7 \qquad \text{A1.55}$$

$$b_7 = \left[\frac{m_8}{2}\right] L_8 \qquad \text{A1.56}$$

$$\sum_{n=1}^{8} K.E_n = \frac{1}{2}a_0\dot{x}+\frac{1}{2}a_1\dot{\theta}_1^2+\frac{1}{2}a_2\dot{\theta}_2^2+\frac{1}{2}a_3\dot{\theta}_3^2+\frac{1}{2}a_4\dot{\theta}_4^2+\frac{1}{2}a_5\dot{\theta}_5^2+\frac{1}{2}a_6\dot{\theta}_6^2+\frac{1}{2}a_7\dot{\theta}_7^2+\frac{1}{2}a_8\dot{\theta}_8^2+$$

$$b_0\dot{x}\dot{\theta}_1\cos\theta_1+b_1\dot{x}\dot{\theta}_2\cos\theta_2+b_2\dot{x}\dot{\theta}_3\cos\theta_3+b_3\dot{x}\dot{\theta}_4\cos\theta_4+b_4\dot{x}\dot{\theta}_5\cos\theta_5+b_5\dot{x}\dot{\theta}_6\cos\theta_6+b_6\dot{x}\dot{\theta}_7\cos\theta_7+$$

$$b_7\dot{x}\dot{\theta}_8\cos\theta_8+b_1L_1\dot{\theta}_1\dot{\theta}_2\cos(\theta_1-\theta_2)+L_1b_2\dot{\theta}_1\dot{\theta}_3\cos(\theta_1-\theta_3)+L_1b_3\dot{\theta}_1\dot{\theta}_4\cos(\theta_1-\theta_4)+$$

$$L_1b_4\dot{\theta}_1\dot{\theta}_5\cos(\theta_1-\theta_5)+L_1b_5\dot{\theta}_1\dot{\theta}_6\cos(\theta_1-\theta_6)+L_1b_6\dot{\theta}_1\dot{\theta}_7\cos(\theta_1-\theta_7)+L_1b_7\dot{\theta}_1\dot{\theta}_8\cos(\theta_1-\theta_8)+$$

$$L_2b_2\dot{\theta}_2\dot{\theta}_3\cos(\theta_2-\theta_3)+L_2b_3\dot{\theta}_2\dot{\theta}_4\cos(\theta_2-\theta_4)+L_2b_4\dot{\theta}_2\dot{\theta}_5\cos(\theta_2-\theta_5)+L_2b_5\dot{\theta}_2\dot{\theta}_6\cos(\theta_2-\theta_6)+$$

$$L_2b_6\dot{\theta}_2\dot{\theta}_7\cos(\theta_2-\theta_7)+L_2b_7\dot{\theta}_2\dot{\theta}_8\cos(\theta_2-\theta_8)+L_3b_3\dot{\theta}_3\dot{\theta}_4\cos(\theta_3-\theta_4)+L_3b_4\dot{\theta}_3\dot{\theta}_5\cos(\theta_3-\theta_5)+$$

$$L_3b_5\dot{\theta}_3\dot{\theta}_6\cos(\theta_3-\theta_6)+L_3b_6\dot{\theta}_3\dot{\theta}_7\cos(\theta_3-\theta_7)+L_3b_7\dot{\theta}_3\dot{\theta}_7\cos(\theta_3-\theta_8)+L_4b_4\dot{\theta}_4\dot{\theta}_5\cos(\theta_4-\theta_5)+$$

$$L_4b_5\dot{\theta}_4\dot{\theta}_6\cos(\theta_4-\theta_6)+L_4b_6\dot{\theta}_4\dot{\theta}_7\cos(\theta_4-\theta_7)+L_4b_7\dot{\theta}_4\dot{\theta}_8\cos(\theta_4-\theta_8)+L_5b_5\dot{\theta}_5\dot{\theta}_6\cos(\theta_5-\theta_6)+$$

$$L_5b_6\dot{\theta}_5\dot{\theta}_7\cos(\theta_5-\theta_7)+L_5b_7\dot{\theta}_5\dot{\theta}_8\cos(\theta_5-\theta_8)+L_6b_6\dot{\theta}_6\dot{\theta}_7\cos(\theta_6-\theta_7)+L_6b_7\dot{\theta}_6\dot{\theta}_8\cos(\theta_6-\theta_8)+$$

$$L_7b_7\dot{\theta}_7\dot{\theta}_8\cos(\theta_7-\theta_8)$$

A1.57

$$\sum_{n=1}^{8} P.E_n = b_0g\cos\theta_1+b_1g\cos\theta_2+b_2g\cos\theta_3+b_3g\cos\theta_4+b_4g\cos\theta_5+b_5g\cos\theta_6+b_6g\cos\theta_7$$ A1.58

$$+b_7g\cos\theta_8$$

The Lagrangian L that describes the dynamics of the system is obtained by the difference between equation (57) and (58) (JNi, 2011,);

$$L=\sum_{n=1}^{8} K.E_n-\sum_{n=1}^{8} P.E_n$$ A1.59

$$
\begin{aligned}
L = {} & \frac{1}{2}a_0\dot{x}+\frac{1}{2}a_1\dot{\theta}_1^2+\frac{1}{2}a_2\dot{\theta}_2^2+\frac{1}{2}a_3\dot{\theta}_3^2+\frac{1}{2}a_4\dot{\theta}_4^2+\frac{1}{2}a_5\dot{\theta}_5^2+\frac{1}{2}a_6\dot{\theta}_6^2+\frac{1}{2}a_7\dot{\theta}_7^2+\frac{1}{2}a_8\dot{\theta}_8^2+ \\
& b_0\dot{x}\dot{\theta}_1\cos\theta_1+b_1\dot{x}\dot{\theta}_2\cos\theta_2+b_2\dot{x}\dot{\theta}_3\cos\theta_3+b_3\dot{x}\dot{\theta}_4\cos\theta_4+b_4\dot{x}\dot{\theta}_5\cos\theta_5+b_5\dot{x}\dot{\theta}_6\cos\theta_6+b_6\dot{x}\dot{\theta}_7\cos\theta_7+ \\
& b_7\dot{x}\dot{\theta}_8\cos\theta_8+b_1L_1\dot{\theta}_1\dot{\theta}_2\cos(\theta_1-\theta_2)+L_1b_2\dot{\theta}_1\dot{\theta}_3\cos(\theta_1-\theta_3)+L_1b_3\dot{\theta}_1\dot{\theta}_4\cos(\theta_1-\theta_4)+ \\
& L_1b_4\dot{\theta}_1\dot{\theta}_5\cos(\theta_1-\theta_5)+L_1b_5\dot{\theta}_1\dot{\theta}_6\cos(\theta_1-\theta_6)+L_1b_6\dot{\theta}_1\dot{\theta}_7\cos(\theta_1-\theta_7)+L_1b_7\dot{\theta}_1\dot{\theta}_8\cos(\theta_1-\theta_8)+ \\
& L_2b_2\dot{\theta}_2\dot{\theta}_3\cos(\theta_2-\theta_3)+L_2b_3\dot{\theta}_2\dot{\theta}_4\cos(\theta_2-\theta_4)+L_2b_4\dot{\theta}_2\dot{\theta}_5\cos(\theta_2-\theta_5)+L_2b_5\dot{\theta}_2\dot{\theta}_6\cos(\theta_2-\theta_6)+ \\
& L_2b_6\dot{\theta}_2\dot{\theta}_7\cos(\theta_2-\theta_7)+L_2b_7\dot{\theta}_2\dot{\theta}_8\cos(\theta_2-\theta_8)+L_3b_3\dot{\theta}_3\dot{\theta}_4\cos(\theta_3-\theta_4)+L_3b_4\dot{\theta}_3\dot{\theta}_5\cos(\theta_3-\theta_5)+ \\
& L_3b_5\dot{\theta}_3\dot{\theta}_6\cos(\theta_3-\theta_6)+L_3b_6\dot{\theta}_3\dot{\theta}_7\cos(\theta_3-\theta_7)+L_3b_7\dot{\theta}_3\dot{\theta}_7\cos(\theta_3-\theta_8)+L_4b_4\dot{\theta}_4\dot{\theta}_5\cos(\theta_4-\theta_5)+ \\
& L_4b_5\dot{\theta}_4\dot{\theta}_6\cos(\theta_4-\theta_6)+L_4b_6\dot{\theta}_4\dot{\theta}_7\cos(\theta_4-\theta_7)+L_4b_7\dot{\theta}_4\dot{\theta}_8\cos(\theta_4-\theta_8)+L_5b_5\dot{\theta}_5\dot{\theta}_6\cos(\theta_5-\theta_6)+ \\
& L_5b_6\dot{\theta}_5\dot{\theta}_7\cos(\theta_5-\theta_7)+L_5b_7\dot{\theta}_5\dot{\theta}_8\cos(\theta_5-\theta_8)+L_6b_6\dot{\theta}_6\dot{\theta}_7\cos(\theta_6-\theta_7)+L_6b_7\dot{\theta}_6\dot{\theta}_8\cos(\theta_6-\theta_8)+ \\
& L_7b_7\dot{\theta}_7\dot{\theta}_8\cos(\theta_7-\theta_8)-b_0g\cos\theta_1+b_1g\cos\theta_2+b_2g\cos\theta_3+b_3g\cos\theta_4+b_4g\cos\theta_5+b_5g\cos\theta_6+b_6g\cos\theta_7 \\
& +b_7g\cos\theta_8
\end{aligned}
\qquad \text{A1.6}
$$

The energy of the system (both cart and pendulum links) due to friction is given by Raleigh function and this describes the frictional (viscous) force within the system (Li et al, 2002 and Jadlovska and Sarnovsky, 2011).

For the cart;

$$F_0 = \frac{1}{2}\mu_0\dot{x}^2 \qquad \text{A1.61}$$

For the pendulum joints;

$$F_n = \frac{1}{2}\mu_n\left(\dot{\theta}_n - \dot{\theta}_{n-1}\right)^2 \qquad \text{A1.62}$$

F_0 is the fricative energy between the cart and the surface track. *F_n* is the fricative energy at the various nth pivot pendulum joints. μ_0 and μ_n are the coefficient of friction of the cart and the pendulums respectively.

Total energy due to friction is given by;

$$F = F_0 + F_n \qquad \text{A1.63}$$

$$F = \frac{1}{2}\mu_0\dot{x}^2 + \frac{1}{2}\sum_{n=1}^{8}\mu_n\left(\dot{\theta}_n - \dot{\theta}_{n-1}\right)^2 \qquad \text{A1.64}$$

First pendulum;

$$F_1 = \frac{1}{2}\left(\mu_1\dot{\theta}_1^2\right) \qquad \text{A1.65}$$

Second pendulum;

$$F_2 = \frac{1}{2}\left(\mu_2\left(\dot{\theta}_2 - \dot{\theta}_1\right)^2\right) \qquad \text{A1.66}$$

Third pendulum;

$$F_3 = \frac{1}{2}\left(\mu_3\left(\dot{\theta}_3 - \dot{\theta}_2\right)^2\right) \qquad \text{A1.67}$$

Forth pendulum;

$$F_4 = \frac{1}{2}\left(\mu_4\left(\dot{\theta}_4 - \dot{\theta}_3\right)^2\right) \qquad \text{A1.68}$$

Fifth pendulum;

$$F_5 = \frac{1}{2}\left(\mu_5\left(\dot{\theta}_5 - \dot{\theta}_4\right)^2\right) \qquad \text{A1.69}$$

Sixth pendulum;

$$F_6 = \frac{1}{2}\left(\mu_6\left(\dot{\theta}_6 - \dot{\theta}_5\right)^2\right) \qquad \text{A1.70}$$

Seventh pendulum;

$$F_7 = \frac{1}{2}\left(\mu_7\left(\dot{\theta}_7 - \dot{\theta}_6\right)^2\right) \qquad \text{A1.71}$$

Eighth pendulum;

$$F_8 = \frac{1}{2}\mu_8\left(\dot{\theta}_8 - \dot{\theta}_7\right)^2 \qquad \text{A1.72}$$

Using Lagrange equation of motion to the cart position and the pendulum angles, the Lagrangian function, *L* described by equation A1.59 gives the resultant

nonlinear dynamic equations that represent the Double-quad inverted pendulum (DQIP) are as follows:

Non-linear dynamic equation of motion for the cart position;

$$\frac{d}{dt}\left(\frac{\partial L}{\partial \dot{x}}\right)-\frac{\partial L}{\partial x}+\frac{\partial F}{\partial \dot{x}}=\psi \quad , (\psi = u) \qquad \text{A1.73}$$

Non-linear dynamic equation of motions for the pendulum angles is given by;

$$\frac{d}{dt}\left(\frac{\partial L}{\partial \dot{\theta}}\right)-\frac{\partial L}{\partial \theta}+\frac{\partial F}{\partial \dot{\theta}}=\psi \qquad \text{A1.74}$$

($\psi = 0$, since the control force u was only applied to the cart)

(Bogdanov, 2004).

$$\begin{aligned}&a_0\ddot{x}+b_0\cos\theta_1\ddot{\theta}_1+b_1\cos\theta_2\ddot{\theta}_2+b_2\cos\theta_3\ddot{\theta}_3+b_2\cos\theta_3\ddot{\theta}_3+b_3\cos\theta_4\ddot{\theta}_4+b_4\cos\theta_5\ddot{\theta}_5+b_5\cos\theta_6\ddot{\theta}_6+\\&b_6\cos\theta_7\ddot{\theta}_7+b_7\cos\theta_8\ddot{\theta}_8+\mu_0\dot{x}-b_0\dot{\theta}_1\sin\theta_1(\dot{\theta}_1)-b_1\dot{\theta}_2\sin\theta_2(\dot{\theta}_2)-b_2\dot{\theta}_3\sin\theta_3(\dot{\theta}_3)-b_3\dot{\theta}_4\sin\theta_4(\dot{\theta}_4)-\\&b_4\dot{\theta}_5\sin\theta_5(\dot{\theta}_5)-b_5\dot{\theta}_6\sin\theta_6(\dot{\theta}_6)-b_6\dot{\theta}_7\sin\theta_7(\dot{\theta}_7)-b_7\dot{\theta}_8\sin\theta_8(\dot{\theta}_8)=u\end{aligned} \qquad \text{A1.75}$$

$$\begin{aligned}&b_0\cos\theta_1\ddot{x}+a_1\ddot{\theta}_1+L_1b_1\cos(\theta_1-\theta_2)\ddot{\theta}_2+L_1b_2\cos(\theta_1-\theta_3)\ddot{\theta}_3+L_1b_3\cos(\theta_1-\theta_4)\ddot{\theta}_4+L_1b_4\cos(\theta_1-\theta_5)\ddot{\theta}_5+\\&L_1b_5\cos(\theta_1-\theta_6)\ddot{\theta}_6+L_1b_6\cos(\theta_1-\theta_7)\ddot{\theta}_7+L_1b_7\cos(\theta_1-\theta_8)\ddot{\theta}_8+(\mu_1+\mu_2)\dot{\theta}_1+(L_1b_1\dot{\theta}_2\sin(\theta_1-\theta_2)-\mu_2)\dot{\theta}_2+\\&L_1b_2\dot{\theta}_3\sin(\theta_1-\theta_3)\dot{\theta}_3+L_1b_3\dot{\theta}_4\sin(\theta_1-\theta_4)\dot{\theta}_4+L_1b_4\dot{\theta}_5\sin(\theta_1-\theta_5)\dot{\theta}_5+L_1b_5\dot{\theta}_6\sin(\theta_1-\theta_6)\dot{\theta}_6+L_1b_6\dot{\theta}_7\sin(\theta_1-\theta_7)\dot{\theta}_7+\\&L_1b_7\dot{\theta}_8\sin(\theta_1-\theta_8)\dot{\theta}_8-b_0g\sin\theta_1=0\end{aligned} \qquad \text{A1.76}$$

$$\begin{aligned}&b_1\cos\theta_2\ddot{x}+L_1b_1\cos(\theta_1-\theta_2)\ddot{\theta}_1+a_2\ddot{\theta}_2+L_2b_2\cos(\theta_2-\theta_3)\ddot{\theta}_3+L_2b_3\cos(\theta_2-\theta_4)\ddot{\theta}_4+L_2b_4\cos(\theta_2-\theta_5)\ddot{\theta}_5+\\&L_2b_5\cos(\theta_2-\theta_6)\ddot{\theta}_6+L_2b_6\cos(\theta_2-\theta_7)\ddot{\theta}_7+L_2b_7\cos(\theta_2-\theta_8)\ddot{\theta}_8-(L_1b_1\dot{\theta}_1\sin(\theta_1-\theta_2)+\mu_2)\dot{\theta}_1+(\mu_2+\mu_3)\dot{\theta}_2+\\&(L_2b_2\dot{\theta}_3\sin(\theta_2-\theta_3)-\mu_3)\dot{\theta}_3+L_2b_3\dot{\theta}_4\sin(\theta_2-\theta_4)\dot{\theta}_4+L_2b_4\dot{\theta}_5\sin(\theta_2-\theta_5)\dot{\theta}_5+L_2b_5\dot{\theta}_6\sin(\theta_2-\theta_6)\dot{\theta}_6+\\&L_2b_6\dot{\theta}_7\sin(\theta_2-\theta_7)\dot{\theta}_7+L_2b_7\dot{\theta}_8\sin(\theta_2-\theta_8)\dot{\theta}_8-b_1g\sin\theta_2=0\end{aligned} \qquad \text{A1.77}$$

$$\begin{aligned}&b_2\cos\theta_3\ddot{x}+L_1b_2\cos(\theta_1-\theta_3)\ddot{\theta}_1+L_2b_2\cos(\theta_2-\theta_3)\ddot{\theta}_2+a_3\ddot{\theta}_3+L_3b_3\cos(\theta_3-\theta_4)\ddot{\theta}_4+L_3b_4\cos(\theta_3-\theta_5)\ddot{\theta}_5+\\&L_3b_5\cos(\theta_3-\theta_6)\ddot{\theta}_6+L_3b_6\cos(\theta_3-\theta_7)\ddot{\theta}_7+L_3b_7\cos(\theta_3-\theta_8)\ddot{\theta}_8-L_1b_2\dot{\theta}_1\sin(\theta_1-\theta_3)\dot{\theta}_1-(L_2b_2\dot{\theta}_2\sin(\theta_2-\theta_3)+\mu_3)\dot{\theta}_2+\\&(\mu_3+\mu_4)\dot{\theta}_3+(L_3b_3\dot{\theta}_4\sin(\theta_3-\theta_4)-\mu_4)\dot{\theta}_4+L_3b_4\dot{\theta}_5\sin(\theta_3-\theta_5)\dot{\theta}_5+L_3b_5\dot{\theta}_6\sin(\theta_3-\theta_6)\dot{\theta}_6+L_3b_6\dot{\theta}_7\sin(\theta_3-\theta_7)\dot{\theta}_7+\\&L_3b_7\dot{\theta}_8\sin(\theta_3-\theta_8)\dot{\theta}_8-b_2g\sin\theta_3=0\end{aligned} \qquad \text{A.178}$$

$$\begin{aligned}&b_3 \cos\theta_4 \ddot{x} + L_1 b_3 \cos(\theta_1-\theta_4)\ddot{\theta}_1 + L_2 b_3 \cos(\theta_2-\theta_4)\ddot{\theta}_2 + L_3 b_3 \cos(\theta_3-\theta_4)\ddot{\theta}_3 + a_4\ddot{\theta}_4 + L_4 b_4 \cos(\theta_4-\theta_5)\ddot{\theta}_5 + \\ &L_4 b_5 \cos(\theta_4-\theta_6)\ddot{\theta}_6 + L_4 b_6 \cos(\theta_4-\theta_7)\ddot{\theta}_7 + L_4 b_7 \cos(\theta_4-\theta_8)\ddot{\theta}_8 - L_1 b_3 \dot{\theta}_1 \sin(\theta_1-\theta_4)\dot{\theta}_1 - L_2 b_3 \dot{\theta}_2 \sin(\theta_2-\theta_4)\dot{\theta}_2 - \\ &(L_3 b_3 \dot{\theta}_3 \sin(\theta_3-\theta_4) + \mu_4)\dot{\theta}_3 + (\mu_4+\mu_5)\dot{\theta}_4 + (L_4 b_4 \dot{\theta}_5 \sin(\theta_4-\theta_5) - \mu_5)\dot{\theta}_5 + L_4 b_5 \dot{\theta}_6 \sin(\theta_4-\theta_6)\dot{\theta}_6 + \\ &L_4 b_6 \dot{\theta}_7 \sin(\theta_4-\theta_7)\dot{\theta}_7 + L_4 b_7 \dot{\theta}_8 \sin(\theta_4-\theta_8)\dot{\theta}_8 - b_3 g \sin\theta_4 = 0\end{aligned} \tag{A1.79}$$

$$\begin{aligned}&b_4 \cos\theta_5 \ddot{x} + L_1 b_4 \cos(\theta_1-\theta_5)\ddot{\theta}_1 + L_2 b_4 \cos(\theta_2-\theta_5)\ddot{\theta}_2 + L_3 b_4 \cos(\theta_3-\theta_5)\ddot{\theta}_3 + L_4 b_4 \cos(\theta_4-\theta_5)\ddot{\theta}_4 + a_5\ddot{\theta}_5 + \\ &L_5 b_5 \cos(\theta_5-\theta_6)\ddot{\theta}_6 + L_5 b_6 \cos(\theta_5-\theta_7)\ddot{\theta}_7 + L_5 b_7 \cos(\theta_5-\theta_8)\ddot{\theta}_8 - L_1 b_4 \dot{\theta}_1 \sin(\theta_1-\theta_5)\dot{\theta}_1 - L_2 b_4 \dot{\theta}_2 \sin(\theta_2-\theta_5)\dot{\theta}_2 - \\ &L_3 b_4 \dot{\theta}_3 \sin(\theta_3-\theta_5)\dot{\theta}_3 - (L_4 b_4 \dot{\theta}_4 \sin(\theta_4-\theta_5) + \mu_5)\dot{\theta}_4 + (\mu_5+\mu_6)\dot{\theta}_5 + (L_5 b_5 \dot{\theta}_6 \sin(\theta_5-\theta_6) - \mu_6)\dot{\theta}_6 + \\ &L_5 b_6 \dot{\theta}_7 \sin(\theta_5-\theta_7)\dot{\theta}_7 + L_5 b_7 \dot{\theta}_8 \sin(\theta_5-\theta_8)\dot{\theta}_8 - b_4 g \sin\theta_5 = 0\end{aligned} \tag{A1.80}$$

$$\begin{aligned}&b_5 \cos\theta_6 \ddot{x} + L_1 b_5 \cos(\theta_1-\theta_6)\ddot{\theta}_1 + L_2 b_5 \cos(\theta_2-\theta_6)\ddot{\theta}_2 + L_3 b_5 \cos(\theta_3-\theta_6)\ddot{\theta}_3 + L_4 b_5 \cos(\theta_4-\theta_6)\ddot{\theta}_4 + \\ &L_5 b_5 \cos(\theta_5-\theta_6)\ddot{\theta}_5 + a_6\ddot{\theta}_6 + L_6 b_6 \cos(\theta_6-\theta_7)\ddot{\theta}_7 + L_6 b_7 \cos(\theta_6-\theta_8)\ddot{\theta}_8 - L_1 b_5 \dot{\theta}_1 \sin(\theta_1-\theta_6)\dot{\theta}_1 - \\ &L_2 b_5 \dot{\theta}_2 \sin(\theta_2-\theta_6)\dot{\theta}_2 - L_3 b_5 \dot{\theta}_3 \sin(\theta_3-\theta_6)\dot{\theta}_3 - L_4 b_5 \dot{\theta}_4 \sin(\theta_4-\theta_6)\dot{\theta}_4 - (L_5 b_5 \dot{\theta}_5 \sin(\theta_5-\theta_6) + \mu_6)\dot{\theta}_5 + \\ &(\mu_6+\mu_7)\dot{\theta}_6 + (L_6 b_6 \dot{\theta}_7 \sin(\theta_6-\theta_7) - \mu_7)\dot{\theta}_7 + L_6 b_7 \dot{\theta}_8 \sin(\theta_6-\theta_8)\dot{\theta}_8 - b_5 g \sin\theta_6 = 0\end{aligned} \tag{A1.81}$$

$$\begin{aligned}&b_6 \cos\theta_7 \ddot{x} + L_1 b_6 \cos(\theta_1-\theta_7)\ddot{\theta}_1 + L_2 b_6 \cos(\theta_2-\theta_7)\ddot{\theta}_2 + L_3 b_6 \cos(\theta_3-\theta_7)\ddot{\theta}_3 + L_4 b_6 \cos(\theta_4-\theta_7)\ddot{\theta}_4 + \\ &L_5 b_6 \cos(\theta_5-\theta_7)\ddot{\theta}_5 + L_6 b_6 \cos(\theta_6-\theta_7)\ddot{\theta}_6 + a_7\ddot{\theta}_7 + L_7 b_7 \cos(\theta_7-\theta_8)\ddot{\theta}_8 - L_1 b_6 \dot{\theta}_1 \sin(\theta_1-\theta_7)\dot{\theta}_1 - \\ &L_2 b_6 \dot{\theta}_2 \sin(\theta_2-\theta_7)\dot{\theta}_2 - L_3 b_6 \dot{\theta}_3 \sin(\theta_3-\theta_7)\dot{\theta}_3 - L_4 b_6 \dot{\theta}_4 \sin(\theta_4-\theta_7)\dot{\theta}_4 - L_5 b_6 \dot{\theta}_5 \sin(\theta_5-\theta_7)\dot{\theta}_5 - \\ &(L_6 b_6 \dot{\theta}_6 \sin(\theta_6-\theta_7) + \mu_7)\dot{\theta}_6 + (\mu_7+\mu_8)\dot{\theta}_7 + (L_7 b_7 \dot{\theta}_8 \sin(\theta_7-\theta_8) - \mu_8)\dot{\theta}_8 - b_6 g \sin\theta_7 = 0\end{aligned} \tag{A1.82}$$

$$\begin{aligned}&b_7 \cos\theta_8 \ddot{x} + L_1 b_7 \cos(\theta_1-\theta_8)\ddot{\theta}_1 + L_2 b_7 \cos(\theta_2-\theta_8)\ddot{\theta}_2 + L_3 b_7 \cos(\theta_3-\theta_8)\ddot{\theta}_3 + L_4 b_7 \cos(\theta_4-\theta_8)\ddot{\theta}_4 + \\ &L_5 b_7 \cos(\theta_5-\theta_8)\ddot{\theta}_5 + L_6 b_7 \cos(\theta_6-\theta_8)\ddot{\theta}_6 + L_7 b_7 \cos(\theta_7-\theta_8)\ddot{\theta}_7 + a_8\ddot{\theta}_8 - L_1 b_7 \dot{\theta}_1 \sin(\theta_1-\theta_8)\dot{\theta}_1 - \\ &L_2 b_7 \dot{\theta}_2 \sin(\theta_2-\theta_8)\dot{\theta}_2 - L_3 b_7 \dot{\theta}_3 \sin(\theta_3-\theta_8)\dot{\theta}_3 - L_4 b_7 \dot{\theta}_4 \sin(\theta_4-\theta_8)\dot{\theta}_4 - L_5 b_7 \dot{\theta}_5 \sin(\theta_5-\theta_8)\dot{\theta}_5 - \\ &L_6 b_7 \dot{\theta}_6 \sin(\theta_6-\theta_8)\dot{\theta}_6 - (L_7 b_7 \dot{\theta}_7 \sin(\theta_7+\theta_8) + \mu_8)\dot{\theta}_7 + \mu_8\dot{\theta}_8 - b_7 g \sin\theta_8 = 0\end{aligned} \tag{A1.83}$$

Equations (A1.75) to (A1.83) are the equations that describe the nonlinear dynamics of the DQIP and thus can be reduced to a single line equation in matrix form:

$$M(x,\theta)\left(\ddot{x}\ddot{\theta}\right) + N((x,\theta),(\dot{x},\dot{\theta}))\left(\dot{x}\dot{\theta}\right) + D(x,\theta) + Gu \tag{A1.84}$$

Where:

$$M(x,\theta)=\begin{pmatrix}
a_0 & b_0\cos\theta_1 & b_1\cos\theta_2 & b_2\cos\theta_3 & b_3\cos\theta_4 & b_4\cos\theta_5 & b_5\cos\theta_6 & b_6\cos\theta_7 & b_7\cos\theta_8 \\
b_0\cos\theta_1 & a_1 & L_1b_1\cos(\theta_1-\theta_2) & L_1b_2\cos(\theta_1-\theta_3) & L_1b_3\cos(\theta_1-\theta_4) & L_1b_4\cos(\theta_1-\theta_5) & L_1b_5\cos(\theta_1-\theta_6) & L_1b_6\cos(\theta_1-\theta_7) & L_1b_7\cos(\theta_1-\theta_8) \\
b_1\cos\theta_2 & L_1b_1\cos(\theta_1-\theta_2) & a_2 & L_2b_2\cos(\theta_2-\theta_3) & L_2b_3\cos(\theta_2-\theta_4) & L_2b_4\cos(\theta_2-\theta_5) & L_2b_5\cos(\theta_2-\theta_6) & L_2b_6\cos(\theta_2-\theta_7) & L_2b_7\cos(\theta_2-\theta_8) \\
b_2\cos\theta_3 & L_1b_2\cos(\theta_1-\theta_3) & L_2b_2\cos(\theta_2-\theta_3) & a_3 & L_3b_3\cos(\theta_3-\theta_4) & L_3b_4\cos(\theta_3-\theta_5) & L_3b_5\cos(\theta_3-\theta_6) & L_3b_6\cos(\theta_3-\theta_7) & L_3b_7\cos(\theta_3-\theta_8) \\
b_3\cos\theta_4 & L_1b_3\cos(\theta_1-\theta_4) & L_2b_3\cos(\theta_2-\theta_4) & L_3b_3\cos(\theta_3-\theta_4) & a_4 & L_4b_4\cos(\theta_4-\theta_5) & L_4b_5\cos(\theta_4-\theta_6) & L_4b_6\cos(\theta_4-\theta_7) & L_4b_7\cos(\theta_4-\theta_8) \\
b_4\cos\theta_5 & L_1b_4\cos(\theta_1-\theta_5) & L_2b_4\cos(\theta_2-\theta_5) & L_3b_4\cos(\theta_3-\theta_5) & L_4b_4\cos(\theta_4-\theta_5) & a_5 & L_5b_5\cos(\theta_5-\theta_6) & L_5b_6\cos(\theta_5-\theta_7) & L_5b_7\cos(\theta_5-\theta_8) \\
b_5\cos\theta_6 & L_1b_5\cos(\theta_1-\theta_6) & L_2b_5\cos(\theta_2-\theta_6) & L_3b_5\cos(\theta_3-\theta_6) & L_4b_5\cos(\theta_4-\theta_6) & L_5b_5\cos(\theta_5-\theta_6) & a_6 & L_6b_6\cos(\theta_6-\theta_7) & L_6b_7\cos(\theta_7-\theta_8) \\
b_6\cos\theta_7 & L_1b_6\cos(\theta_1-\theta_7) & L_2b_6\cos(\theta_2-\theta_7) & L_3b_6\cos(\theta_3-\theta_7) & L_4b_6\cos(\theta_4-\theta_7) & L_5b_6\cos(\theta_5-\theta_7) & L_6b_6\cos(\theta_6-\theta_7) & a_7 & L_7b_7\cos(\theta_7-\theta_8) \\
b_7\cos\theta_8 & L_1b_7\cos(\theta_1-\theta_8) & L_2b_7\cos(\theta_2-\theta_8) & L_3b_7\cos(\theta_3-\theta_8) & L_4b_7\cos(\theta_4-\theta_8) & L_5b_7\cos(\theta_5-\theta_8) & L_6b_7\cos(\theta_6-\theta_8) & L_7b_7\cos(\theta_7-\theta_8) & a_8
\end{pmatrix}$$

A1.85

$$N((x,\theta),(\dot{x},\dot{\theta})=\left(\begin{matrix}
\mu_0 & -b_0\dot{\theta}_1\sin\theta_1 & -b_1\dot{\theta}_2\sin\theta_2 & -b_2\dot{\theta}_3\sin\theta_3 & -b_3\dot{\theta}_4\sin\theta_4 \\
0 & \mu_1+\mu_2 & L_1b_1\dot{\theta}_2\sin(\theta_1-\theta_2)-\mu_2 & L_1b_2\dot{\theta}_3\sin(\theta_1-\theta_3) & L_1b_3\dot{\theta}_4\sin(\theta_1-\theta_4) \\
0 & -L_1b_1\dot{\theta}_1\sin(\theta_1-\theta_2)-\mu_2 & \mu_2+\mu_3 & L_2b_2\dot{\theta}_3\sin(\theta_2-\theta_3)-\mu_3 & L_2b_3\dot{\theta}_4\sin(\theta_2-\theta_4) \\
0 & -L_1b_2\dot{\theta}_1\sin(\theta_1-\theta_3) & -L_2b_2\dot{\theta}_2\sin(\theta_2-\theta_3)-\mu_3 & \mu_3+\mu_4 & L_3b_3\dot{\theta}_4\sin(\theta_3-\theta_4)-\mu_4 \\
0 & -L_1b_3\dot{\theta}_1\sin(\theta_1-\theta_4) & -L_2b_3\dot{\theta}_2\sin(\theta_2-\theta_4) & -L_3b_3\dot{\theta}_3\sin(\theta_3-\theta_4)-\mu_4 & \mu_4+\mu_5 \\
0 & -L_1b_4\dot{\theta}_1\sin(\theta_1-\theta_5) & -L_2b_4\dot{\theta}_2\sin(\theta_2-\theta_5) & -L_3b_4\dot{\theta}_3\sin(\theta_3-\theta_5) & -L_4b_4\dot{\theta}_4\sin(\theta_4-\theta_5)-\mu_5 \\
0 & -L_1b_5\dot{\theta}_1\sin(\theta_1-\theta_6) & -L_2b_5\dot{\theta}_2\sin(\theta_2-\theta_6) & -L_3b_5\dot{\theta}_3\sin(\theta_3-\theta_6) & -L_4b_5\dot{\theta}_4\sin(\theta_4-\theta_6) \\
0 & -L_1b_6\dot{\theta}_1\sin(\theta_1-\theta_7) & -L_2b_6\dot{\theta}_2\sin(\theta_2-\theta_7) & -L_3b_6\dot{\theta}_3\sin(\theta_3-\theta_7) & -L_4b_6\dot{\theta}_4\sin(\theta_4-\theta_7) \\
0 & -L_1b_7\dot{\theta}_1\sin(\theta_1-\theta_8) & -L_2b_7\dot{\theta}_2\sin(\theta_2-\theta_8) & -L_3b_7\dot{\theta}_3\sin(\theta_3-\theta_8) & -L_4b_7\dot{\theta}_4\sin(\theta_4-\theta_8)
\end{matrix}\right.$$

$$\left.\begin{matrix}
-b_4\dot{\theta}_5\sin\theta_5 & -b_5\dot{\theta}_6\sin\theta_6 & -b_6\dot{\theta}_7\sin\theta_7 & -b_7\dot{\theta}_8\sin\theta_8 \\
L_1b_4\dot{\theta}_5\sin(\theta_1-\theta_5) & L_1b_5\dot{\theta}_6\sin(\theta_1-\theta_6) & L_1b_6\dot{\theta}_7\sin(\theta_1-\theta_7) & L_1b_7\dot{\theta}_8\sin(\theta_1-\theta_8) \\
L_2b_4\dot{\theta}_5\sin(\theta_2-\theta_5) & L_2b_5\dot{\theta}_6\sin(\theta_2-\theta_6) & L_2b_6\dot{\theta}_7\sin(\theta_2-\theta_7) & L_2b_7\dot{\theta}_8\sin(\theta_2-\theta_8) \\
L_3b_4\dot{\theta}_5\sin(\theta_3-\theta_5) & L_3b_5\dot{\theta}_6\sin(\theta_3-\theta_6) & L_3b_6\dot{\theta}_7\sin(\theta_3-\theta_7) & L_3b_7\dot{\theta}_8\sin(\theta_3-\theta_8) \\
L_4b_4\dot{\theta}_5\sin(\theta_4-\theta_5)-\mu_5 & L_4b_5\dot{\theta}_6\sin(\theta_4-\theta_6) & L_4b_6\dot{\theta}_7\sin(\theta_4-\theta_7) & L_4b_7\dot{\theta}_8\sin(\theta_4-\theta_8) \\
\mu_5+\mu_6 & L_5b_5\dot{\theta}_6\sin(\theta_5-\theta_6)-\mu_6 & L_5b_6\dot{\theta}_7\sin(\theta_5-\theta_7) & L_5b_7\dot{\theta}_8\sin(\theta_5-\theta_8) \\
-L_5b_5\dot{\theta}_5\sin(\theta_5-\theta_6)-\mu_6 & \mu_6+\mu_7 & L_6b_6\dot{\theta}_7\sin(\theta_6-\theta_7)-\mu_7 & L_6b_7\dot{\theta}_8\sin(\theta_6-\theta_8) \\
-L_5b_6\dot{\theta}_5\sin(\theta_5-\theta_7) & -L_6b_6\dot{\theta}_6\sin(\theta_6-\theta_7)-\mu_7 & \mu_7+\mu_8 & L_7b_7\dot{\theta}_8\sin(\theta_7-\theta_8)-\mu_8 \\
-L_5b_7\dot{\theta}_5\sin(\theta_5-\theta_8) & -L_6b_7\dot{\theta}_6\sin(\theta_6-\theta_8) & -L_7b_7\dot{\theta}_7\sin(\theta_7-\theta_8)-\mu_7 & \mu_8
\end{matrix}\right)$$

A1.86

$$D(x,\theta)=\begin{pmatrix} 0 \\ -b_0 g\sin\theta_1 \\ -b_1 g\sin\theta_2 \\ -b_2 g\sin\theta_3 \\ -b_3 g\sin\theta_4 \\ -b_4 g\sin\theta_5 \\ -b_5 g\sin\theta_6 \\ -b_6 g\sin\theta_7 \\ -b_7 g\sin\theta_8 \end{pmatrix} \qquad \text{A1.87}$$

$$\text{And}\, G=\begin{pmatrix} 1 \\ 0 \\ 0 \\ 0 \\ 0 \\ 0 \\ 0 \\ 0 \\ 0 \end{pmatrix} \qquad \text{A1.88}$$

Replacing the generalized co-ordinates with a single parameter β, equation (A1.84) is further simplified as;

$$M(\beta)\left(\ddot{\beta}\right)+N(\beta,\dot{\beta})\left(\dot{\beta}\right)+D(\beta)=Gu \qquad \text{A1.89}$$

Where $\beta = (x,\ \theta)$

To make the control implementation easier, the system dynamic equations represented in a compact form by equation (A1.89) is reformulated into 18th *(9x9)* order system of ordinary differential equation. In order to achieve this, a state vector z ϵ R^{18} such that $z = \left(\beta\ \dot{\beta}\right)^T$.

By discarding the dependencies and their derivatives of the generalized co-ordinates $(\beta, \dot{\beta})$ in the system matrix, the dynamic equation (A1.89) can be written as;

$$M\ddot{\beta}+N\dot{\beta}+D\beta=Gu \qquad \text{A1.90}$$

$$\ddot{\beta} = -M^{-1}N\dot{\beta} - M^{-1}D + M^{-1}Gu \qquad \text{A1.91}$$

$$\dot{Z} = \begin{pmatrix} 0_{9x9} & I_{9x9} \\ 0_{9x9} & -M^{-1}N \end{pmatrix} Z + \begin{pmatrix} 0_{9x1} \\ -M^{-1}D \end{pmatrix} + \begin{pmatrix} 0_{9x1} \\ M^{-1}G \end{pmatrix} u \qquad \text{A1.92}$$

Equation (A1.92) represents a nonlinear state space dynamics of the DQIP. The equation is converted into its linear equivalent as follows:

APPROXIMATE LINEAR MODEL OF THE SYSTEM

The equivalent linear model of the DQIP is obtained by simply linearizing the equation (A1.91) about an operating point (vertical position). The linear model is obtained by using Taylor series expansion of equation (A1.92) and linear Jacobian matrix transformation.

Equation (A1.92) is linearized about: $Z = 0\left((\beta\dot{\beta})^T = (x, \theta) = (00)^T\right)$ i.e. θ_n is very small and approaching zero.

$$\text{Let } M'Z = \begin{pmatrix} 0_{9x9} & I_{9x9} \\ 0_{9x9} & -M^{-1}(0)N(0) \end{pmatrix} Z \qquad \text{A1.93}$$

In matrix *D*, all $\sin\theta \approx \theta$. Therefore,

$$D(0) \approx \frac{\partial D(\theta)}{\partial \theta}(\boldsymbol{\theta} \approx \mathbf{0}) \approx \frac{\boldsymbol{\partial D(0)}}{\boldsymbol{\partial \theta}} \boldsymbol{x\theta} \qquad \text{A1.94}$$

In order to write equation (A1.94) in terms of $Z = (\beta\ \dot{\beta})^T$, equation (A1.94) becomes;

$$D(0) = \begin{pmatrix} \dfrac{\partial D(0)}{\partial \theta} & 0_{9x1} \end{pmatrix} \begin{pmatrix} \beta \\ \dot{\beta} \end{pmatrix} = \begin{pmatrix} \dfrac{\partial D(0)}{\partial \theta} & 0_{9x1} \end{pmatrix} Z \qquad \text{A1.95}$$

$$\text{Let } N' = \begin{pmatrix} 0_{9x1} \\ -M^{-1}(0)D(0) \end{pmatrix} \qquad \text{A1.96}$$

Then, $N' = \begin{pmatrix} 0_{9x1} \\ -M^{-1}(0)D(0) \end{pmatrix} = \begin{pmatrix} 0_{9x9} & 0_{9x9} \\ -M^{-1}(0)\dfrac{\partial D(0)}{\partial \theta} & 0_{9x9} \end{pmatrix} Z$ A1.97

Adding equations (A1.93) and (A1.97);

$$M'Z + N' = \begin{pmatrix} 0_{9x9} & I_{9x9} \\ 0_{9x9} & -M^{-1}(0)N(0) \end{pmatrix} Z + \begin{pmatrix} 0_{9x9} & 0_{9x9} \\ -M^{-1}(0)\dfrac{\partial D(0)}{\partial \theta} & 0_{9x9} \end{pmatrix} Z \qquad \text{A1.98}$$

Substituting equation (A1.98) into equation (A1.92), the approximate linear equivalent of equation (A1.92) around an upright position will be;

$$\dot{Z} = \begin{pmatrix} 0_{9x9} & I_{9x9} \\ -M^{-1}(0)\dfrac{\partial D(0)}{\partial \theta} & -M^{-1}(0)N(0) \end{pmatrix} Z + \begin{pmatrix} 0_{9x1} \\ M^{-1}(0)G \end{pmatrix} u \qquad \text{A1.99}$$

APPENDIX A2
QUADRUPLE INVERTED PENDULUM (QIP) FROM THE DOUBLE QUAD INVERTED PPENDULUM (DQIP) SYSTEM

The model of the QIP can be extracted from DQIP model by truncating the mathematical modeling at the fourth link. The resulting nonlinear model of the QIP is determined as follows;

$$\begin{aligned}&a_0\ddot{x}+b_0\cos\theta_1\ddot{\theta}_1+b_1\cos\theta_2\ddot{\theta}_2+b_2\cos\theta_3\ddot{\theta}_3+b_2\cos\theta_3\ddot{\theta}_3+b_3\cos\theta_4\ddot{\theta}_4+\mu_0\dot{x}-b_0\dot{\theta}_1\sin\theta_1(\dot{\theta}_1)-b_1\dot{\theta}_2\sin\theta_2(\dot{\theta}_2)\\&-b_2\dot{\theta}_3\sin\theta_3(\dot{\theta}_3)-b_3\dot{\theta}_4\sin\theta_4(\dot{\theta}_4)=u\end{aligned} \tag{A2.1}$$

$$\begin{aligned}&b_0\cos\theta_1\ddot{x}+a_1\ddot{\theta}_1+L_1b_1\cos(\theta_1-\theta_2)\ddot{\theta}_2+L_1b_2\cos(\theta_1-\theta_3)\ddot{\theta}_3+L_1b_3\cos(\theta_1-\theta_4)\ddot{\theta}_4+(\mu_1+\mu_2)\dot{\theta}_1+\\&(L_1b_1\dot{\theta}_2\sin(\theta_1-\theta_2)-\mu_2)\dot{\theta}_2+L_1b_2\dot{\theta}_3\sin(\theta_1-\theta_3)\dot{\theta}_3+L_1b_3\dot{\theta}_4\sin(\theta_1-\theta_4)\dot{\theta}_4-b_0g\sin\theta_1=0\end{aligned} \tag{A2.2}$$

$$\begin{aligned}&b_1\cos\theta_2\ddot{x}+L_1b_1\cos(\theta_1-\theta_2)\ddot{\theta}_1+a_2\ddot{\theta}_2+L_2b_2\cos(\theta_2-\theta_3)\ddot{\theta}_3+L_2b_3\cos(\theta_2-\theta_4)\ddot{\theta}_4-(L_1b_1\dot{\theta}_1\sin(\theta_1-\theta_2)+\mu_2)\dot{\theta}_1+\\&(\mu_2+\mu_3)\dot{\theta}_2+(L_2b_2\dot{\theta}_3\sin(\theta_2-\theta_3)-\mu_3)\dot{\theta}_3+L_2b_3\dot{\theta}_4\sin(\theta_2-\theta_4)\dot{\theta}_4-b_1g\sin\theta_2=0\end{aligned} \tag{A2.3}$$

$$\begin{aligned}&b_2\cos\theta_3\ddot{x}+L_1b_2\cos(\theta_1-\theta_3)\ddot{\theta}_1+L_2b_2\cos(\theta_2-\theta_3)\ddot{\theta}_2+a_3\ddot{\theta}_3+L_3b_3\cos(\theta_3-\theta_4)\ddot{\theta}_4-L_1b_2\dot{\theta}_1\sin(\theta_1-\theta_3)\dot{\theta}_1-\\&(L_2b_2\dot{\theta}_2\sin(\theta_2-\theta_3)+\mu_3)\dot{\theta}_2+(\mu_3+\mu_4)\dot{\theta}_3+(L_3b_3\dot{\theta}_4\sin(\theta_3-\theta_4)-\mu_4)\dot{\theta}_4-b_2g\sin\theta_3=0\end{aligned} \tag{3.14}$$

$$\begin{aligned}&b_3\cos\theta_4\ddot{x}+L_1b_3\cos(\theta_1-\theta_4)\ddot{\theta}_1+L_2b_3\cos(\theta_2-\theta_4)\ddot{\theta}_2+L_3b_3\cos(\theta_3-\theta_4)\ddot{\theta}_3+a_4\ddot{\theta}_4-L_1b_3\dot{\theta}_1\sin(\theta_1-\theta_4)\dot{\theta}_1-\\&L_2b_3\dot{\theta}_2\sin(\theta_2-\theta_4)\dot{\theta}_2-(L_3b_3\dot{\theta}_3\sin(\theta_3-\theta_4)+\mu_4)\dot{\theta}_3+(\mu_4+\mu_5)\dot{\theta}_4-b_3g\sin\theta_4=0\end{aligned} \tag{3.15}$$

Using equations (A2.1) to (A2.5), the compact state-space model of the QIP is given by:

$$\dot{x}=\begin{pmatrix}0_{5x5} & I_{5x5}\\ -M^{-1}(0)\dfrac{\partial D(0)}{\partial\theta} & -M^{-1}(0)N(0)\end{pmatrix}x+\begin{pmatrix}0_{5x1}\\ M^{-1}(0)G\end{pmatrix}u \tag{A2.6}$$

Equation (3.16) corresponds to the standard state-space equation given by (3.17).

$$\dot{x} = Ax + Bu \tag{A2.7}$$

$$y = Cx + Du$$

(A2.8)

Where $A = \begin{pmatrix} 0_{5x5} & I_{5x5} \\ -M^{-1}(0)\dfrac{\partial D(0)}{\partial \theta} & -M^{-1}(0)N(0) \end{pmatrix}$ (A2.9)

$$B = \begin{pmatrix} 0_{5x1} \\ M^{-1}(0)G \end{pmatrix} \tag{A2.10}$$

APPENDIX B1

MATLAB M. FILE FOR QUADRUPLE INVERTED PENDULUM (QIP)

```
%%Parameters used for State Matrix computation of the Quad Inverted
Pendulum.

m0 = 1.3282;    % Mass of the Cart
m1 = 0.2200;    % Mass of the First Pendulum
m2 = m1;        % Mass of the Second Pendulum
m3 = m2;        % Mass of the Third Pendulum
m4 = 0.1870;    % Mass of the Fourth Pendulum
g = 9.81;       % gravitational constant
u0 = 22.9147;   % Frictional Coefficient between the Cart and the Track
u1 = 0.007056;  % Frictional Coefficient between the first pendulum and the
                  cart' pivot point
u2 = 0.002646;  % Frictional Coefficient between the first pendulum and the
                  second
u3 = u2;        % Frictional Coefficient between the second pendulum and
                  the third
u4 = u3;        % Frictional Coefficient between the third pendulum and the
                  fourth

%%State matrix elements computations

n1 = u1 + u2
n2 = u2 + u3
n3 = u3 + u4
L1 = 0.49;
L2 = L1;
L3 = L2;
L4 = 0.452;
a0 = m0 + m1 + m2 + m3 + m4
a1 = (m1/3 + m2 + m3 + m4)*L1^2
a2 = (m2/3 + m3 + m4)*L2^2
a3 = (m3/3 + m4)*L3^2
a4 = (m4/3)*L4^2
b0 = (m1/2 + m2 + m3 + m4)*L1
b1 = (m2/2 + m3 + m4)*L2
b2 = (m3/2 +m4)*L3
b3 = (m4/2)*L4
a11 = L1*b1
a12 = L1*b2
a13 = L1*b3
a22 = L2*b2
a23 = L2*b3
a33 = L3*b3
M0 = [a0 b0 b1 b2 b3; b0 a1 b1*L1 b2*L1 b3*L1; b1 b1*L1 a2 b2*L2 b3*L2; b2
b2*L1 b2*L2 a3 b3*L3; b3 b3*L1 b3*L2 b3*L3 a4]
N0 = [u0 0 0 0 0; 0 n1 -u2 0 0; 0 -u2 n2 -u3 0; 0 0 -u3 n3 -u4; 0 0 0 -u3
u4]
D0 = [0 0 0 0 0; 0 -b0 0 0 0; 0 0 -b1 0 0; 0 0 0 -b2 0; 0 0 0 0 -b3]*g
G = [1; 0; 0; 0; 0]
InvM0 = inv(M0)
A1 = -InvM0*D0
A2 = -InvM0*N0
```

```
B1 = InvM0*G
A = [zeros(5,5) eye(5,5); A1 A2] % State variable Matrix
B = [zeros(5,1); B1]             % Input State Matrix
C = [eye(5,5) zeros(5,5)]        % Output State Matrix
D = 0                            % Transition Disturbance Matrix
ltiview(sys_ss)                  % Find System Linear Configuration
MCr = ctrb(A, B);                % Tests for C  Control Solution
MCo = obsv(A, C);
CONTR = rank(MCr)
OBSVB = rank(MCo)
if rank(MCr)==size(A)
    'THE SYSTEM IS CONTROLLABLE'
else 'THE SYSTEM IS NOT CONTROLLABLE'
end
    if rank(MCo)==size(A)
        'THE SYSTEM IS OBSERVABLE'
    else 'THE SYSTEM IS NOT OBSERVABLE'
    end
>> CONTR = 10

ans =

THE SYSTEM IS CONTROLLABLE

>> OBSVB = 10

ans =

THE SYSTEM IS OBSERVABLE

state = {'x', 'x_dot' 'theta1' 'theta_dot1' 'theta2' 'theta_dot2' 'theta3'
'theta_dot3' 'theta4' 'theta_dot4'}
inputs = {'u'};
outputs = {'x'; 'theta1'; 'theta2'; 'theta3'; 'theta4'}

%ys_ss = ss(A, B, C, D, 'statename',states, 'inputname',inputs,
'outputname',outputs)
sys_ss = ss(A, B, C, D)
ltiview(sys_ss)

%%Design of LQR Controller for Quad Inverted Pendulum.

Q11 = 200;
Q22 = 250;
Q33 = 200;
Q44 = 200;
Q55 = 200;
Q66 = 0;
Q77 = 0;
Q88 = 0;
Q99 = 0;
Q00 = 0;
Q1 = [Q11 Q22 Q33 Q44 Q55 Q66 Q77 Q88 Q99 Q00];
Q = diag(Q1)
R = 1;
[K P E] = lqr(A,B,Q,R)
```

```
sys_LQ = ss(A-B*K, Bc, Cc, Dc)
x0 = [2; -0.04; 0.02; -0.01; 0.005; 0; 0; 0; 0; 0]

t = 0:0.02:10;

x0 = initial(sys_LQ, x, t);

x1 =initial(sys_LQ,
X1 = [1 0 0 0 0 0 0 0 0 0 ]*x0';
X2 = [0 1 0 0 0 0 0 0 0 0 ]*x0';
X3 = [0 0 1 0 0 0 0 0 0 0 ]*x0';
X4 = [0 0 0 1 0 0 0 0 0 0 ]*x0';
X5 = [0 0 0 0 1 0 0 0 0 0 ]*x0';

plot(t, X1);
xlabel('Time (s)')
legend('Velocity of the Cart')
grid;

plot(t, X2)
xlabel('Time (s)')
ylabel('First Pendulum Angle (rad)')
legend('First Pendulum Angular Velocity')
title('Time Response of the First Pendulum')
grid;

plot(t, X2)
xlabel('Time (s)')
ylabel('First Pendulum Angle (rad)')
legend('First Pendulum Angular Velocity')
title('Time Response of the First Pendulum')
grid;

plot(t, X3)
xlabel('Time (s)')
ylabel('Second Pendulum Angle (rad)')
legend('Second Pendulum Angular Velocity')
grid;

plot(t, X4)
xlabel('Time (s)')
ylabel('Third Pendulum Angle (rad)')
legend('Third Pendulum Angular Velocity')
grid;
plot(t, X5)
xlabel('Time (s)')
ylabel('Fourth Pendulum Angle (rad)')
legend('Fourth Pendulum Angular Velocity')
title('Time Response of the Fourth Pendulum Angle')
grid;
```

APPENDIX B2

MATLAB M.FILE FOR DOUBLE QUAD INVERTED PENDULUM (DQIP)

```
%%Parameters used for State Matrices computations of the Double Quad
Inverted Pendulum.

m0 = 1.3282;   % Mass of the Cart
m1 = 0.220;     % Mass of the first Pendulum rod
m2 = 0.220;     % Mass of the second Pendulum rod
m3 = 0.220;     % Mass of the third Pendulum rod
m4 = 0.220;     % Mass of the fourth Pendulum rod
m5 = 0.220;     % Mass of the fifth Pendulum rod
m6 = 0.220;     % Mass of the sixth Pendulum rod
m7 = 0.220;     % Mass of the seventh Pendulum rod
m8 = 0.187;     % Mass of the eighth Pendulum rod
L1 = 0.500;     % Length of the first Pendulum rod
L2 = 0.500;     % Length of the second Pendulum rod
L3 = 0.500;     % Length of the third Pendulum rod
L4 = 0.500;     % Length of the fourth Pendulum rod
L5 = 0.500;     % Length of the fifth Pendulum rod
L6 = 0.500;     % Length of the sixth Pendulum rod
L7 = 0.500;     % Length of the seventh Pendulum rod
L8 = 0.700;     % Length of the eighth Pendulum rod
g = 9.81;         % Gravitational constant
u0 = 22.9147;   % Frictional coefficient between the Cart and the
                  horizontal Track
u1 = 0.007056; % Frictional coefficient between the pivot point of the
            first Pendulum and the Cart
u2 = 0.002;    % Frictional coefficient between the pivot point of the
            first and second Pendulum
u3 = 0.002;    % Frictional coefficient between the pivot point of the
                  second and third Pendulum
u4 = 0.002;    % Frictional coefficient between the pivot point of the
            third and fourth Pendulum
u5 = 0.002;    % Frictional coefficient between the pivot point of the
            fourth and fifth Pendulum
u6 = 0.002;    % Frictional coefficient between the pivot point of the
            fifth and sixth Pendulum
u7 = 0.002;   % Frictional coefficient between the pivot point of the
                  sixth and seventh Pendulum
u8 = 0.002;   % Frictional coefficient between the pivot point of the
                  seventh and eight Pendulum

%%Computation of state space matrices elements

a0 = m0 +m1 + m2 + m3 + m4 + m5 + m6 + m7 + m8;
a1 = (m1/3 + m2 + m3 + m4+ m5 + m6 + m7 + m8)*L1^2;
a2 = (m2/3 + m3 + m4 + m5 + m6 + m7 + m8)*L2^2;
a3 = (m3/3 + m4 + m5 + m6 + m7 + m8)*L3^2;
a4 = (m4/3 + m5 + m6 + m7 + m8)*L4^2;
a5 = (m5/3 + m6 + m7 + m8)*L5^2;
a6 = (m6/3 + m7 + m8)*L6^2;
a7 = (m7/3 + m8)*L7^2;
a8 = (m8/3)*L8^2;
b0 = (m1/2 + m2 + m3 + m4 + m5 + m6 + m7 +m8)*L1;
```

```
b1 = (m2/2 + m3 + m4 + m5 + m6 + m7 +m8)*L2;
b2 = (m3/2 + m4 + m5 + m6 + m7 +m8)*L3;
b3 = (m4/2 + m5 + m6 + m7 +m8)*L4;
b4 = (m5/2 + m6 + m7 +m8)*L5;
b5 = (m6/2 + m7 +m8)*L6;
b6 = (m7/2 +m8)*L7;
b7 = (m8/2)*L8;

%%State Space Matrices Representation

M0 = [a0 b0 b1 b2 b3 b4 b5 b6 b7; b0 a1 L1*b1 L1*b2 L1*b3 L1*b4 L1*b5
L1*b6 L1*b7;
    b1 L1*b1 a2 L2*b2 L2*b3 L2*b4 L2*b5 L2*b6 L2*b7; b2 L1*b2 L2*b2 a3
L3*b3 L3*b4 L3*b5 L3*b6 L3*b7;
    b3 L1*b3 L2*b3 L3*b3 a4 L4*b4 L4*b5 L4*b6 L4*b7; b4 L1*b4 L2*b4 L3*b4
L4*b4 a5 L5*b5 L5*b6 L5*b7;
    b5 L1*b5 L2*b5 L3*b5 L4*b5 L5*b5 a6 L6*b6 L6*b7; b6 L1*b6 L2*b6 L3*b6
L4*b6 L5*b6 L6*b6 a7 L7*b7;
    b7 L1*b7 L2*b7 L3*b7 L4*b7 L5*b7 L6*b7 L7*b7 a8];
DE0 = [0 0 0 0 0 0 0 0 0; 0 -b0 0 0 0 0 0 0 0; 0 0 -b1 0 0 0 0 0 0;
    0 0 0 -b2 0 0 0 0 0; 0 0 0 0 -b3 0 0 0 0; 0 0 0 0 0 -b4 0 0 0;
    0 0 0 0 0 0 -b5 0 0; 0 0 0 0 0 0 0 -b6 0; 0 0 0 0 0 0 0 0 -b7]*g;
n1 = u1 + u2;
n2 = u2 + u3;
n3 = u3 + u4;
n4 = u4 + u5;
n5 = u5 + u6;
n6 = u6 + u7;
n7 = u7 + u8;
N0 = [u0 0 0 0 0 0 0 0 0; 0 n1 -u2 0 0 0 0 0 0; 0 -u2 n2 -u3 0 0 0 0 0;
    0 0 -u3 n3 -u4 0 0 0 0; 0 0 0 -u4 n4 -u5 0 0 0; 0 0 0 0 -u5 n5 -u6 0
0;
    0 0 0 0 0 -u6 n6 -u7 0; 0 0 0 0 0 0 -u7 n7 -u8; 0 0 0 0 0 0 0 -u7 u8];
G = [1; 0; 0; 0; 0; 0; 0; 0; 0];
InvM0 = inv(M0);
A1 = -InvM0*DE0;
A2 = -InvM0*N0;
B1 = inv(M0)*G;   %Inverse of M0 multiply by G
A = [zeros (9,9) eye(9,9); A1 A2];
B = [zeros (9,1); B1];
C = ([1 0 0 0 0 0 0 0 0 0 0 0 0 0 0 0 0 0; 0 1 0 0 0 0 0 0 0 0 0 0 0 0 0
0 0;
    0 0 1 0 0 0 0 0 0 0 0 0 0 0 0 0 0 0; 0 0 0 1 0 0 0 0 0 0 0 0 0 0 0 0
0;
    0 0 0 0 1 0 0 0 0 0 0 0 0 0 0 0 0 0; 0 0 0 0 0 1 0 0 0 0 0 0 0 0 0 0
0;
    0 0 0 0 0 0 1 0 0 0 0 0 0 0 0 0 0 0; 0 0 0 0 0 0 0 1 0 0 0 0 0 0 0 0
0;
    0 0 0 0 0 0 0 0 1 0 0 0 0 0 0 0 0 0]);


%% Test for Control Solution on an un-scaled DQIP

MCr = ctrb(A, B);
MCo = obsv(A, C);
CONTR = rank(MCr)
OBSVB = rank(MCo)
```

```
if rank(MCr)==size(A)
    'THE SYSTEM IS CONTROLLABLE'
else 'THE SYSTEM IS NOT CONTROLLABLE'
end
    if rank(MCo)==size(A)
        'THE SYSTEM IS OBSERVABLE'
    else 'THE SYSTEM IS NOT OBSERVABLE'
    end
>> CONTR = 13

ans =

THE SYSTEM IS NOT CONTROLLABLE

>> OBSVB = 17

ans =

THE SYSTEM IS NOT OBSERVABLE

%% State Model Scaling

As = 0.75e-1*([zeros (9,9) eye(9,9); A1 A2]);
Bs = 0.75e-1*([zeros (9,1); B1]);
Cs = [1 0 0 0 0 0 0 0 0 0 0 0 0 0 0 0 0 0; 0 1 0 0 0 0 0 0 0 0 0 0 0 0 0 0
0 0;
    0 0 1 0 0 0 0 0 0 0 0 0 0 0 0 0 0 0; 0 0 0 1 0 0 0 0 0 0 0 0 0 0 0 0
0;
    0 0 0 0 1 0 0 0 0 0 0 0 0 0 0 0 0 0; 0 0 0 0 0 1 0 0 0 0 0 0 0 0 0 0
0;
    0 0 0 0 0 0 1 0 0 0 0 0 0 0 0 0 0 0; 0 0 0 0 0 0 0 1 0 0 0 0 0 0 0 0
0;
    0 0 0 0 0 0 0 0 1 0 0 0 0 0 0 0 0 0];
Ds = zeros (9,1);
G1 = ss(As, Bs, Cs, Ds);
prescale(G1)
G1 = ss(As, Bs, Cs, Ds);
Gn = ssbal(G1);

%% Control Tests Solution on the DQIP Scaled Model

MCr = ctrb(As, Bs);
Mc = rank (MCr);
MCo = obsv(As, Cs);
Mo = rank(MCo);

if rank(MCr)==size(As)
    'THE SYSTEM IS CONTROLLABLE'
else 'THE SYSTEM IS NOT CONTROLLABLE'
end
    if rank(MCo)==size(A)
        'THE SYSTEM IS OBSERVABLE'
    else 'THE SYSTEM IS NOT OBSERVABLE'
    end
>> CONTR = 18
```

```
ans =

THE SYSTEM IS CONTROLLABLE

>> OBSVB = 18

ans =

THE SYSTEM IS OBSERVABLE

ltiview(sys_ss);      %% Linear Configuration Plots of the DQIP without
the                   feedback Controller


%% Design of a feedback controller
% start by selecting R = 1 and Q

R = 1;
Q = eye(18);    % please edit this to emphasize or penalize different
                  states as required.
% larger value of Q penalizes a state more;
R = 0.6; Q1 = 100; Q2 = 500; Q3 = 500; Q4 = 500; Q5 = 500; Q6 = 500; Q7 =
500; Q8 = 500; Q9 = 500;
Q10 = 1; Q11 = 1; Q12 = 1; Q13 = 1; Q14 = 1; Q15 = 1; Q16 = 1; Q17 = 1;
Q18 = 1;

R = 0.8; Q1 = 500; Q2 = 5000; Q3 = 5000; Q4 = 5000; Q5 = 5000; Q6 = 5000;
Q7 = 5000; Q8 = 5000; Q9 = 5000;
Q10 = 1; Q11 = 1; Q12 = 1; Q13 = 1; Q14 = 1; Q15 = 1; Q16 = 1; Q17 = 1;
Q18 = 1;
Q = diag(Qn)

R = 0.4; Q1 = 1000; Q2 = 10000; Q3 = 10000; Q4 = 10000; Q5 = 10000; Q6 =
10000; Q7 = 10000; Q8 = 10000; Q9 = 10000;
Q10 = 1; Q11 = 1; Q12 = 1; Q13 = 1; Q14 = 1; Q15 = 1; Q16 = 1; Q17 = 1;
Q18 = 1;
  t = 0:0.02:40;
x0 = initial(sys_LQ, x, t);
x1 =initial(sys_LQ,
X1 = [1 0 0 0 0 0 0 0 0 0 0 0 0 0 0 0 0 0]*x0';
X2 = [0 1 0 0 0 0 0 0 0 0 0 0 0 0 0 0 0 0]*x0';
X3 = [0 0 1 0 0 0 0 0 0 0 0 0 0 0 0 0 0 0]*x0';
X4 = [0 0 0 1 0 0 0 0 0 0 0 0 0 0 0 0 0 0]*x0';
X5 = [0 0 0 0 1 0 0 0 0 0 0 0 0 0 0 0 0 0]*x0'
X6 = [0 0 0 0 0 1 0 0 0 0 0 0 0 0 0 0 0 0]*x0';
X7 = [0 0 0 0 0 0 1 0 0 0 0 0 0 0 0 0 0 0]*x0';
X8 = [0 0 0 0 0 0 0 1 0 0 0 0 0 0 0 0 0 0]*x0';
X9 = [0 0 0 0 0 0 0 0 1 0 0 0 0 0 0 0 0 0]*x0'

% % LQR controller Design

[K,P,E]=lqr(A,B,Q,R)     % K is the controller gain matrix, E is the
                           position of the new poles

Ac = [(As-Bs*K)];
Bc = [Bs];
Cc = [Cs];
```

```
Dc = [Ds];
sys_cl = ss(Ac, Bc, Cc, Dc);

ltiview(sys_cl);      %% Linear Configuration Plots of the DQIP with the
                      feedback Controller

 %% Select observer poles such that, the dynamics are 3 - 3 times faster
than the dynamics of plant

lam = 4*real(E) + 1i*imag(E);
 lam = lam';
 L = place(A',C',lam);
 L=L';

T = 0:0.01:350;
u = 1*ones(size(T));
[y,x]=lsim(A-B*K,B,C,D,u,T);
figure(2)
plot(T,y)
```

MATLAB M.File for the System Responses

```
plot(Cartp_1.time,Cartp_1.signals.values,'linewidth',3)
xlabel('time(seconds)','fontsize',16);ylabel('CartDisplacement(m)','fontsi
ze',16);
legend('Cart response','location','northeast')
set(1,'color','white');
grid;

stairs(in_data.time,in_data.signals.values,'linewidth',3)
xlabel('time(seconds)','fontsize',16);ylabel('Controlinput(N)','fontsize',
16);
set(2,'color','white');
grid;

plot(Theta_1.time,Theta_1.signals.values,'linewidth',3)
xlabel('time(seconds)','fontsize',12);ylabel('Theta1(rad)','fontsize',16);
legend('First Pendulum Response','location','northeast')
set(1,'color','white');
grid;

plot(Theta_2.time,Theta_2.signals.values,'linewidth',3)
xlabel('time(seconds)','fontsize',16);ylabel('Theta2(rad)','fontsize',16);
legend('Second Pendulum Response','location','northeast')
set(1,'color','white');
grid;

plot(Theta_3.time,Theta_3.signals.values,'linewidth',3)
xlabel('time(seconds)','fontsize',16);ylabel('Theta3(rad)','fontsize',16);
legend('Third Pendulum Response','location','northeast')
set(1,'color','white');
grid;

plot(Theta_4.time,Theta_4.signals.values,'linewidth',3)
xlabel('time(seconds)','fontsize',16);ylabel('Theta4(rad)','fontsize',16);
legend('Fourth Pendulum Response','location','northeast')
```

```
set(1,'color','white');
grid;

plot(Theta_5.time,Theta_5.signals.values,'linewidth',3)
xlabel('time(seconds)','fontsize',16);ylabel('Theta5(rad)','fontsize',16);
legend('Fifth Pendulum Response','location','northeast')
set(1,'color','white');
grid;

plot(Theta_6.time,Theta_6.signals.values,'linewidth',3)
xlabel('time(seconds)','fontsize',16);ylabel('Theta6(rad)','fontsize',16);
legend('Sixth Pendulum Response','location','northeast')
set(1,'color','white');
grid;

plot(Theta_7.time,Theta_7.signals.values,'linewidth',3)
xlabel('time(seconds)','fontsize',16);ylabel('Theta7(rad)','fontsize',16);
legend('Seventh Pendulum Response','location','northeast')
set(1,'color','white');
grid;

plot(Theta_8.time,Theta_8.signals.values,'linewidth',3)
xlabel('time(seconds)','fontsize',16);ylabel('Theta8(rad)','fontsize',16);
legend('Eighth Pendulum Response','location','northeast')
set(1,'color','white');
grid;
```

APPENDIX C
MATLAB SOURCE CODES OF THE DQIP WITH THE CONTROLLER

```
Model {
  Name "LQR Controller Model of the DQIP"
  Version         8.1 MdlSubVersion       0 GraphicalInterface {
NumRootInports      0 NumRootOutports     1 Outport { BusObject
""
      BusOutputAsStruct       "off"
      Name "x_hat"} ParameterArgumentNames  "" ComputedModelVersion
"1.2"
    NumModelReferences 0 NumTestPointedSignals 0
  }
  SavedCharacterEncoding  "windows-1252 slprops.hdlmdlprops {$PropName
"HDLParams" $ObjectID 1
    Array {
      Type  "Cell"
      Dimension 2
      Cell            "HDLSubsystem"
      Cell            "untitled"
      PropName            "mdlProps"
    }
  }
  SaveDefaultBlockParams  on
  ScopeRefreshTime    0.035000
  OverrideScopeRefreshTime on
  DisableAllScopes    off
  DataTypeOverride    "UseLocalSettings"
  DataTypeOverrideAppliesTo "AllNumericTypes"
  MinMaxOverflowLogging   "UseLocalSettings"
  MinMaxOverflowArchiveMode "Overwrite"
  FPTRunName          "Run 1"
  MaxMDLFileLineLength    120
  Object {
    $PropName           "BdWindowsInfo"
    $ObjectID           2
    $ClassName          "Simulink.BDWindowsInfo"
    Object {
      $PropName           "WindowsInfo"
      $ObjectID           3
      $ClassName          "Simulink.WindowInfo"
      IsActive            [1]
      Location            [456.0, 46.0, 1091.0, 900.0]
      Object {
    $PropName       "ModelBrowserInfo"
    $ObjectID       4
    $ClassName      "Simulink.ModelBrowserInfo"
    Visible         [1]
    DockPosition        "Left"
    Width           [50]
    Height          [50]
    Filter          [8]
      }
      Object {
    $PropName       "ExplorerBarInfo"
    $ObjectID       5
```

```
    $ClassName      "Simulink.ExplorerBarInfo"
    Visible         [1]
      }
      Array {
    Type            "Simulink.EditorInfo"
    Dimension       3
    Object {
      $ObjectID       6
      IsActive        [1]
      ViewObjType         "SimulinkTopLevel"
      LoadSaveID          "0"
      Extents         [845.0, 694.0]
      ZoomFactor          [1.0]
      Offset          [-19.525006264448166, -167.3625071644783]
    }
    Object {
      $ObjectID       7
      IsActive        [0]
      ViewObjType         "SimulinkSubsys"
      LoadSaveID          "1"
      Extents         [845.0, 694.0]
      ZoomFactor          [1.0]
      Offset          [0.0, 0.0]
    }
    Object {
      $ObjectID       8
      IsActive        [0]
      ViewObjType         "SimulinkSubsys"
      LoadSaveID          "42"
      Extents         [845.0, 694.0]
      ZoomFactor          [1.25]
      Offset          [0.0, 0.0]
    }
    PropName        "EditorsInfo"
      }
    }
  }
  Created         "Sat Feb 22 13:28:59 2014"
  Creator         "Yusuf S"
  UpdateHistory       "UpdateHistoryNever"
  ModifiedByFormat    "%<Auto>"
  LastModifiedBy      "Yusuf S"
  ModifiedDateFormat      "%<Auto>"
  LastModifiedDate    "Sat Feb 22 21:04:42 2014"
  RTWModifiedTimeStamp    315003844
  ModelVersionFormat      "1.%<AutoIncrement:2>"
  ConfigurationManager    "None"
  SampleTimeColors    off
  SampleTimeAnnotations   off
  LibraryLinkDisplay      "disabled"
  WideLines       off
  ShowLineDimensions      off
  ShowPortDataTypes   off
  ShowDesignRanges    off
  ShowLoopsOnError    on
  IgnoreBidirectionalLines off
  ShowStorageClass    off
```

```
ShowTestPointIcons      on
ShowSignalResolutionIcons on
ShowViewerIcons     on
SortedOrder         off
ExecutionContextIcon    off
ShowLinearizationAnnotations on
BlockNameDataTip    off
BlockParametersDataTip  off
BlockDescriptionStringDataTip off
ToolBar         on
StatusBar       on
BrowserShowLibraryLinks off
BrowserLookUnderMasks   off
SimulationMode      "normal"
LinearizationMsg    "none"
Profile         off
ParamWorkspaceSource    "MATLABWorkspace"
AccelSystemTargetFile   "accel.tlc"
AccelTemplateMakefile   "accel_default_tmf"
AccelMakeCommand    "make_rtw"
TryForcingSFcnDF    off
Object {
  $PropName           "DataLoggingOverride"
  $ObjectID           9
  $ClassName          "Simulink.SimulationData.ModelLoggingInfo"
  model_          "Model_2"
  overrideMode_       [0U]
  Array {
    Type            "Cell"
    Dimension           1
    Cell            "Model_2"
    PropName            "logAsSpecifiedByModels_"
  }
  Array {
    Type            "Cell"
    Dimension           1
    Cell            []
    PropName            "logAsSpecifiedByModelsSSIDs_"
  }
}
RecordCoverage      off
CovPath         "/"
CovSaveName         "covdata"
CovMetricSettings   "dw"
CovNameIncrementing     off
CovHtmlReporting    on
CovForceBlockReductionOff on
covSaveCumulativeToWorkspaceVar on
CovSaveSingleToWorkspaceVar on
CovCumulativeVarName    "covCumulativeData"
CovCumulativeReport     off
CovReportOnPause    on
CovModelRefEnable   "Off"
CovExternalEMLEnable    off
ExtModeBatchMode    off
ExtModeEnableFloating   on
ExtModeTrigType     "manual"
```

```
ExtModeTrigMode     "normal"
ExtModeTrigPort     "1"
ExtModeTrigElement      "any"
ExtModeTrigDuration     1000
ExtModeTrigDurationFloating "auto"
ExtModeTrigHoldOff      0
ExtModeTrigDelay    0
ExtModeTrigDirection    "rising"
ExtModeTrigLevel    0
ExtModeArchiveMode      "off"
ExtModeAutoIncOneShot   off
ExtModeIncDirWhenArm    off
ExtModeAddSuffixToVar   off
ExtModeWriteAllDataToWs off
ExtModeArmWhenConnect   on
ExtModeSkipDownloadWhenConnect off
ExtModeLogAll       on
ExtModeAutoUpdateStatusClock on
BufferReuse         on
ShowModelReferenceBlockVersion off
ShowModelReferenceBlockIO off
Array {
  Type             "Handle"
  Dimension           1
  Simulink.ConfigSet {
    $ObjectID           10
    Version             "1.13.0"
    Array {
  Type             "Handle"
  Dimension       9
  Simulink.SolverCC {
    $ObjectID       11
    Version         "1.13.0"
    StartTime       "0.0"
    StopTime        "100"
    AbsTol          "auto"
    FixedStep       "auto"
    InitialStep         "auto"
    MaxNumMinSteps      "-1"
    MaxOrder        5
    ZcThreshold         "auto"
    ConsecutiveZCsStepRelTol "10*128*eps"
    MaxConsecutiveZCs   "1000"
    ExtrapolationOrder      4
    NumberNewtonIterations  1
    MaxStep         "auto"
    MinStep         "auto"
    MaxConsecutiveMinStep   "1"
    RelTol          "1e-3"
    SolverMode          "Auto"
    EnableConcurrentExecution off
    ConcurrentTasks     off
    Solver          "ode45"
    SolverName          "ode45"
    SolverJacobianMethodControl "auto"
    ShapePreserveControl    "DisableAll"
    ZeroCrossControl    "UseLocalSettings"
```

```
    ZeroCrossAlgorithm      "Nonadaptive"
    AlgebraicLoopSolver     "TrustRegion"
    SolverResetMethod   "Fast"
    PositivePriorityOrder   off
    AutoInsertRateTranBlk   off
    SampleTimeConstraint    "Unconstrained"
    InsertRTBMode       "Whenever possible"
  }
  Simulink.DataIOCC {
    $ObjectID       12
    Version         "1.13.0"
    Decimation          "1"
    ExternalInput       "[t, u]"
    FinalStateName      "xFinal"
    InitialState        "xInitial"
    LimitDataPoints     on
    MaxDataPoints       "1000"
    LoadExternalInput   off
    LoadInitialState    off
    SaveFinalState      off
    SaveCompleteFinalSimState off
    SaveFormat          "Array"
    SignalLoggingSaveFormat "Dataset"
    SaveOutput          on
    SaveState       off
    SignalLogging       on
    DSMLogging          on
    InspectSignalLogs   off
    SaveTime        on
    ReturnWorkspaceOutputs  off
    StateSaveName       "xout"
    TimeSaveName        "tout"
    OutputSaveName      "yout"
    SignalLoggingName   "logsout"
    DSMLoggingName      "dsmout"
    OutputOption        "RefineOutputTimes"
    OutputTimes         "[]"
    ReturnWorkspaceOutputsName "out"
    Refine          "1"
  }
  Simulink.OptimizationCC {
    $ObjectID       13
    Version         "1.13.0"
    Array {
      Type            "Cell"
      Dimension           8
      Cell            "BooleansAsBitfields"
      Cell            "PassReuseOutputArgsAs"
      Cell            "PassReuseOutputArgsThreshold"
      Cell            "ZeroExternalMemoryAtStartup"
      Cell            "ZeroInternalMemoryAtStartup"
      Cell            "OptimizeModelRefInitCode"
      Cell            "NoFixptDivByZeroProtection"
      Cell            "UseSpecifiedMinMax"
      PropName            "DisabledProps"
    }
    BlockReduction      on
```

```
  BooleanDataType     on
  ConditionallyExecuteInputs on
  InlineParams        off
  UseIntDivNetSlope   off
  UseFloatMulNetSlope     off
  UseSpecifiedMinMax      off
  InlineInvariantSignals  off
  OptimizeBlockIOStorage  on
  BufferReuse         on
  EnhancedBackFolding     off
  StrengthReduction   off
  ExpressionFolding   on
  BooleansAsBitfields     off
  BitfieldContainerType   "uint_T"
  EnableMemcpy        on
  MemcpyThreshold     64
  PassReuseOutputArgsAs   "Structure reference"
  ExpressionDepthLimit    128
  FoldNonRolledExpr   on
  LocalBlockOutputs   on
  RollThreshold       5
  SystemCodeInlineAuto    off
  StateBitsets        off
  DataBitsets         off
  UseTempVars         off
  ZeroExternalMemoryAtStartup on
  ZeroInternalMemoryAtStartup on
  InitFltsAndDblsToZero   off
  NoFixptDivByZeroProtection off
  EfficientFloat2IntCast  off
  EfficientMapNaN2IntZero on
  OptimizeModelRefInitCode off
  LifeSpan        "inf"
  MaxStackSize        "Inherit from target"
  BufferReusableBoundary  on
  SimCompilerOptimization "Off"
  AccelVerboseBuild   off
  ParallelExecutionInRapidAccelerator on
}
```